AFFDL-TR-73-19
VOLUME I

WRIGHT-PATTERSON
TECHNICAL LIBRARY
WPAFB, O.

STOL TACTICAL AIRCRAFT INVESTIGATION

Volume I

Configuration Definition : Medium STOL Transport with Vectored Thrust/Mechanical Flaps

Richard H. Carroll
John W. Jants
Peter Milns

THE BOEING COMPANY

TECHNICAL REPORT AFFDL-TR-73-19 – VOLUME I

MAY, 1973

Approved for public release; distribution unlimited.

Air Force Flight Dynamics Laboratory
Air Force Systems Command
Wright-Patterson Air Force Base, Ohio 45433

Notice

When Government drawings, specifications, or other data are used for any purpose other than in connection with a definitely related Government procurement operation, the United States Government thereby incurs no responsibility nor any obligation whatsoever; and the fact that the Government may have formulated, furnished, or in any way supplied the said drawings, specifications, or other data, is not to be regarded by implication or otherwise as in any manner licensing the holder or any other person or corporation or conveying any rights or permission to manufacture, use, or sell any patented invention that may in any way be related thereto.

Copies of this report should not be returned unless return is required by security considerations, contractual obligations, or notice on a specific document.

AIR FORCE/56780/20 August 1973 — 150

STOL TACTICAL AIRCRAFT INVESTIGATION

Volume I

Configuration Definition : Medium STOL Transport with Vectored Thrust/Mechanical Flaps

Richard H. Carroll
John W. Jants
Peter Milns

Approved for public release ; distribution unlimited.

FOREWORD

This report was prepared for the United States Air Force by The Boeing Company, Seattle, Washington in partial fulfillment of Contract F33615-71-C-1757, Project No. 643A. It is one of eight related documents covering the results of investigations of vectored-thrust and jet-flap powered lift technology, under the STOL Tactical Aircraft Investigation (STAI) Program sponsored by the Air Force Flight Dynamics Laboratory, Air Force Systems Command, Wright-Patterson Air Force Base, Ohio. The relation of this report to the others of this series is indicated below:

AFFDL TR-73-19 STOL TACTICAL AIRCRAFT INVESTIGATION

Vol I	Configuration Definition: Medium STOL Transport with Vectored Thrust/Mechanical Flaps	THIS REPORT
Vol II Part I	Aerodynamic Technology: Design Compendium, Vectored Thrust/Mechanical Flaps	
Vol II Part II	A Lifting Line Analysis Method for Jet-Flapped Wings	
Vol III	Takeoff and Landing Performance Ground Rules for Powered Lift STOL Transport Aircraft	
Vol IV	Analysis of Wind Tunnel Data, Vectored Thrust/Mechanical Flaps and Internally Blown Jet Flaps	
Vol V Part I	Flight Control Technology: System Analysis and Trade Studies for a Medium STOL Transport with Vectored Thrust and Mechanical Flaps	
Vol V Part II	Flight Control Technology: Piloted Simulation of a Medium STOL Transport with Vectored Thrust/Mechanical Flaps	
Vol VI	Air Cushion Landing System Study	

The work reported here was performed in the period 8 June 1971 through 12 January 1973 by the Aero/Propulsion Staff of the Research and Engineering Division and by the Tactical Airlift Program, aeronautical and Information Systems Division, both of the Aerospace Group, The Boeing Company. Mr. Franklyn J. Davenport served as Program Manager.

The authors gratefully acknowledge the contributions of the following individuals to the work reported here:

Configuration Development: David M. Dolliver, Michael R. Stanley, David L. Womeldorff and Gerald G. Upton.

Aerodynamics: Fred W. May, J. Patrick Palmer, Bernard F. Ray, Arnold E. Rengstorff and Donald E. West.

Flight Controls: Kenneth J. Crandall.

Propulsion: Joe P. Zeeben.

Structures: Bryce A. Bolton, Allan L. Brown and Roman F. Michalak.

Mass Properties: William F. Mannick.

The Air Force Project Engineer for this investigation was Mr. Garland S. Oates, Air Force Flight Dynamics Laboratory, PTA, Wright-Patterson Air Force Base, Ohio.

This report was released within The Boeing Company as Document D180-14408-1, and submitted to the USAF in January 1973.

This technical report has been reviewed and is approved.

E. J. Cross Jr., Lt. Col., USAF
Chief, Prototype Division
Air Force Flight Dynamics Laboratory

(iv blank)

ABSTRACT

A configuration for an Advanced Medium STOL Transport (AMST) using vectored thrust for powered lift is defined in detail. Capability to operate from an austere forward airfield of 2000 feet length at the midpoint of 500 nm radius mission with 28,000 lbs. of payload is substantiated by aerodynamic, propulsion, structural, and weights data. The vectored thrust powered lift concept is compared with other powered lift schemes considered for the AMST. A program of continuing research and development in tactical airlift and STOL technology is recommended.

(vi blank)

TABLE OF CONTENTS

LIST OF ILLUSTRATIONS

LIST OF ILLUSTRATIONS (Cont'd)

LIST OF ILLUSTRATIONS (Cont'd)

LIST OF ILLUSTRATIONS (Cont'd)

LIST OF ILLUSTRATIONS (Cont'd)

LIST OF TABLES

LIST OF SYMBOLS

Symbol	Definition
C_D	Drag coefficient, D/qS
C_J	Gross thrust coefficient, (total F_G)/qS
C_L	Lift coefficient, L/qS
C_ℓ	Rolling moment coefficient, ℓ/qSb
C_n	Yawing moment coefficient, n/qSb
C_μ	BLC momentum coefficient, μ_{BLC}/qS
D	Drag, lbs
F_G	Gross thrust, lbs
F_N	Net thrust, lbs
K	Control gain
L	Lift, lbs
M	Mach number
S	Wing area, sq ft
V_H	Level flight placard speed, knots
$\bar{V}_H$	Horizontal tail volume coefficient
W	Airplane weight, lbs
BL	Buttock line, inches
BS	Body station, inches
WL	Water line, inches
T/W	Thrust to weight ratio
CBR	California bearing ratio
SFC	Specific fuel consumption, lbs fuel/hr per lb thrust

LIST OF SYMBOLS (continued)

Symbol	Definition
b	Wing span, ft
$\bar{c}$	Mean aerodynamic chord, ft
f	Drag area, sq ft
ℓ	Rolling moment, ft-lb
n	Yawing moment, ft-lb
q	Dynamic pressure, lbs/sq ft
s	Laplace transform variable
$t_{(\ )}$	Time to reach dynamic condition (as indicated by subscript), sec
α_w	Wing angle of attack
β	Sideslip angle
γ	Flight path angle
δ	Air pressure ratio
$\delta_{(\ )}$	Control deflection (as indicated by subscript)
ζ_{DR}	Dutch roll mode damping ratio
η_v	Thrust vectoring efficiency
θ	Pitch attitude angle, or air temperature ratio (evident from context)
σ	Thrust vector angle
ϕ	Bank angle
ψ	Yaw angle
τ_R	Roll subsidence mode time constant, sec

Symbol	Definition
τ_s	Spiral mode time constant, sec
ω_{DR}	Dutch roll mode undamped natural frequency, rad/sec
μ_{BLC}	BLC momentum flux, lbs

SECTION I

INTRODUCTION AND SUMMARY

1.1 Introduction

The U.S. Air Force has determined the requirement to modernize its Tactical Airlift capability. The Tactical Airlift Technology Advanced Development Program (TAT-ADP) was established as a first step in meeting this requirement, contributing to the technology base for development of an Advanced Medium STOL Transport (AMST).

The AMST must be capable of handling substantial payloads and using airfields considerably shorter than those required by large tactical transports now in the Air Force inventory. If this short-field requirement is to be met without unduly compromising aircraft speed, economy, and ride quality, an advanced-technology powered-lift concept will be required.

The STOL Tactical Aircraft Investigation (STAI) is a major part of the TAT-ADP, and comprises studies of the aerodynamics and flight control technology of powered lift systems under consideration for use on the AMST. Under the STAI, The Boeing Company was awarded Contract No. F33615-71-C-1757 by the USAF Flight Dynamics Laboratory to conduct investigations of the technology of the vectored-thrust powered lift concept.

Early in the STAI, an assessment of the state of the art of vectored thrust aerodynamic technology was made. It indicated a severe lack of experimental aerodynamic data on vectored thrust effects for configurations suitable for tactical transport aircraft.

A wind tunnel test program was therefore conducted to provide an adequate data base. More than 600 hours were spent in the Boeing V/STOL wind tunnel establishing the aerodynamic interaction effects of vectored thrust over a wide range of configuration and flight condition variables, including:

- Wing sweepback angle and aspect ratio,
- Nacelle placement,
- Vector nozzle angle,
- Ground proximity,

and many others.

The results of that test program are reported in Volume IV of this series. These results were used as the basis for an aerodynamic technology design compendium for vectored thrust transports, presented as Part I of Volume II of this series.

The aerodynamics effort was parallelled by a study of thrust reversing and vectoring concepts sponsored by the Air Force Aero Propulsion Laboratory, reported in Reference 1. This study (not restricted to AMST applications) provided a basis for improved understanding of both weights and efficiency of thrust vectoring devices.

Meanwhile, an intensive study of the flight control technology of the vectored thrust powered lift concept was underway as another major task of the STAI, as reported in Volume V of this series. Control force and moment producers for low dynamic pressure STOL flight were evaluated. Stability and control augmentation systems were investigated, considering not only mathematical "control laws" but also the realistic mechanization of the system. More than 400 hours of piloted flight simulation, including 57 hours in the NASA-Ames FSAA moving-base simulator, were spent evaluating candidate concepts and validating the selected system.

The results of the aerodynamic, propulsion, and control technology studies provided a firm basis for definition of a vectored thrust tactical transport configuration with a high degree of technical confidence. This report presents the results of that configuration definition effort. In addition, recommendations are made for further research and development in the tactical airlift area, as indicated both by STAI work and by results to date of the Boeing AMST prototype program.

1.2 Summary

A STOL tactical transport using the vectored thrust/mechanical flap powered lift concept has been configurated and analyzed in detail. Figure 1 shows an artist's concept of this airplane in flight. It is similar in appearance to the Baseline Configuration designed on the basis of preliminary data early in the STAI. Significant differences are:

(1) More weight. At 158,000 lbs STOL mission takeoff weight, the airplane is 12,500 lbs heavier than the original baseline.

(2) More forward engine placement to provide better clearance between the reverse-thrust exhaust plume and the leading edge of the wing.

(3) Revised fuselage lines reflecting an improved flight deck arrangement and low drag landing gear fairings.

Two areas of technical risk were identified:

(1) The mass and stiffness distribution of the wing and engines results in unsatisfactory flutter margins in some flight conditions. In the time available it was not possible to determine the degree to which the problem could be relieved by minor rearrangement or the required additional weight for stiffening.

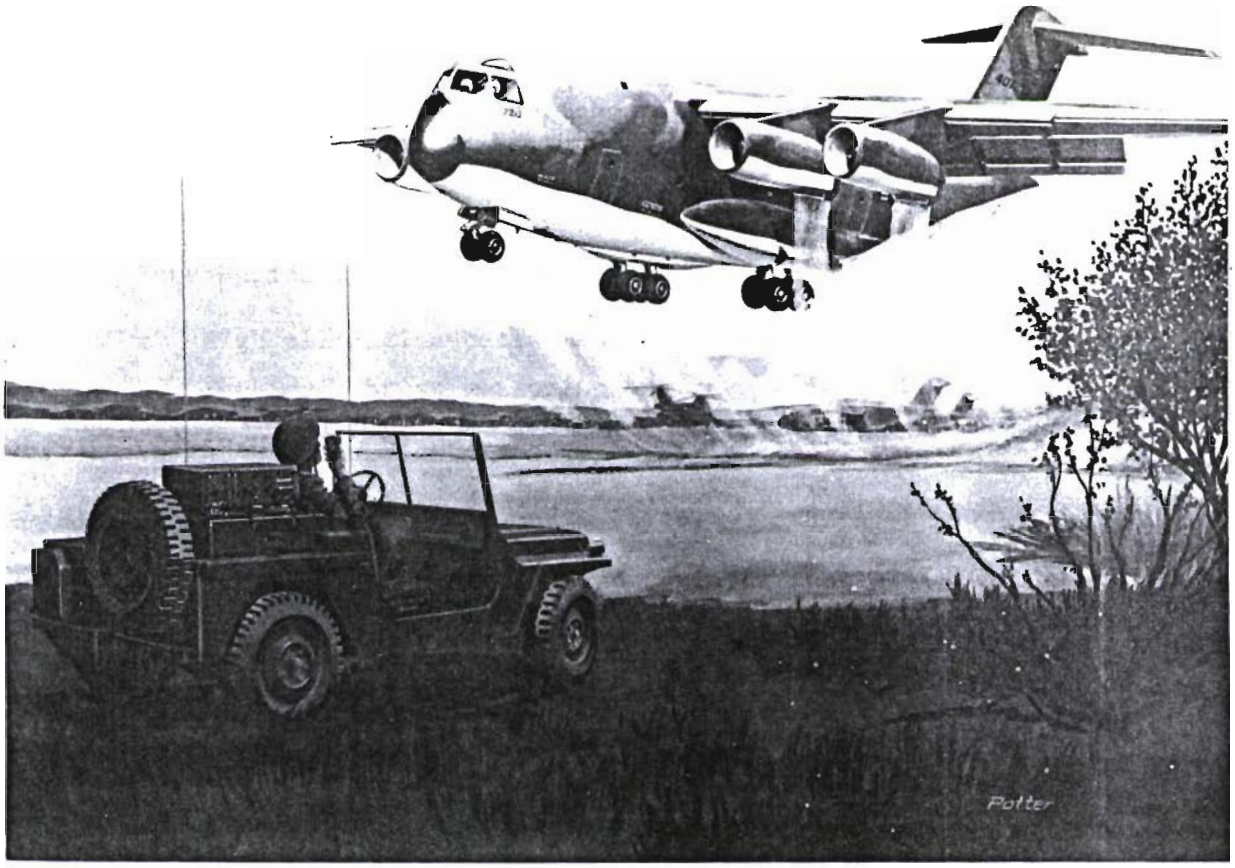

Figure 1: Vectored Thrust Medium STOL Transport

(7) Vision-designed cockpit lines and windows:

- o Visibility superior to best of current TAC Transport aircraft (C-7) with six large windows rather than 12, as on the C-130.
- o Assured wing tip clearance during taxi.

(8) Large cargo compartment:

- o Effective utilization when longer runways are available. (Payloads up to 58,000 pounds)
- o Capability to carry cargo outsize to current tactical aircraft. (Cargo box size = 12 x 12 x 61 feet)

2.2 Performance Summary

2.2.1 Payload Distance

The airplane's payload-range/radius performance is presented in Figure 5. The design payload of 28,000 pounds carried to a 500-nautical mile radius and return results in a takeoff gross weight of 158,000 pounds. With zero payload and 58,000 pounds of fuel, the maximum radius is 1470 nautical miles.

The ferry range with maximum internal fuel of 67,400 pounds is 3700 nautical miles. The long-range cruise (99% of maximum range) Mach number is approximately .71 for the radius and ferry missions.

2.2.2 Takeoff and Landing

Figure 6 shows takeoff and landing field lengths, computed for two different sets of ground rules:

(1) "Normal" rules. They require that in the event of engine failure during a STOL takeoff, the pilot must be able either to stop within the available distance or to complete the takeoff with the remaining engines. In the event of engine failure during final approach, the pilot must be able to continue to a safe landing. These rules were defined in detail by the Air Force for all STAI contractors, and are those applying to the 2000-foot field length designed criterion.

(2) "Assault" rules. In some circumstances, combat or emergency requirements may demand operation where engine failure could be expected to cause a crash. Performance determined using assault rules is airplane's maximum capability.

The rules are stated in full in Appendix II.

(2) The forward engine location may cause unacceptable buffeting in the STOL landing approach condition. Adverse lift interference is evident in the wind tunnel data at low angles of attack. Whether this is associated with buffet-producing flow separation could not be determined without further wind tunnel testing.

The airplane is equipped with an advanced flight control system featuring the modulation of thrust vector angle as a primary longitudinal control in the STOL approach condition. The pilot leaves the throttle setting fixed, controlling the airplane's speed and pitch altitude with the thrust vector lever and the control column, respectively. The control system adjusts the actual vector angle and the direct lift control spoilers so as to decouple speed and altitude (or path angle) responses.

SECTION II

CONFIGURATION DESCRIPTION AND CHARACTERISTICS

2.1 Description

The Model 953-815 is a military tactical transport aircraft which uses vectored thrust and mechanical flaps to fulfill the high-lift requirements of STOL performance. This airplane is designed for a 500-nautical mile radius mission into and out of an austere forward field, with a payload of 28,000 pounds, achieving a cruise Mach number of 0.75. It will also perform a 3600-nautical mile ferry mission with no payload, unrefueled. Figure 2 shows the general arrangement and principal dimensions of the 953-815. The inboard profile is presented in Figures 3 and 4.

Features of the 953-815 include:

(1) Four engines:

- o High all-engine performance (field length = 900 feet).
- o Combined thrust vectoring and reversing mechanization.

(2) Variable camber leading-edge flaps.

(3) Triple-slotted trailing-edge flaps.

(4) Leading-edge and aileron boundary layer control (BLC).

- o High-lift coefficient ($\Delta C_{L_{max}} = +0.9$).
- o Gentle stall characteristics.

(5) Advanced flight controls and displays:

- o Precise control during approach and landing (Cooper/Harper Rating = 2.0).
- o Safe recovery following failure of critical engine.
- o Full exploitation of low-speed performance envelope.

(6) Long-stroke, high-flotation landing gear:

- o Sustained operation on austere airfields (400 passes, CBR = 6.0).
- o Energy absorption on steep approach landings (design sink rate = 15 feet per second).
- o Operation at gross weight of 200,000 pounds on the same paved runways as the T43A (Boeing 737) at 100,000-pound gross weight.

(7) Vision-designed cockpit lines and windows:

- o Visibility superior to best of current TAC Transport aircraft (C-7) with six large windows rather than 12, as on the C-130.
- o Assured wing tip clearance during taxi.

(8) Large cargo compartment:

- o Effective utilization when longer runways are available. (Payloads up to 58,000 pounds)
- o Capability to carry cargo outsize to current tactical aircraft. (Cargo box size = 12 x 12 x 61 feet)

2.2 Performance Summary

2.2.1 Payload Distance

The airplane's payload-range/radius performance is presented in Figure 5. The design payload of 28,000 pounds carried to a 500-nautical mile radius and return results in a takeoff gross weight of 158,000 pounds. With zero payload and 58,000 pounds of fuel, the maximum radius is 1470 nautical miles.

The ferry range with maximum internal fuel of 67,400 pounds is 3700 nautical miles. The long-range cruise (99% of maximum range) Mach number is approximately .71 for the radius and ferry missions.

2.2.2 Takeoff and Landing

Figure 6 shows takeoff and landing field lengths, computed for two different sets of ground rules:

(1) "Normal" rules. They require that in the event of engine failure during a STOL takeoff, the pilot must be able either to stop within the available distance or to complete the takeoff with the remaining engines. In the event of engine failure during final approach, the pilot must be able to continue to a safe landing. These rules were defined in detail by the Air Force for all STAI contractors, and are those applying to the 2000-foot field length designed criterion.

(2) "Assault" rules. In some circumstances, combat or emergency requirements may demand operation where engine failure could be expected to cause a crash. Performance determined using assault rules is airplane's maximum capability.

The rules are stated in full in Appendix II.

MODEL 953.815

AERODYNAMIC DATA

		WING	HORIZ. TAIL	VERT. TAIL
AREA	FT^2	1700.00	533.60	385.65
SPAN	FT	112.92	46.20	19.64
ASPECT RATIO		7.5	4.0	1.0
SWEEP, C/4		6.35°	10°	37°
DIHEDRAL		0°	- 4°	—
INCIDENCE		0°	+4°,-15°	—
TAPER RATIO		.30	.5	.8
THICKNESS RATIO	BODY SIDE	.150	.13	.13
	.55 b/2	.132	.13	.13
	TIP	.132	.13	.13
MAC	IN.	198.13	143.83	235.66
VOLUME COEFFICIENT		——	1.28	.112

POWER PLANT

4 BY PASS 5.25 TURBOFANS WITH THRUST VECT. & REV. 18,600 LB THR

LANDING GEAR

MAIN	8	40 x 18.0 - 17 TIRES
NOSE	2	40 x 18.0 - 17 TIRES

CARGO COMPARTMENT

144" w 144"/148" H 540" L (734 L INCL RAMP)

WEIGHTS

DESIGN GROSS	158,000 LB	STOL MISSION
DESIGN STOL	145,000 LB	STOL MISSION
STOL PAYLOAD	28,000 LB	STOL MISSION
O.E.W.	100,000 LB	
MAX. GROSS	225,000 LB	CTOL MISSION
MAX. PAYLOAD	58,000 LB	CTOL MISSION

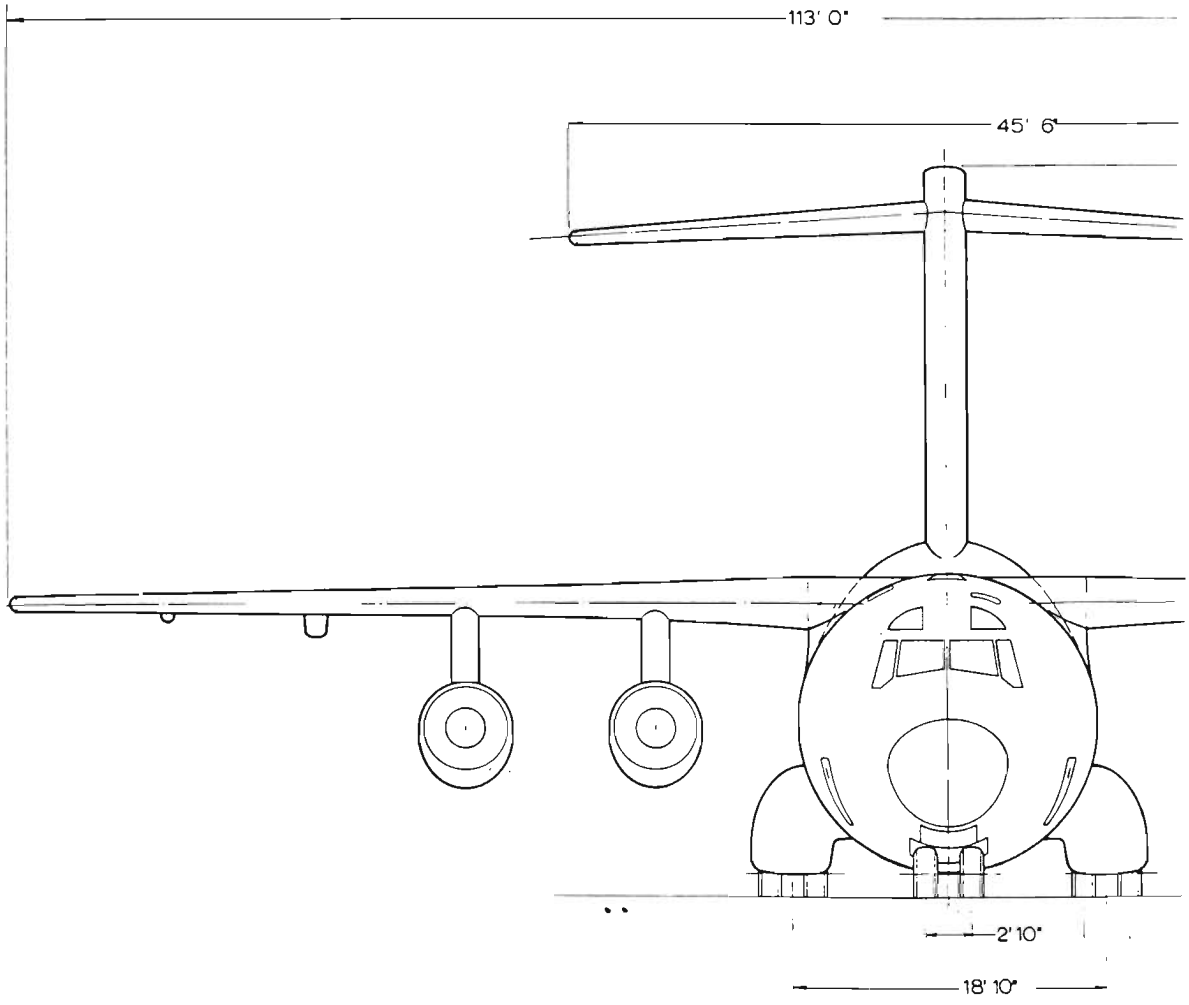

& REV. 18,600 LB THRUST

FUEL	
TANK NO. 1 & 6	13,700 LB
TANK NO. 2 & 5	16,300 LB
TANK NO. 3 & 4	16,800 LB
SUB TOTAL	46,800 LB
CENTER TANK	20,600 LB
TOTAL	67,400 LB

)

SION

SION

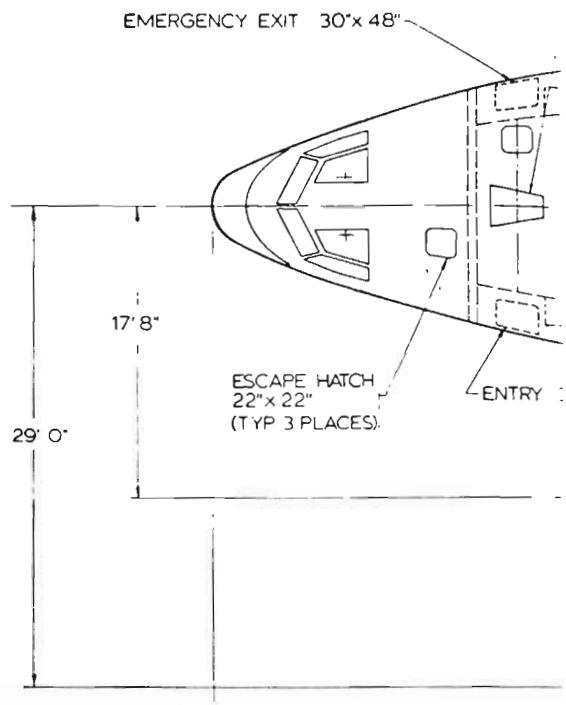

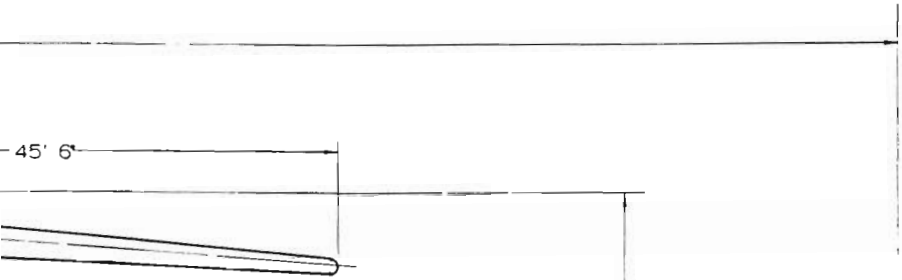

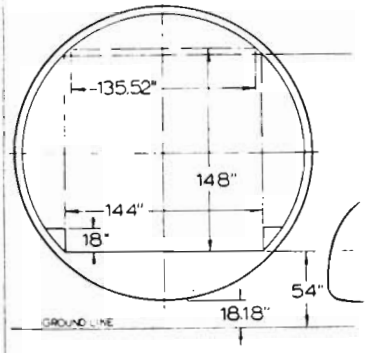

44' 2"

44' 5"

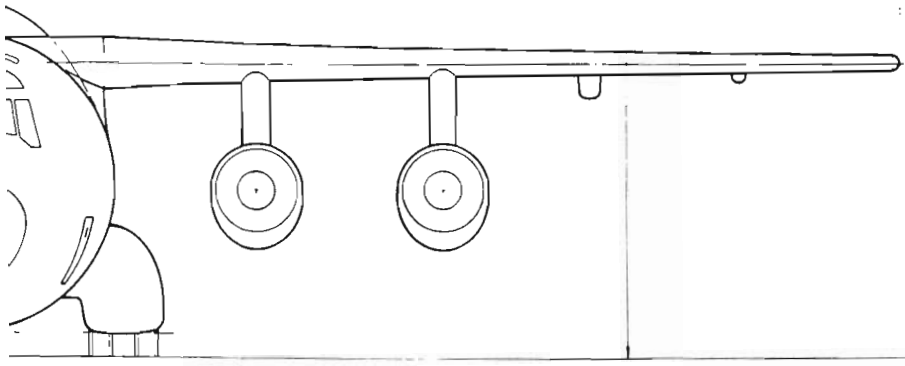

19' 6"

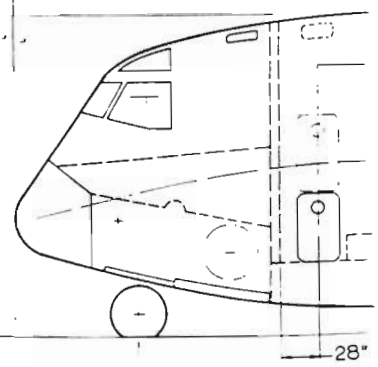

-2' 10"

10"

7'5"

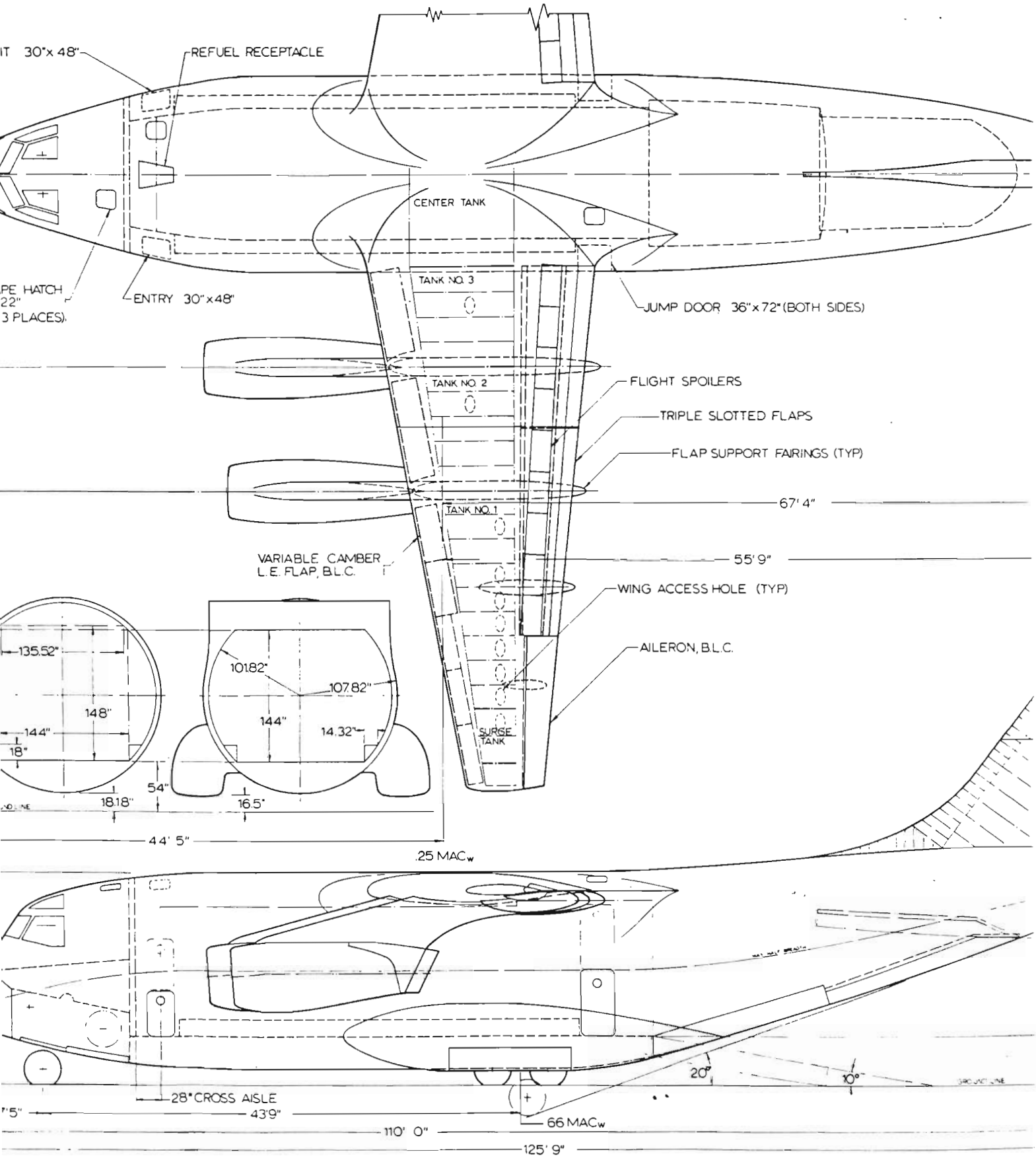
IT 30"x 48"
REFUEL RECEPTACLE
CENTER TANK
PE HATCH
22"
3 PLACES).
ENTRY 30"x48"
TANK NO. 3
JUMP DOOR 36"x72"(BOTH SIDES)
TANK NO. 2
FLIGHT SPOILERS
TRIPLE SLOTTED FLAPS
FLAP SUPPORT FAIRINGS (TYP)
67' 4"
TANK NO. 1
VARIABLE CAMBER
L.E. FLAP, B.L.C.
55' 9"
WING ACCESS HOLE (TYP)
AILERON, B.L.C.
135.52"
148"
144"
18"
101.82"
107.82"
144"
14.32"
SURGE
TANK
54"
18.18"
16.5"
44' 5"
.25 MAC$_w$
20°
10°
28"CROSS AISLE
43'9"
66 MAC$_w$
110' 0"
125' 9"

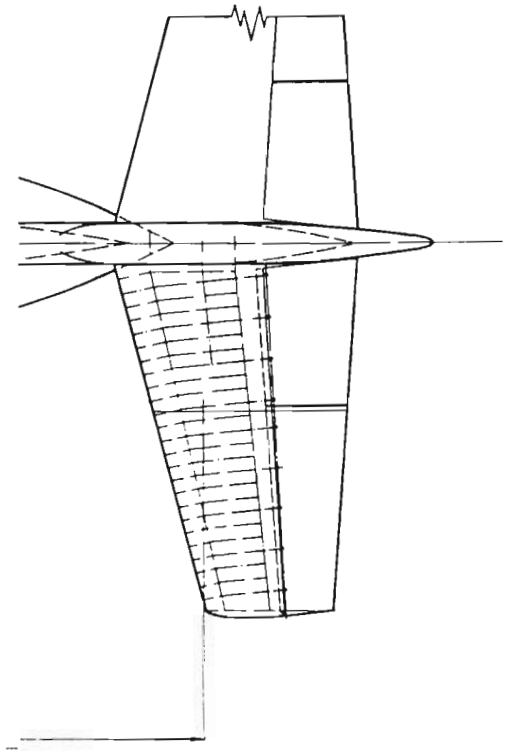

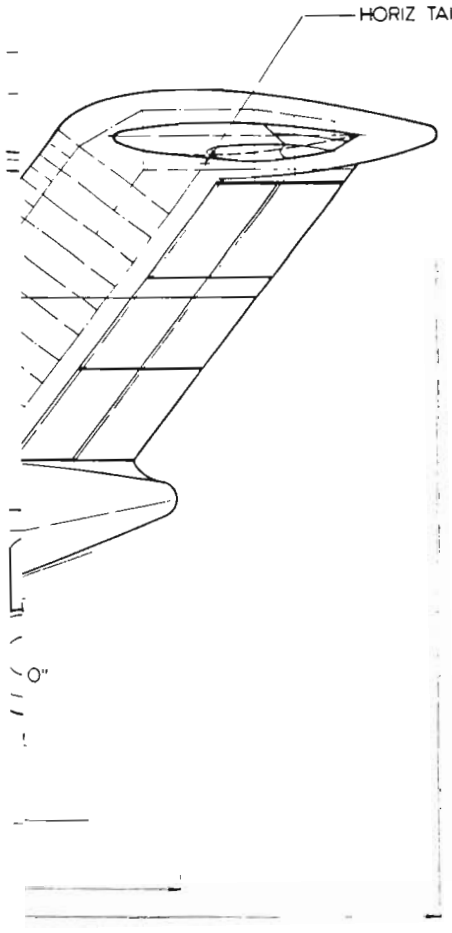

0 50 100 200 300 400
SCALE IN INCHES

0 2 4 6 8 10
SCALE IN METERS

Figure 2: General Arrangement—Model 953-815

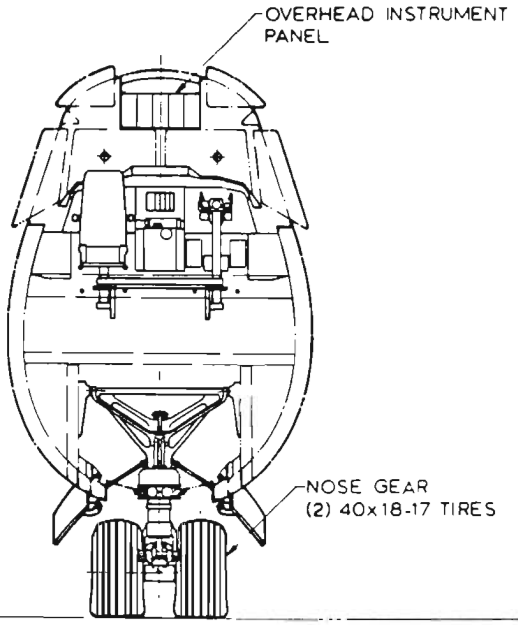

STA 210

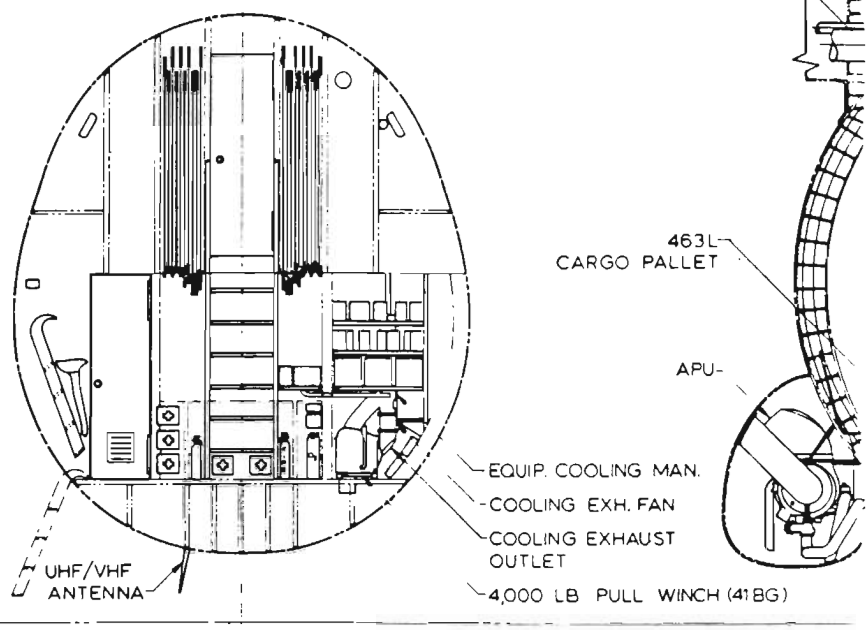

STA 300

INFL

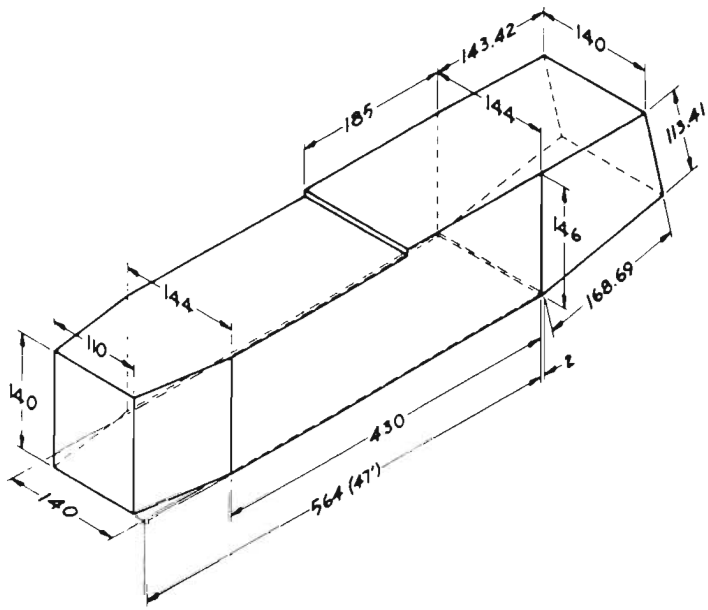

CARGO COMPARTMENT

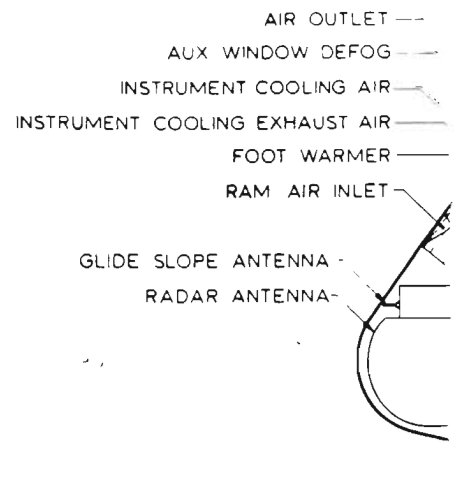

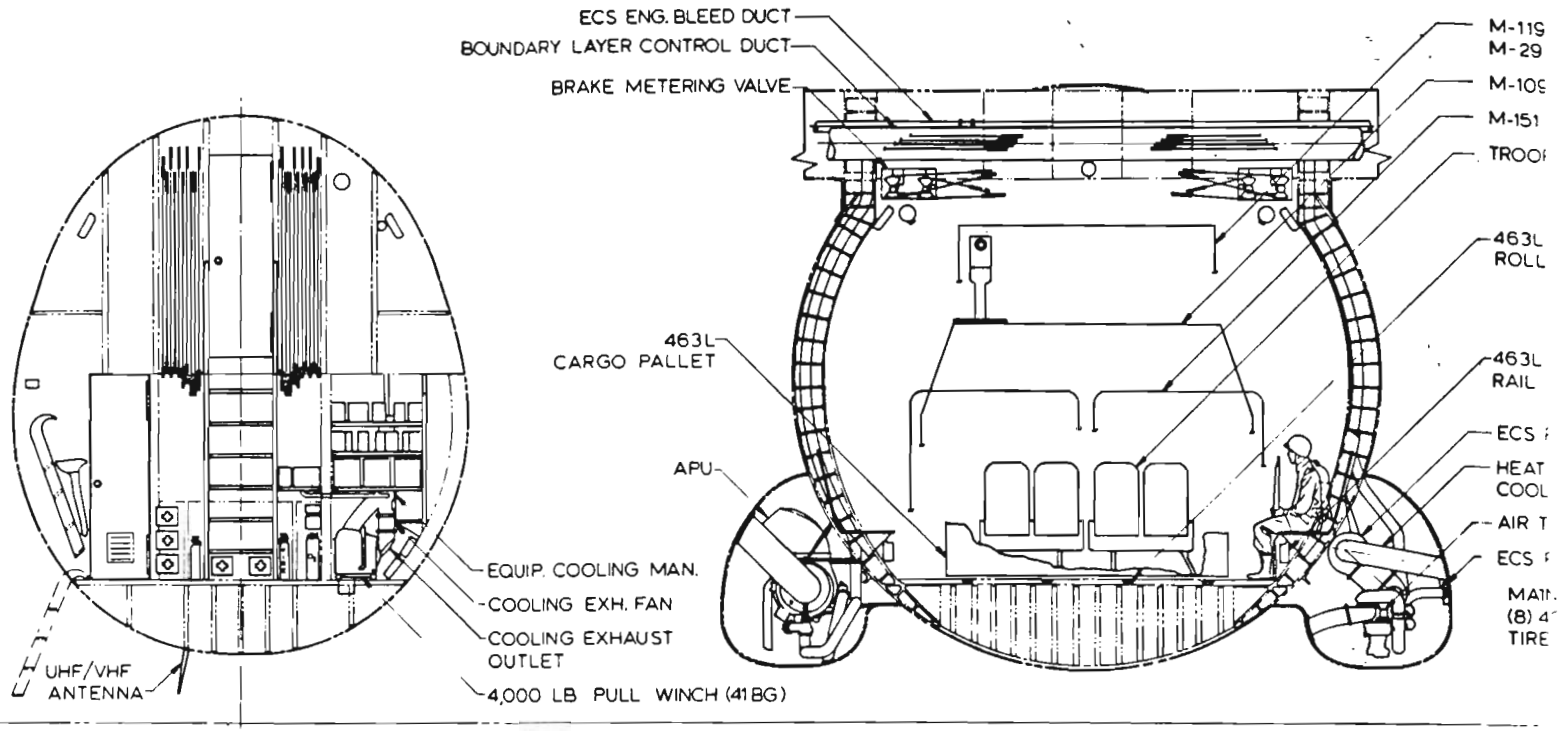
ECS ENG. BLEED DUCT
BOUNDARY LAYER CONTROL DUCT
BRAKE METERING VALVE
M-11
M-29
M-10
M-151
TROO
463L
ROLL
463L
CARGO PALLET
463L
RAIL
APU
ECS
HEAT
COOL
AIR T
ECS
MAI
(8) 4
TIRE
EQUIP. COOLING MAN.
COOLING EXH. FAN
COOLING EXHAUST
OUTLET
UHF/VHF
ANTENNA
4,000 LB PULL WINCH (41BG)
STA 300
STA 610

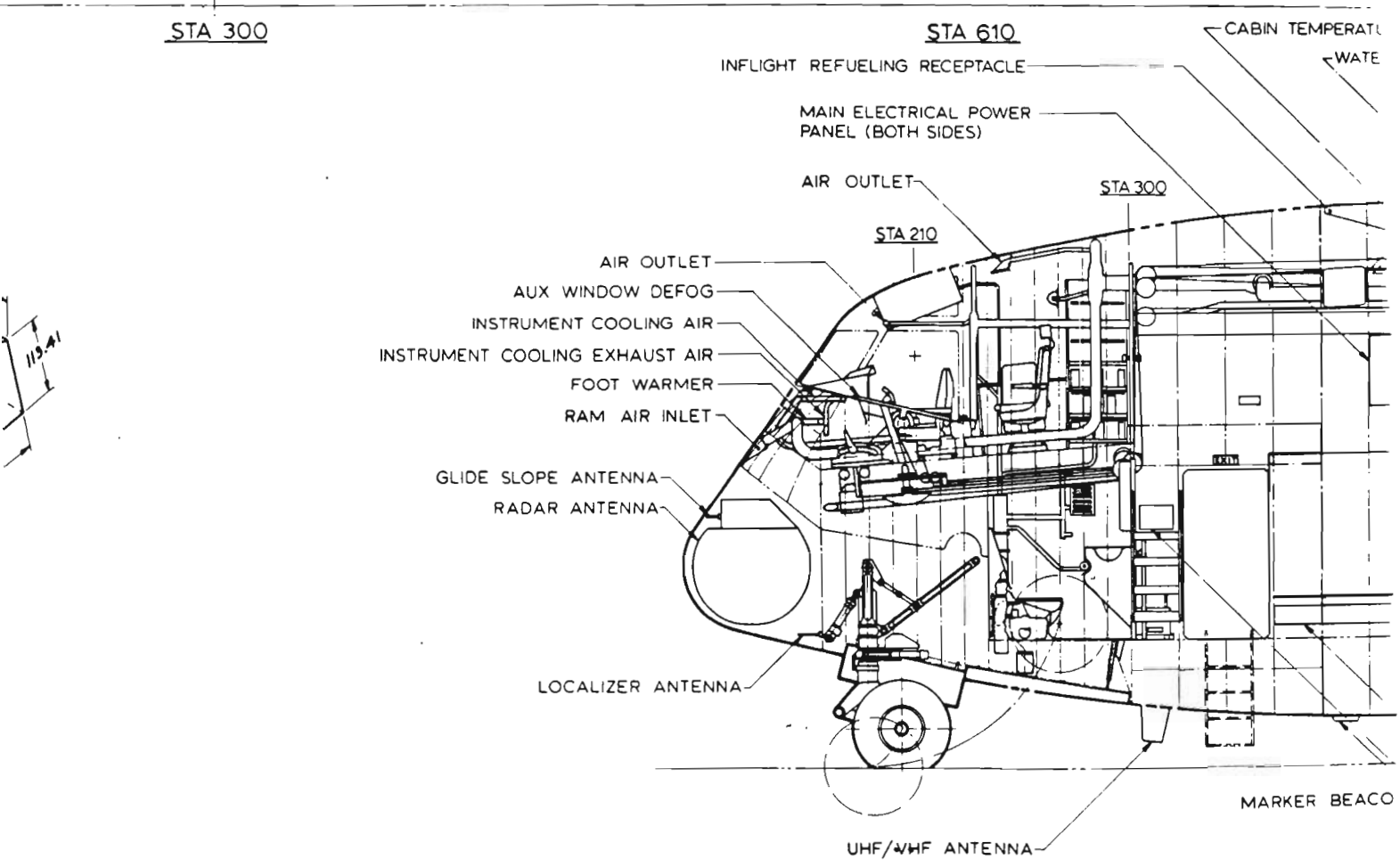
CABIN TEMPERATU
WATE
INFLIGHT REFUELING RECEPTACLE
MAIN ELECTRICAL POWER
PANEL (BOTH SIDES)
AIR OUTLET
STA 300
STA 210
AIR OUTLET
AUX WINDOW DEFOG
INSTRUMENT COOLING AIR
INSTRUMENT COOLING EXHAUST AIR
FOOT WARMER
RAM AIR INLET
GLIDE SLOPE ANTENNA
RADAR ANTENNA
LOCALIZER ANTENNA
MARKER BEACO
UHF/VHF ANTENNA

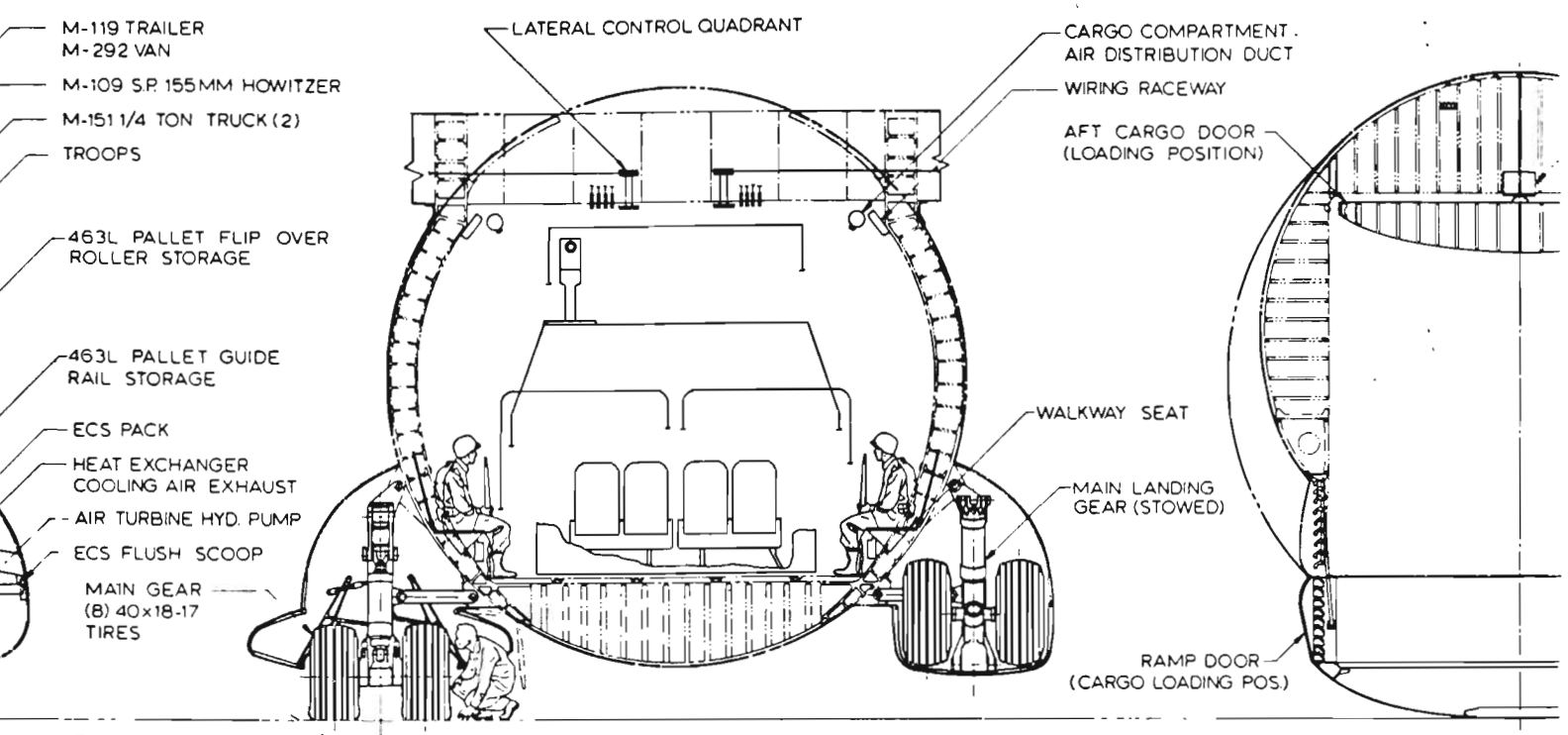
M-119 TRAILER
M-292 VAN
M-109 S.P. 155MM HOWITZER
M-151 1/4 TON TRUCK (2)
TROOPS
463L PALLET FLIP OVER ROLLER STORAGE
463L PALLET GUIDE RAIL STORAGE
ECS PACK
HEAT EXCHANGER COOLING AIR EXHAUST
AIR TURBINE HYD. PUMP
ECS FLUSH SCOOP
MAIN GEAR (8) 40x18-17 TIRES
LATERAL CONTROL QUADRANT
CARGO COMPARTMENT AIR DISTRIBUTION DUCT
WIRING RACEWAY
AFT CARGO DOOR (LOADING POSITION)
WALKWAY SEAT
MAIN LANDING GEAR (STOWED)
RAMP DOOR (CARGO LOADING POS.)
STA 730
STA 103

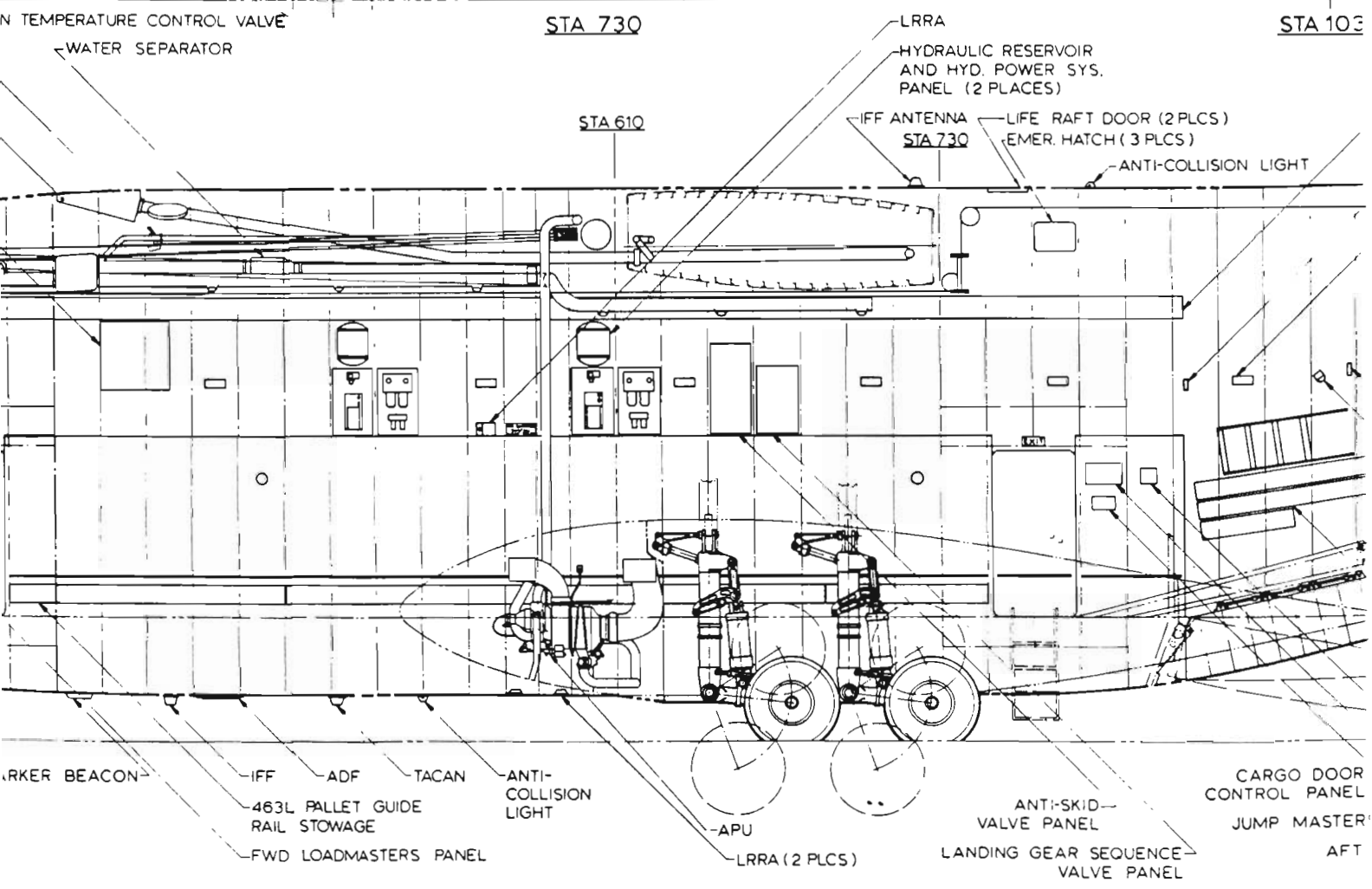
N TEMPERATURE CONTROL VALVE
WATER SEPARATOR
LRRA
HYDRAULIC RESERVOIR AND HYD. POWER SYS. PANEL (2 PLACES)
STA 610
IFF ANTENNA
STA 730
LIFE RAFT DOOR (2 PLCS)
EMER. HATCH (3 PLCS)
ANTI-COLLISION LIGHT
RKER BEACON
IFF
ADF
TACAN
ANTI-COLLISION LIGHT
463L PALLET GUIDE RAIL STOWAGE
FWD LOADMASTERS PANEL
APU
LRRA (2 PLCS)
ANTI-SKID VALVE PANEL
LANDING GEAR SEQUENCE VALVE PANEL
CARGO DOOR CONTROL PANEL
JUMP MASTER
AFT

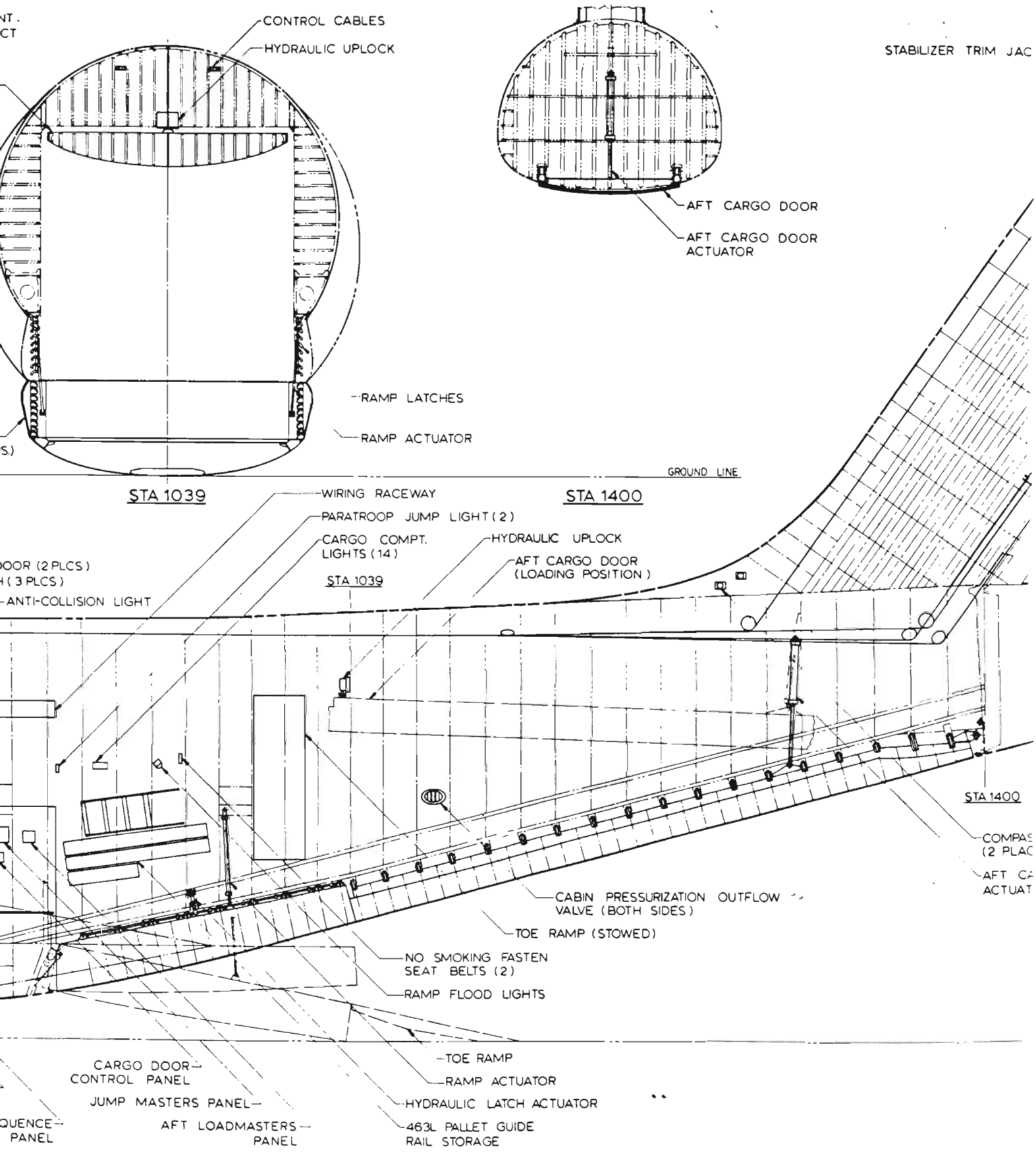
CONTROL CABLES
HYDRAULIC UPLOCK
STABILIZER TRIM JAC
AFT CARGO DOOR
AFT CARGO DOOR ACTUATOR
RAMP LATCHES
RAMP ACTUATOR
GROUND LINE
STA 1039
STA 1400
WIRING RACEWAY
PARATROOP JUMP LIGHT (2)
CARGO COMPT. LIGHTS (14)
HYDRAULIC UPLOCK
AFT CARGO DOOR (LOADING POSITION)
STA 1039
ANTI-COLLISION LIGHT
STA 1400
CABIN PRESSURIZATION OUTFLOW VALVE (BOTH SIDES)
TOE RAMP (STOWED)
NO SMOKING FASTEN SEAT BELTS (2)
RAMP FLOOD LIGHTS
TOE RAMP
RAMP ACTUATOR
HYDRAULIC LATCH ACTUATOR
463L PALLET GUIDE RAIL STORAGE
CARGO DOOR CONTROL PANEL
JUMP MASTERS PANEL
AFT LOADMASTERS PANEL

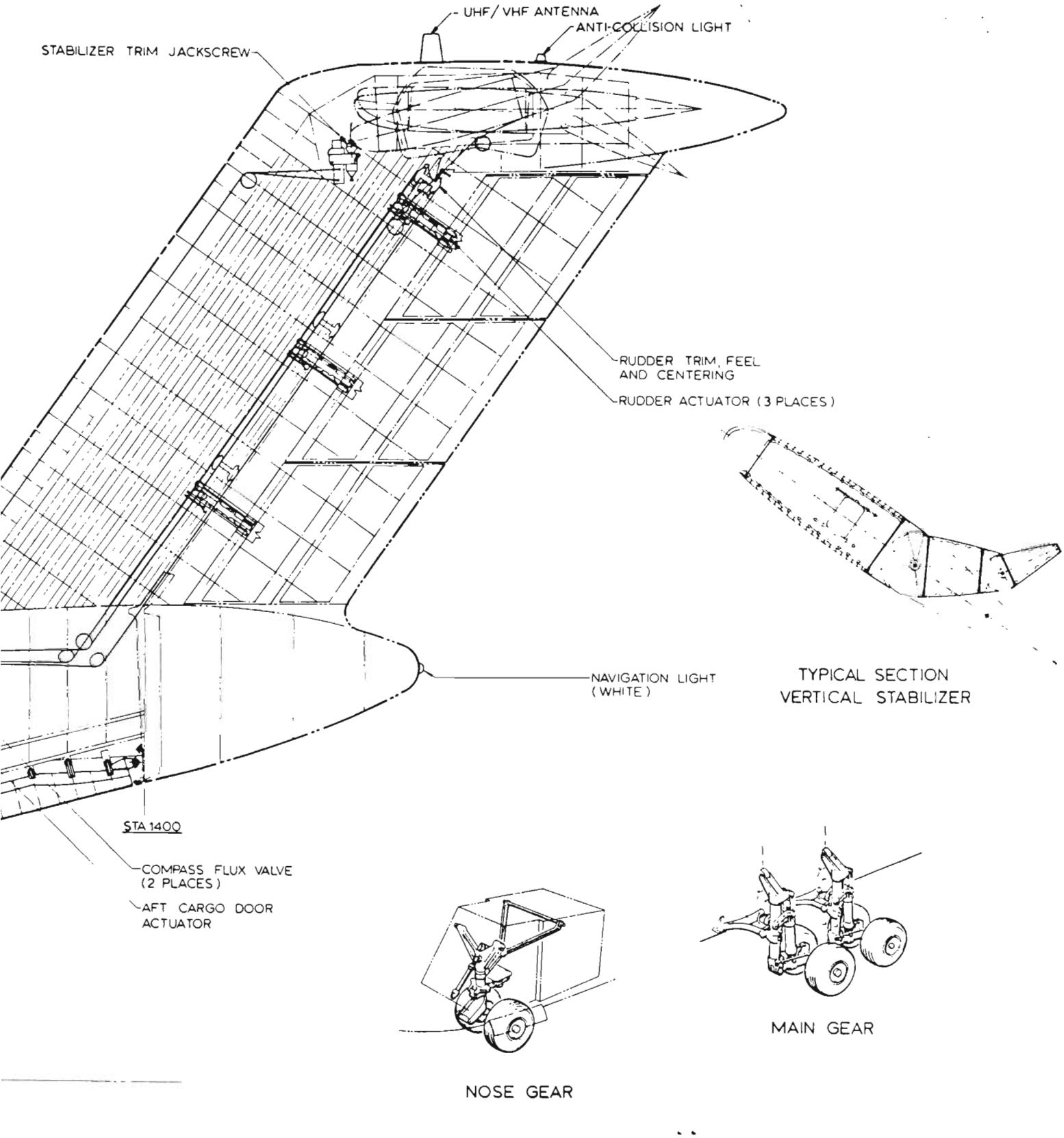

Figure 3: Inboard

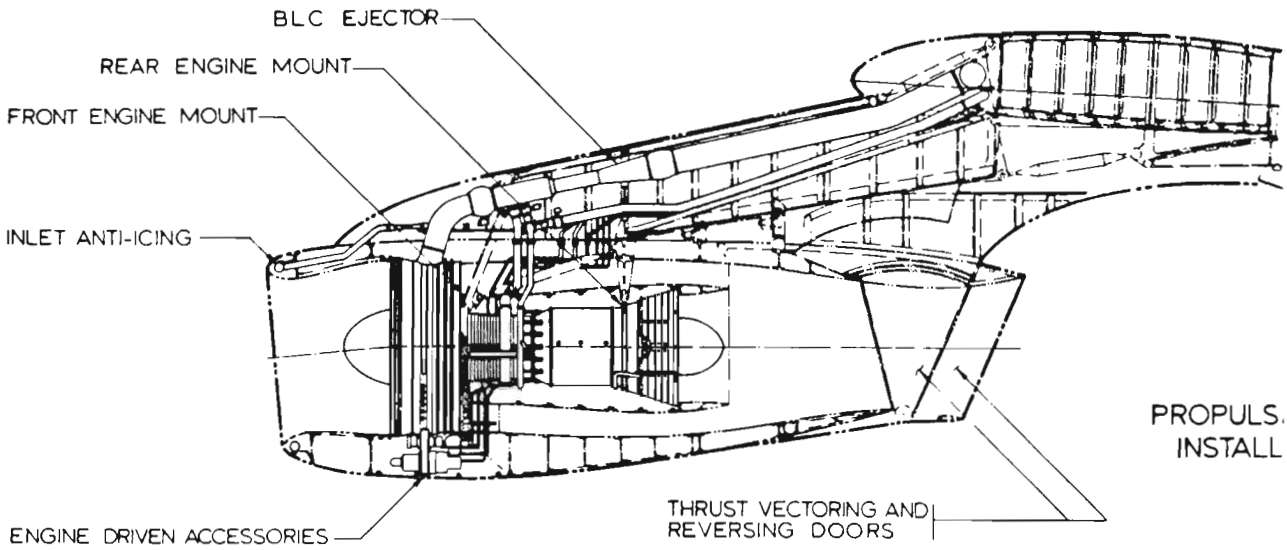
BLC EJECTOR
REAR ENGINE MOUNT
FRONT ENGINE MOUNT
INLET ANTI-ICING
ENGINE DRIVEN ACCESSORIES
THRUST VECTORING AND REVERSING DOORS
PROPULS
INSTALL

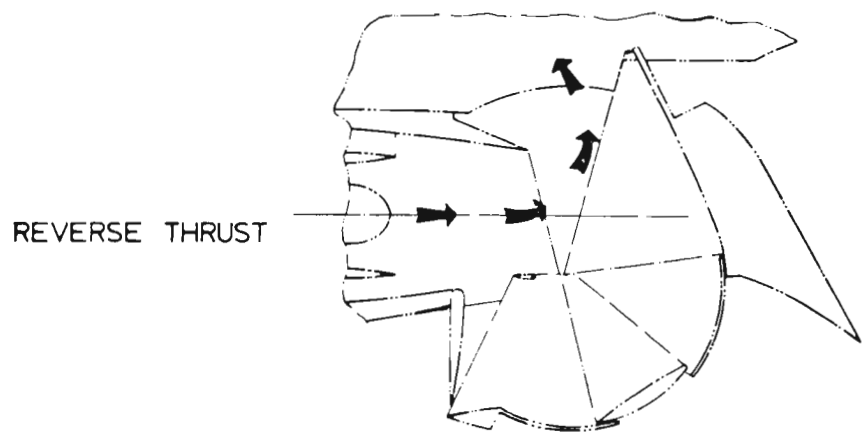
REVERSE THRUST

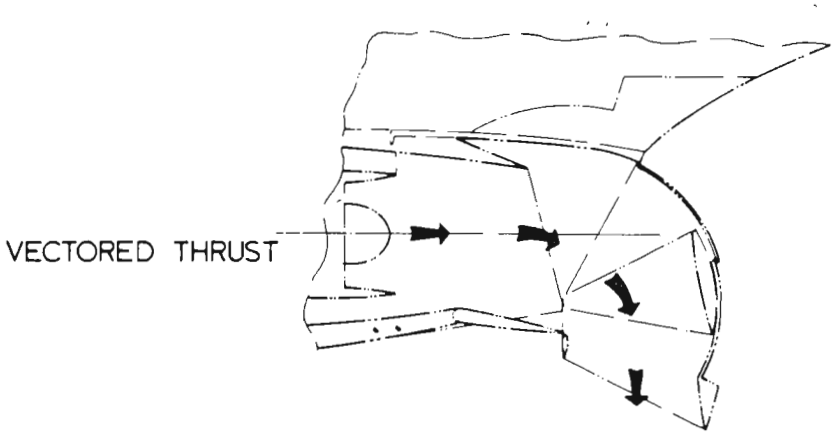
VECTORED THRUST

ELEVATOR

TYPICAL HORIZONTA

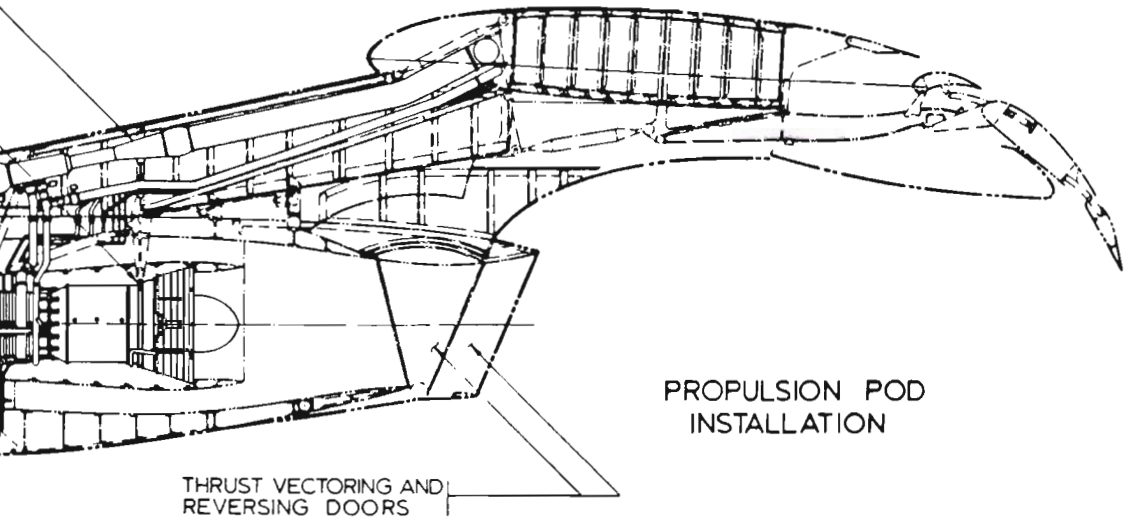

PROPULSION POD
INSTALLATION

THRUST VECTORING AND
REVERSING DOORS

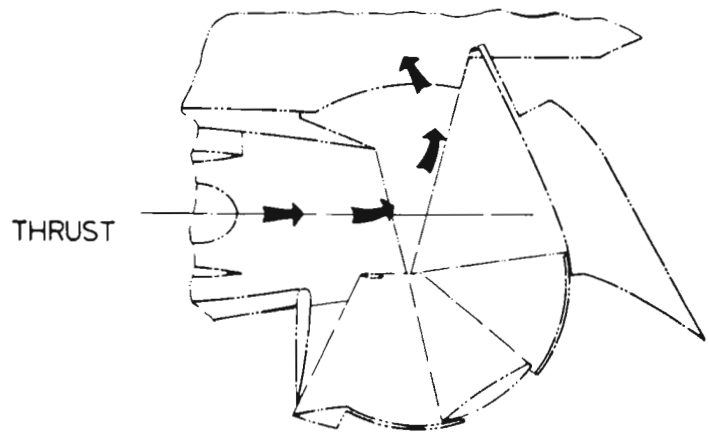

THRUST

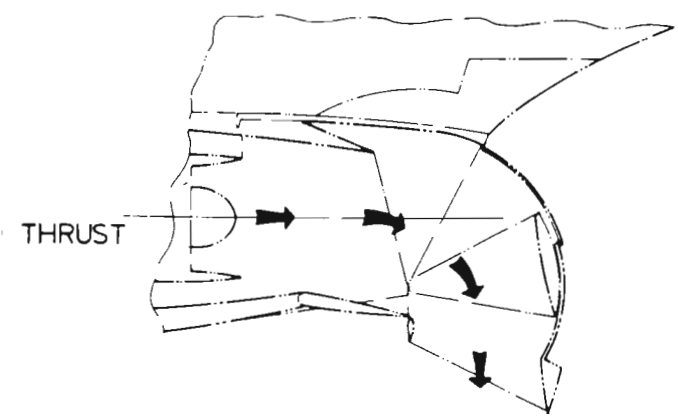

THRUST

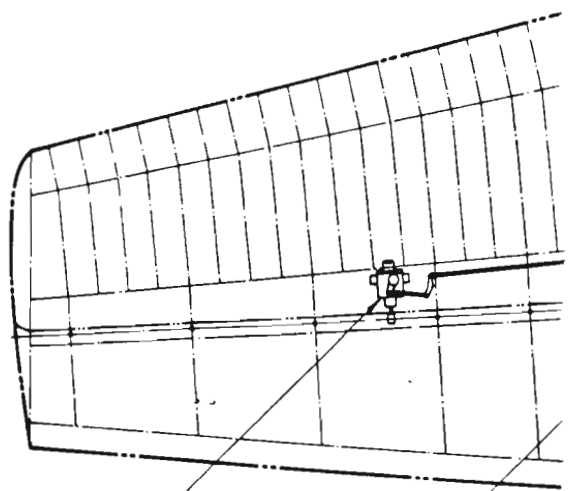

OUTB'D ELEVATOR ACTUATOR

INB'D ELEVATOR ACTUATOR

HORIZONTAL TAIL

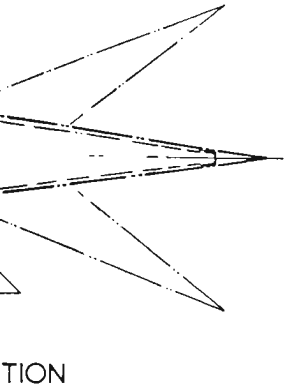

TION

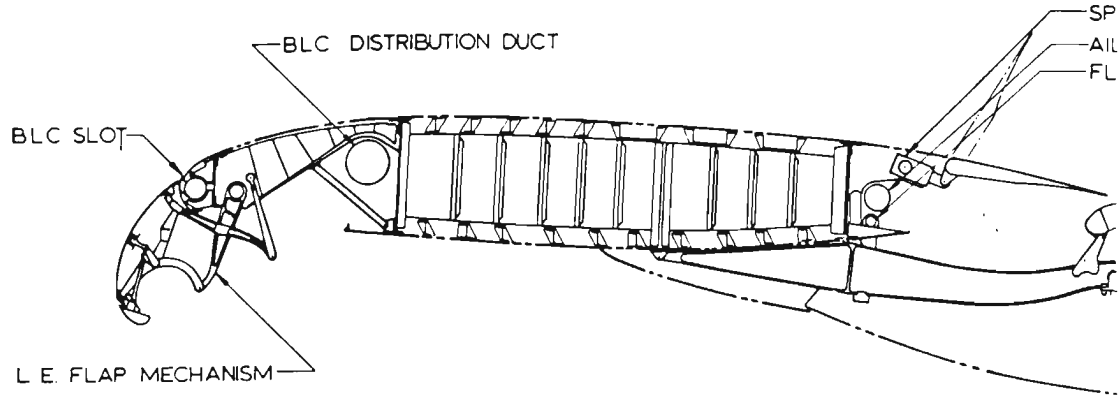

TYPICAL WING SECTION

NO SCALE

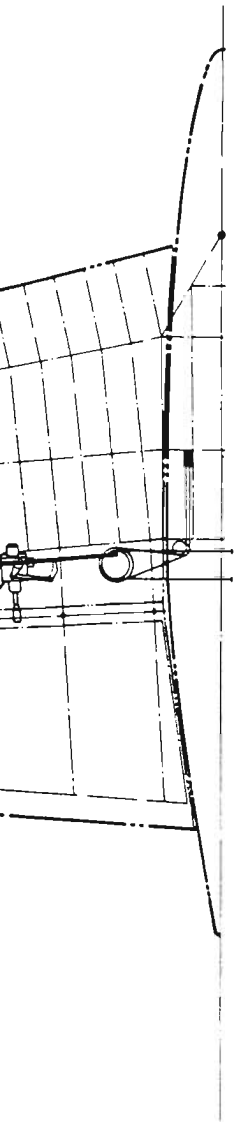

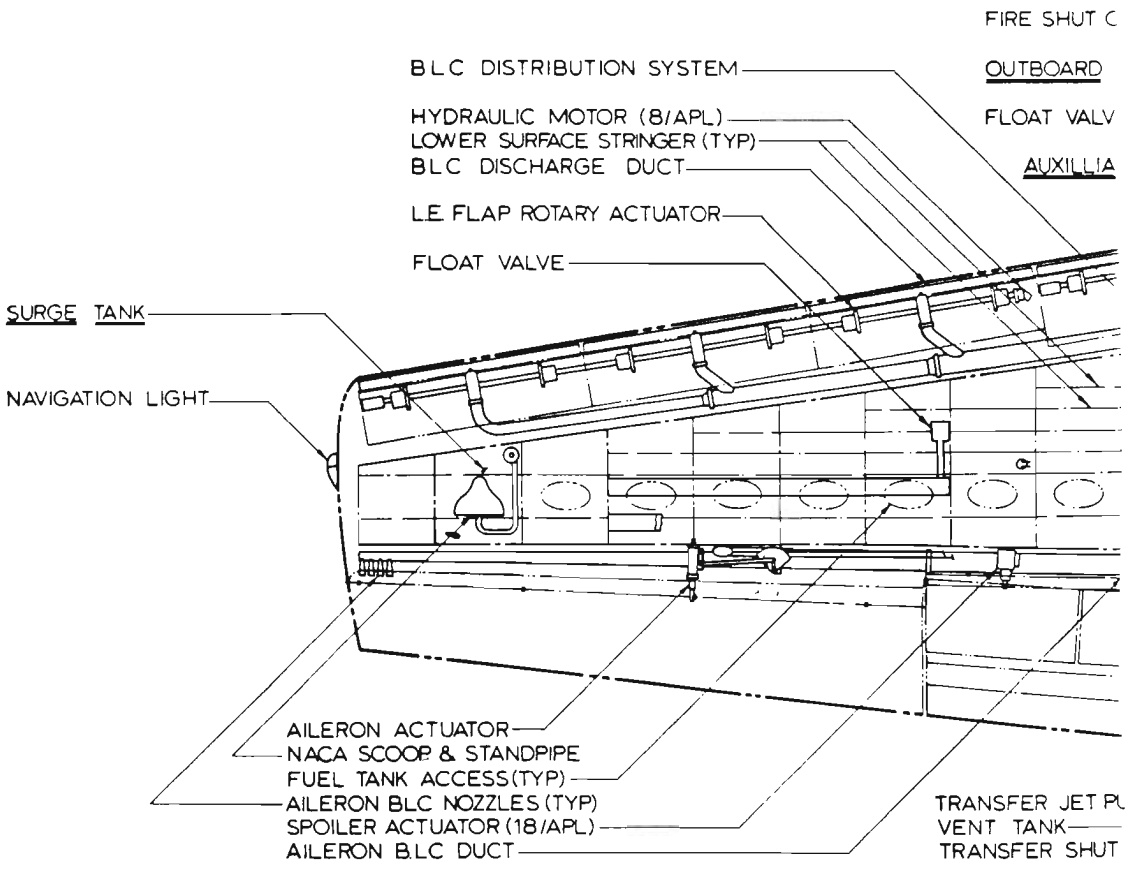

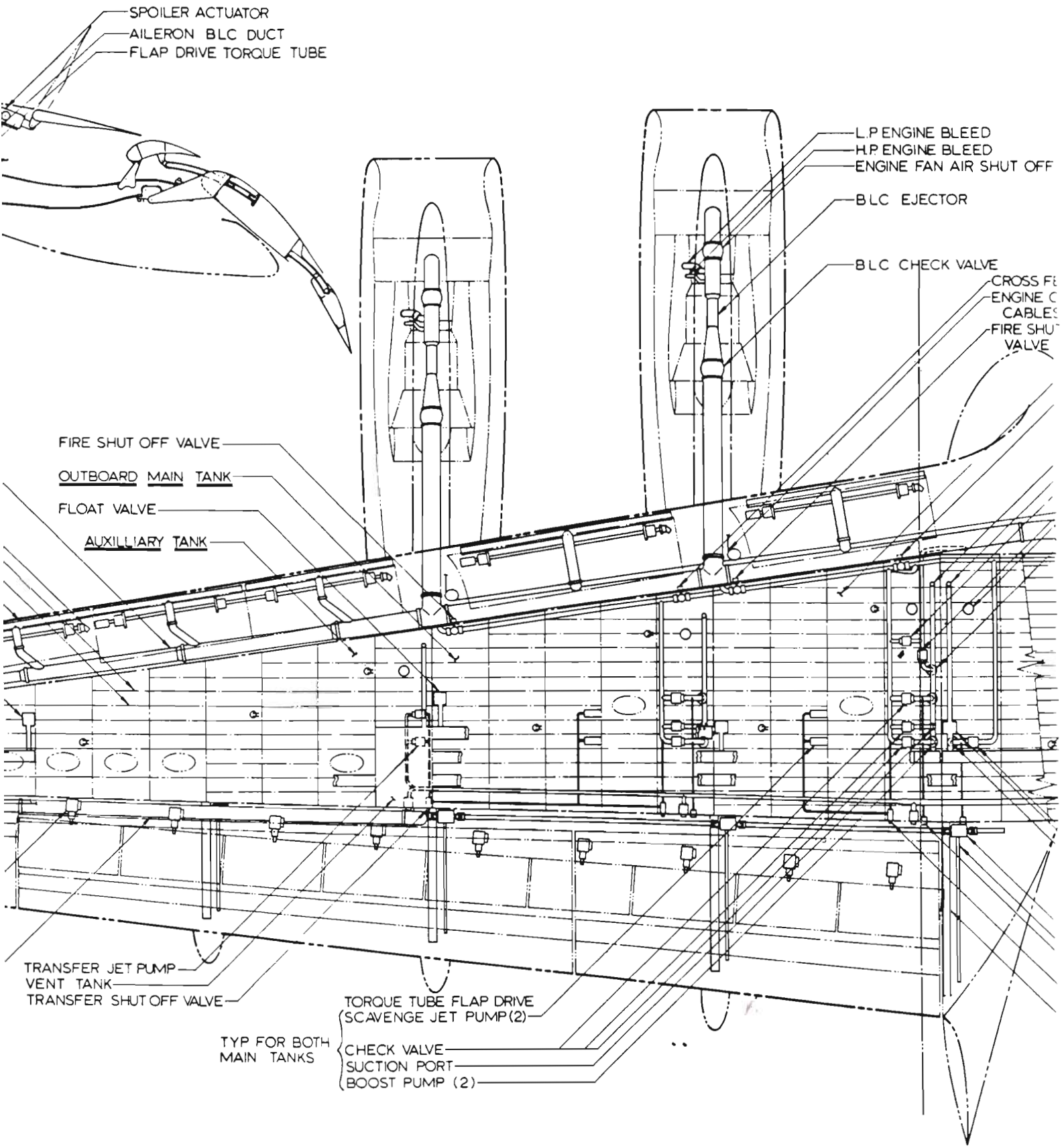
SPOILER ACTUATOR
AILERON BLC DUCT
FLAP DRIVE TORQUE TUBE
L.P ENGINE BLEED
H.P. ENGINE BLEED
ENGINE FAN AIR SHUT OFF
BLC EJECTOR
BLC CHECK VALVE
CROSS FE
ENGINE C
CABLES
FIRE SHUT
VALVE
FIRE SHUT OFF VALVE
OUTBOARD MAIN TANK
FLOAT VALVE
AUXILLIARY TANK
TRANSFER JET PUMP
VENT TANK
TRANSFER SHUT OFF VALVE
TORQUE TUBE FLAP DRIVE
SCAVENGE JET PUMP (2)
TYP FOR BOTH MAIN TANKS
CHECK VALVE
SUCTION PORT
BOOST PUMP (2)

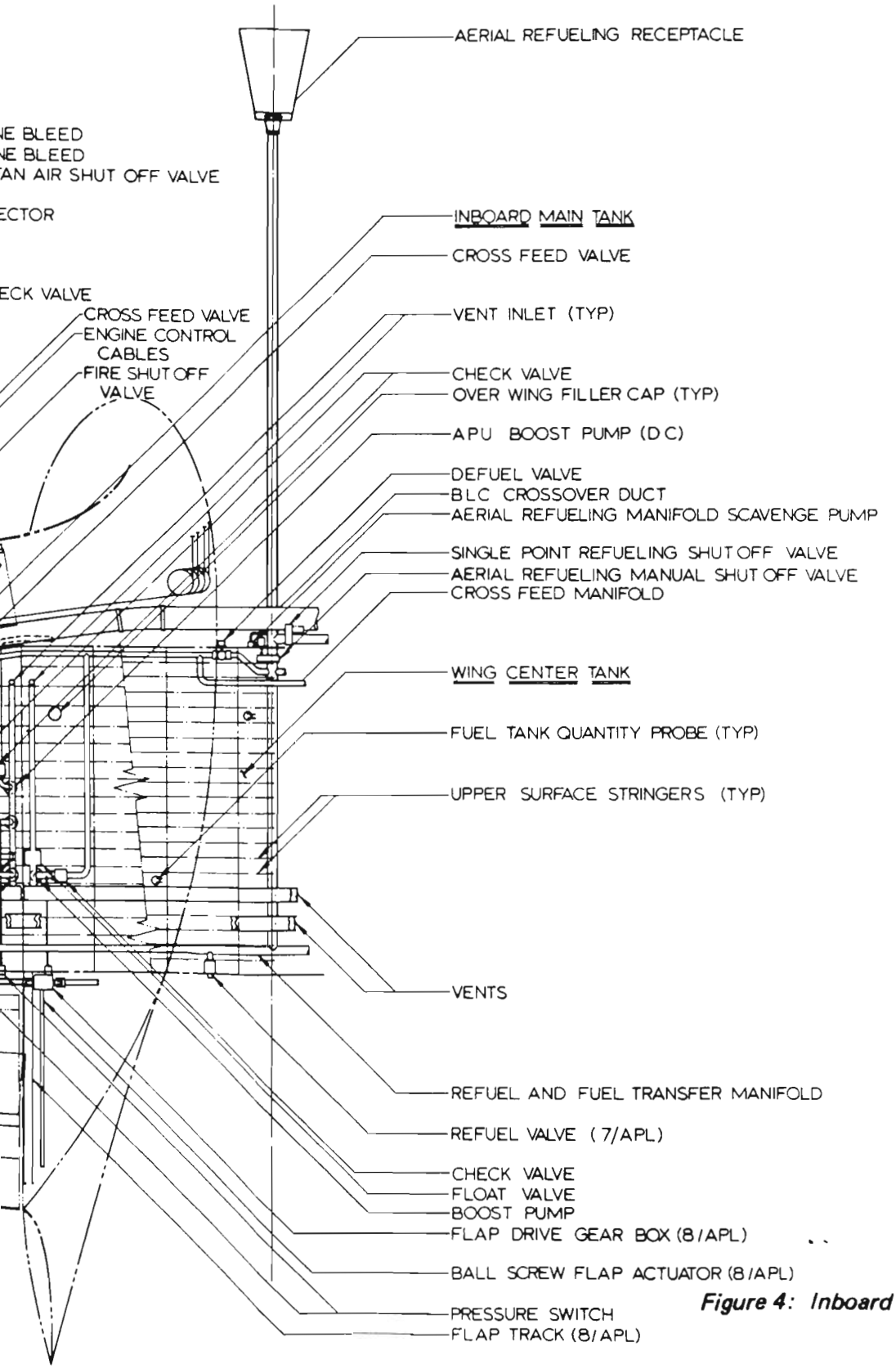

Figure 4: Inboard Profile (Continued)

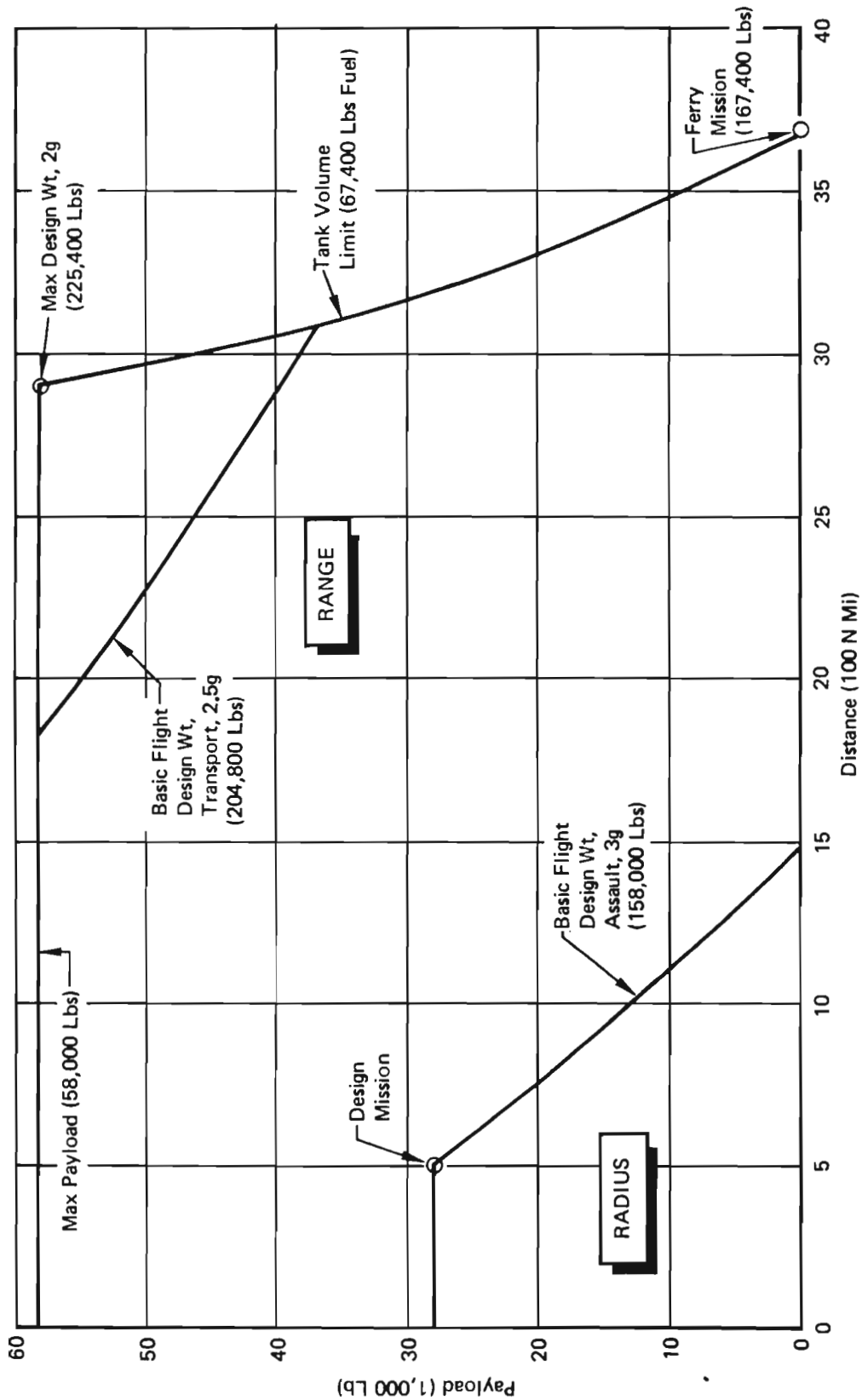

Figure 5: Payload vs Distance

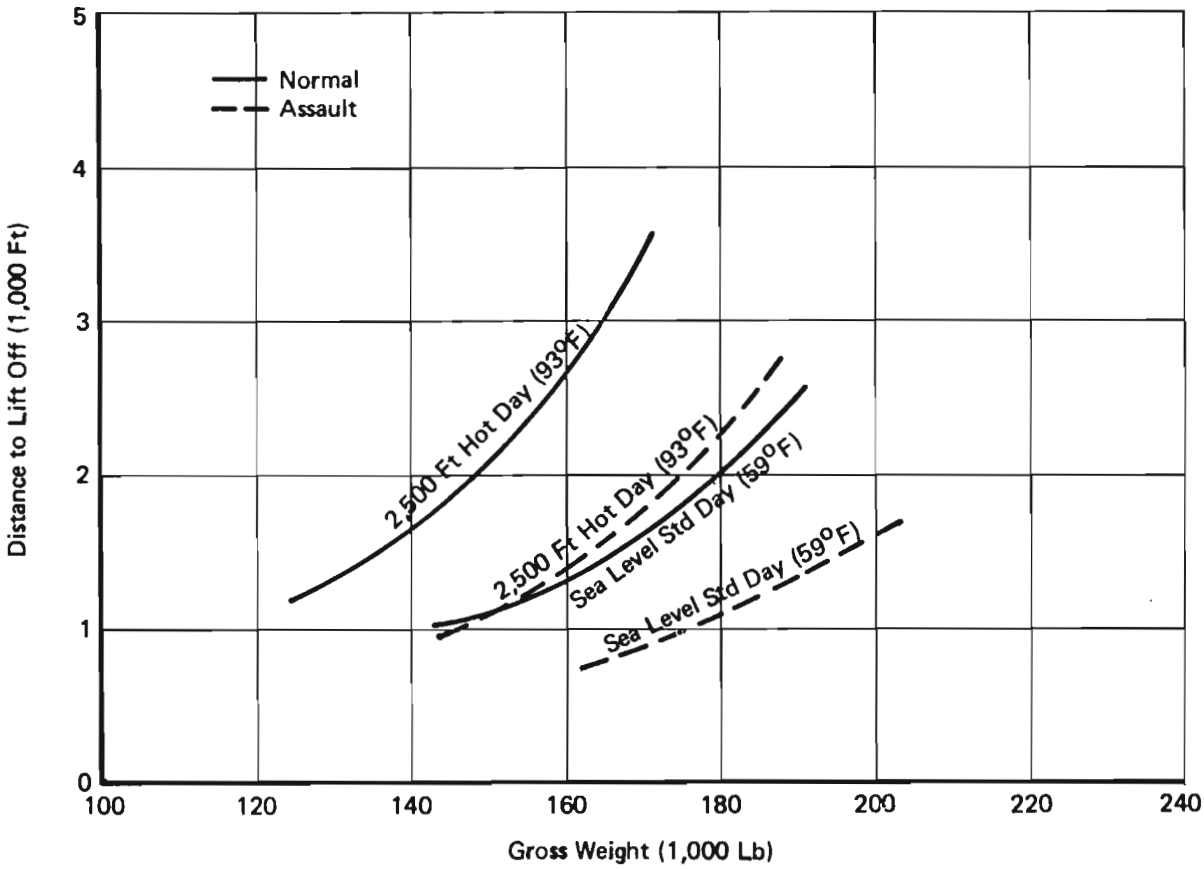

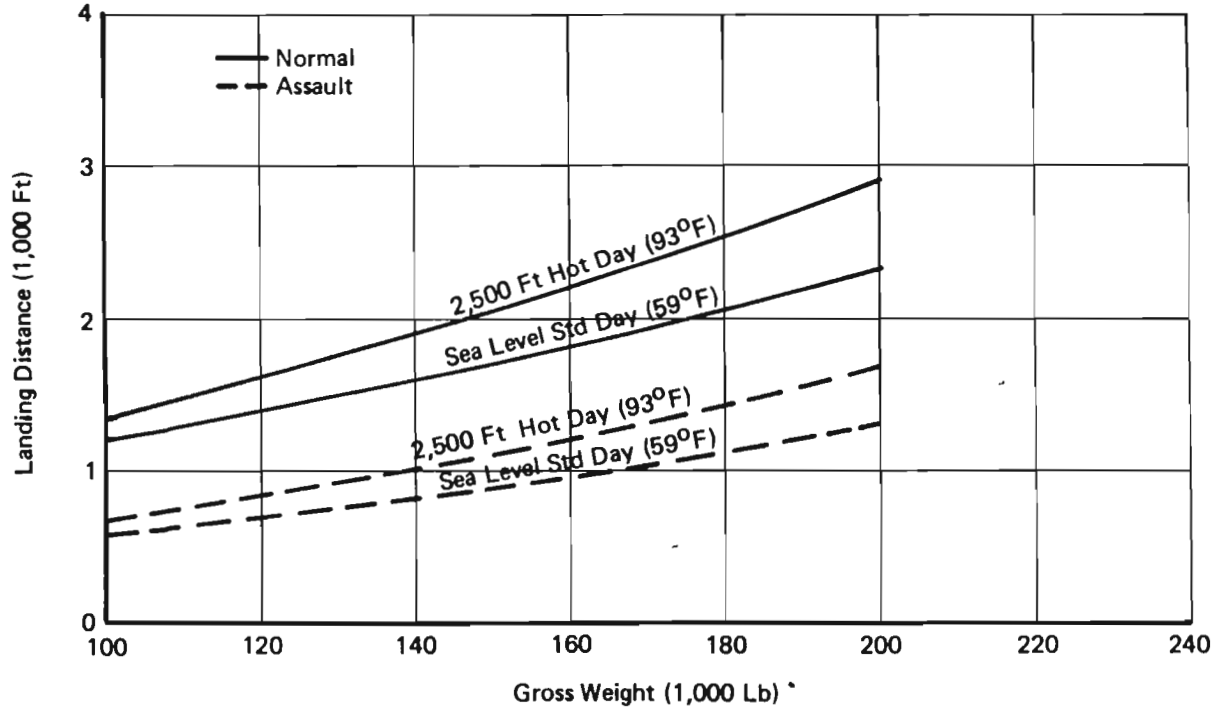

Figure 6 : Takeoff and Landing Distance Summary

2.2.3 Speed Altitude Performance

The speed-altitude capability using maximum cruise thrust at the initial cruise weights for both the outbound and inbound legs of the radius mission are shown in Figure 7. The airplane is capable of flying faster than Mach 0.75 at normal power.

2.3 Weights Summary

Weights of the Model 953-815 are summarized below.

Condition	Weight (Lbs.)
Weight Empty	98,540
Operating Weight	100,000
Basic Flight Design Weight	158,000
STOL Flight Design Weight	145,000
Maximum Design Weight	225,400
STOL Payload	28,000
Maximum Payload	58,000
Full Internal Fuel Weight	67,400

A detailed discussion of the mass properties of the airplane is given in Section VI.

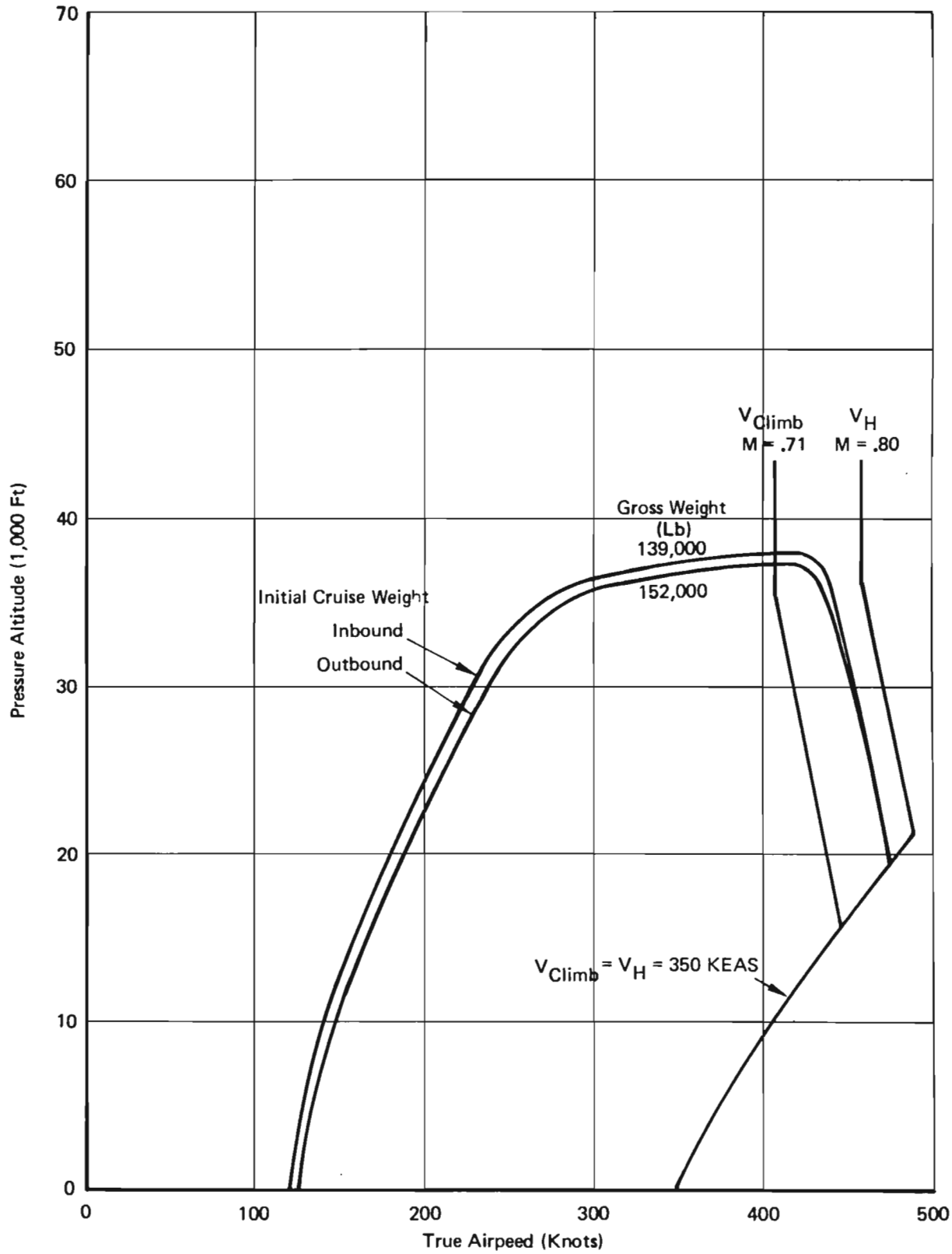

Figure 7: Speed – Altitude Envelope

SECTION III

PARAMETRIC ANALYSIS

3.1 DAMPS

Configuration definition was aided by a parametric analysis computer program. This parametric analysis, called DAMPS (Dynamic Airplane Matching Program System) integrates aerodynamics, parametric weights, and propulsion technology into an iterative solution for a specific STOL payload-mission problem. Data output includes required wing and tail dimensions, weights, and engine size to accomplish the required mission.

3.2 Technology Variables

DAMPS is readily adaptable to change in the technology variables contained in the high speed aerodynamics, weights, and propulsion systems analysis. DAMPS was used in the Baseline Configuration Study (Appendix II) to arrive at the Model 953-801. The vectored thrust wind tunnel test results reported in Volume IV of this series (Reference 6) and embodied in the high lift methodology of Volume II (Reference 7) affect the technology variables. These technology variables were also updated to reflect data generated by the Boeing AMST proposal study. The AMST proposal particularly affected the weights and aerodynamics inputs.

A high speed aerodynamic model of the AMST airplane was tested during the AMST proposal effort and, since no high speed data was generated for the STAI study, the MST data was used to update the high speed aerodynamic characteristics.

3.3 Configuration Selection

Using the updated technology variables, airplanes were sized at a series of thrust to weight ratios and wing loading combinations to meet the STAI mission. (500 nautical mile radius with 28,000 lb. payload) Equal takeoff gross weight contours were then plotted on the T/W versus W/S plane, as shown in Figure 8.

Lines of constant 2,000 ft. landing and takeoff distance, as functions of W/S and T/W, were calculated to comply with the performance rules outlined in Appendix B. In addition, the maximum W/S was determining which provided enough internal fuel tank volume to fly 3,600 nautical miles at zero payload. This led to determination of the design point: a 158,000 lb. airplane with a wing loading of 93 pounds per square foot and a thrust-to-weight ratio of .470 which meets all the requirements of the STAI mission.

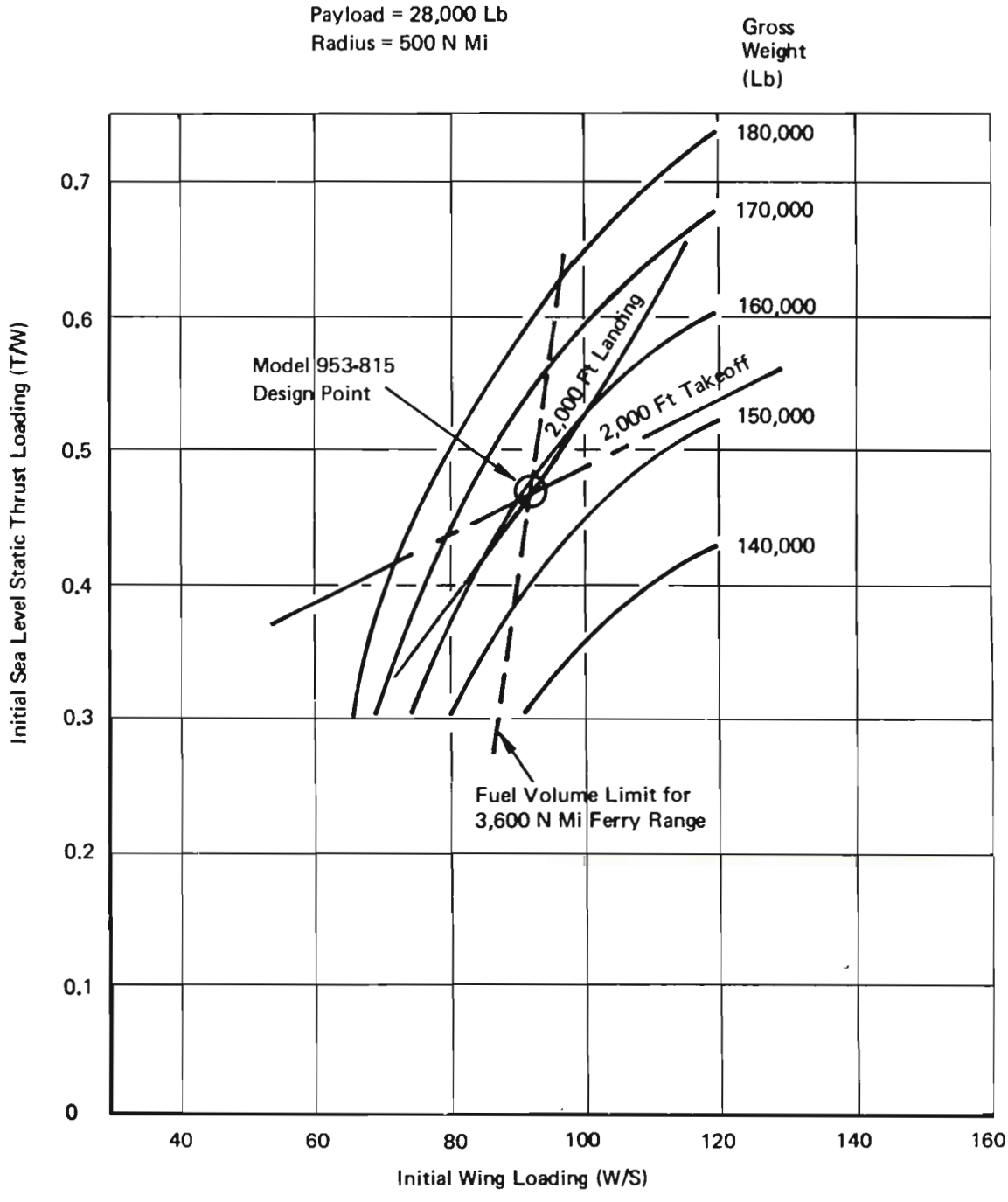

Figure 8: Parametric Design -- Model 953-815

SECTION IV

AERODYNAMIC AND PROPULSION SYSTEM CHARACTERISTICS

4.1 Aerodynamic Characteristics

4.1.1 High Speed Drag

Total airplane drag is defined by the following equation:

$$C_D = C_{D_{Profile}} + \Delta C_{D_{Lift}} + \Delta C_{D_{Compressibility}}$$

The sketch in Figure 9 depicts the elements that build up the drag polar. These are:

Profile Drag - $C_{D_{Profile}}$

Profile drag as defined here includes skin friction drag (including corrections for airfoil thickness) pressure drag (including effects of angle of attack) interference drag, excrescence and roughness drag. Separation effects are included in the pressure and interference drag. Profile drag calculations were made at M = .6 and an altitude of 38,000 ft.

Drag Due to Lift - $\Delta C_{D_{Lift}}$

The elements that comprise drag due to lift are vortex drag and trim drag. The vortex drag calculations include the effects of the body and non-ellipticity of the spanwise load distribution. The trim drag estimates account for changes in wing induced drag (caused by the tail load), tail induced drag and the tail drag increment caused by the induced wing downwash.

Compressibility Drag - $\Delta C_{D_{Compressibility}}$

Compressibility drag is defined as the increase in drag above its level at M = .60. Most of the compressibility drag arises from energy losses in shock waves. Variations in induced drag, interference drag, and trim drag with Mach number are included in the calculation of compressibility drag.

The estimated profile drag values for the various components of the airplane are presented in Table I. The drag polars for M = .60, .71, .73, .75, and .77 are shown in Figure 10.

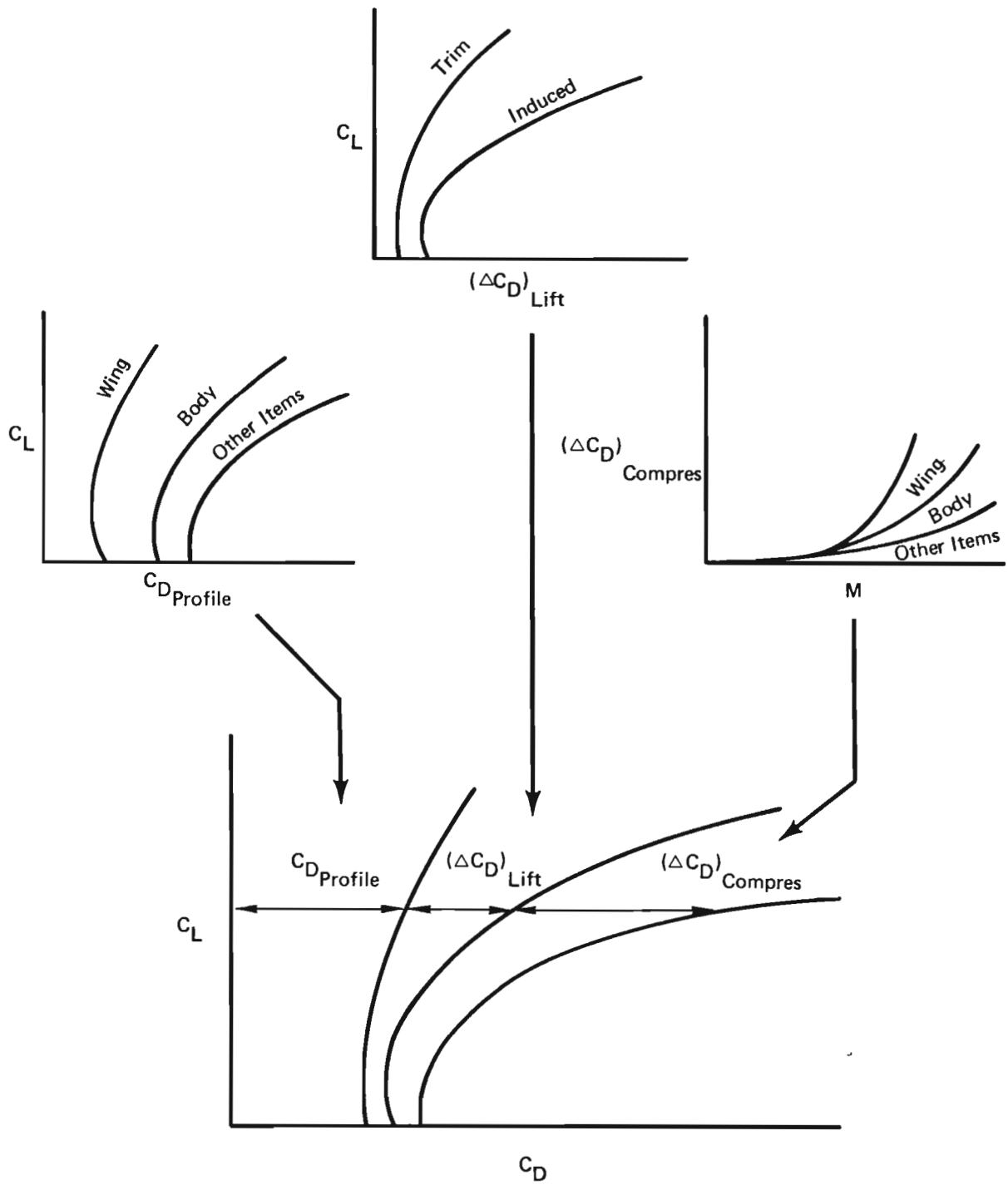

Figure 9: Drag Polar Buildup

TABLE I

PROFILE DRAG BUILDUP

Component	Wetted Area (Sq. Ft.)	C_{D_P}	f (Sq. Ft.)	$C_{f_{eff.}}$
Wing	2735	.00641	10.90	.00398
Body	4307	.00552	9.38	.00218
Empennage	1881	.00386	6.56	.00349
Nacelles and Struts	1828	.00384	6.53	.00357
Landing Gear Pods	720	.00127	2.16	.00300
Flap Tracks	28	.00020	.34	.01210
Roughness and Excrescences		.00158	2.68	
TOTAL AIRPLANE	11499	.02268	38.55	.00335

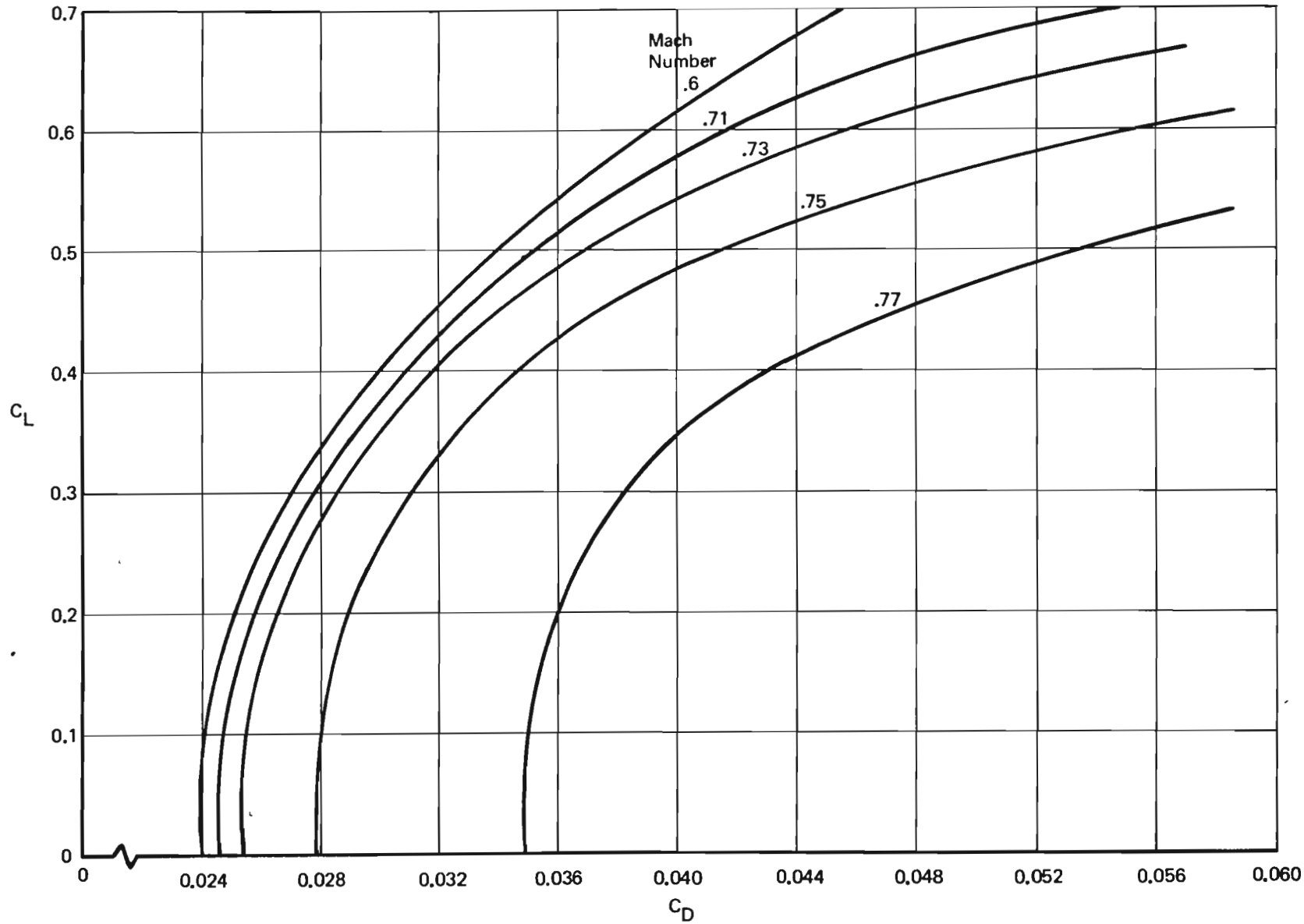

Figure 10: High-Speed Drag Polar

4.1.2 High Lift Characteristics

The high lift system consists of triple-slotted trailing edge flaps and aerodynamically shaped leading edge flaps.

Twenty-five percent chord triple-slotted trailing edge flaps extend from the side of the body to 75 percent span. They are a development of similar highly successful systems used on existing Boeing commercial aircraft.

The aerodynamically shaped Krueger leading edge flap is designed to be used with leading edge blowing. Aerodynamic data are presented in this section for a leading edge blowing momentum coefficient of 0.04.

Lift, drag and moment data were estimated using the methods given in the design compendium (Reference 7). The airplane was trimmed for the forward c.g. location, and for an outboard engine inoperative, where applicable.

The trimmed high lift characteristics of the airplane are shown in Figures 11 through 19 for a range of thrust vector angles (σ) which covers typical settings encountered during takeoff and landing. These data are in free air and in ground effect and include effects of one engine inoperative as well as all engines operating. Data at a thrust vector angle of 0° is shown in Figures 11-13, at $\sigma = 30°$ in Figures 14-17 and at $\sigma = 60°$ in Figures 18 and 19.

4.1.3 Engine Placement Influence on Aerodynamic Interference Effects

At large thrust vector angles and low angle of attack, substantial negative lift interference is present on this configuration. Selection of a more rearward nacelle location would have reduced this effect substantially. In fact, the wind tunnel test results indicated that locating the nozzles close to the trailing edge would have led to favorable interference at all angles of attack. The selection of a forward engine location therefore demands explanation.

To meet the requirement for effective thrust reversal down to very low forward speed, it was necessary to prevent re-ingestion of the exhaust plumes by the engines. With four engines on the wing, this can only be done if the exhaust is not contained under the wing. The engine must therefore either be far enough aft for the reverser plume to clear the trailing edge, or far enough forward for it to clear the leading edge.

The aft location is beyond the region where favorable interference would be expected, and is unfavorable because of mass-balance effects on flutter characteristics. Furthermore, large nose-down pitching moments would be generated in the vectored thrust mode, tending to nullify possible lift gains by adverse trim effects.

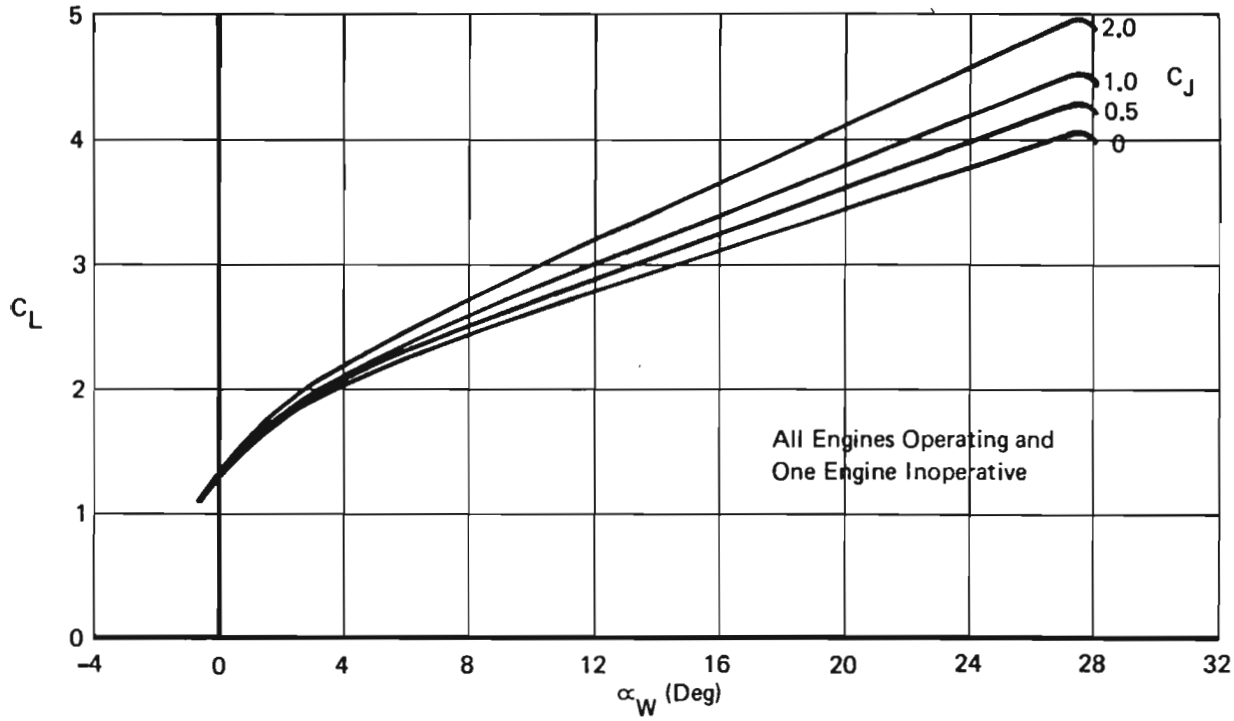

Figure 11: Trimmed Lift — Free Air, Thrust Vector = 0°

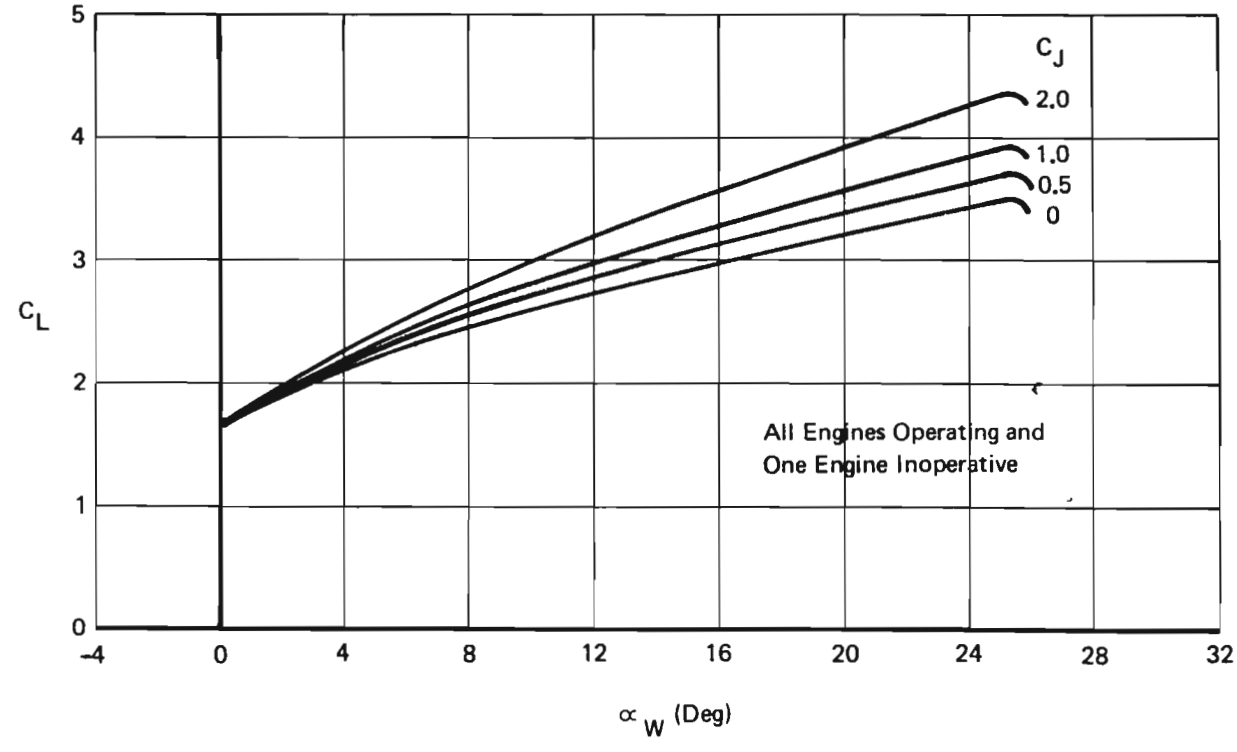

Figure 12: Trimmed Lift — Ground Effect, Thrust Vector = 0°

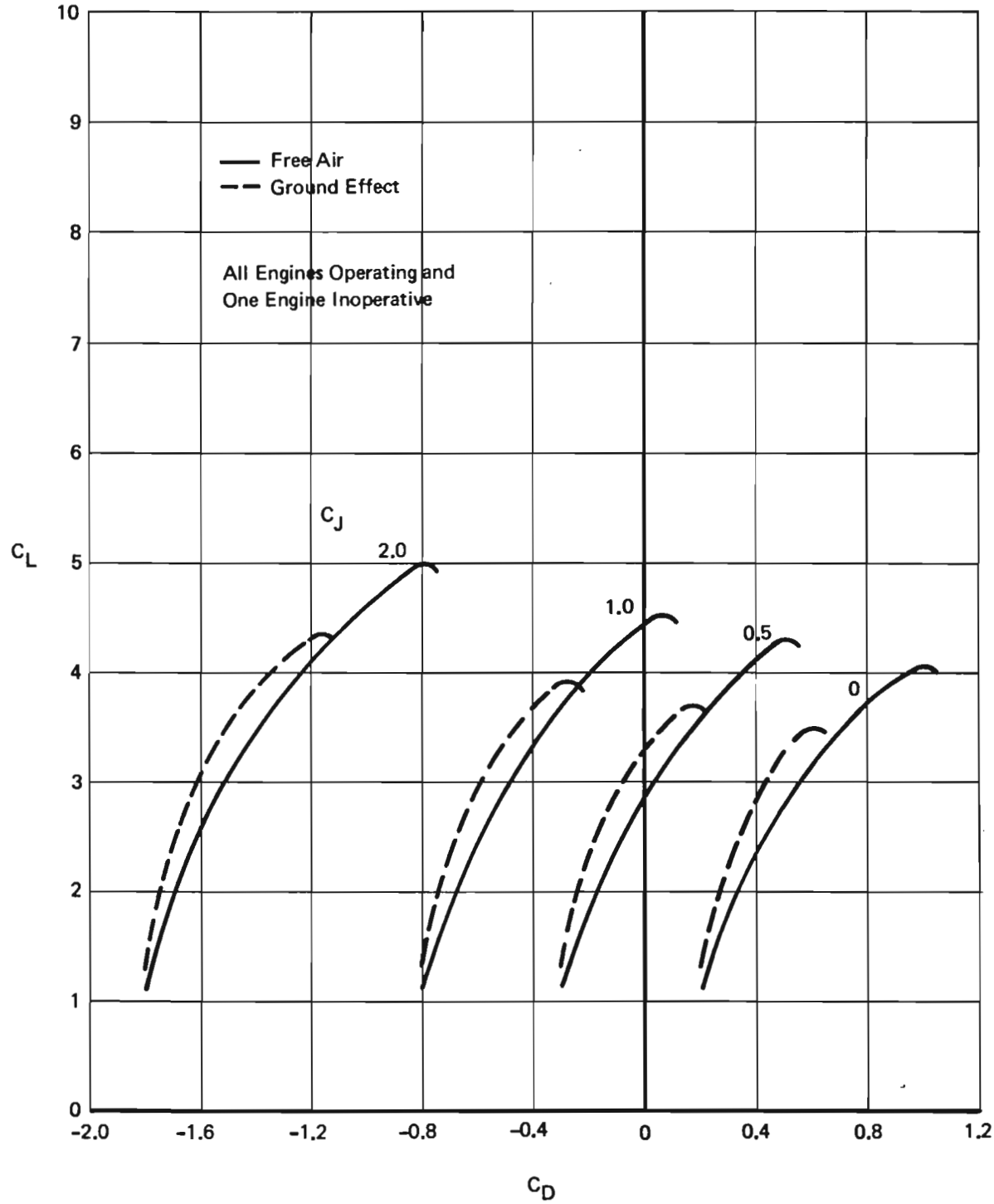

Figure 13: Trimmed Drag Polar — Thrust Vector = 0^o

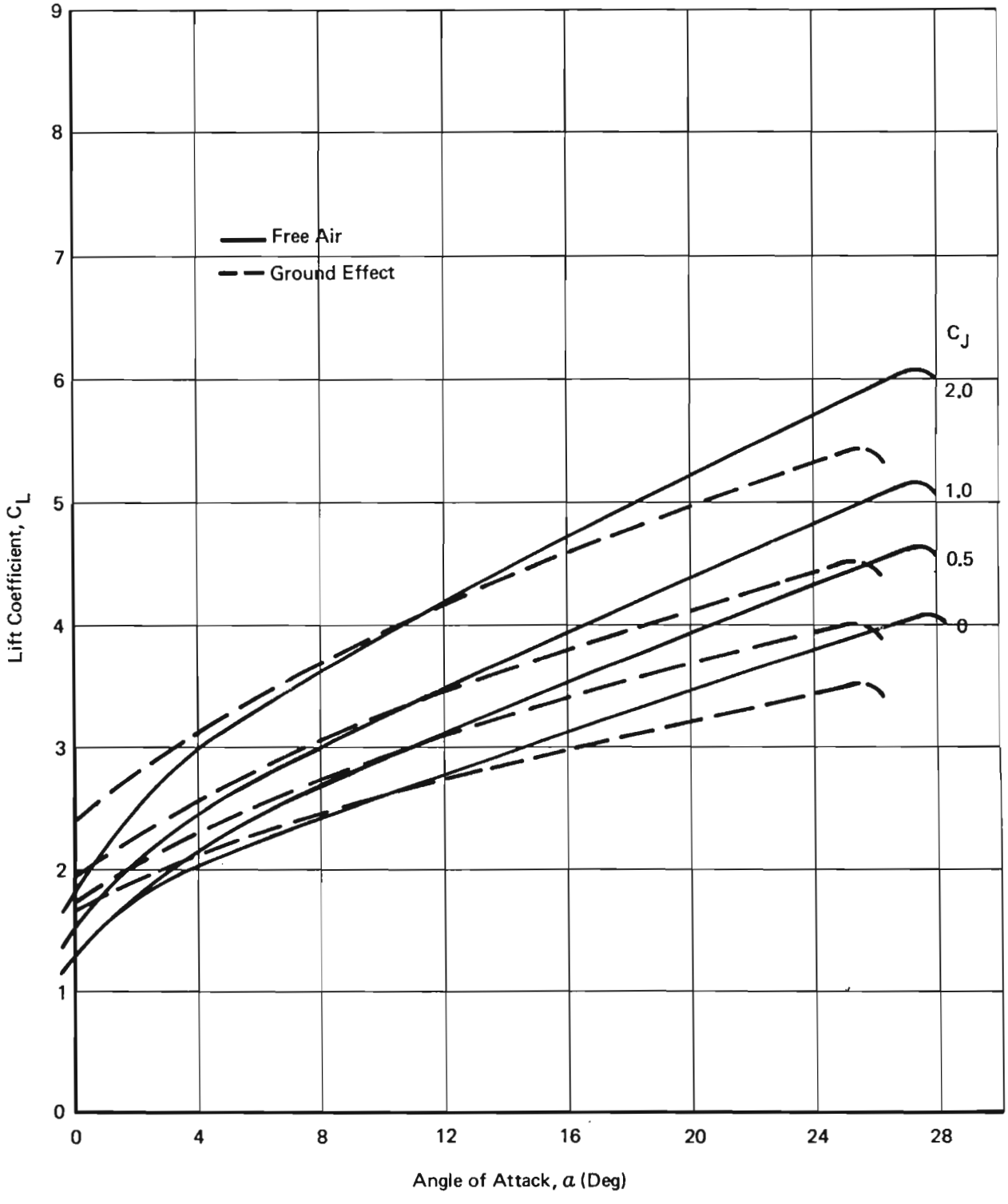

Figure 14: Trimmed Lift – All Engines Operating, Thrust Vector = 30°

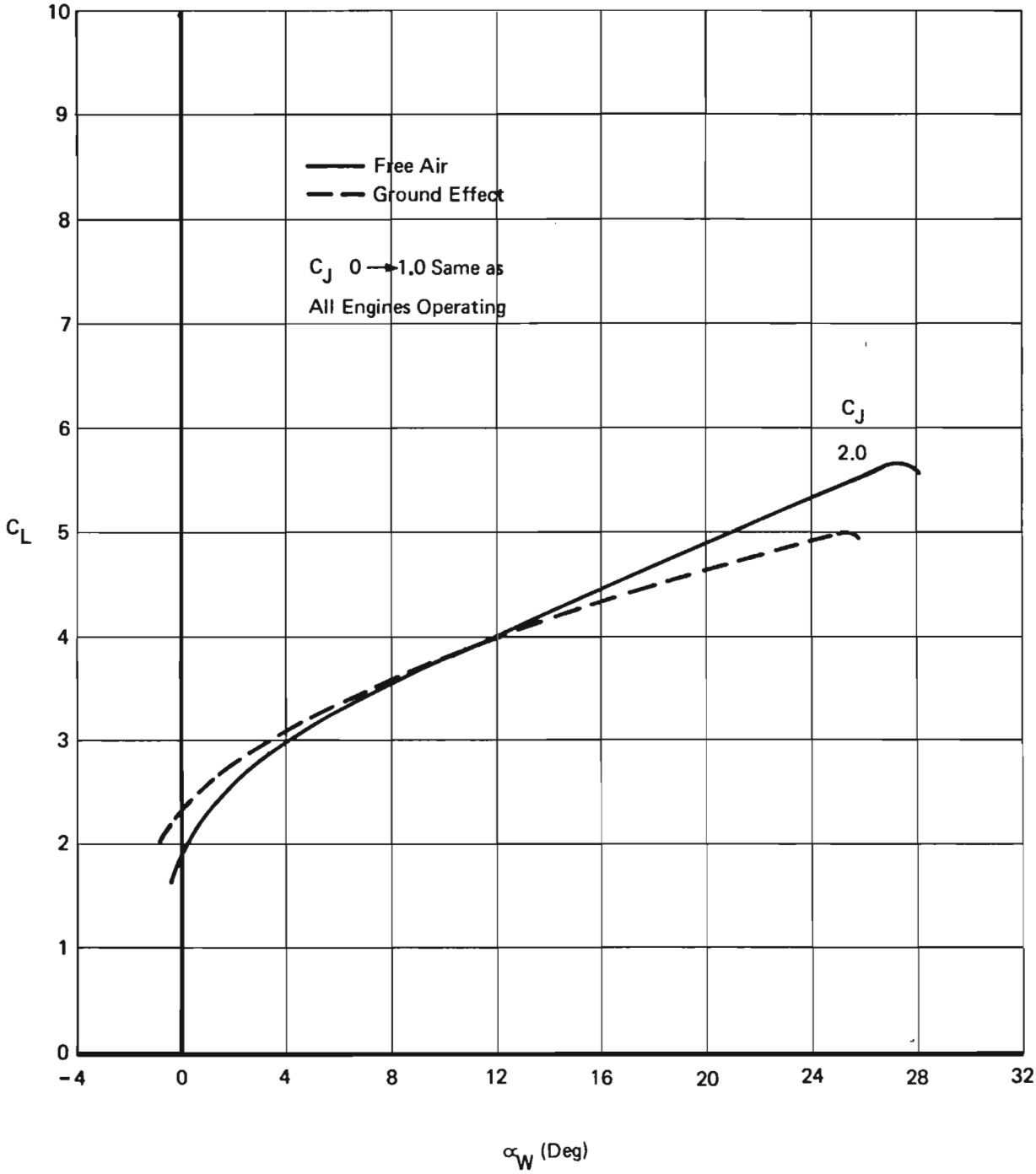

Figure 15: Trimmed Lift — One Engine Inoperative, Thrust Vector = 30°

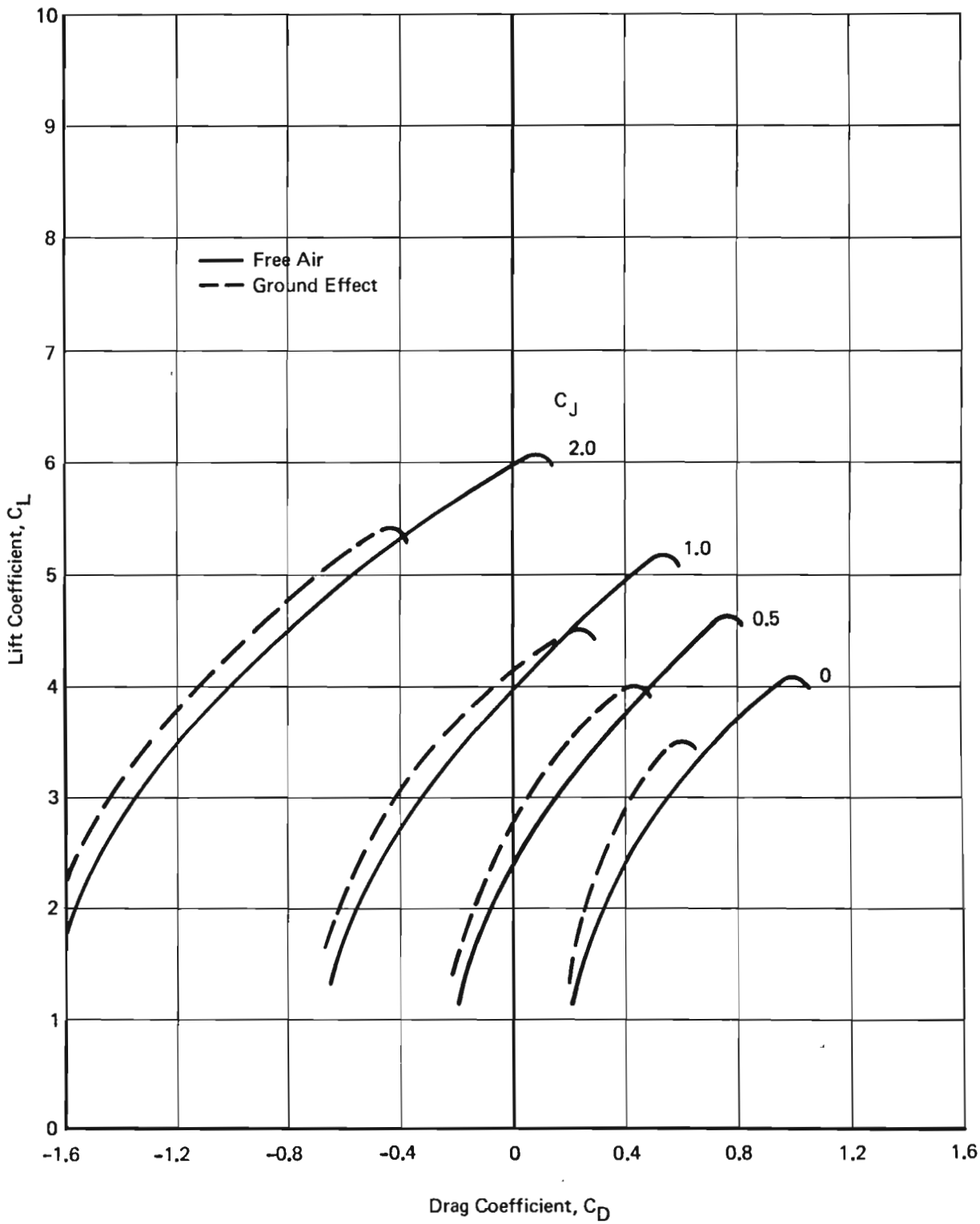

Figure 16: Trimmed Drag Polars — All Engines Operating, Thrust Vector = 30°

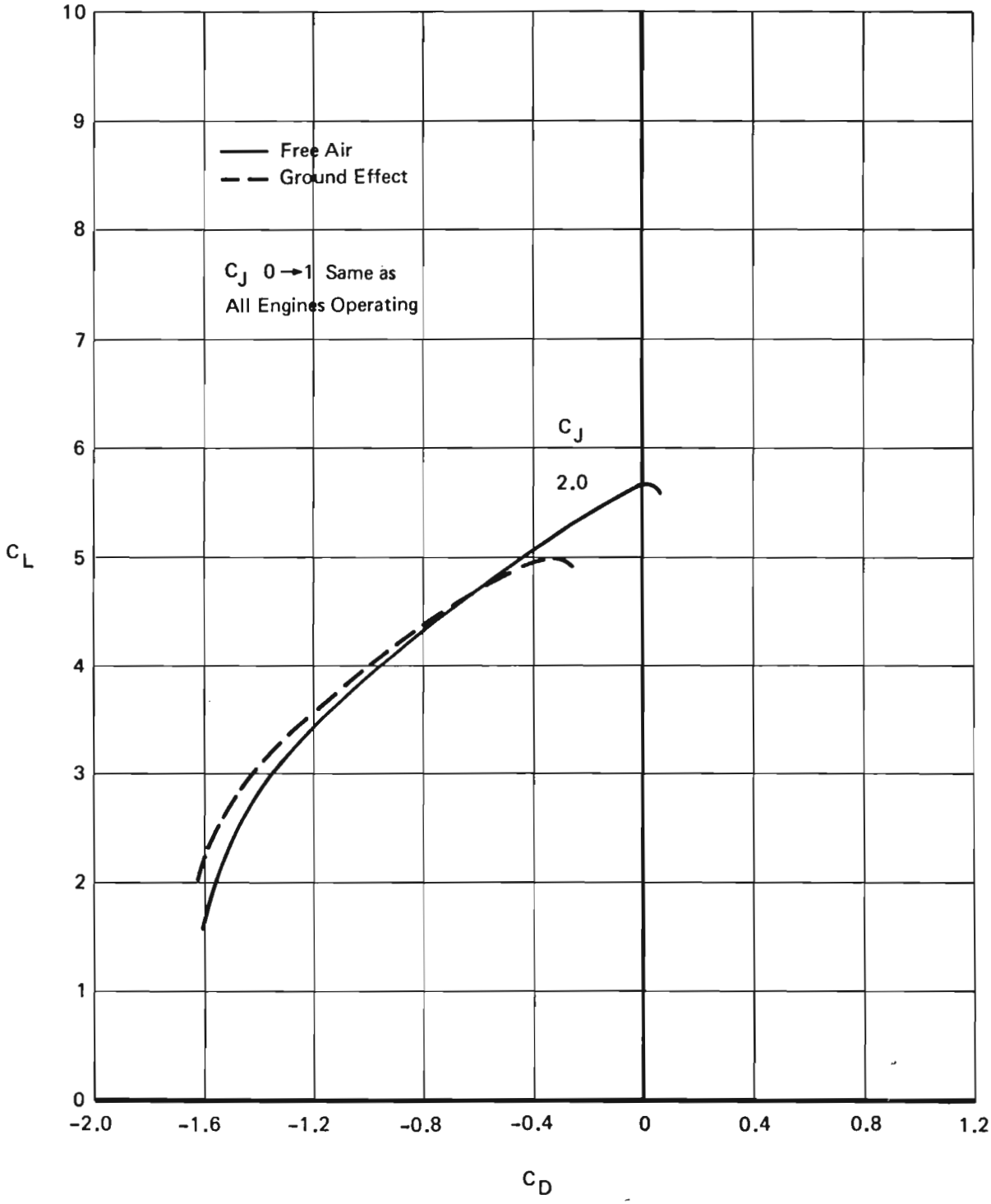

Figure 17: Trimmed Drag Polar – One Engine Inoperative, Thrust Vector = 30°

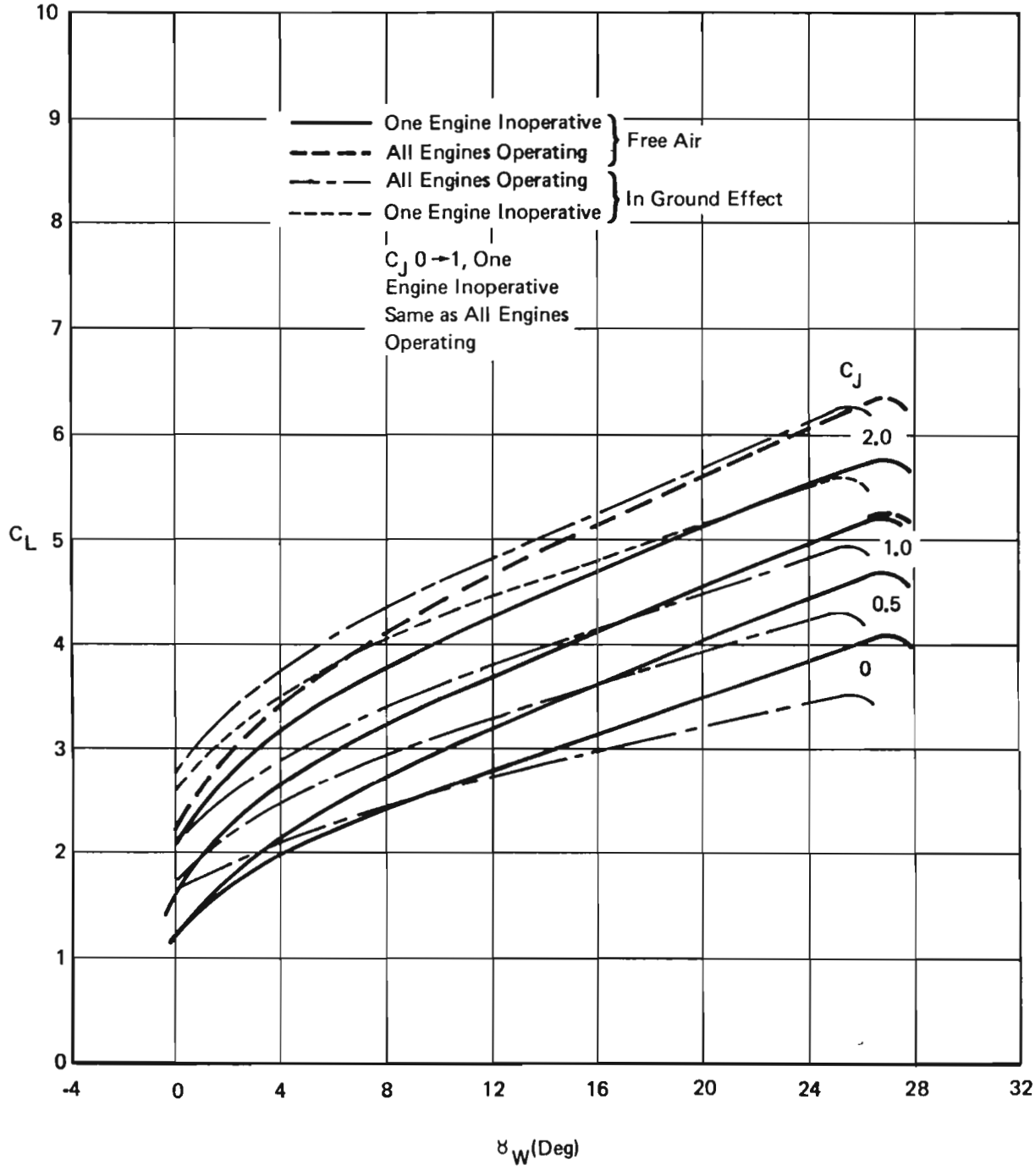

Figure 18: Trimmed Lift — Free Air and in Ground Effect, Thrust Vector = 60°

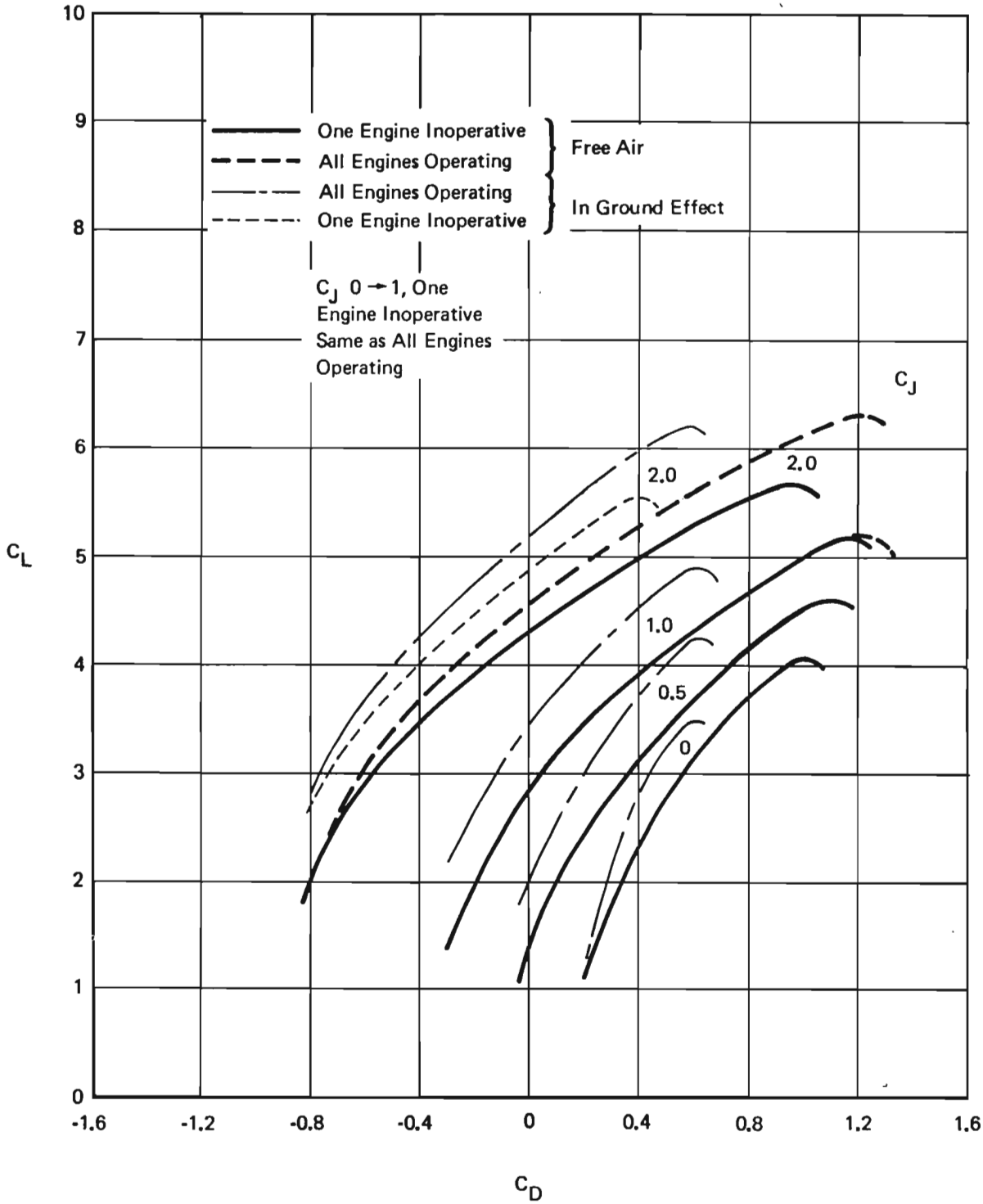

Figure 19: Trimmed Drag Polar — Free Air and in Ground Effect, Thrust Vector = 60°

It was noted in the analysis of wind tunnel results that the adverse interference effects disappeared at high angle of attack, with a net favorable effect at stall, for all fore-and-aft nacelle locations. Since the stall condition determined the minimum speed, the adverse effects at low α did not affect takeoff and landing performance. The forward nacelle location was therefore selected, though a small $C_{L_{max}}$ penalty was paid because of a smaller favorable interference at stall.

It was recognized that this choice involved the risk that the unfavorable low - α lift interference was associated with buffet-producing flow separation. This problem would have to be resolved by properly instrumented wind tunnel tests before further configuration development could proceed.

4.2 Propulsion

4.2.1 Engine Selection

The propulsion system selected for this study required a high bypass ratio engine which would be available in the 1975 to 1980 time period.

The engine selected was the Allison Model PD351-73. Engine characteristics are listed below:

Thrust, SLS	18,600 lb
Total Airflow	590 lb/sec
Bypass ratio	5.25
Compressor Pressure Ratio (P3/P2)	24.5
Turbine Inlet Temperature	2465°F
Engine Weight	2,280 lb

Figure 20 shows the engine outline and basic dimensions, and the scaling rules. For study purposes, it was assumed that the thrust-to-weight ratio was a constant over a thrust range of 15,000 to 25,000 pounds.

The engine performance data was calculated with a digital computer program described in an Allison EDR 7141 dated 22 October 1971. Performance was calculated with 100% inlet recovery, .42 lb/sec high pressure bleed, and 25 horsepower per engine extracted for all attitudes and flight speeds. Takeoff net thrust and gross thrust are shown in Figures 21, 22 and 23 for standard day and hot day at sea level, 2500, and 5000 feet. Sufficient bleed air is required to provide a momentum

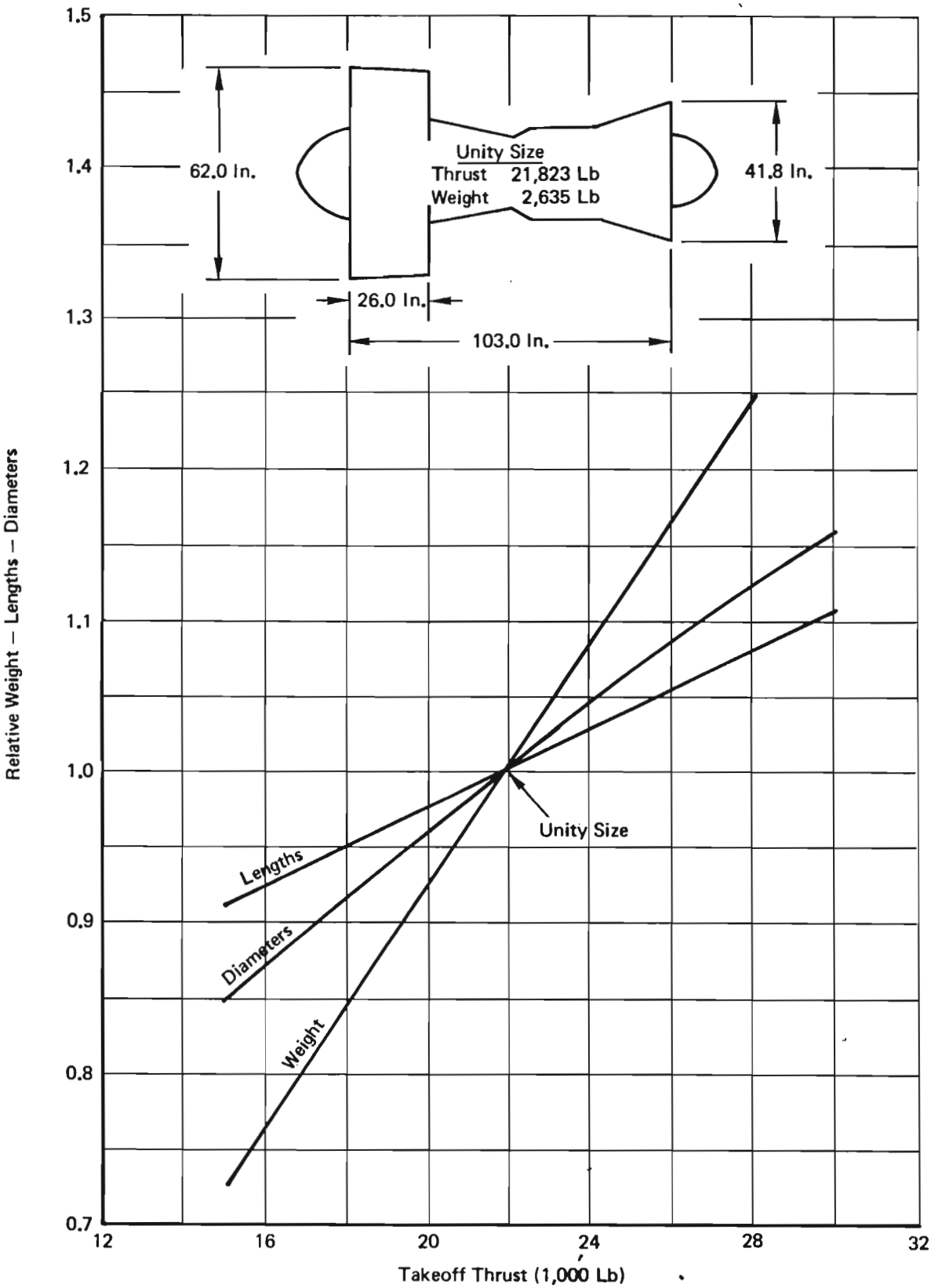

Figure 20: Engine Sizing Chart

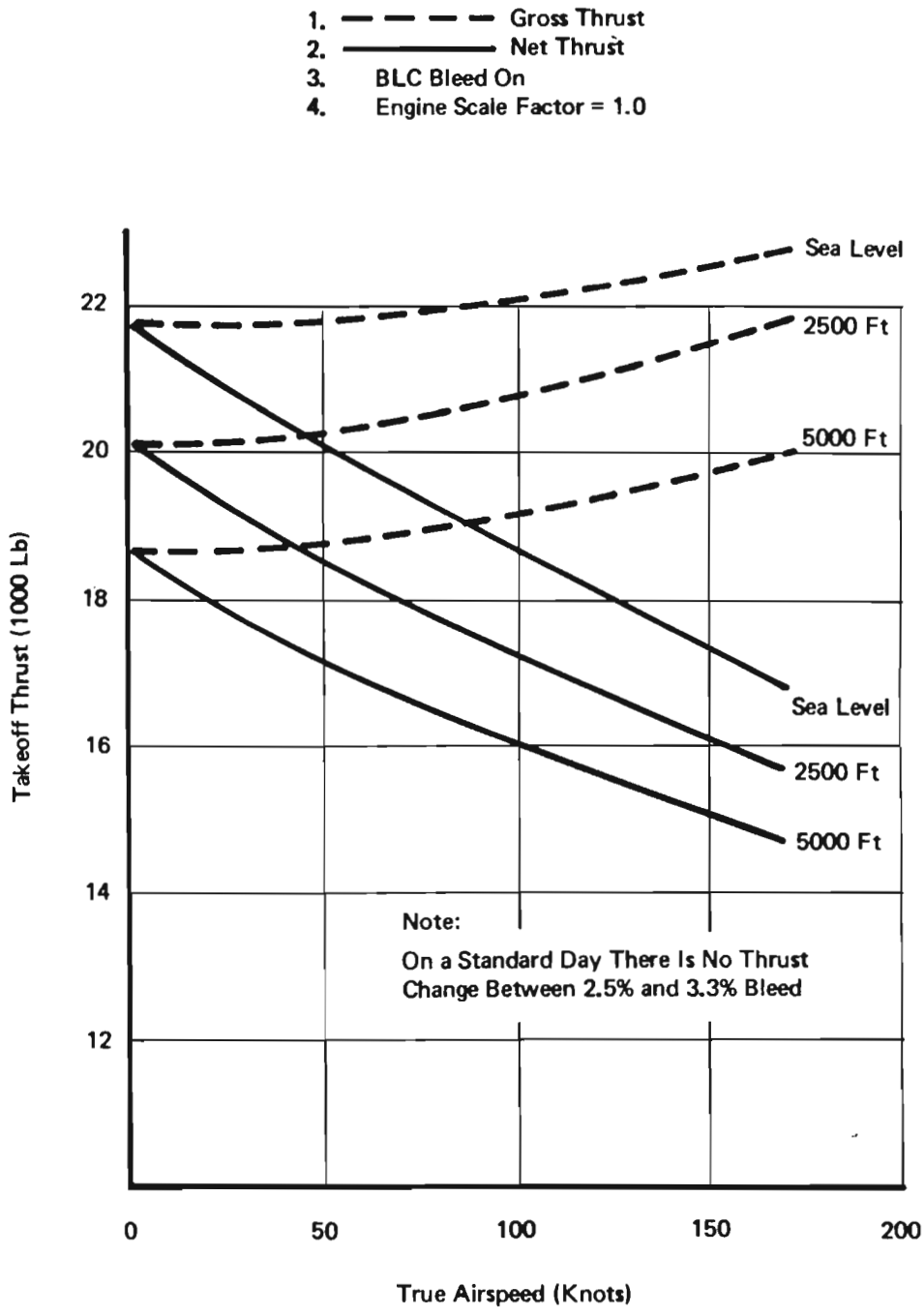

Figure 21: PD351-73 Takeoff Thrust – Standard Day

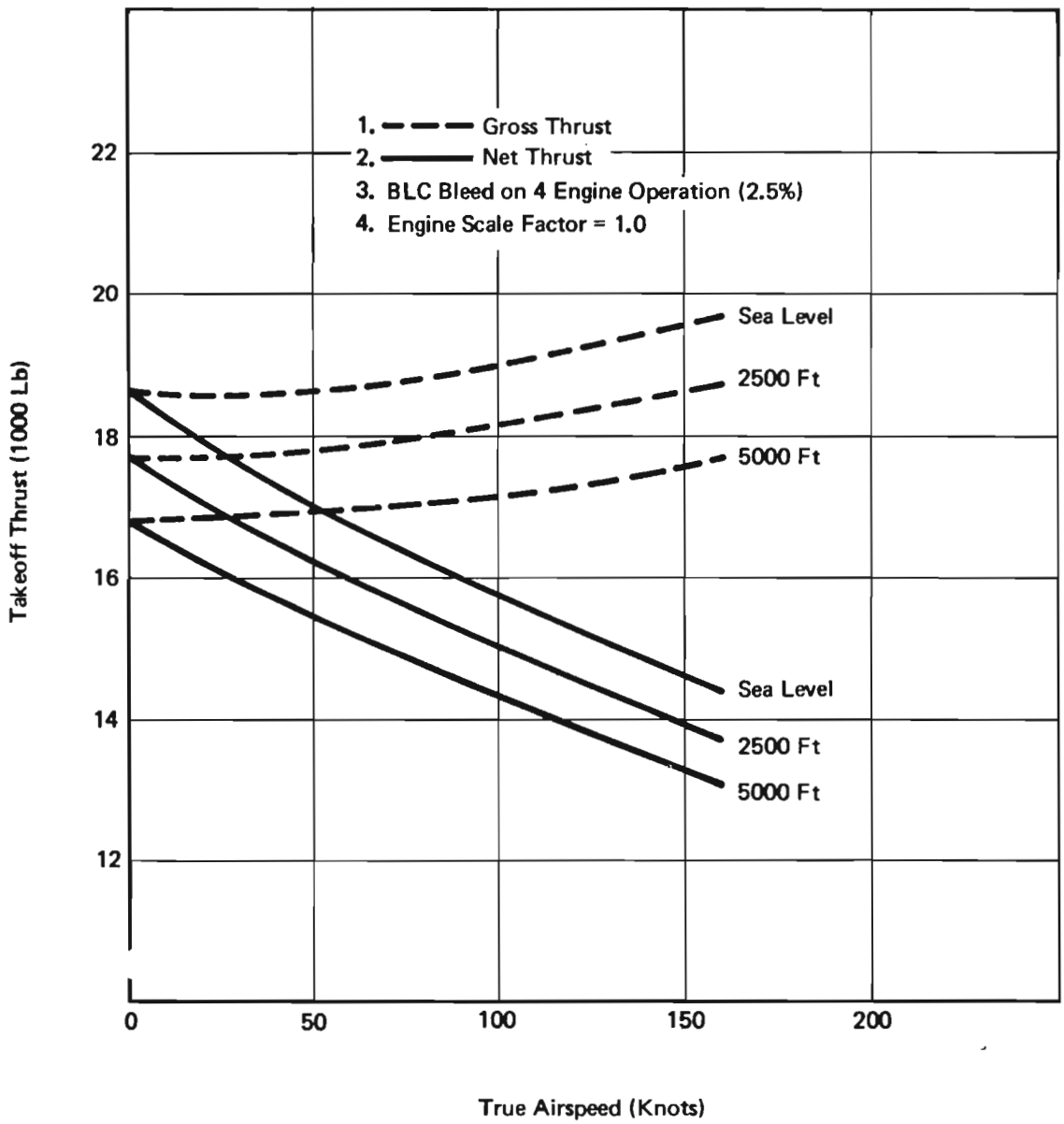

Figure 22: PD 351-73 Takeoff Thrust – Hot Day

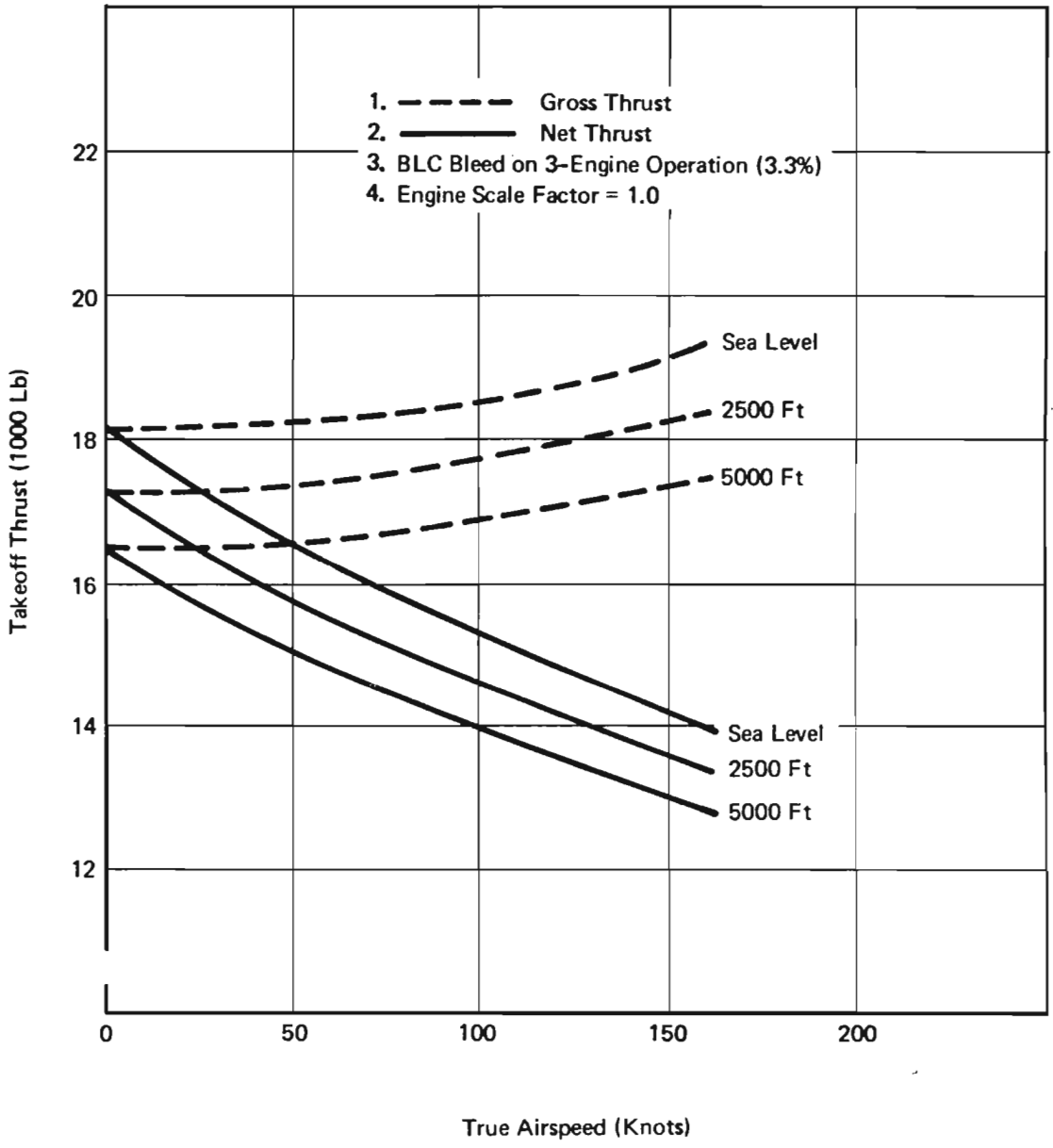

Figure 23 : PD 351-73 Takeoff Thrust — Hot Day, 3-Engine Bleed

flux of 1500 pounds at the BLC nozzles, under sea level static conditions, for either three-engine operation (3.3% compressor discharge bleed) or four-engine operation (2.5% compressor discharge bleed).

Intermediate thrust as a function of altitude and Mach number is shown in Figure 24. Corrected net thrust and corrected specific fuel consumption are also shown in Figure 24.

The vector efficiency for a "hood-type" nozzle is given in Figure 25. This data was obtained from tests performed in the STOL Transport Thrust Reverser Vectoring Program (Reference 1).

4.2.2 Engine Installation

The engines are arranged in single pods mounted on struts below and forward of the wing, shown in Figure 26. The struts are cantilevered off the wing. The engine mounting points on top of the engine at the engine core are attached to the strut with tension bolts for easy engine removal. Controls and services are routed through the structural strut from the front spar to the engine fire wall. Inspection, maintenance, and engine change are facilitated by opening the cowl panels that are hinged to the engine support strut. A four-foot high maintenance stand gives access to engine and airplane accessories, engine core exterior, and boroscope ports. The engine can be removed by lowering vertically on hoists attached to the engine support strut.

Fire safety is provided by the fire detection and extinguishing systems, and by firewalls that are used to compartment the engine accessory areas. Jet airplane experience has shown that the most effective means to control engine fires is with a positive fuel shutoff. Fuel shutoff is at the front spar near the engine centerline.

Each engine is equipped with a pneumatic starter, powered by the Auxiliary Power Unit (APU) installed in the main landing gear fairing (Figure 3). Each engine can also be started from existing Air Force ground carts. Standard day start times will be less than 45 seconds per engine.

Each engine has a full-length fan duct in conjunction with a single exhaust nozzle. This allows for a single device to be used for thrust reversing and thrust vectoring (Figure 26).

4.2.3 Fuel System

Fuel is carried in integral tanks between spars of the wing. (Figure 4). A separate tank is provided for each engine, with additional fuel carried in two outboard tanks and a center wing tank. Usable fuel capacity is approximately 67,400 pounds.

Two AC-powered boost pumps supply fuel from each main tank to the engines. A crossfeed manifold and valves permit the delivery

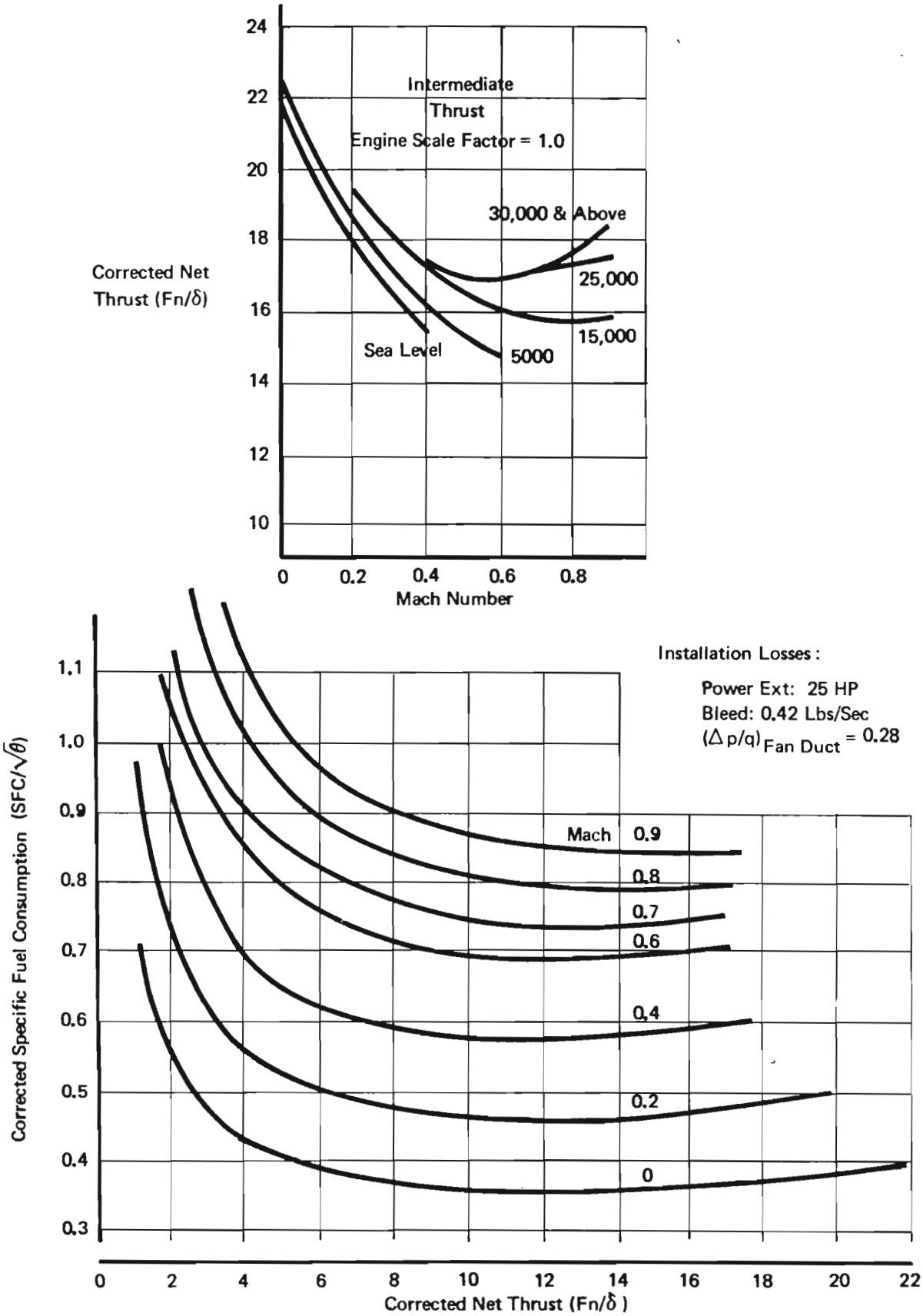

Figure 24 : Allison PD 351-73 Installed Performance

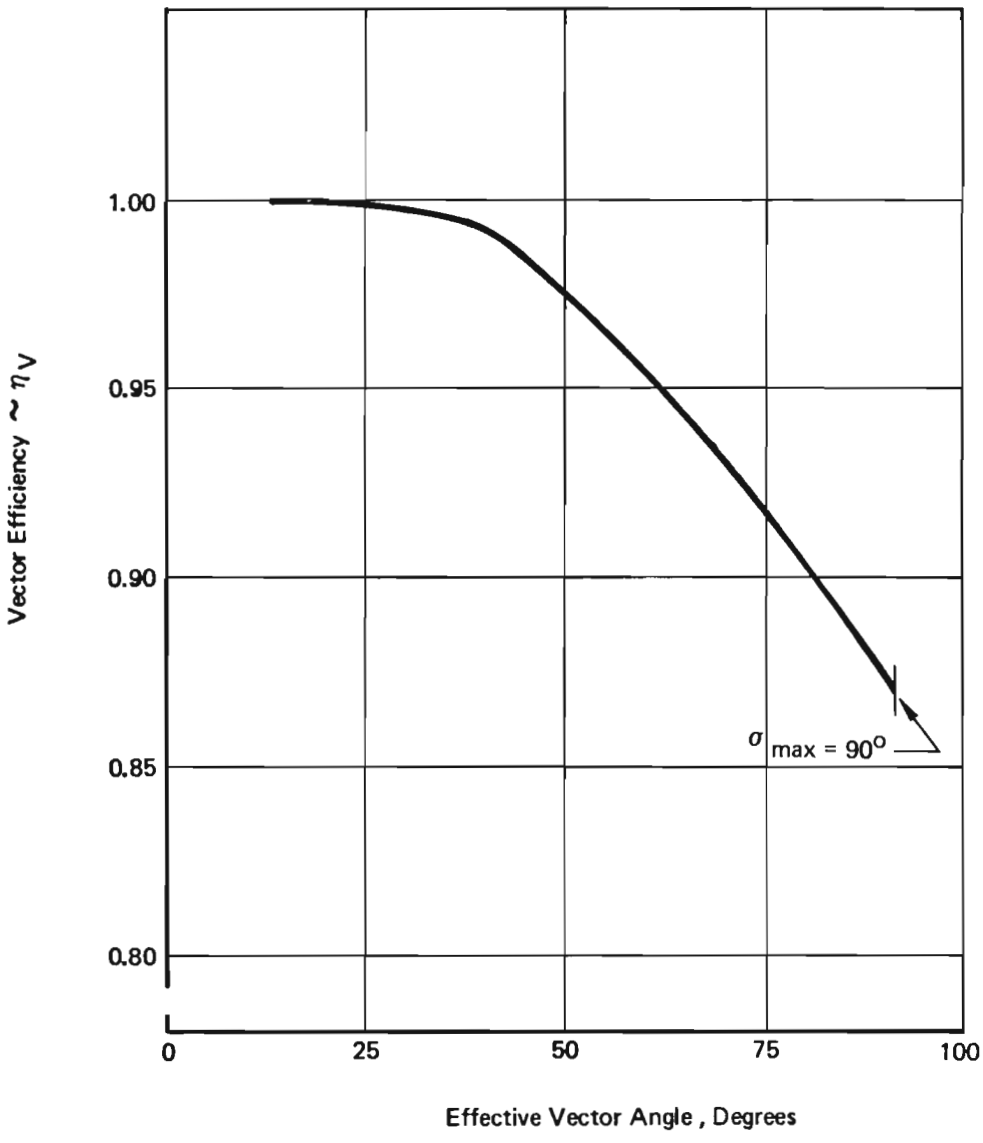

Figure 25: Vector Nozzle Angle Turning Efficiency

of fuel from any tank or tanks to any or all engines. The center wing tank boost pumps can override the main tank pumps until center wing fuel is depleted. Suction feed capability is provided in each main tank to supply each engine should the boost pumps be inoperative.

Each tank is vented through integral wing structural members and connecting tubing. The vent lines terminate in wing-tip surge tanks to minimize fuel spillage. The surge tanks are connected to static air vent scoops in the lower surface of the wing tip.

4.2.4 Thrust Reversing/Vectoring

A thrust reverser efficiency of 40% was estimated for this installation, based on the results of Ref. 1. The reverser can be operated down to zero velocity with negligible engine ingestion of exhaust gas or ground debris. Hot gas impingement on airplane structure and flap drag loss due to engine exhaust are eliminated.

The thrust vectoring system used on the baseline configuration, Model 953-801 (Appendix I), was of the sliding plug/rotating cascade type. This type of system was found in later testing (Ref. 1) not to be as efficient as assumed, particularly below 45°. Therefore, a rotating hood type system was selected for the Model 953-815, Figure 26. This system has high efficiency in the required vector angle range (Figures 25 and 30). The vectoring modulation mechanism is incorporated into the primary flight control system, Figure 46.

The system basically consists of a lower ramp, which is used to increase the flow area in the turning region, and four deflector doors which either deflect the thrust down for vectoring or up and forward for reversing. The deflector doors are stowed in the aft nacelle cowling during cruise.

The mechanism required to operate the system consists of a simple gear box located at each hinge for the deflector doors and four power hinges for the ramp. A hydraulic motor located in the cowl near the strut drives the mechanism. The ramp and deflector doors are geared together.

4.2.5 Boundary Layer Control (BLC)

4.2.5.1 System Description

Engine bleed is used for the wing leading edge and aileron BLC system. An ejector design operating in single or two-stage mode mixes HP bleed, LP bleed, and fan air. The ejector boosts fan pressure to meet the BLC requirement and lowers the manifold temperature to

acceptable limits. HP and LP bleed form the first stage; the second stage uses the output of the first as the primary nozzle to boost the fan air. This is simpler than using flow multipliers (such as turbo-compressors driven by high pressure bleed) and has similar performance (Figure 27).

The principal features of the system are fixed geometry ejectors, simple on-off valve control, redundant BLC air supply from the running engines if one engine fails, and a distribution system in the wing with no valves or moving parts. One ejector for each engine is provided. The mixed flow is delivered through a manifold along the front spar, then into the feeder ducts, and out through the leading edge and aileron nozzles (Figure 27).

Engine high and low pressure bleed air is cooled to 500°F maximum temperature by the ejector and fan bleed pressure is boosted to 28 psia for more efficient leading edge and aileron blowing. Duct Mach number is below 0.30.

For normal four-engine operation, all four ejectors are used (Figure 28). In the event of a single engine failure, the ejectors have been sized so that three will fulfill the airplane's BLC requirement.

Each set of engine bleed valves is programmed by simple pressure sensing pneumatic servo controls. Adequate pressure and flow is maintained at engine power settings associated with takeoff, approach, and go-around.

Leading edge and aileron nozzles and plenum ducts made of stainless steel and titanium are installed in segments along the entire wing leading edge and aileron to minimize accumulation of thermal expansion effects. Nozzles are full span, fixed convergent nozzles (Figure 27).

Valves are not used to isolate duct failures since symmetrical decay of BLC performance is preferred for this case. Leading and trailing edge cavity over temperatures that could occur from duct rupture are sensed and signalled by a warning light on the system control panel. Malfunction of the BLC control valves that could cause excessive duct air temperature also signals a warning light for manual shutdown of the system by the flight crew.

4.2.5.2 System Operation and Performance

Prior to takeoff or landing approach, the BLC system is turned on by pilot actuation of the BLC selector switch. This action opens the bleed valves feeding the ejectors. With the selector switch in the takeoff position, only LP and fan bleed are used to supply BLC air. In the approach position LP, HP, and fan bleed are used (Figure 28) after takeoff or landing, LE flap retraction or pilot action shuts off the BLC air. An interconnect between the thrust reverser and the bleed system shuts off the bleed air during reverse mode.

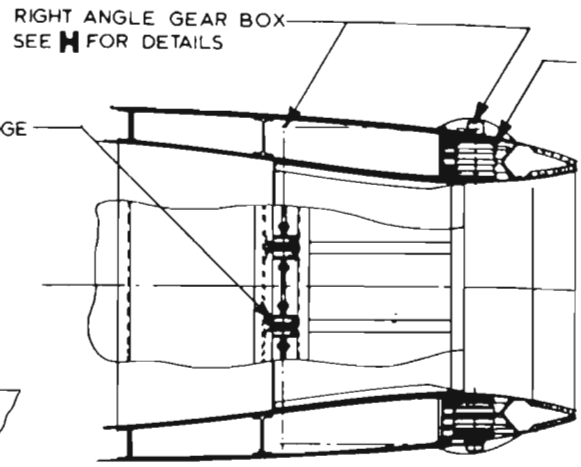

B B

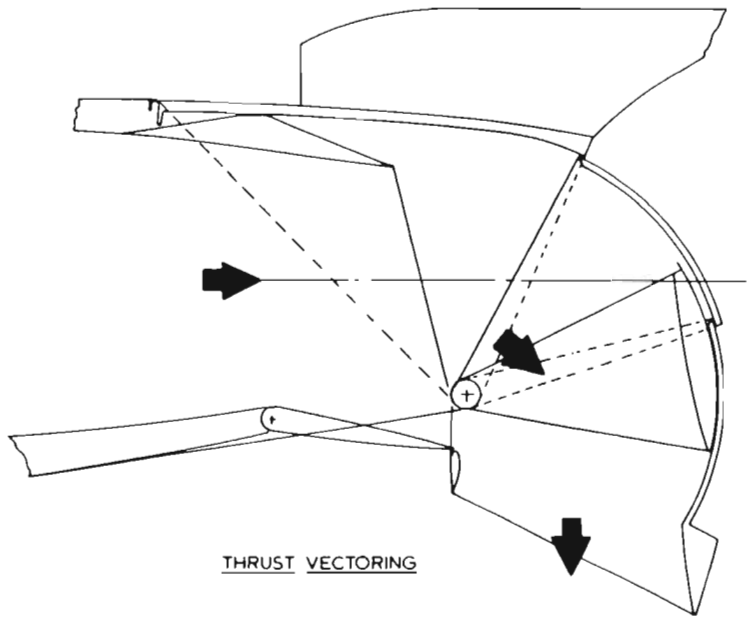

THRUST VECTORING

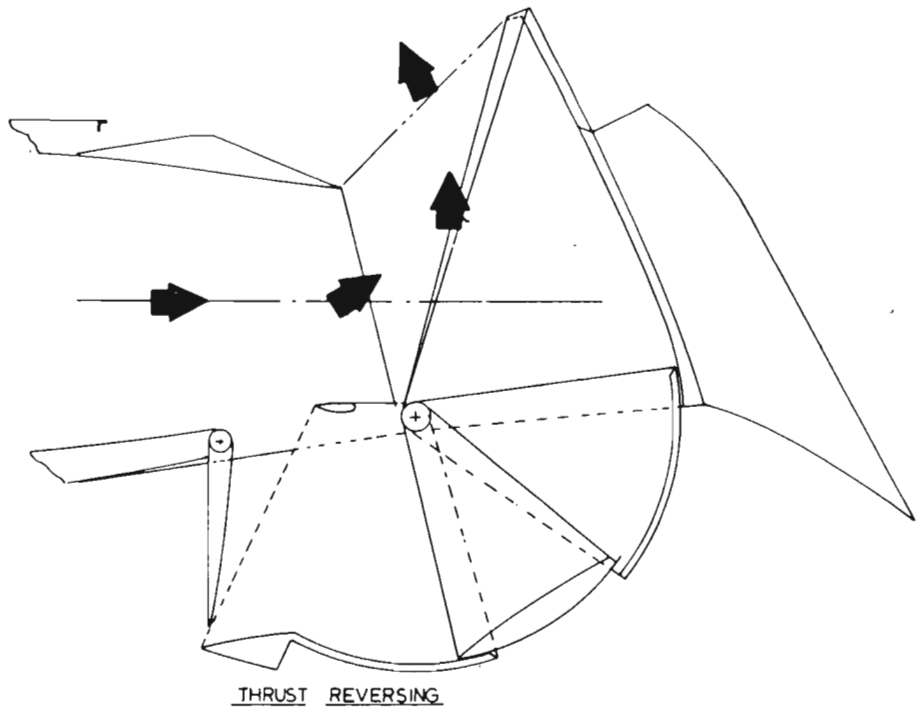

THRUST REVERSING

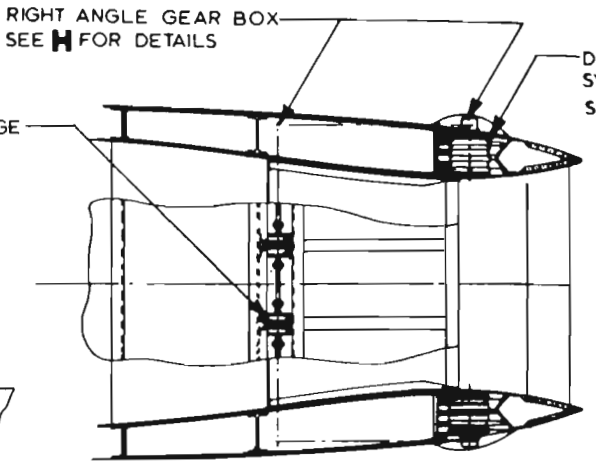

B B

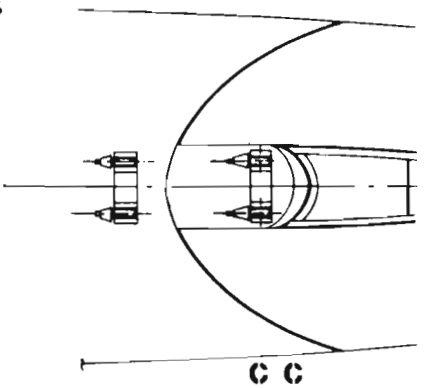

C C

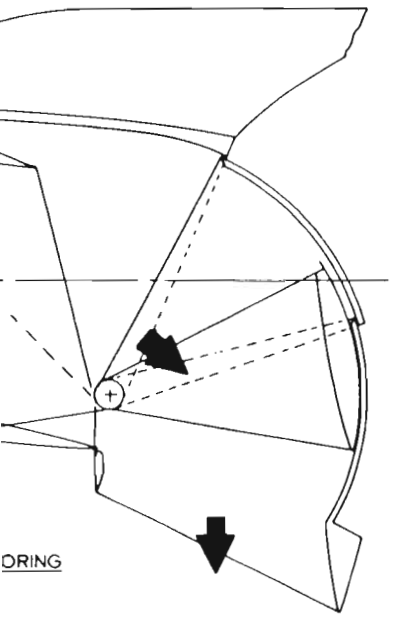

DRING

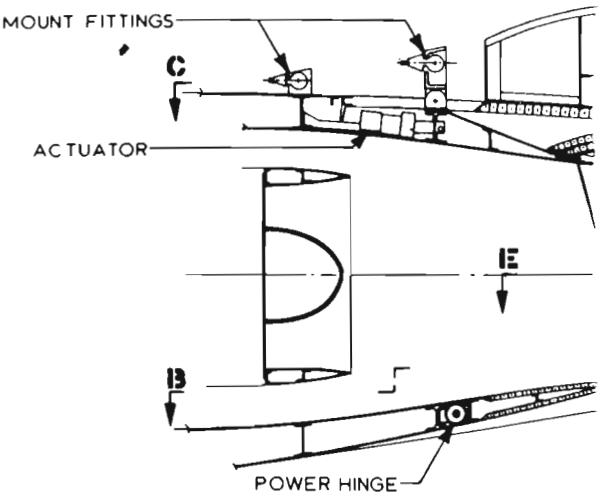

STRUCTURAL ARRANGEMI
PRIMARY NOZZLE, VECTORING, REVER

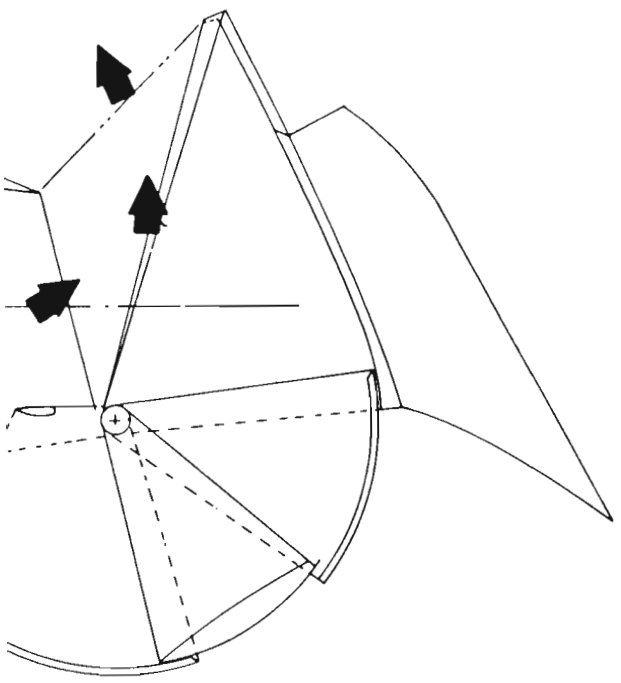

REVERSING

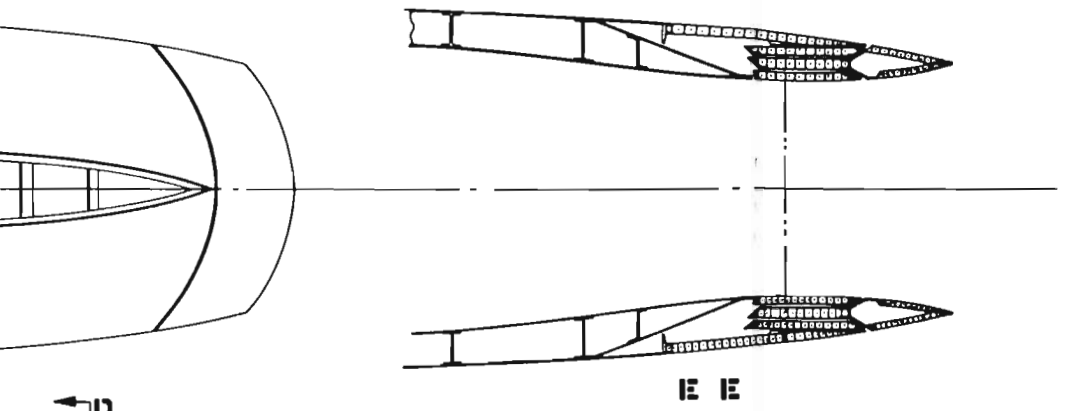

E E

D

STRUT FAIRING

C

E

B

DEFLECTOR DOOR
HINGE POINT

D

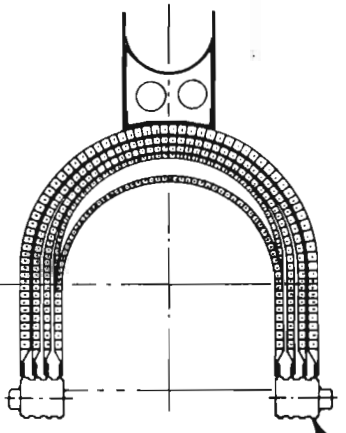

D D

DEFLECTOR DOOR
SYNCRONIZING GEAR BOX
SEE H FOR DETAILS

INLET ANTI-IC

EMENT
VERSING DOORS

HYDRAULIC ACTUATOR

℄ RAMP HINGE

RIGHT ANGLE GEAR BOX

F

F F
SCALE ½

F

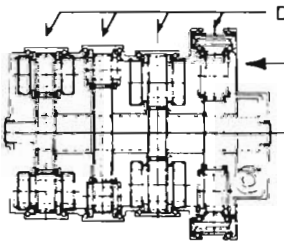

DOOR ℄'S

NOTE : SYNCRONIZING GEAR BOX
IS SIMILAR TO A POWER
HINGE (I.E. SUN AND PLANE
GEARS DRIVING A RING G
GEAR REDUCTION APPRO

G G
GEAR BOX DETAIL
SCALE ½

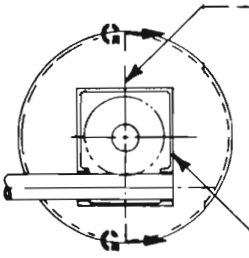

℄ DEFLECTOR DOOR H

G

G

DEFLECTOR DOORS
SYNCRONIZING GEAR

H
VECTORING, REVERSING ACTUATION DETAILS
SCALE ½

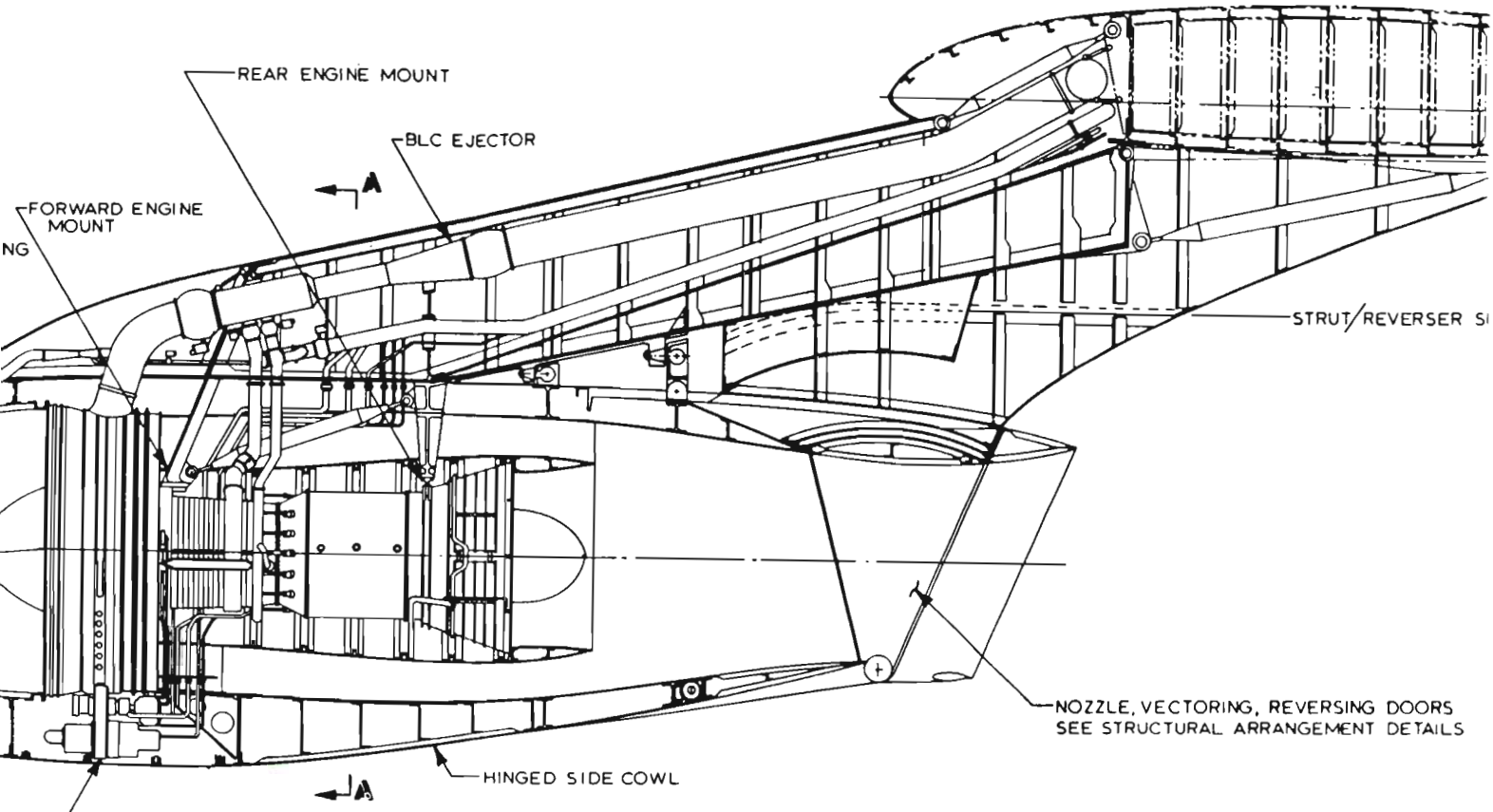

T
EAR).
. 50:1

VIEW LOOKING AT ENGINE (NEAR SIDE COWLING REMOVED)

NGE

BOX

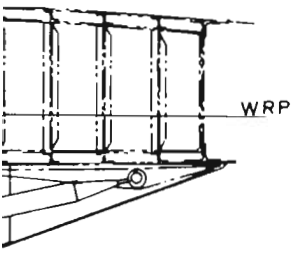

EVERSER SPLIT LINE

DOORS
DETAILS

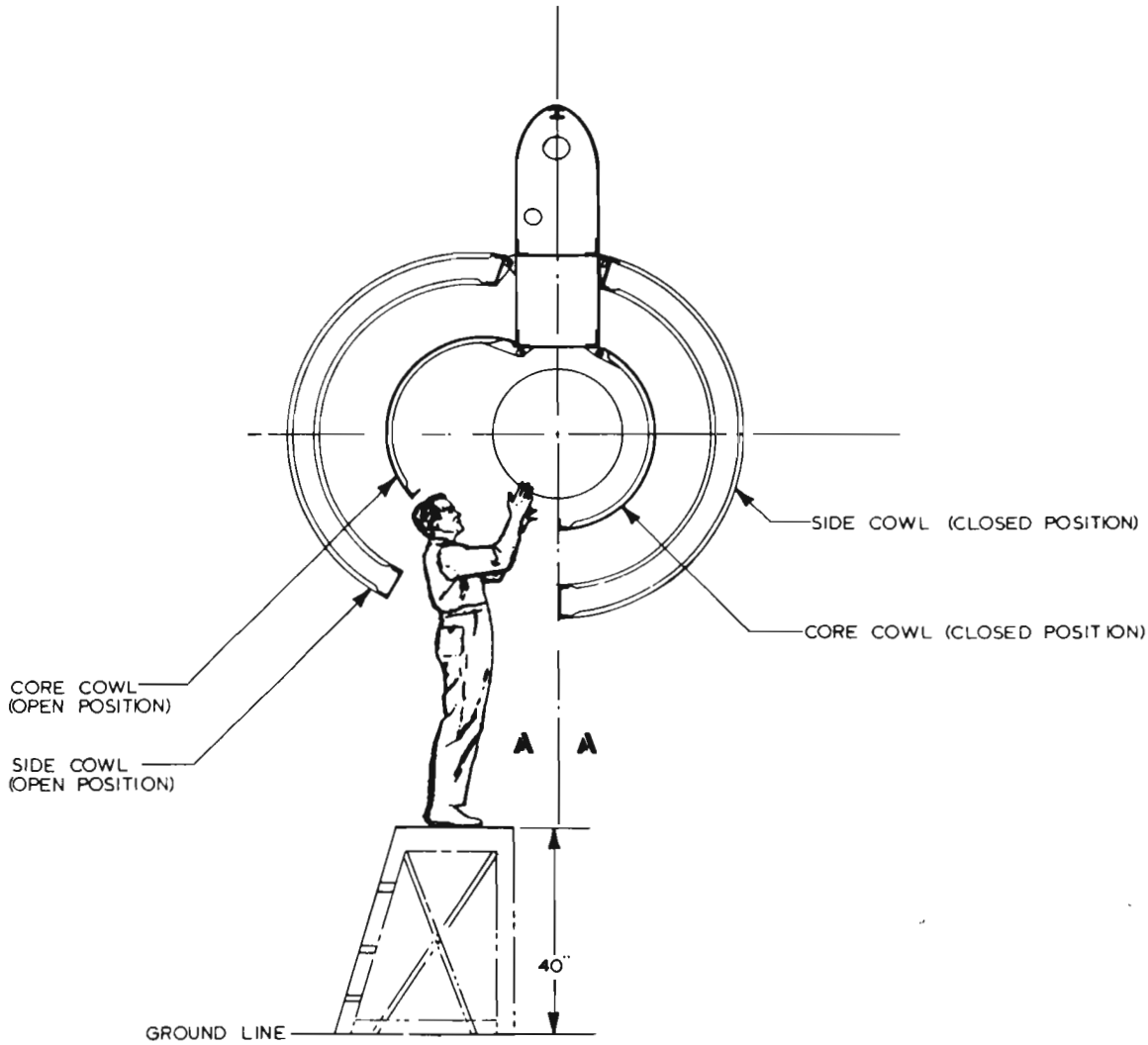

Figure 26: Engine Installation

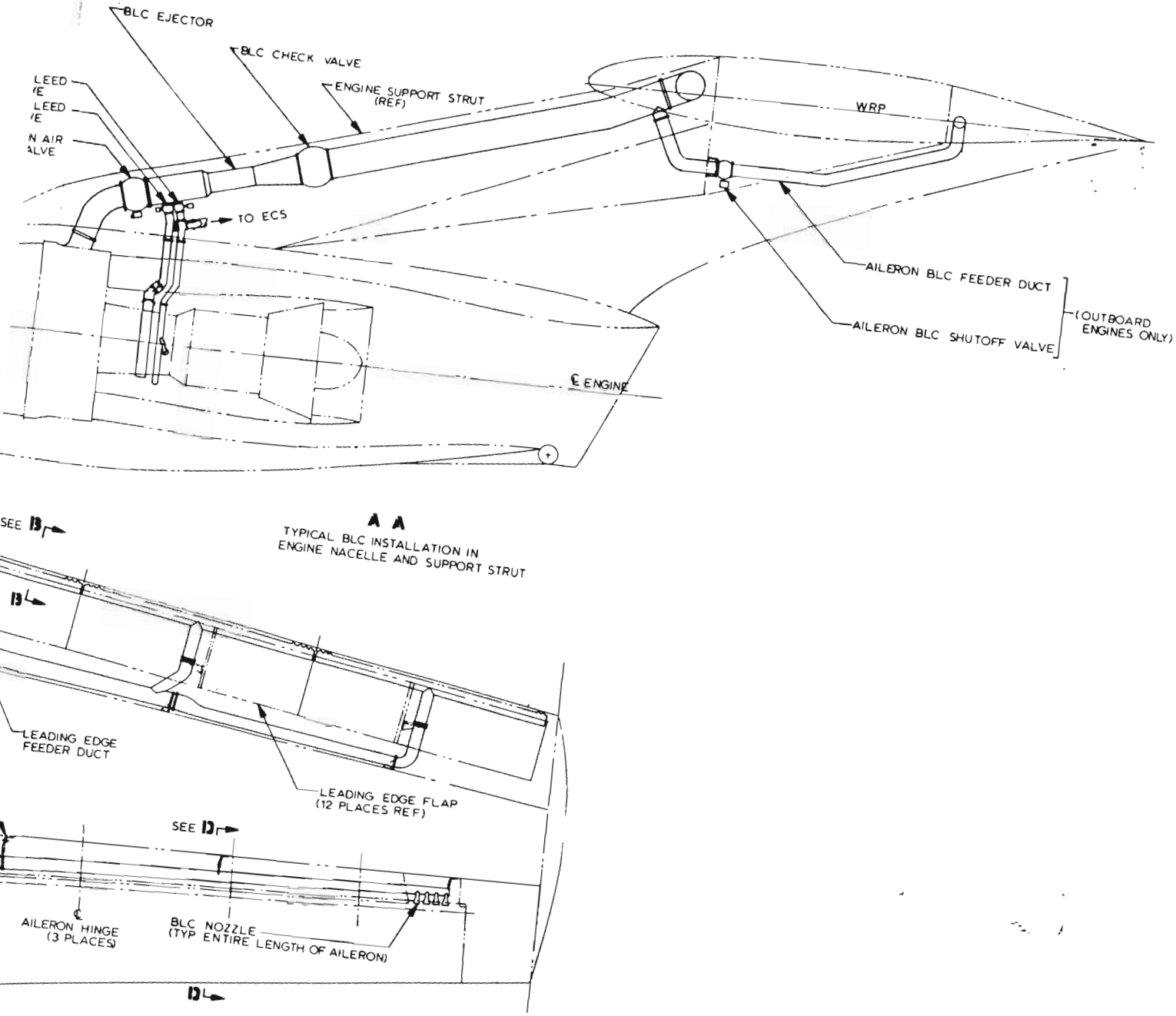

Figure 27: BLC Installation

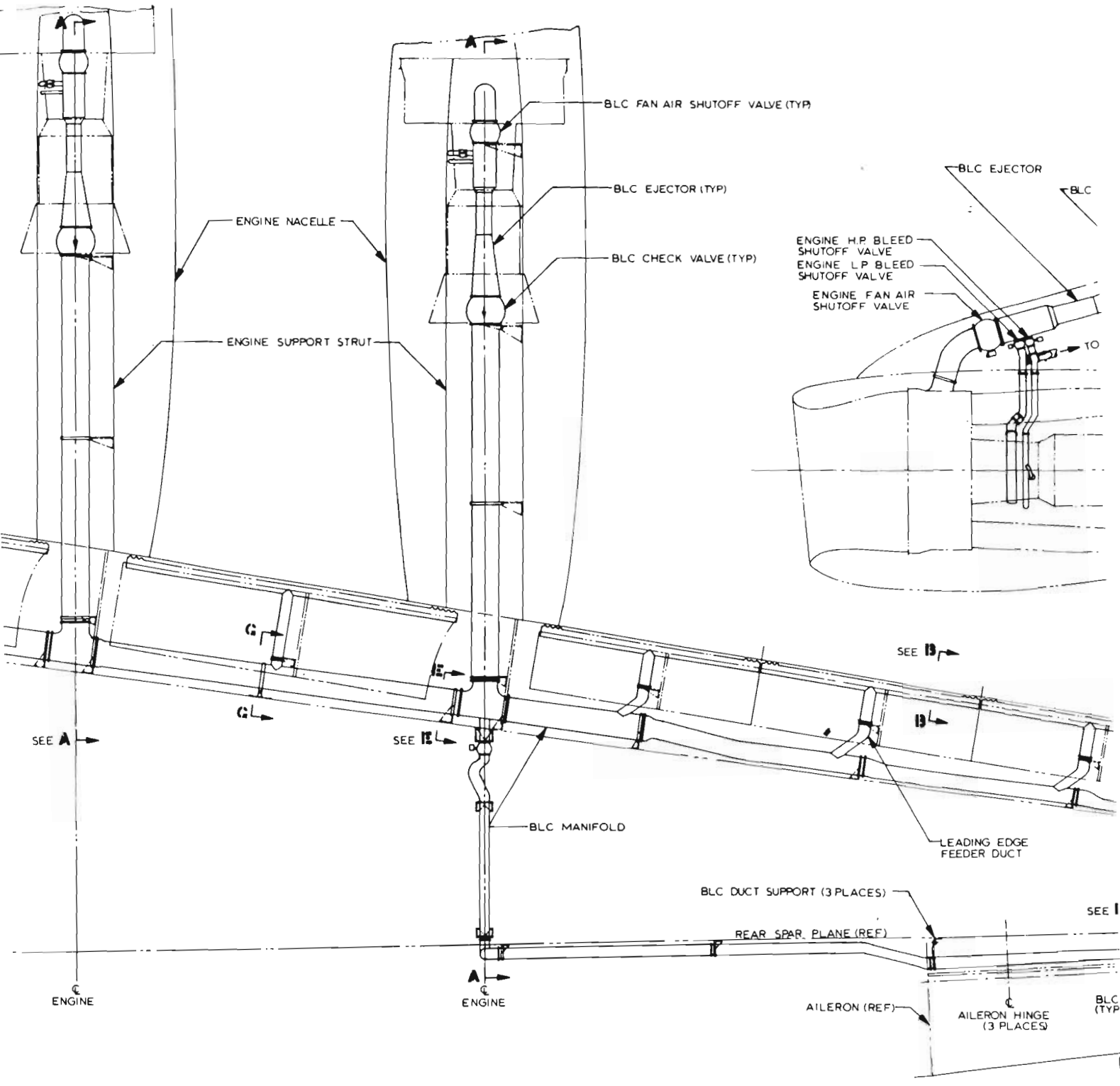
BLC FAN AIR SHUTOFF VALVE (TYP)
BLC EJECTOR (TYP)
BLC CHECK VALVE (TYP)
ENGINE NACELLE
ENGINE SUPPORT STRUT
BLC EJECTOR
BLC
ENGINE H.P. BLEED SHUTOFF VALVE
ENGINE L.P. BLEED SHUTOFF VALVE
ENGINE FAN AIR SHUTOFF VALVE
TO
SEE B
SEE A
SEE E
BLC MANIFOLD
LEADING EDGE FEEDER DUCT
BLC DUCT SUPPORT (3 PLACES)
REAR SPAR PLANE (REF)
SEE I
℄ ENGINE
℄ ENGINE
AILERON (REF)
℄ AILERON HINGE (3 PLACES)
BLC (TYP

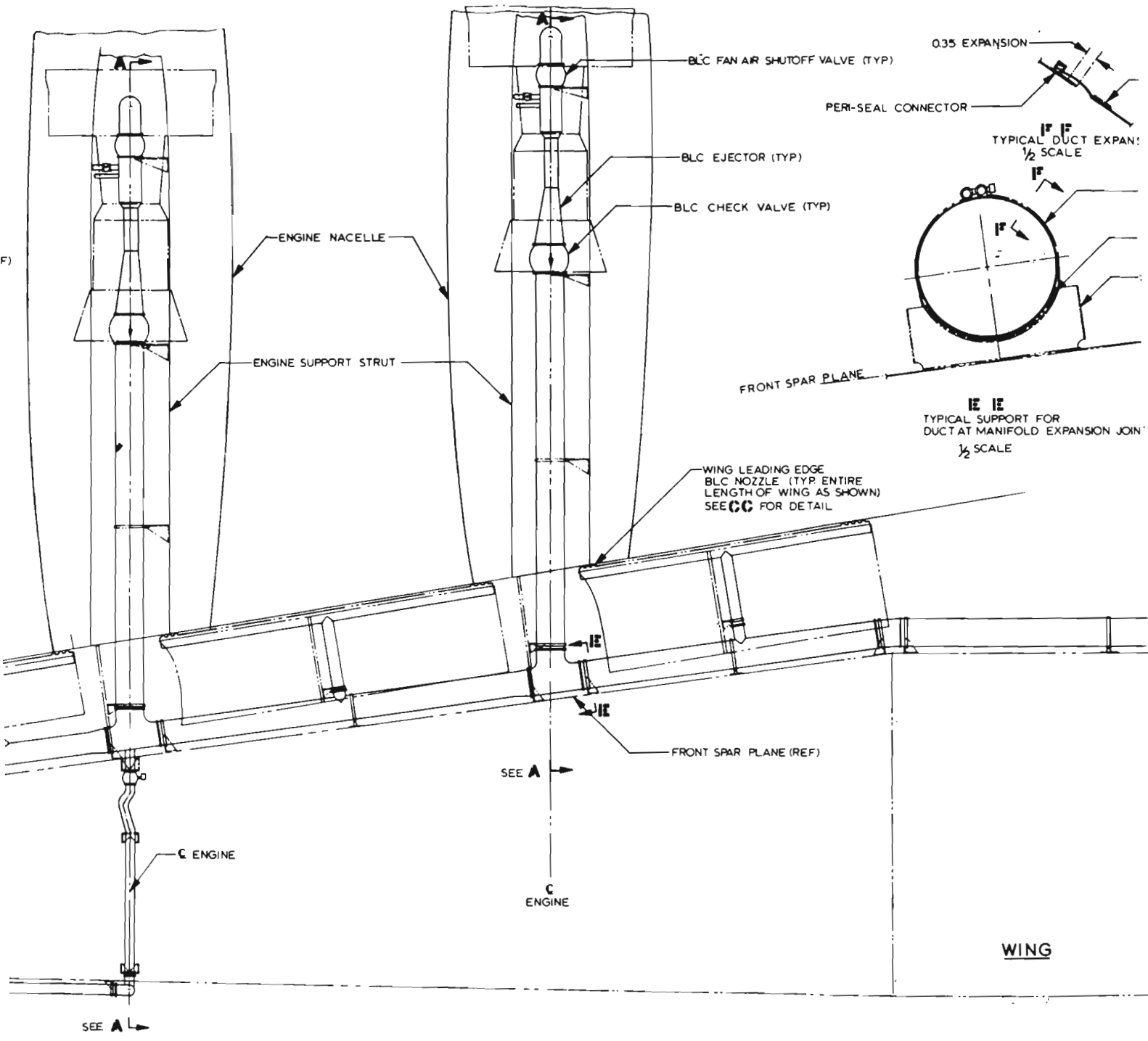
BLC FAN AIR SHUTOFF VALVE (TYP)
BLC EJECTOR (TYP)
BLC CHECK VALVE (TYP)
ENGINE NACELLE
ENGINE SUPPORT STRUT
WING LEADING EDGE
BLC NOZZLE (TYP ENTIRE
LENGTH OF WING AS SHOWN)
SEE CC FOR DETAIL
FRONT SPAR PLANE (REF)
SEE A
℄ ENGINE
℄
ENGINE
SEE A
0.35 EXPANSION
PERI-SEAL CONNECTOR
TYPICAL DUCT EXPANS
½ SCALE
FRONT SPAR PLANE
TYPICAL SUPPORT FOR
DUCT AT MANIFOLD EXPANSION JOIN
½ SCALE
WING

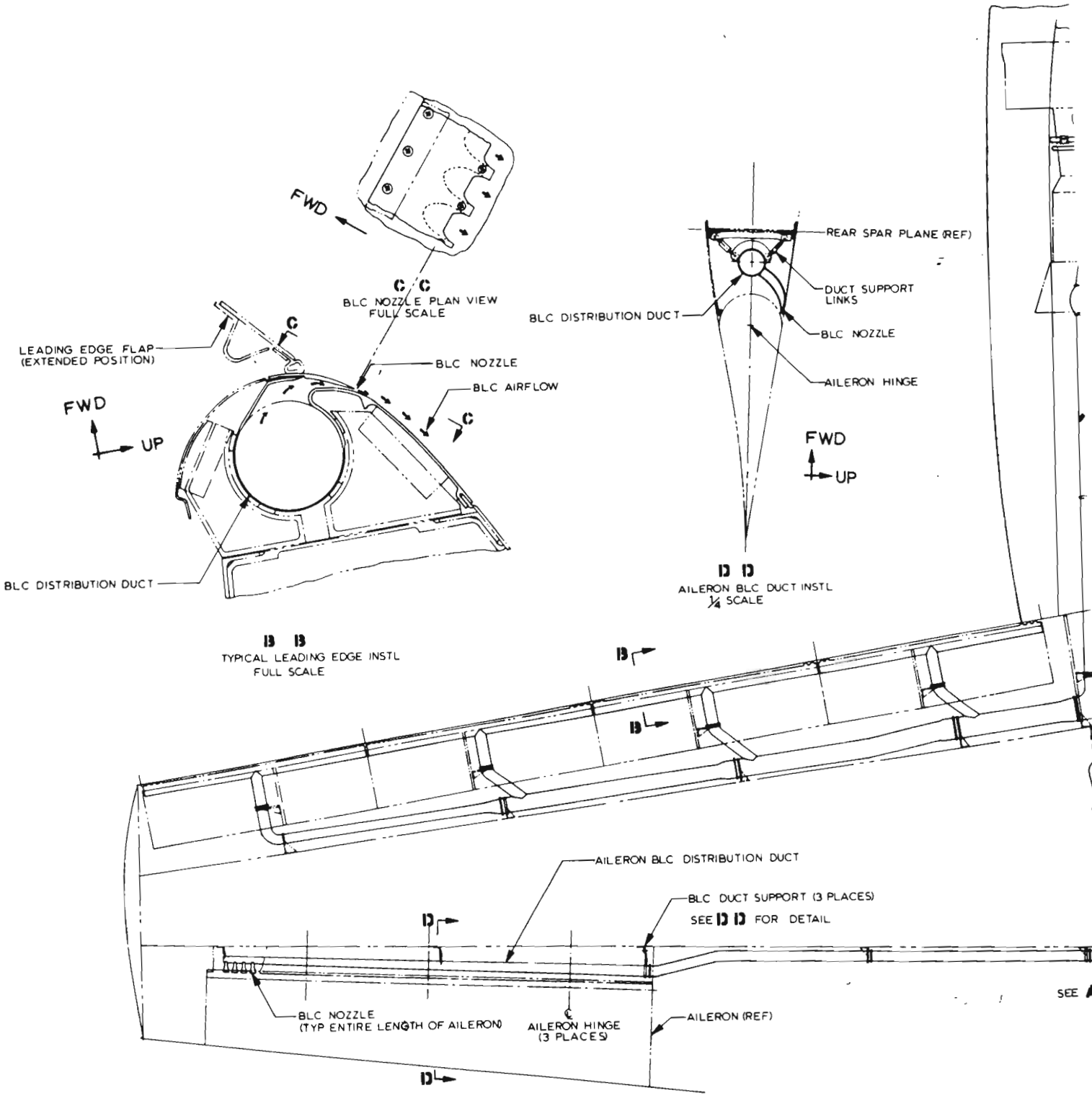
FWD
C C
BLC NOZZLE PLAN VIEW
FULL SCALE
LEADING EDGE FLAP
(EXTENDED POSITION)
C
BLC NOZZLE
BLC AIRFLOW
FWD
UP
C
BLC DISTRIBUTION DUCT
REAR SPAR PLANE (REF)
DUCT SUPPORT
LINKS
BLC DISTRIBUTION DUCT
BLC NOZZLE
AILERON HINGE
FWD
UP
D D
AILERON BLC DUCT INSTL
1/4 SCALE
B B
TYPICAL LEADING EDGE INSTL
FULL SCALE
B
B
AILERON BLC DISTRIBUTION DUCT
BLC DUCT SUPPORT (3 PLACES)
SEE D D FOR DETAIL
D
BLC NOZZLE
(TYP ENTIRE LENGTH OF AILERON)
AILERON HINGE
(3 PLACES)
AILERON (REF)
D

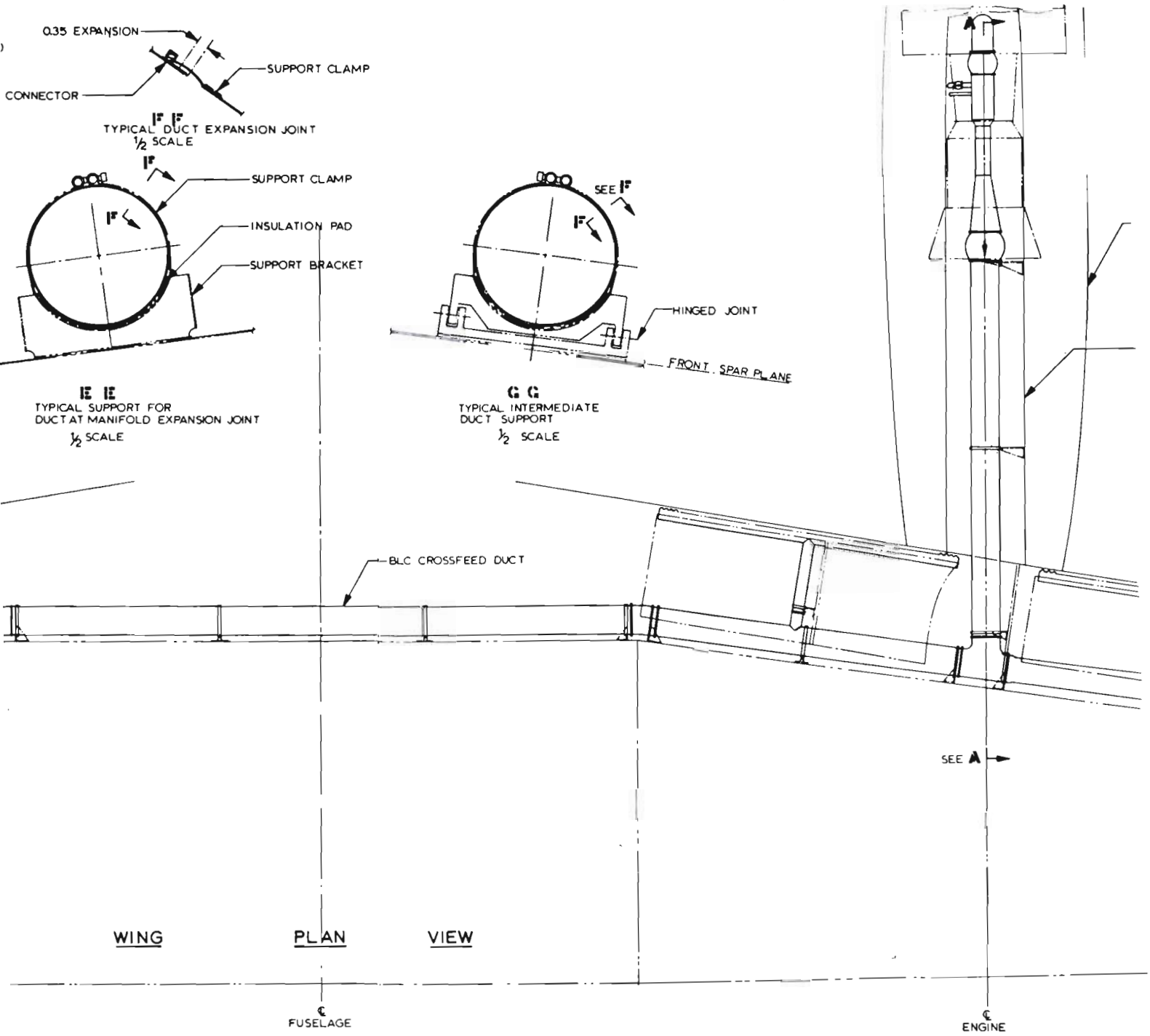
0.35 EXPANSION
SUPPORT CLAMP
CONNECTOR
F F
TYPICAL DUCT EXPANSION JOINT
½ SCALE
F
SUPPORT CLAMP
INSULATION PAD
SUPPORT BRACKET
F
E E
TYPICAL SUPPORT FOR
DUCT AT MANIFOLD EXPANSION JOINT
½ SCALE
SEE F
F
HINGED JOINT
FRONT SPAR PLANE
G G
TYPICAL INTERMEDIATE
DUCT SUPPORT
½ SCALE
A
BLC CROSSFEED DUCT
SEE A
WING PLAN VIEW
℄
FUSELAGE
℄
ENGINE

Mode	4 Engines Normal	1 Engine Out
Takeoff	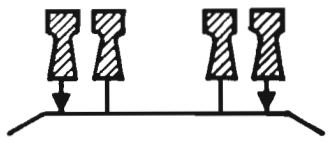	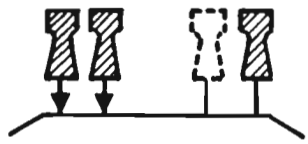
$C_{\mu_{Net}} = \frac{F_N \text{ Blowing}}{q \times \text{Wing Area}}$	Engine F_G	
	$C_{\mu_{Net}}$ =	0.0492 / 0.0369
	=	18,550 Lb / 18,100 Lb
Manifold: Total Temp	=	500°F / 500°F
Manifold: Total Air Flow	=	48.5 Lb/Sec / 36.4 Lb/Sec
Manifold: Total Pressure	=	28 Psia / 29 Psia
Engine Bleed	=	3.3% LP / 3.3% LP
		3.3% HP / 3.3% HP
V_∞ = 88 Kt		
T_{Amb} = 103°F		
Approach	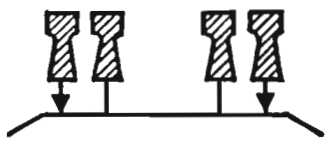	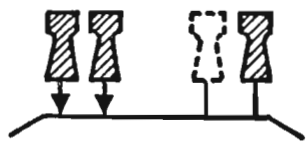
	Engine F_G	
	$C_{\mu_{Net}}$ =	0.0374 / 0.0369
	=	18,500 Lb / 18,100 Lb
Manifold: Total Temp	=	500°F / 500°F
Manifold: Total Air Flow	=	50.2 Lb/Sec / 36.4 Lb/Sec
Manifold: Total Pressure	=	28 Psia / 29 Psia
Engine Bleed	=	3.3% LP / 3.3% LP
		3.3% HP / 3.3% HP
V_∞ = 88 Kt		
T_{Amb} = 103°F		

Figure 28: Performance of Multiple Ejector BLC System

4.3 Performance Charts

This section contains estimated takeoff, landing, climb, and cruise performance for the 953-815 airplane with four .857 scale Allison PD 351-73 engines. Installed thrust and fuel flow rates are contained in Section 4.2. Aerodynamic characteristics were obtained from Section 4.1. Structural weight limitations for determining payload range capability were obtained from Section 6. The performance was determined in accordance with the mission and takeoff and landing rules presented in Appendix II.

4.3.1 Takeoff and Landing

The high-lift configuration was the same for both takeoff and landing except for the thrust vector angle. The high lift characteristics described in Section 4.1.2 were used for both takeoff and landing.

4.3.1.1 Normal Takeoff and Landing

Normal (critical engine inoperative) takeoff distance (Figure 29) was based on the critical field length. Normal landing distance (also Figure 29) was based on the distance to clear 50 ft. and come to a stop utilizing maximum braking and two engine thrust reversal.

Full flap deflection and full span leading edge blowing was used for both takeoff and landing. The thrust vector was set at 7° (so the thrust would not impinge on the flaps) during takeoff ground roll in order to maximize the acceleration. At rotation speed, the thrust vector was changed to the maximum angle that could be used and still meet the 3° climbout angle requirement with the critical engine inoperative. (See Figure 30 for vector angles.) This minimized the liftoff speeds (Figure 31) which were based on the stall and maneuver requirements given in Appendix II.

Normal landing vector angles shown on Figure 30 were selected to provide a 10 fps sink rate with the critical engine inoperative and the remaining engines at takeoff thrust in order to minimize the landing speed. Engine out go-around requires a 20 to 30 degree reduction in the vector angle. Landing speeds were then selected to meet the required stall and maneuver margin requirements.

Normal takeoff and landing distances for standard atmospheric conditions are shown on Figure 32.

4.3.1.2 Assault Takeoff and Landing

Assault (all engines operating) takeoff performance was determined by setting the thrust vector at 7° during the ground acceleration and then rotating the nozzles (just prior to liftoff) to the angle that would provide a climb angle of 3° in free air with all

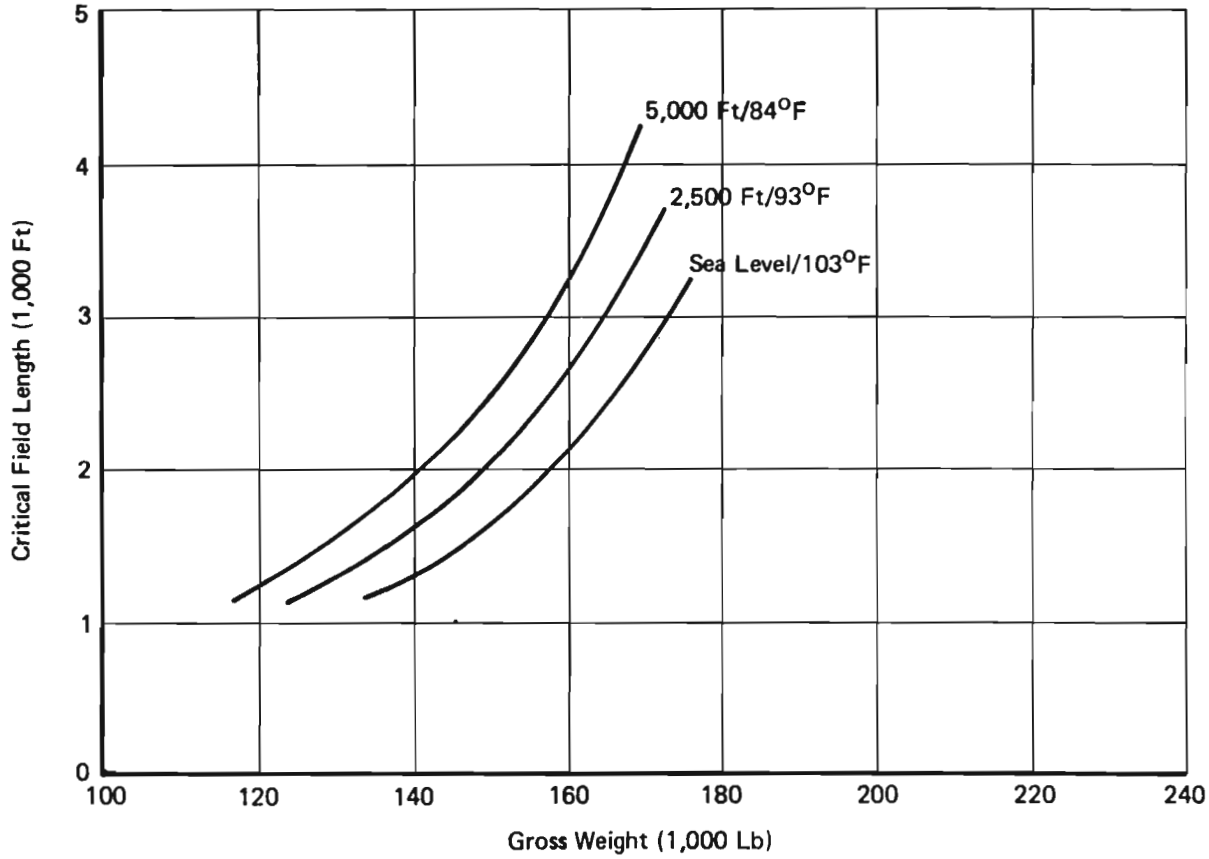

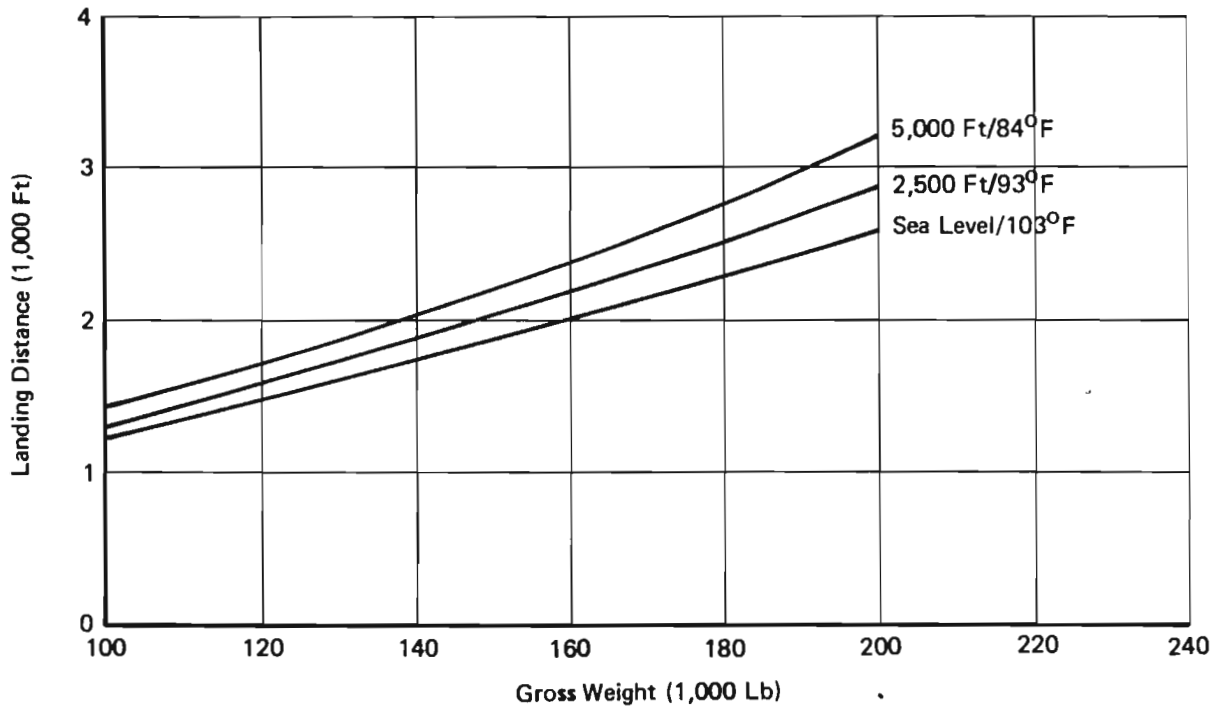

Figure 29: Normal Takeoff & Landing – Hot Atmosphere

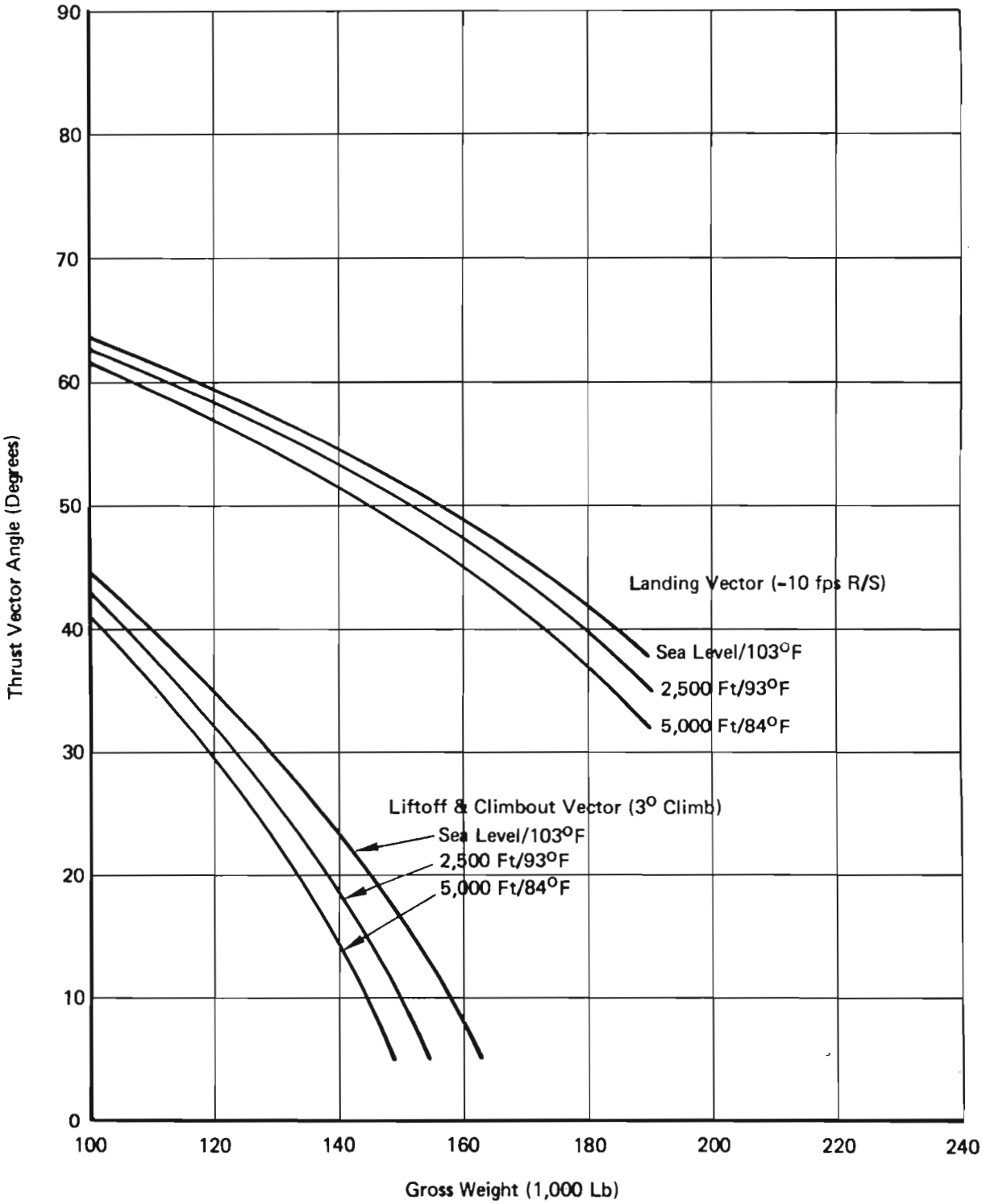

Figure 30: Normal Takeoff & Landing Thrust Vectors — Hot Atmosphere

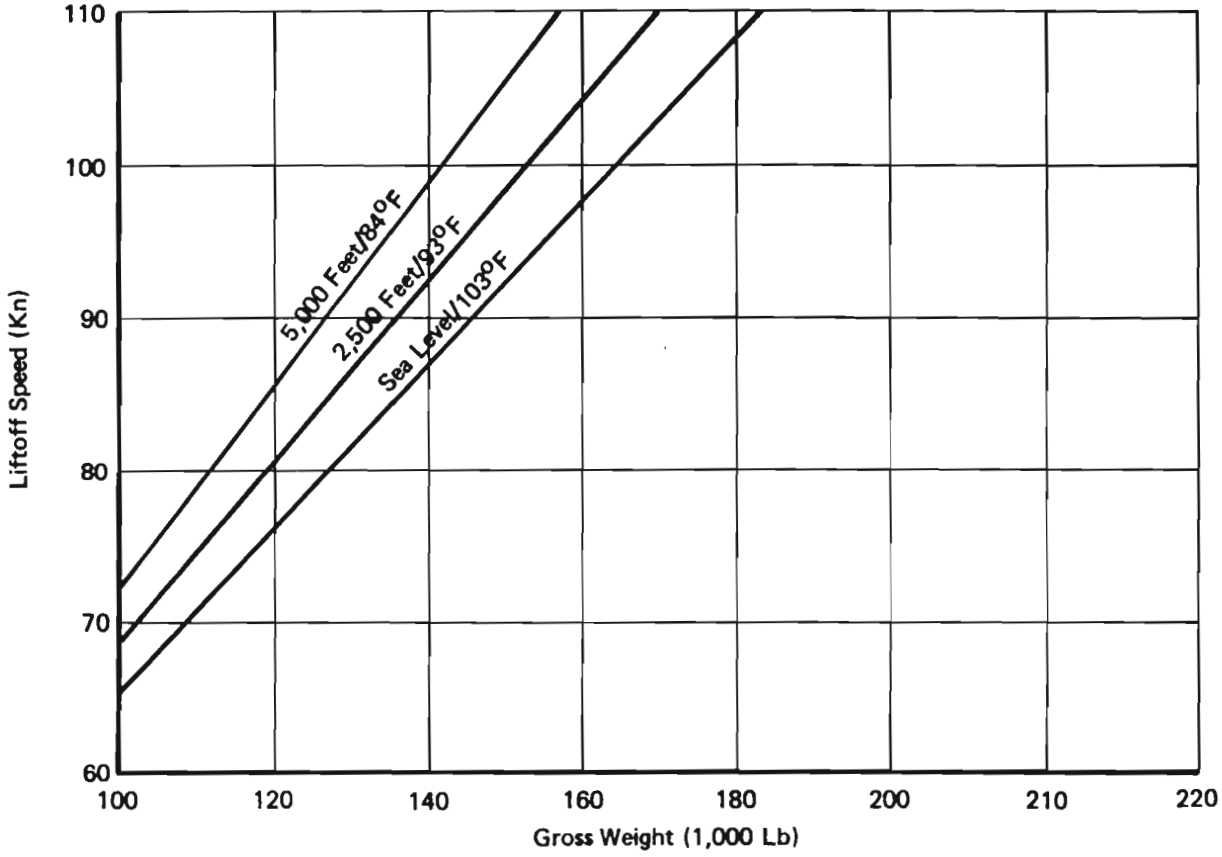

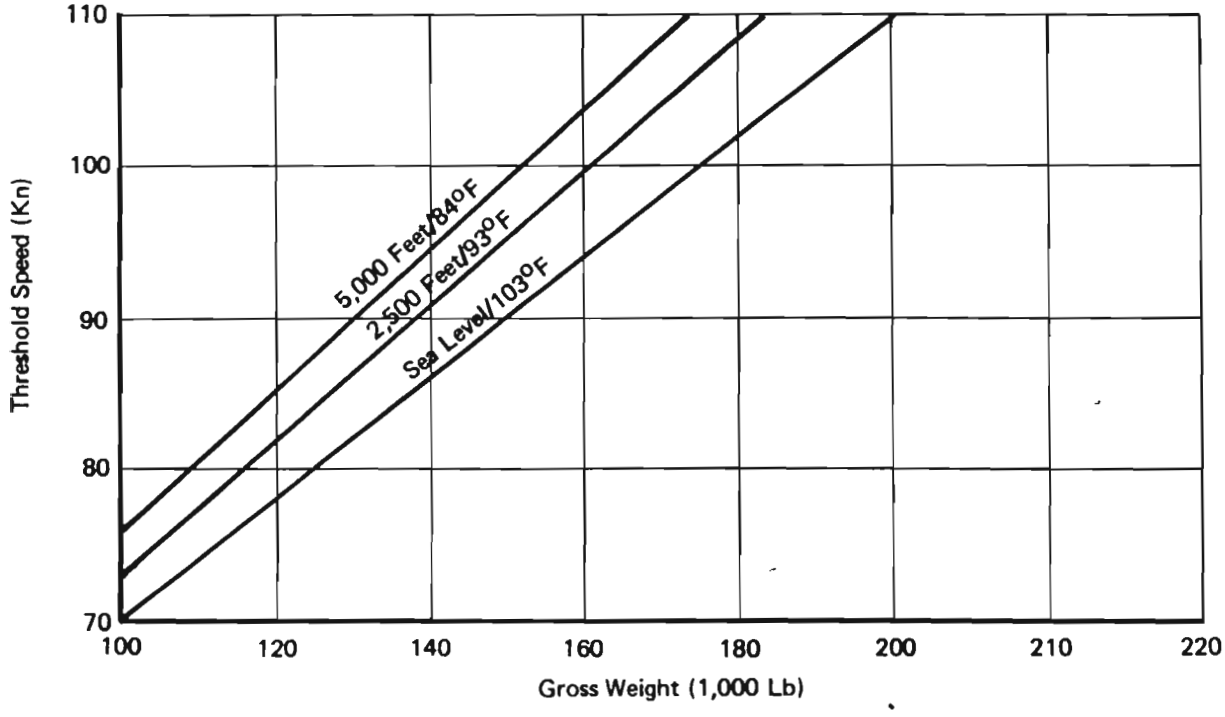

Figure 31: Normal Liftoff & Threshold Speeds – Hot Atmosphere

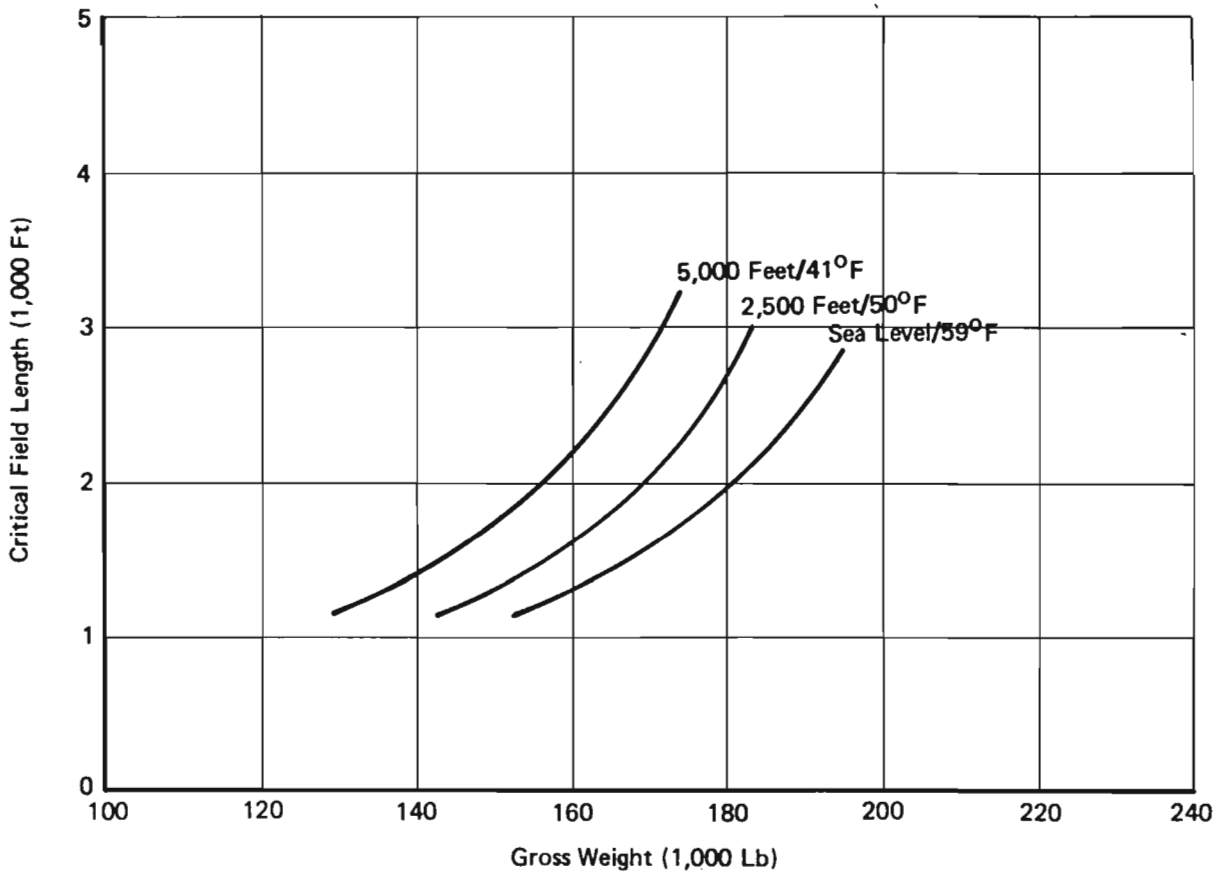

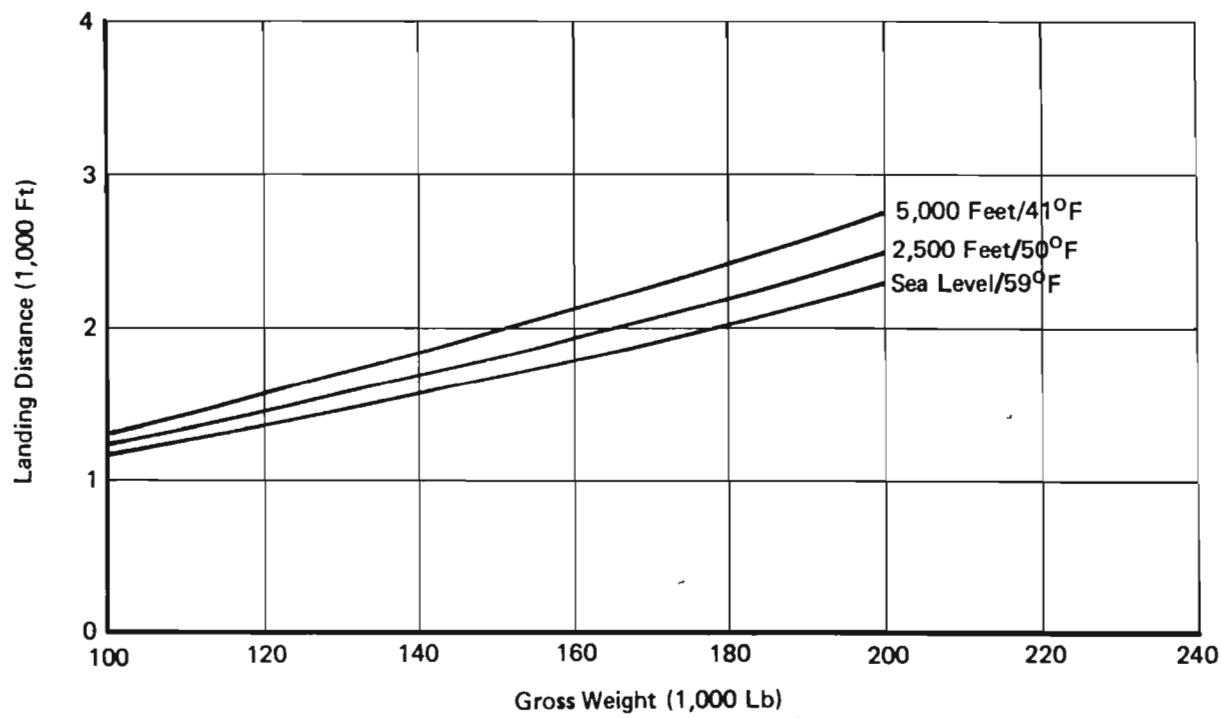

Figure 32: Normal Takeoff & Landing — Standard Atmosphere

engines operating. Liftoff speed was then selected to meet the stall and maneuver requirements given in Appendix B. Distances required to accelerate to liftoff speed are shown on Figure 33 for hot atmospheric conditions and on Figure 34 for standard conditions.

Assault landing distances (also shown on Figures 33 and 34) were based on a 300 ft air distance and a stopping distance utilizing maximum braking and maximum four engine thrust reversal. Thrust vector angles and landing speeds were selected to meet a 10 fps sink rate and minimum stall and maneuver margin requirements (see appendix II) with all engines operating.

4.3.1.3 Minimum Flight Speeds

Minimum flight speeds on the 953-815 are limited by wing stall. Minimum flight speeds with four engines at takeoff thrust and three engines at takeoff thrust (outboard engine inoperative) are shown on Figures 35 and 36 for sea level/standard and 2500 ft/93°F conditions.

4.3.2 Mission Capability

The airplane payload-distance performance is summarized in Figure 5 of Section 2.2. The 500 nautical mile radius mission with a maximum payload of 28,000 pounds is accomplished at the design gross weight of 158,000 pounds. Trading all of the payload for fuel results in a radius of 1470 nautical miles with a fuel load of 58,000 pounds.

The ferry mission range with maximum internal fuel of 67,400 pounds resulting in a takeoff weight of 167,400 pounds, is 3700 nautical miles. The long range cruise Mach number is .71 for both the radius and ferry missions.

A summary of fuel used and distance for the radius and ferry range missions is presented in Table II. The radius mission profile is shown in Figure 37.

The speed-altitude capability using maximum cruise thrust is illustrated in Figure 7, Section 2.2 by the speed-altitude envelope for the initial cruise weights for both the outbound and inbound legs of the radius mission.

4.3.3 Segment Performance

The airplane climb, cruise, and loiter performance are presented in this section.

The climb performance as shown in Figure 38 is presented in the form of time, fuel, and distance required for climb from sea level to cruise ceiling on a standard day. The climb speed schedule is 350 knots EAS to Mach .71.

Cruise performance is presented as fuel mileage and integrated range. Fuel mileage (nautical miles per pound) is shown for altitudes of sea level, 20,000, 30,000, 35,000, and 40,000 feet in Figures 39 through 43. Maximum range and long range cruise conditions are noted on the figures. The integrated range, speed, and altitude for long range cruise is presented in Figure 44.

Loiter performance is shown in Figure 45 as speed and fuel flow required for holding at any altitude. The speeds shown are in excess of those for maximum L/D to permit improved handling characteristics.

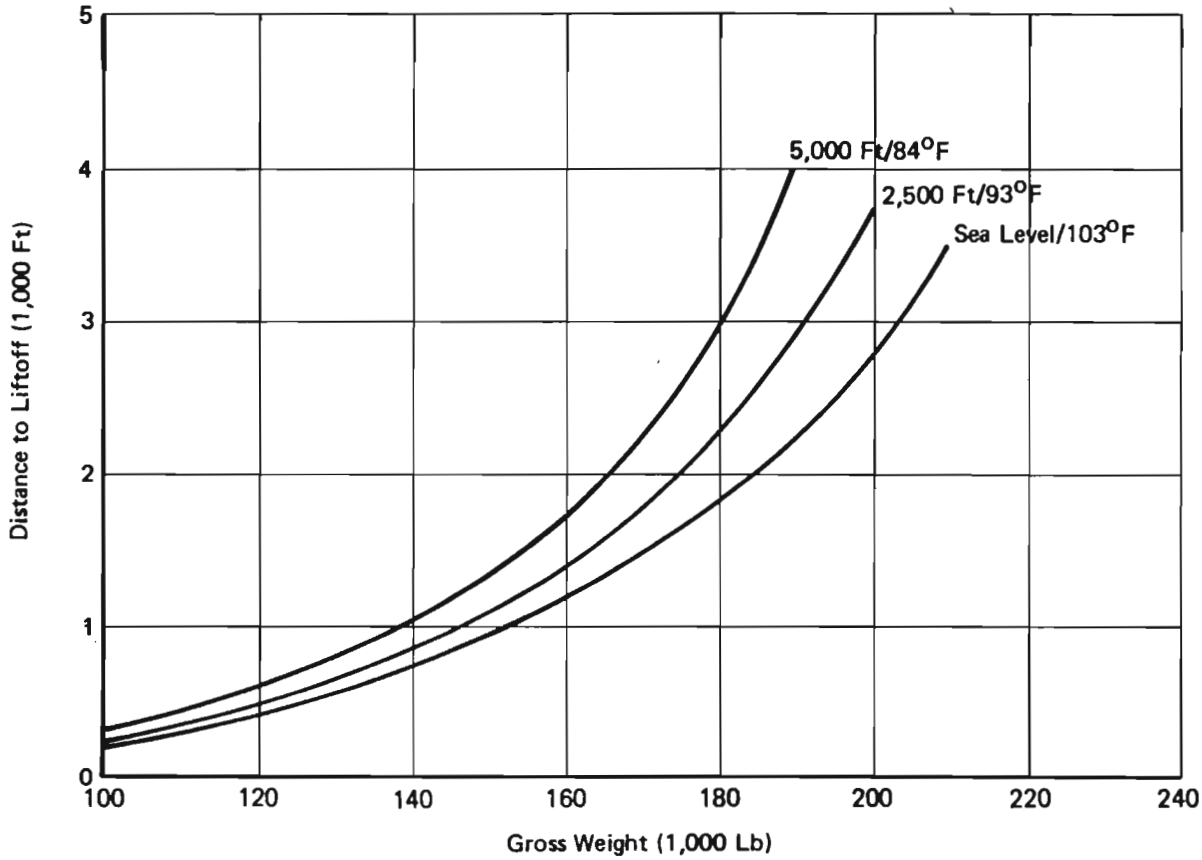

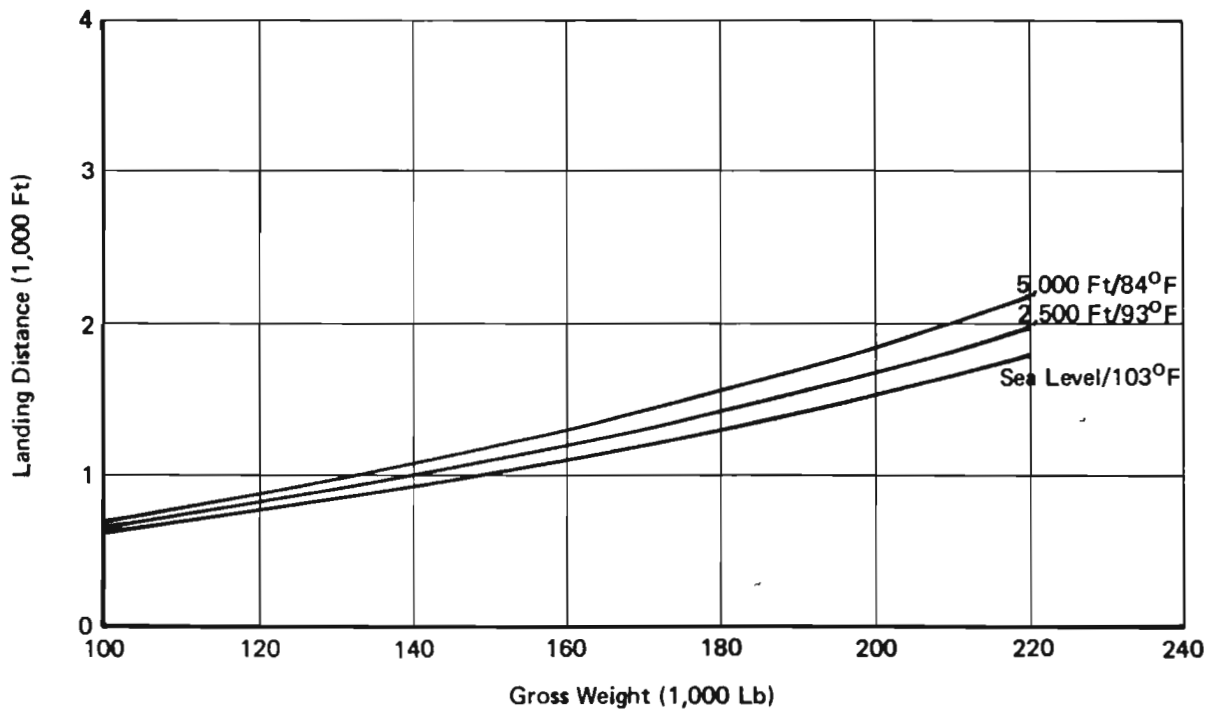

Figure 33: Assault Takeoff and Landing – Hot Atmosphere

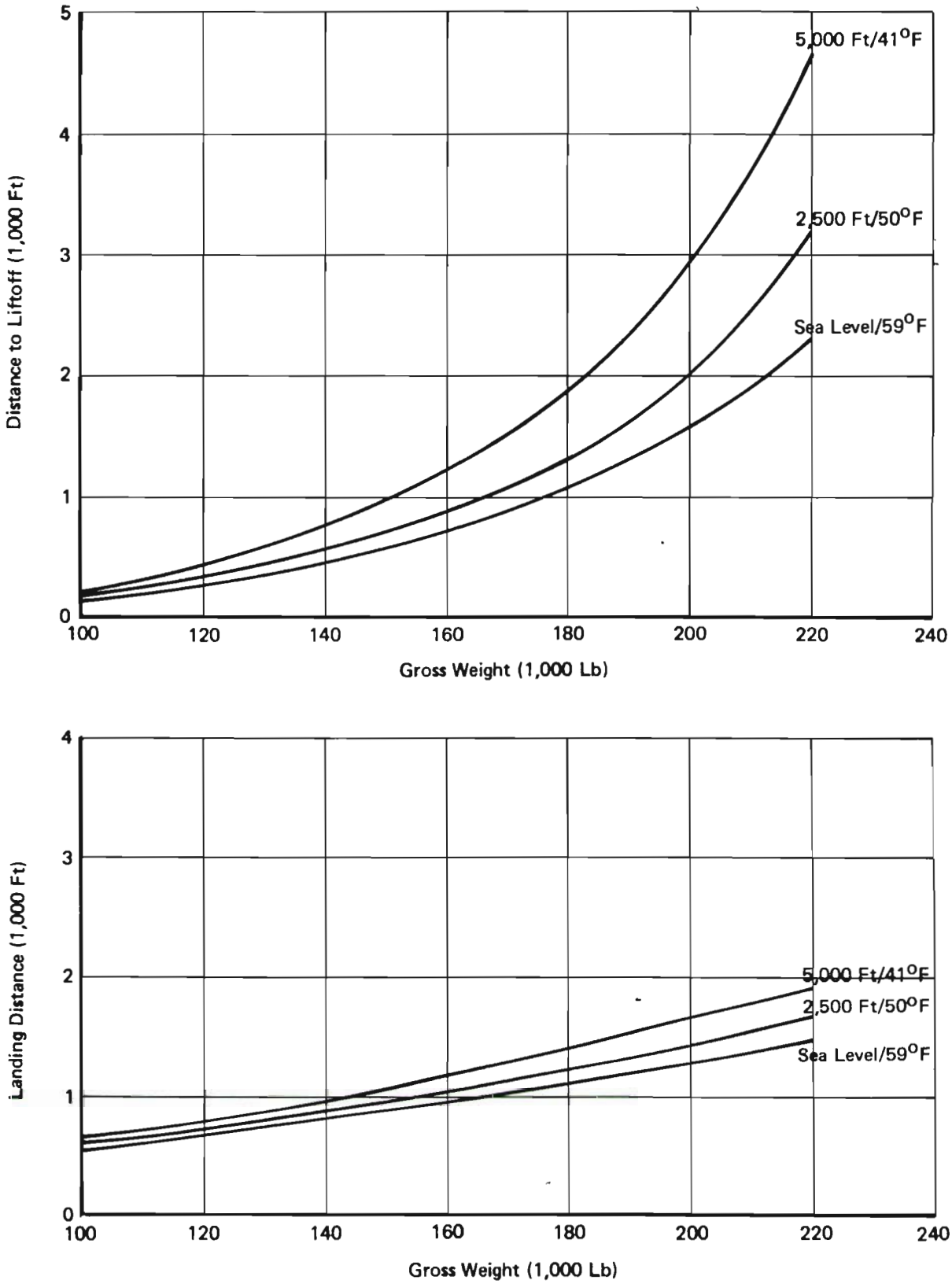

Figure 34: Assault Takeoff and Landing — Standard Atmosphere

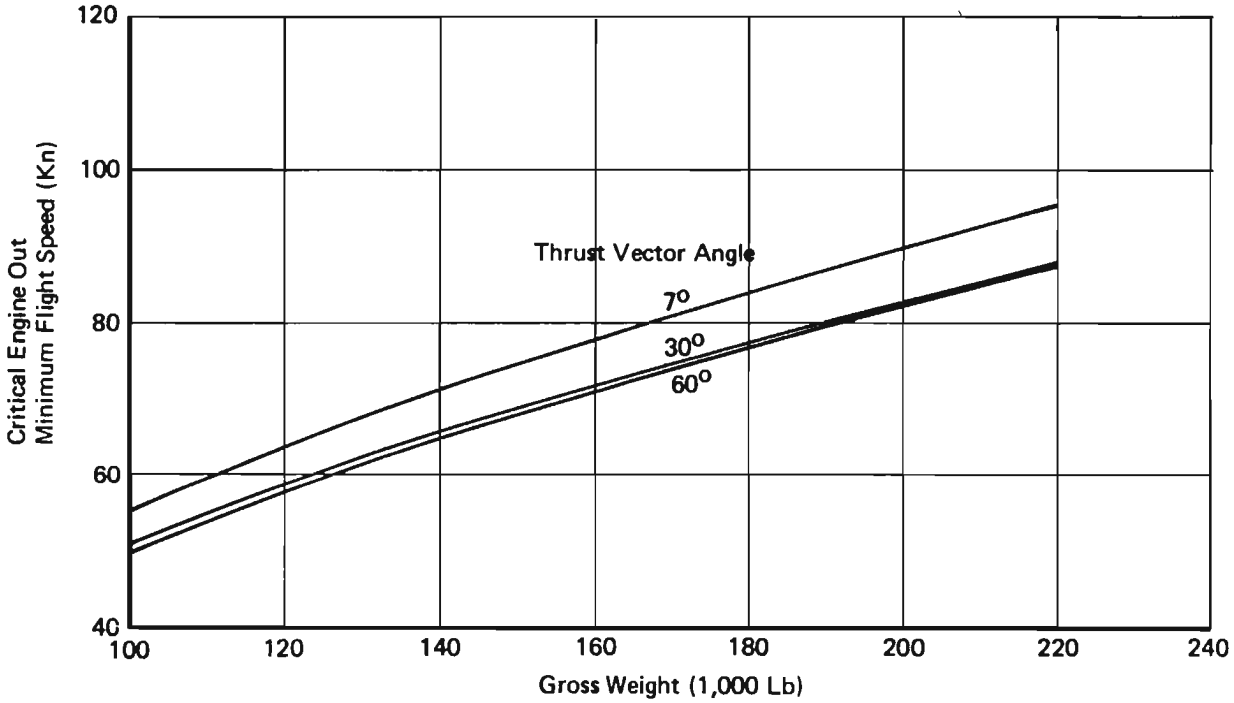

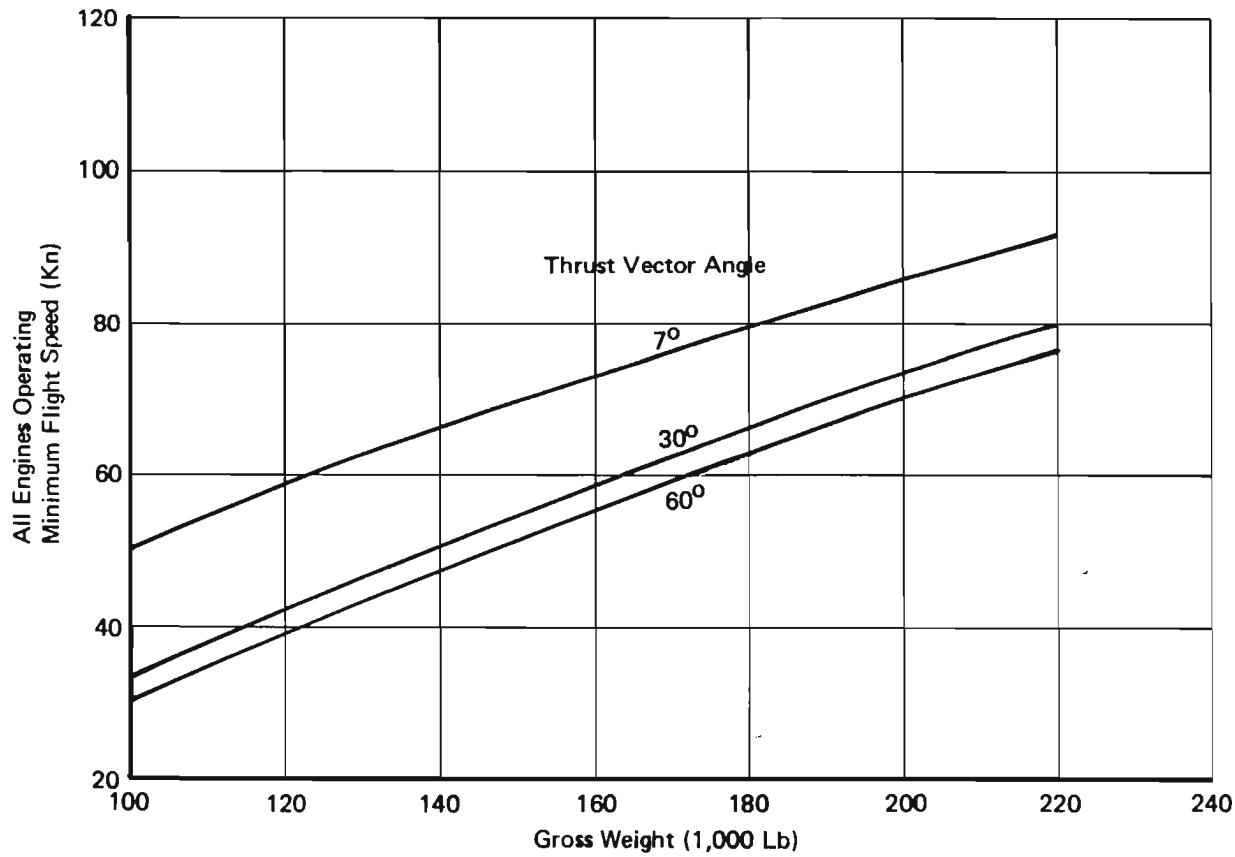

Figure 35: Minimum Flight Speeds — Sea Level Standard

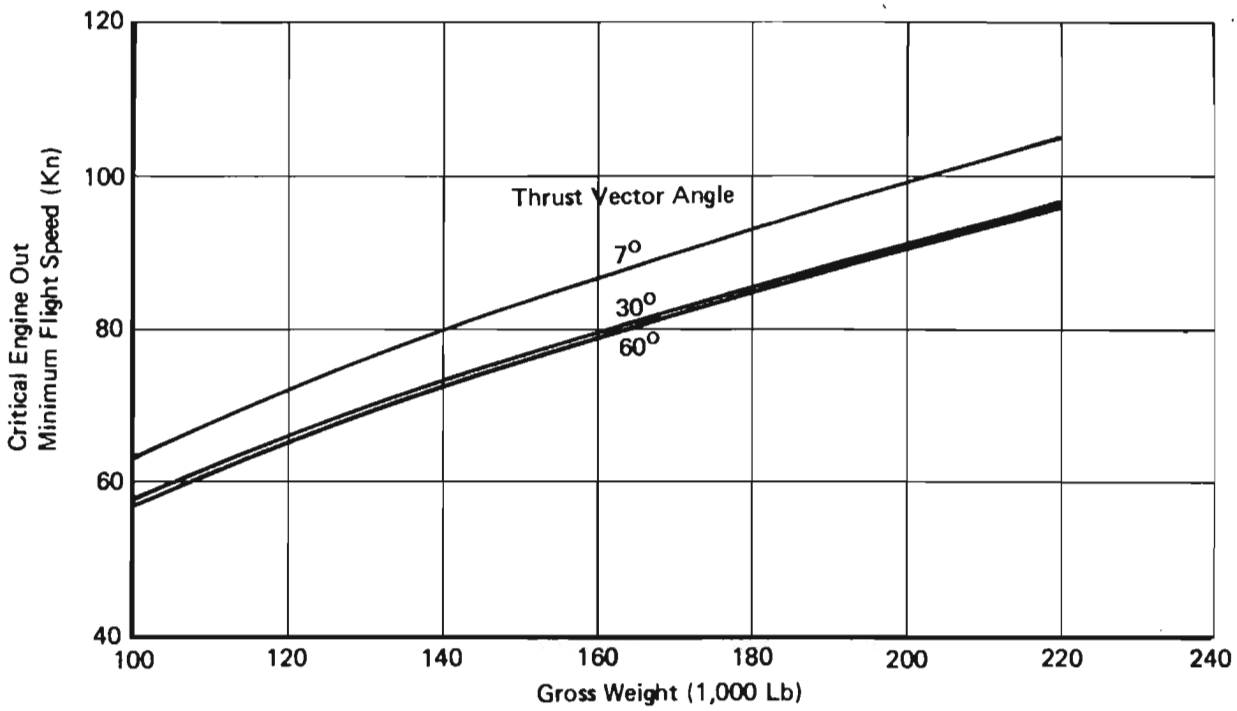

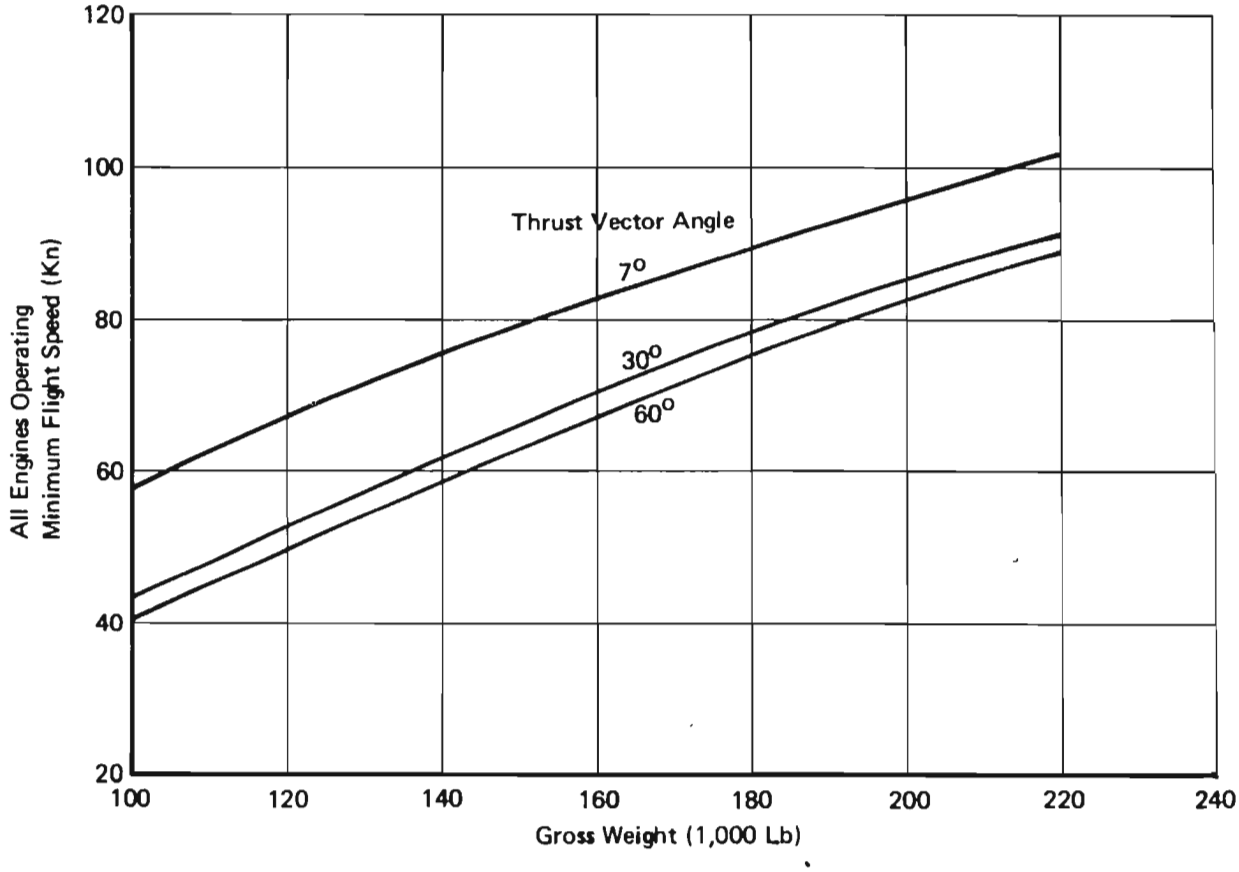

Figure 36: Minimum Flight Speeds – 2,500 Feet/93°F

TABLE II - MISSION SUMMARY

RADIUS MISSION - T.O. DESIGN G.W. = 158000 LB.

	Segment	Distance (n.mi.)	Fuel Used (lb.)	Weight At End Of Segment (lb.)
				158000
(1)	Takeoff	0	2550	
				155450
(2)	Climb	75.5	3130	
				152320
(3)	Cruise-Outbound	424.5	7220	
				145100
(4)	Descent	0	0	
				145100
(5)	Midpoint Landing	0	0	
				145100
(6)	Midpoint Takeoff	0	2550	
				142550
(7)	Climb	86	3200	
				139350
(8)	Cruise-Inbound	414	6550	
				132800
(9)	Descent	0	0	
				132800
(10)	Reserve	0	4800	
				128000
	Payload			28000
	Total	500	30000	100000

FERRY MISSION - T.O. DESIGN G.W. = 167400 LB.

	Segment	Distance (n.mi.)	Fuel Used (lb.)	Weight At End Of Segment (lb.)
				167400
(1)	Takeoff	0	2550	
				164850
(2)	Climb	69	3100	
				161750
(3)	Cruise-Outbound	3632	55500	
				106250
(4)	Descent	0	0	
				106250
(10)	Reserve	0	6250	
				100000
	Total	3701	67400	100000

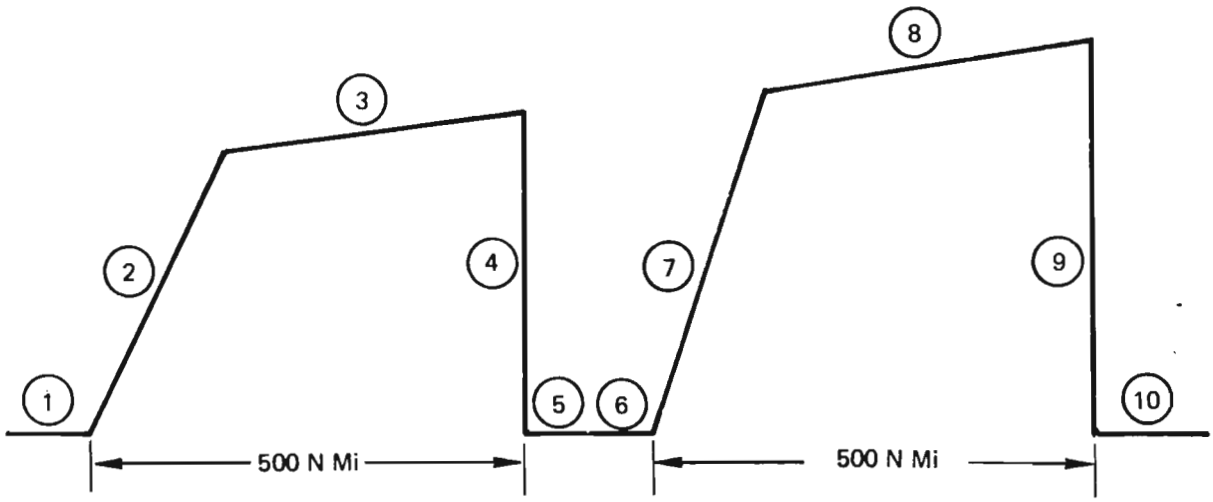

MIL-C-5011A Rules

(6) (1) Taxi, Takeoff and Accelerate to Climb Fuel Allowance is Determined with the Engines Operating at Normal Power for 5 Minutes at Seal Level

(7) (2) Climb Fuel and Distance is Determined at the Speed for Maximum Rate of Climb

(8) (3) Cruise is Performed at the Speed and Altitude for Long Range Cruise

(9) (4) Descent – No Allowance is Made for Range or Fuel Burned in Descent

(5) Midpoint Landing is Conducted Without Refueling and With No Reduction in Payload

(10) Reserve Fuel Allowance is 5 Percent of Initial Fuel Plus 30 Minutes Holding. In Addition, All Fuel Consumption is Increased by 5 Percent to Allow for In-Service Tolerances.

Figure 37: Mission Profile

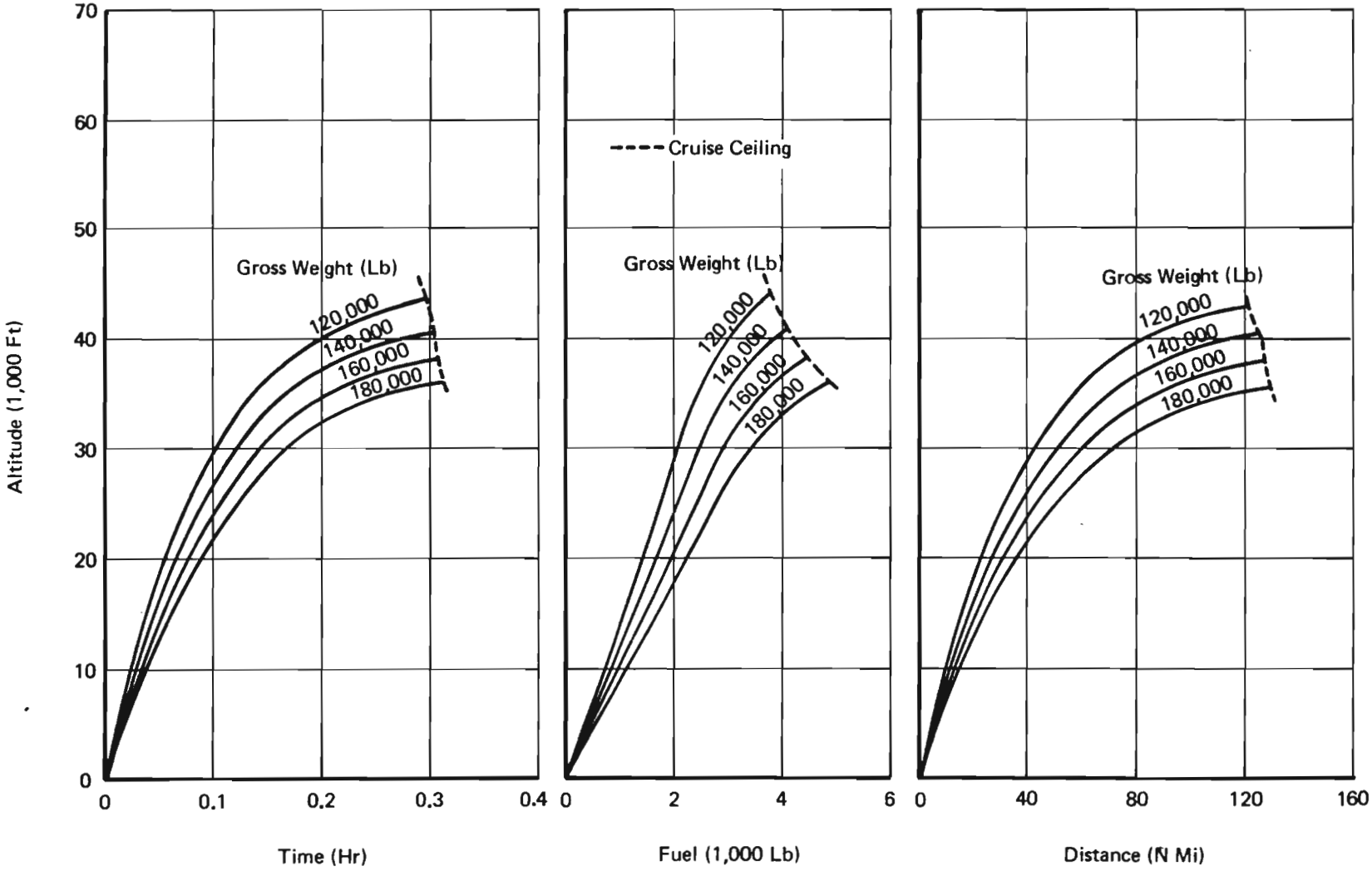

Figure 38: Time, Fuel and Distance to Climb to Cruise Altitude

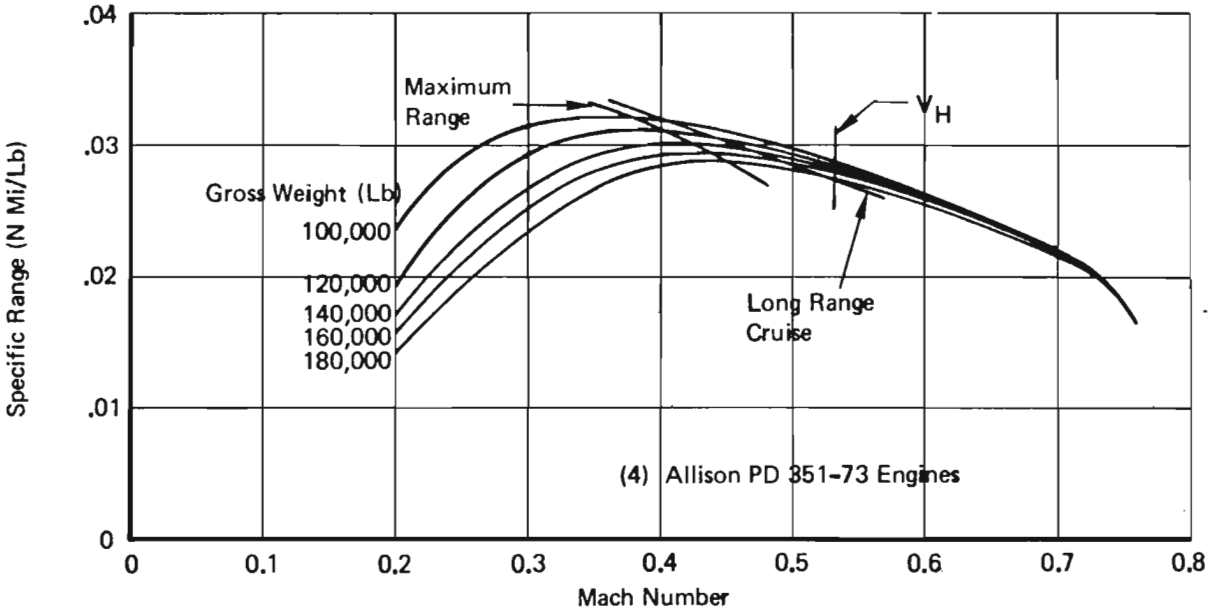

Figure 39: Fuel Mileage at Sea Level – Standard Day

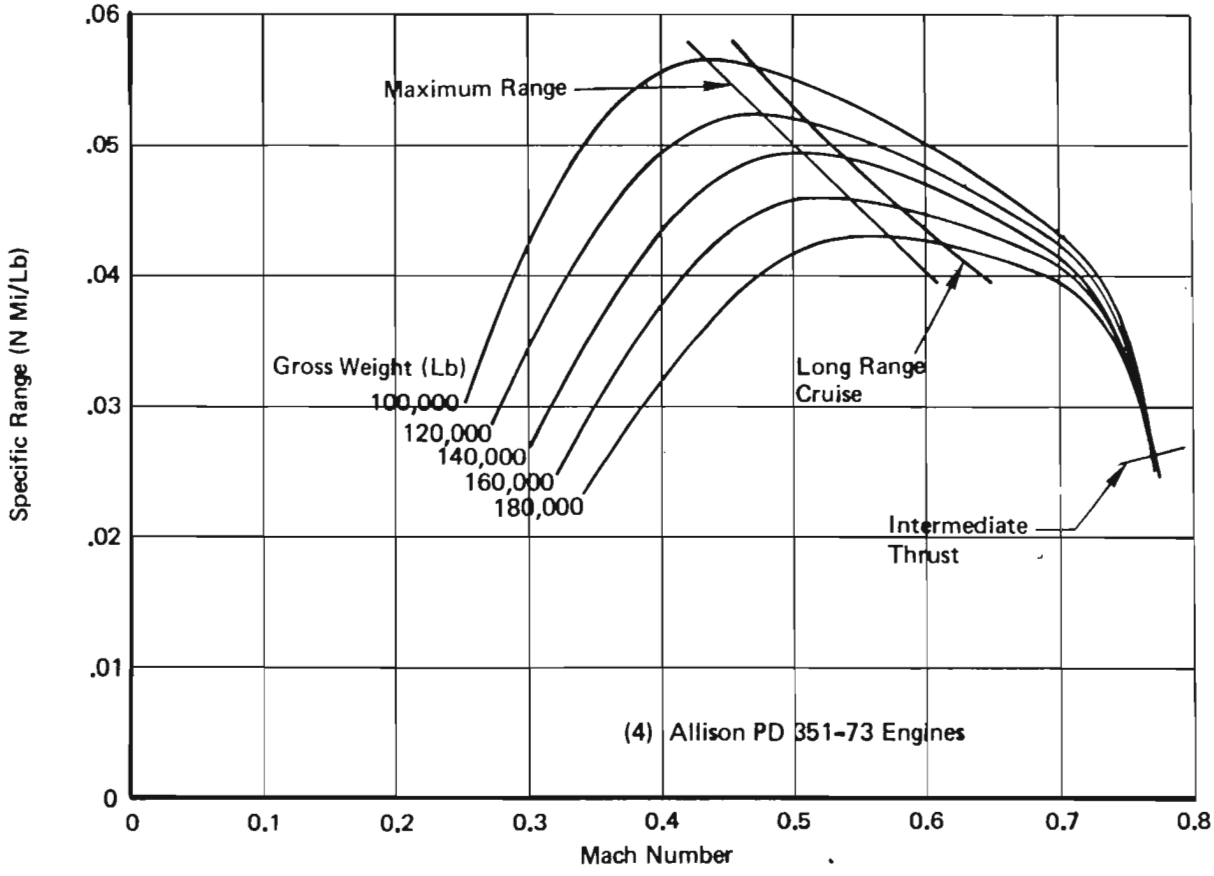

Figure 40: Fuel Mileage at 20,000 Feet – Standard Day

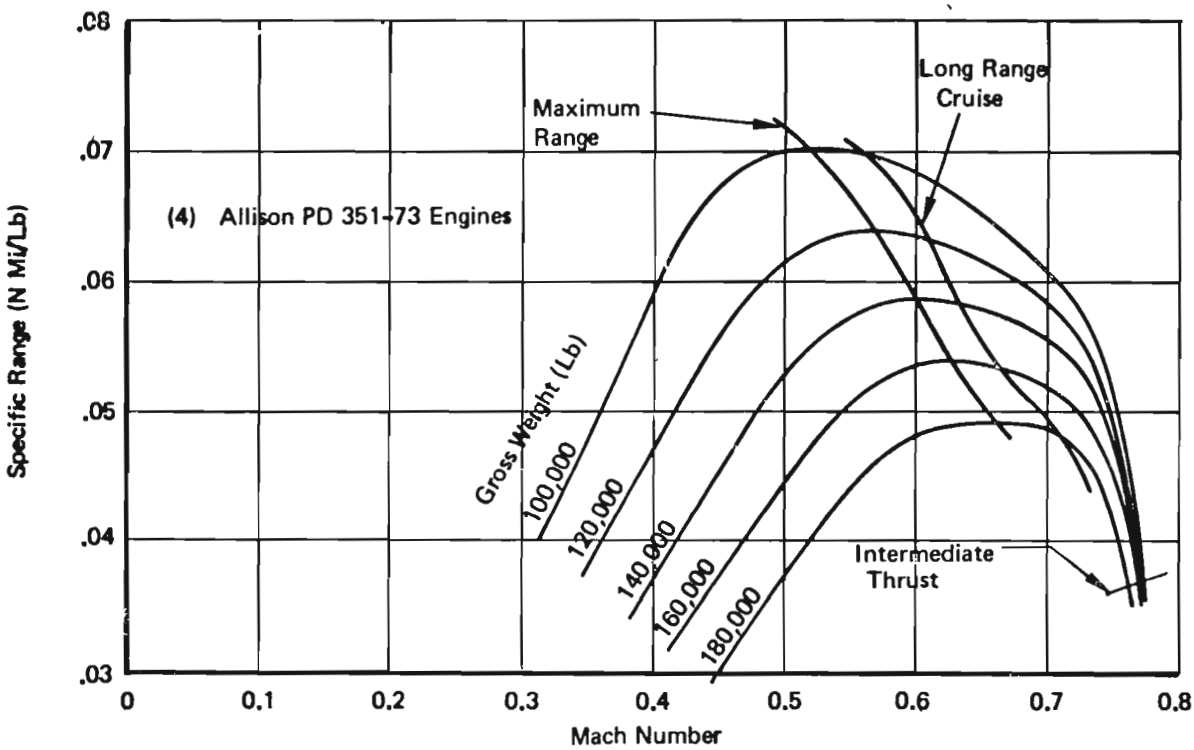

Figure 41: Fuel Mileage at 30,000 Feet — Standard Day

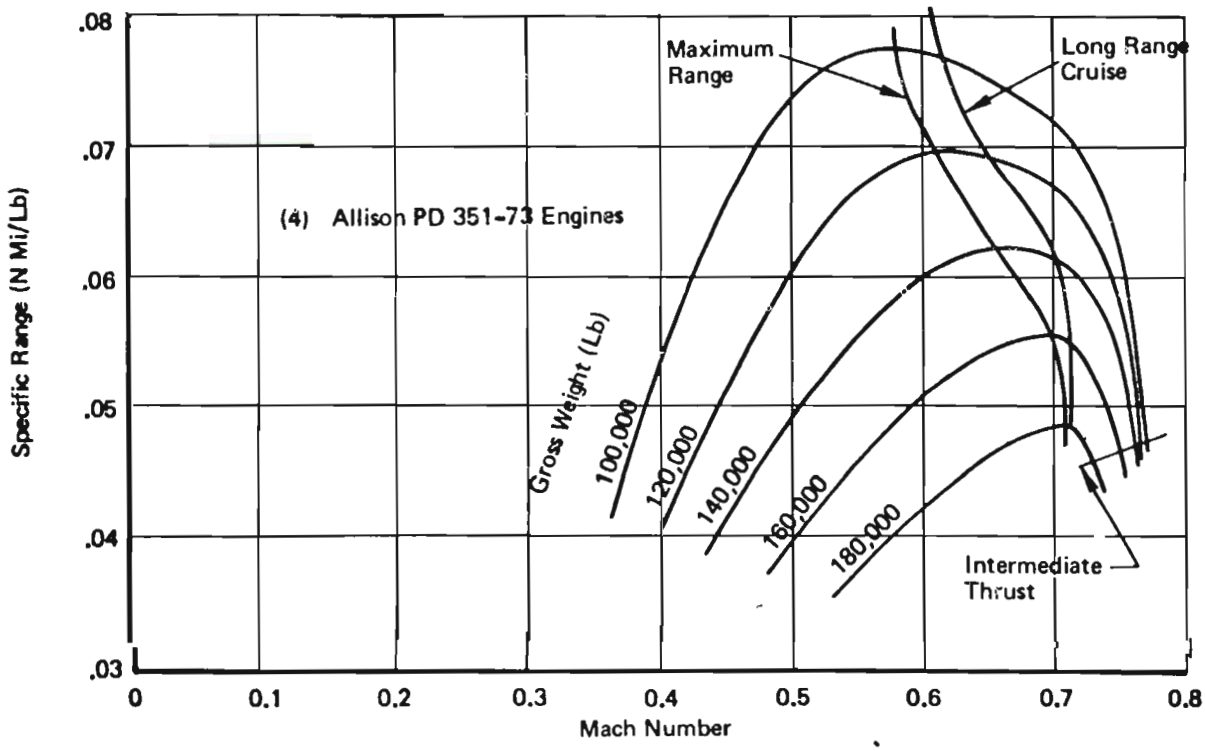

Figure 42: Fuel Mileage at 35,000 Feet — Standard Day

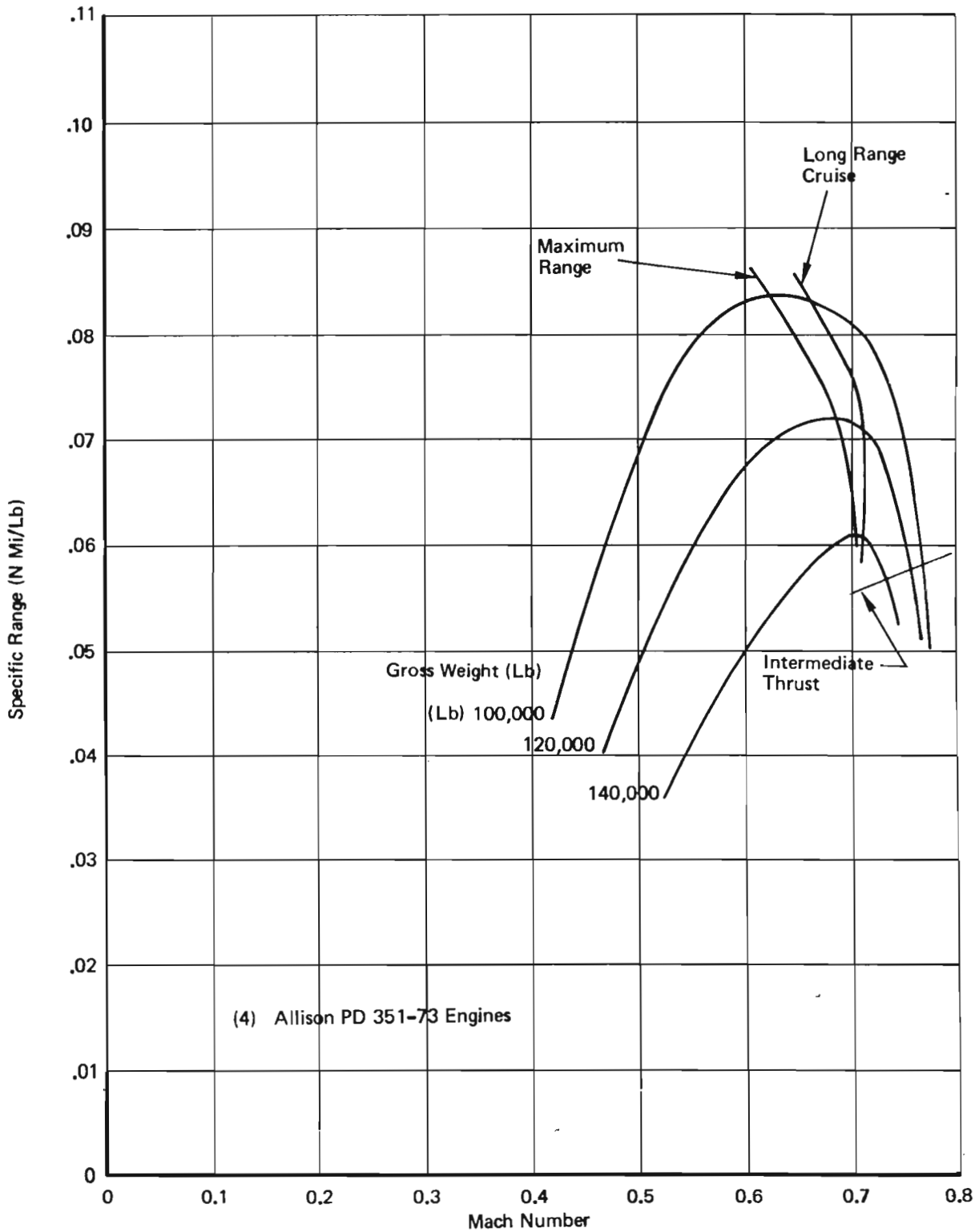

Figure 43: Fuel Mileage at 40,000 Feet — Standard Day

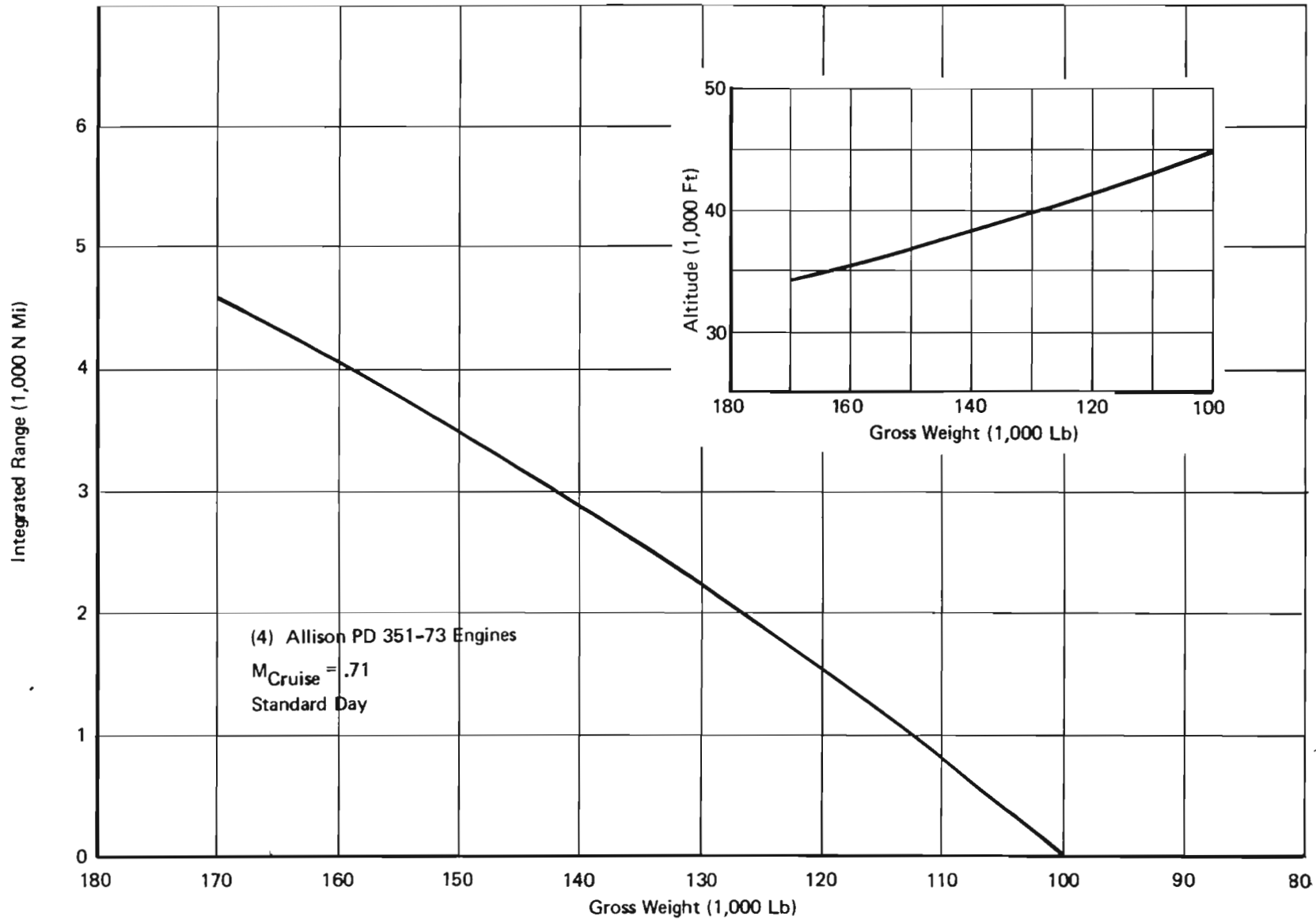

Figure 44: Long Range Cruise Performance

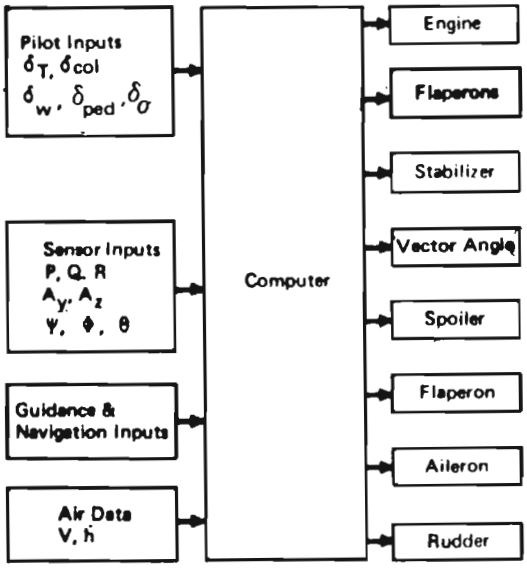

AUTOMATIC FLIGHT CONTROL SYSTEM (AFCS)

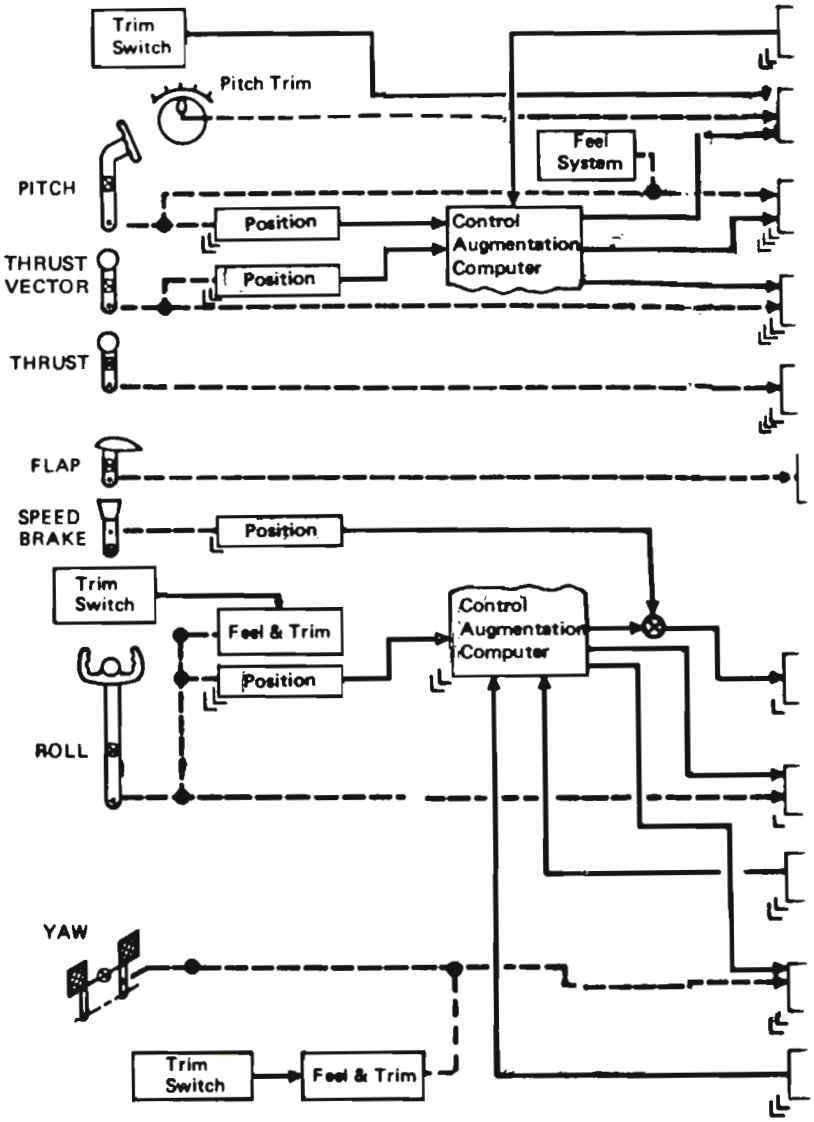

FLIGHT CONTROL SYSTEM

Notes:

1. Path Symbols are:
   - Mechanical
   - Electrical
   - Airplane Motion
2. Parallel redundant electric signal paths and computers are isolated and nonvoting
3. Left-hand corner block symbol indicates degree of redundancy
   e.g.  = 3 elements
4. Control surface symbol includes Power Control and Automatic Flight Control Actuators
5. Pilot Commands
   - δ_T = Thrust
   - δ_{col} = Pitch (Column)
   - δ_w = Roll (Wheel)
   - δ_{ped} = Yaw (Pedal)
   - δ_σ = Vector Angle

CONTROL SYSTEM FEATURES

- MULTIPLE CONTROL PATHS FOR SURVIVABILITY
- MASS BALANCED SURFACES OR DUAL LOAD PATH RESTRAINT
- REDUNDANT CONTROL SYSTEM ON EACH AIRPLANE AXIS
- SUMMED-ELECTRICAL (AFCS) AND MECHANICAL SURFACE CONTROL
- THREE CHANNEL AUTOMATIC FLIGHT CONTROL SYSTEM (AFCS) INCLUDING AUTOMATIC PATH GUIDANCE
- THREE HYDRAULIC SYSTEMS ON EACH AIRPLANE AXIS

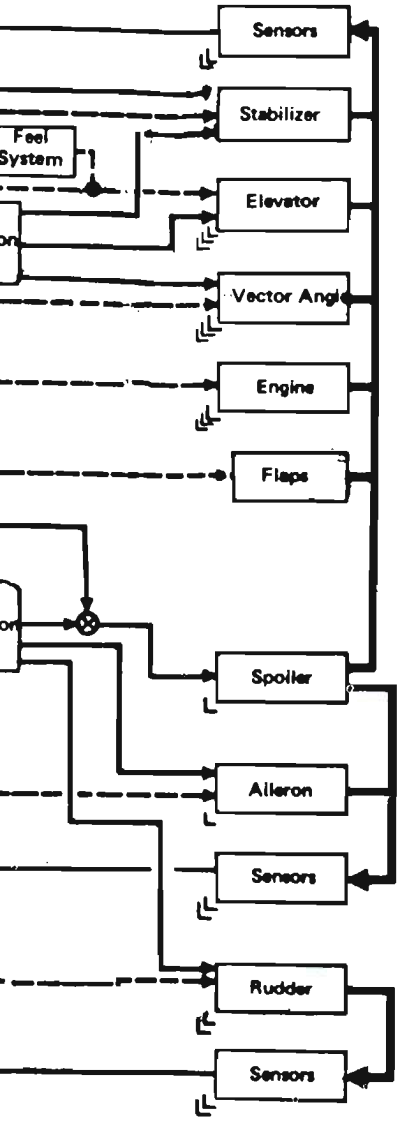
Sensors
Stabilizer
Feel System
Elevator
Vector Angl
Engine
Flaps
Spoiler
Aileron
Sensors
Rudder
Sensors

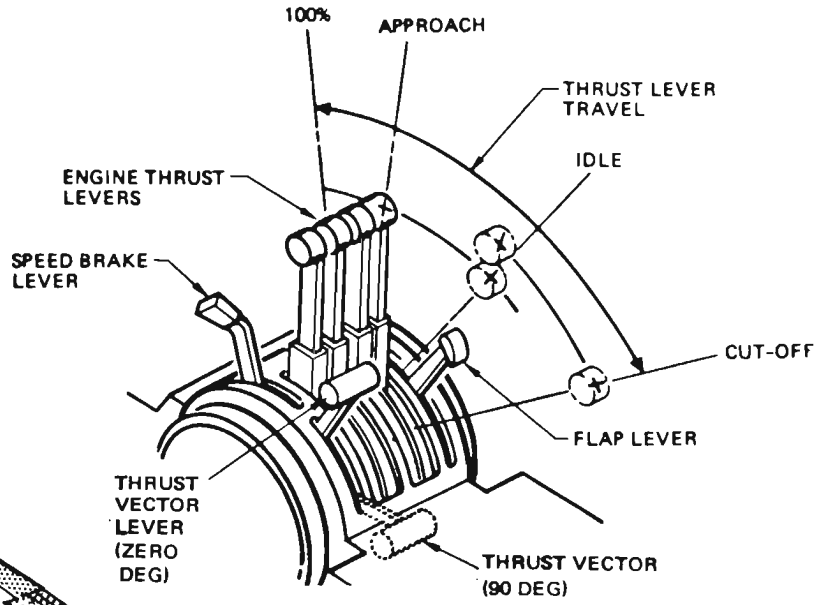
100%
APPROACH
THRUST LEVER TRAVEL
IDLE
ENGINE THRUST LEVERS
SPEED BRAKE LEVER
CUT-OFF
FLAP LEVER
THRUST VECTOR LEVER (ZERO DEG)
THRUST VECTOR (90 DEG)

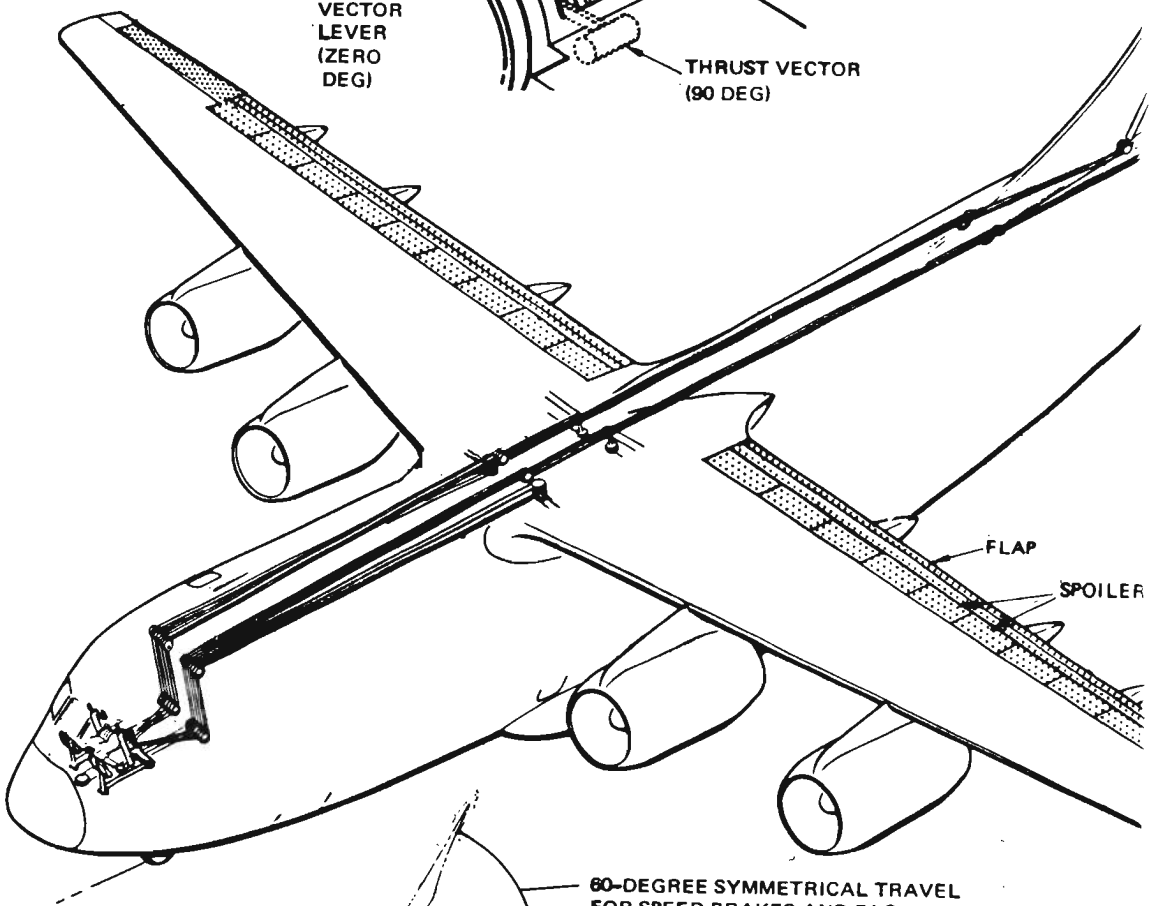
FLAP
SPOILER

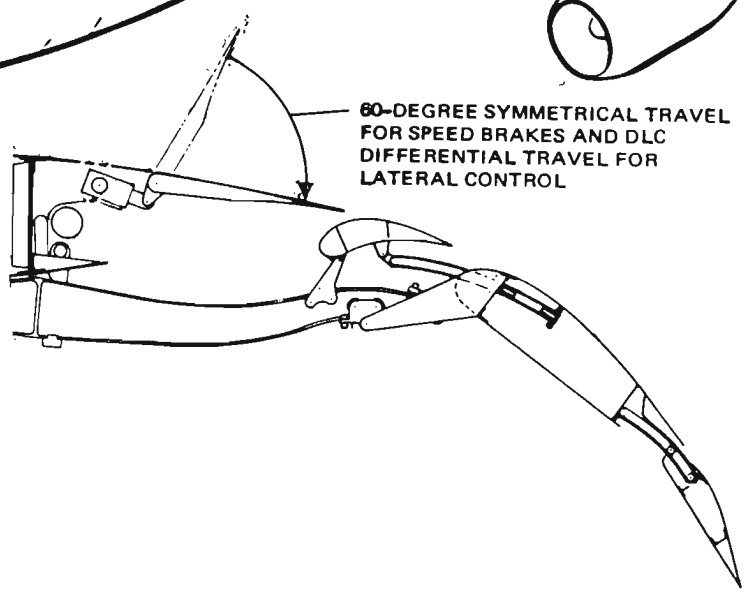
60-DEGREE SYMMETRICAL TRAVEL FOR SPEED BRAKES AND DLC
DIFFERENTIAL TRAVEL FOR LATERAL CONTROL

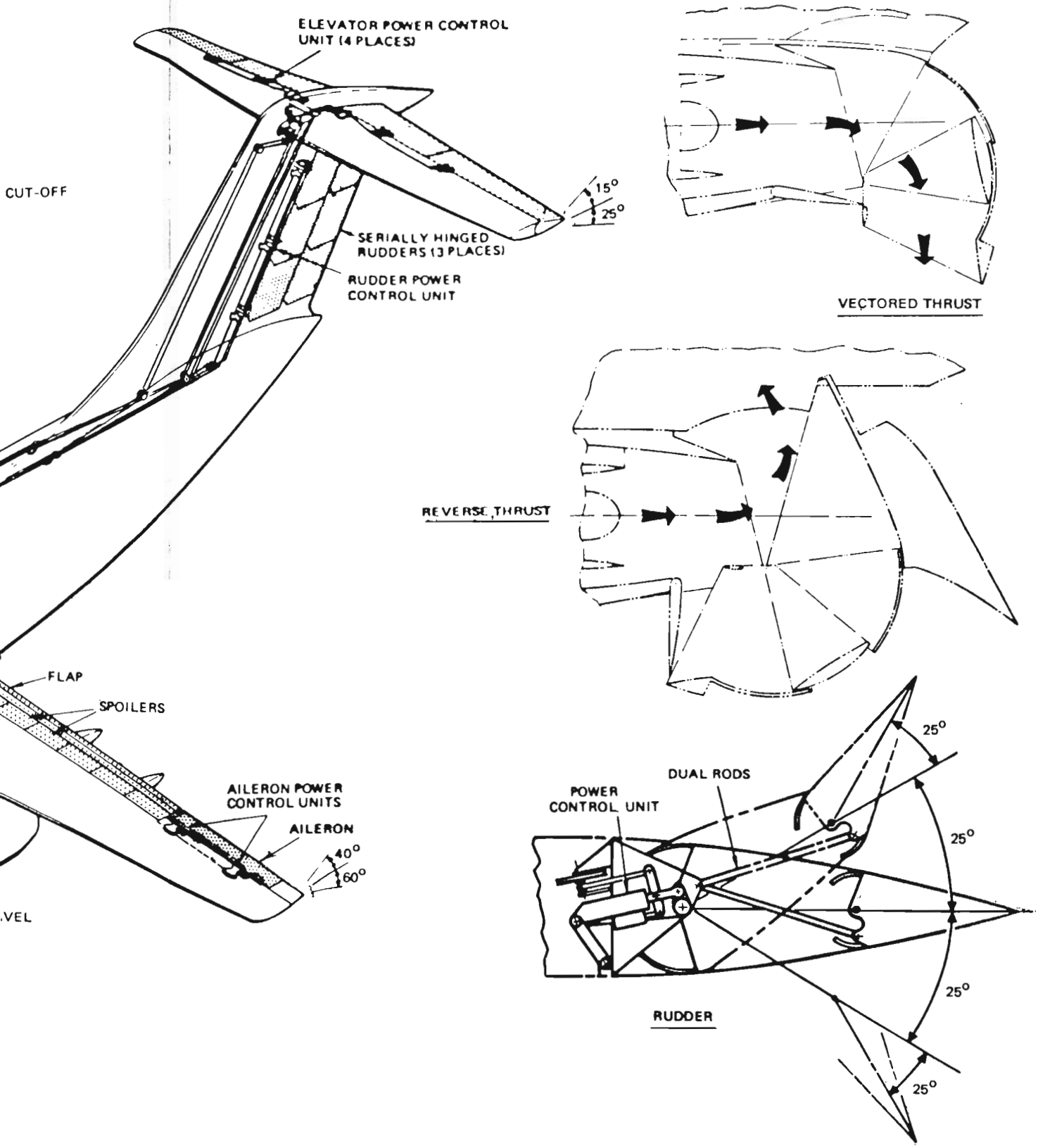

Figure 46: Primary Flight Control System

5.2 Basic Aerodynamic Characteristics

5.2.1 Horizontal Tail

The 953-815 configuration has a "T" tail with an aspect ratio of 4.0 and 10 degrees of sweep. An elevator, with hinge line at 63% chord, is used for maneuvering. Trim is accomplished by controlling the incidence of the stabilizer.

The use of vectored thrust powered lift to achieve STOL performance introduces effects not present (or of negligible magnitude) on conventional airplanes which must be considered in sizing the horizontal tail. These are:

(1) The moment due to the deflected propulsive force of the engines. Because the engine gross thrust is essentially independent of speed, this effect contributes a substantial increment to the speed derivative of the pitching moment coefficient.

(2) Thrust interference effects on the angle of attack derivatives.

(3) Thrust interference effects on the speed derivatives.

The above three effects, together with the power-off aerodynamic center, establish the neutral point of the airplane. The first item, thrust moment, is by far the largest effect for a vectored thrust STOL airplane. Since the balancing aerodynamic moment is negative (i.e. nose down) for the 953-815 configuration, the neutral point is forward of the aerodynamic center. For the takeoff condition, the neutral point is 22% MAC ahead of the aerodynamic center. For the approach condition, the neutral point is 16% MAC ahead of the aerodynamic center.

Horizontal tail volume coefficient requirements are shown in Figure 47. The 953-815 configuration has a horizontal tail volume coefficient of 1.28. Figure 47 shows that, at this volume coefficient, the forward c.g. limit is determined by STOL takeoff rotation and is at 11% MAC. The loading range only extends forward as far as 14% MAC, so adequate longitudinal control power is assured. The close match between CTOL trim and STOL takeoff rotation capability allowed the utilization of the simpler conventional single hinge elevator.

Aft. c.g. limits are set by minimum stability considerations. Figure 47 shows that with the flaps up the aerodynamic center is at 54% MAC, which is about 30% MAC aft of the neutral point in the climbout or approach condition. In the approach and climb conditions the neutral points are at 21.5% MAC and 26% MAC, respectively. The loading range extends to 28% MAC causing a speed instability of 6.5 percent MAC. However, results of the control system trade study showed that the control augmentation system alters the airplane response characteristics to provide good STOL flying qualitites for a speed instability of up to 16 percent. The 6.5 percent figure would be applicable to SAS "off" operation and will provide Level 3 capability.

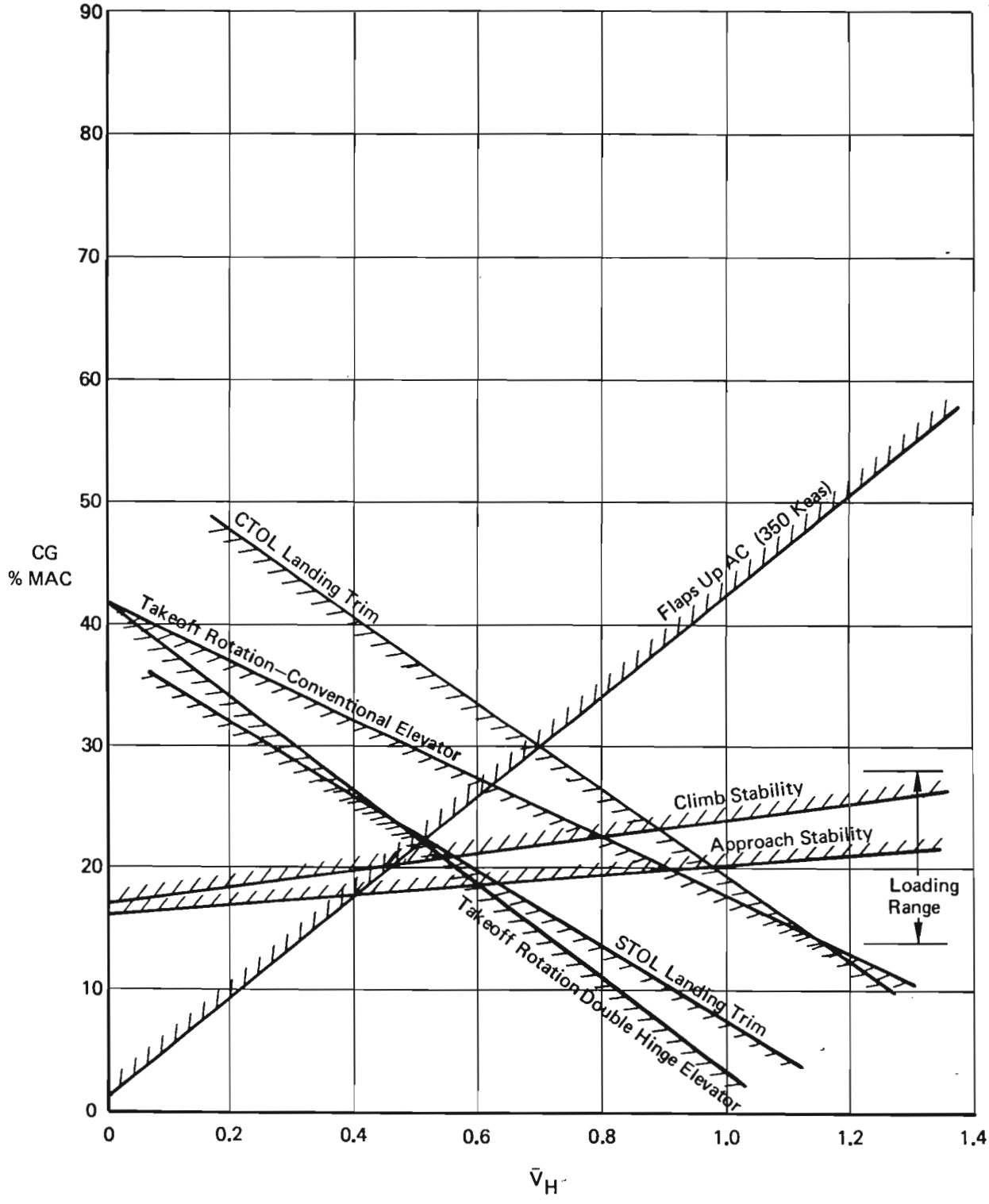

Figure 47: Horizontal Tail Size

5.2.2 Vertical Tail

The vertical tail is a constant chord surface with 37 degrees of sweep and an aspect ratio of 1.0. The rudder is double hinged with the hinge lines at 63% and 77% chord. The vertical tail volume coefficient is .112.

Vertical tail size is determined by directional stability requirements, control during a crosswind landing, or yawing moment required to balance an engine failure. For the 953-815 configuration, the critical case is the yawing moment due to an outboard engine failure. Figure 48 shows the yawing moment requirement for an engine failure during the takeoff ground run. With the aid of nose wheel steering, the pilot can maintain a straight path along the ground, following engine failure, down to a speed of 66 knots at a gross weight of 120,000 lbs. or 63 knots at a gross weight of 160,000 lbs. Since V_1 is 73 knots, ample control is available to handle an engine failure on takeoff.

5.2.3 Roll Control

The roll control system consists of wing mounted spoilers and blown ailerons. The spoilers have a 22 inch chord and extend from 15% to 67.5% semispan. The ailerons extend for 67.5% semispan to the wing tip with the hinge line at 75% chord. Boundary layer control (BLC) is used on the ailerons. BLC extends the linear range of the ailerons and allows the use of higher deflection angles. Enough energy is added so that the ailerons are effective up to deflection angles of 60 degrees.

The critical roll control case occurs with an outboard engine failure when the thrust is vectored vertically. With the outboard engine at 51% semispan and a thrust coefficient of .5 on each engine, a rolling moment coefficient of .128 will result due to the effect of direct thrust. An additional increment of as much as .03, depending upon angle of attack, may be present due to thrust-aerodynamic interference affects. Therefore, enough roll control is required to be able to produce a rolling moment coefficient of .16, plus that needed for maneuver. Roll control power is shown in Figure 49. About 85% of the rolling moment required to balance an outboard engine failure is available from the ailerons, minimizing the required spoiler deflection. When an engine failure occurs it is important to keep the required spoiler deflections small in order to minimize the lift loss and the drag increase. Most of the spoiler power is available for maneuver following an engine failure.

5.3 Control Augmentation System

5.3.1 Design Requirements

The Boeing Model 953-815 exhibits conventional flying qualities at all speeds except the extremely low speeds needed for STOL performance. Because of the basic airplane flight characteristics inherent in powered lift at high lift coefficients, a control augmentation system is required to achieve superior flying qualities during STOL flight. Conventional flight requires only a yaw damper.

Control of an airplane at STOL flight speeds requires larger control surfaces and improved control surface effectiveness because of the low dynamic pressure. Without control augmentation high $C_{L_{max}}$ STOL airplanes exhibit poor turn coordination, low spiral stability, and long flight-path time constants. Control quickening and response damping is required to achieve routine operational STOL landings and takeoffs. The control augmentation system was designed specifically for precise path control in the STOL flight mode. The control surface configuration provides fine resolution, rapid response, and redundancy. The redundancy is sufficient to complete a STOL landing following any single failure. Crosswind and engine-out control power requirements have been met.

5.3.2 System Concept

The control augmentation system utilizes both pilot command and airplane response feedback signals to provide superior STOL flying qualities. It allows individual engagement of the lateral/directional, longitudinal, and speed modes. The lateral/directional mode provides roll rate command. The longitudinal mode provides pitch rate command. The speed mode provides airspeed command and hold. Separation of these modes allows the pilot more flexibility in his descent and deceleration pattern.

Flightpath and attitude changes are accomplished through the control column. STOL speed changes are made by moving the thrust vector control (Figure 50). The attitude, attitude rate and speed feedback signals automatically compensate for the coupling between thrust and attitude changes, increase attitude damping, and reduce the airplane sensitivity to gusts. The same signals correct for nonlinearities of the pitching moments at high angles of attack. Precision flightpath control is enhanced by providing pilot control of speed and pitch attitude free of interactions. Pilot ratings obtained in simulated IFR tracking averaged 2.5 for the augmented system. With the augmentation disengaged, the rating deteriorated to 7.0.

Since the control augmented lateral/directional system (Figure 51) provides good turn coordination, heading changes are generally accomplished with the wheel only, although small heading corrections can be accomplished with the rudder. The turn coordination

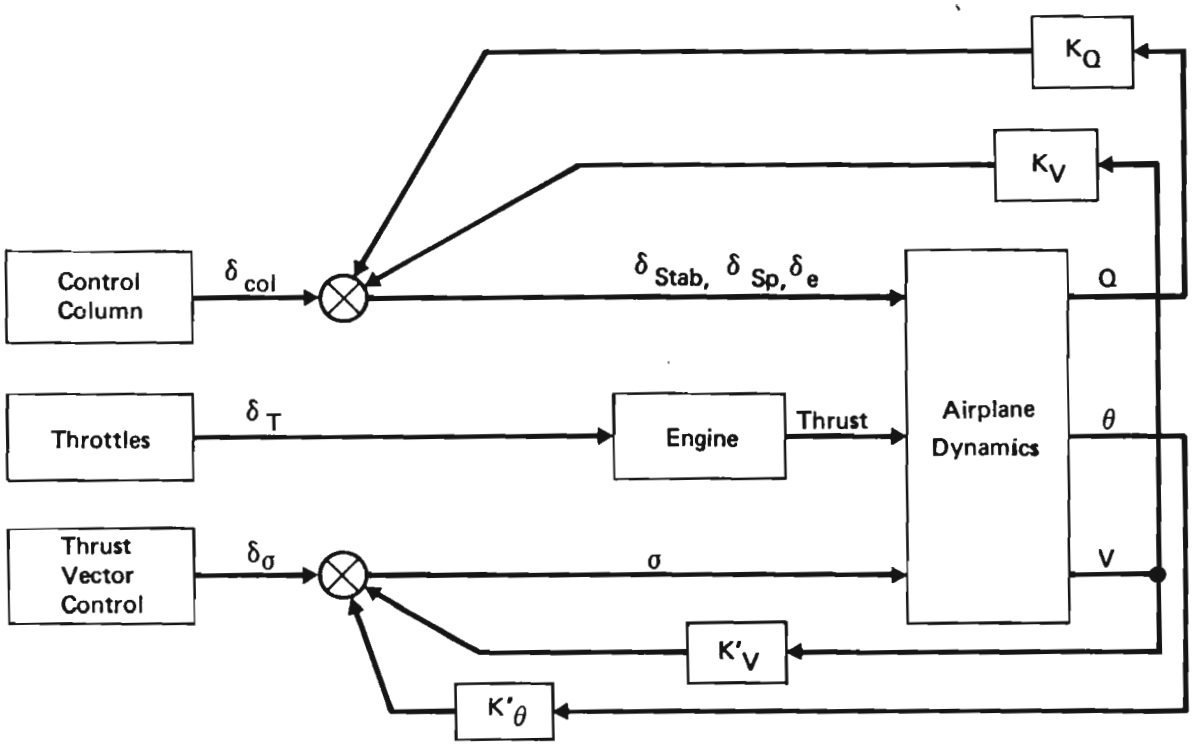

Figure 50: Longitudinal Control Augmentation System

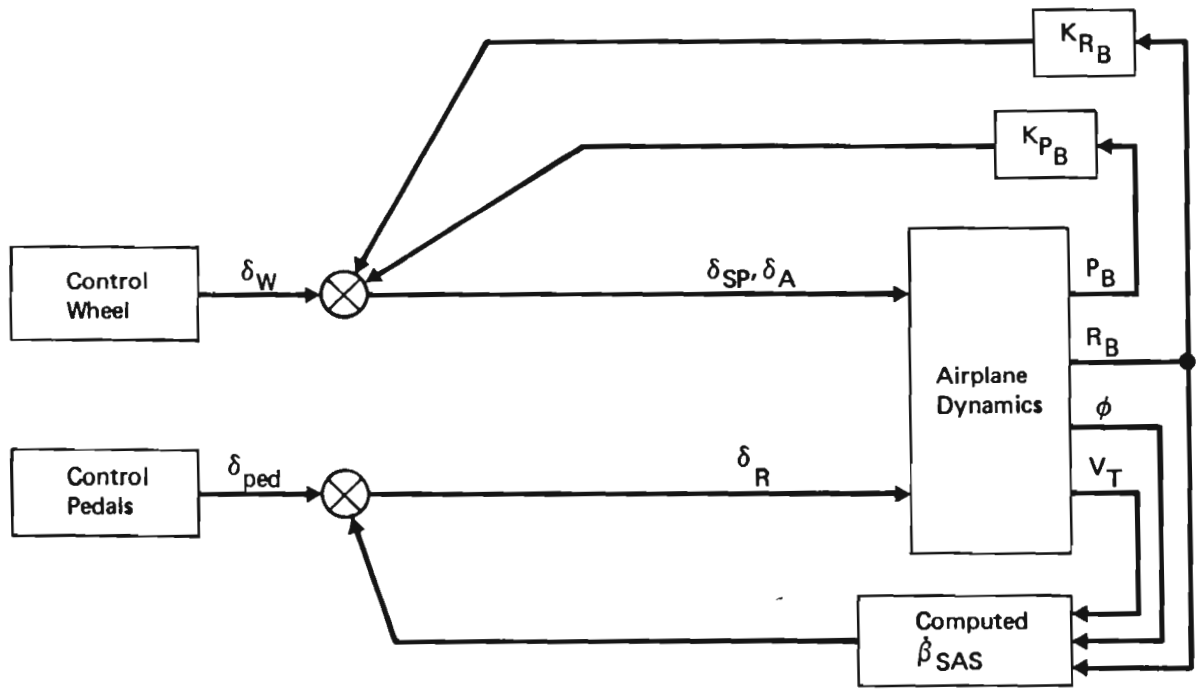

Figure 51: Lateral/Directional Control Augmentation System

is provided by the computed slideslip feedback to the rudder. The roll rate and yaw rate feedback to the lateral axis improve roll response and spiral mode characteristics.

Pilot ratings were obtained in simulated IFR tracking and averaged 2.5 for the augmented lateral directional system. With the augmentation disengaged, this rating deteriorated to 9.0.

SECTION VI

STRUCTURES AND WEIGHT

6.1 Structural Analysis

6.1.1 Structures Description

The airframe structure consists primarily of conventional, state-of-the-art aluminum components which have been sized in sufficient detail to provide "Class II" weight estimates.* The airplane configuration and its principal characteristics are shown in Figure 2. The inboard profile, shown in Figures 3 and 4, provides details of the major structural components described in this section. Table IV lists materials.

6.1.1.1 Body

The body is designed with a conventional aluminum stiffened sheet metal shell and frames. The pressurized cabin extends from the forward bulkhead, over the nose wheel well, under the wing and aft to the fin rear spar bulkhead. The cab structure has frames at 10-inch spacing continuously attached to the skin. The cargo compartment monocoque structure is skin-stringer construction, stabilized by frames. Frames forward of the constant section are locally attached to the skin to resist bending in the flat areas due to cabin pressure. Cargo compartment frames are basically at twenty-inch spacing to obtain minimum weight in monocoque and cargo floor and are attached to the skin only at the floor level. The aft body monocoque structure is skin-stringer construction, stabilized by upper frames at approximately 20-inch spacing, with box section longerons above the cutout for the ramp and cargo door. The tail cone is nonpressurized fiberglass construction with full ring frames at 40-inch spacing.

Entry doors at the forward end of the cargo compartment are overhead opening plug type doors and are opposite installations. Troop jump doors at the aft end of the cargo compartment are identical overhead opening plug type doors positioned at floor level. A portion of the main landing gear fairing articulates to provide jump clearance. A hinged cargo loading ramp and an inward opening door with actuating and latching systems are installed in the aft body. The cargo floor includes cargo tie-downs and cargo pallet/airdrop pallet handling provisions. Some of the major features of this body are:

- Constant circular cross section in major portion of the body to minimize weight of pressure vessel and minimize cost of parts and tooling.

---

* "Class I" weights are parametric or statistical.
"Class II" weights are based on dimensions, areas, etc. of major components sized to carry the computed loads.

Table IV: Structure Materials

Component	Material
Wing Skin & Stringers - Upper	7075-T6
Wing Skin & Stringers - Lower	2024-T3
Wing Spars	
Upper Chords	7075-T6
Lower Chords	2024-T3
Webs	2024-T3
Flaps & Fairings	Fiberglass H/C
Control Surfaces	Aluminum H/C
Tails	7075-T6
Body	
Skins	2024-T3 Clad
Stringers & Frames	7075-T6 Clad
Bulkheads & Longerons	7075-T73
Landing Gear	4340M Var (275 - 305 ksi)
Windows & Windshields	Stretched Acrylic & Glass
Engine Pylons	6Al-4V Ti & 2024-T3 Clad
Thrust Vectoring & Reversing	347 Stainless Steel

- Maximum use of common skin-stringer-frame details.

- Circular aft body cross section above ramp and door longeron to minimize pressure induced bending.

- Main landing gear does not penetrate body pressure shell.

6.1.1.2 Wing

The wing is designed with conventional stiffened aluminum panels, spars and ribs, with leading and trailing edge devices attached to the front and rear spars respectively. Both the upper surface and lower surface inspar panels have skins stiffened by zee sections oriented spanwise. The panels are pre-formed in the streamwise direction and draped onto the gentle spanwise contour. The spars are continuous members with no splices in the highly loaded center wing. They have upper and lower chords, webs, and stiffeners. The stiffeners are zee and tee sections. Separate fittings attached to the spars provide support for high lift and control devices. All structural box ribs are oriented streamwise and consist of upper and lower chords, web, and zee stiffeners with many common parts. The structural box is an integral fuel tank with access doors in the lower outboard section for inspection and maintenance.

The leading edge variable camber flaps extend from body intersection outboard to the wing tip interrupted at the engine support struts. They consist of fiberglass panels supported by machined ribs attached to the front spar. The fiberglass flap panel is extended by a rotary actuator.

The triple-slotted trailing edge flaps, spoilers, and ailerons are of bonded honeycomb panel construction.

Some major features of the wing are:

- Damage tolerant skin-stringer multiple panels

- 113-foot-long skin panels, stringer, and spars eliminate splices in the highly-loaded center wing and reduce part number count by 50 per cent

- Variable camber leading edge flap panels with boundary layer control (BLC)

- Triple-slotted trailing edge flaps

- Ailerons with BLC

- Trailing edge spoilers interchangeable LH to RH

- Engine nacelles interchangeable

6.1.1.3 Horizontal Tail

The horizontal tail is designed with conventional aluminum skin, spar, and rib construction. The multispar box with dual load-paths provides damage tolerance.

6.1.1.4 Vertical Tail

The vertical tail is designed with conventional stiffened aluminum panel, spar, and rib construction. Its constant airfoil section allows the multiple use of parts such as leading edge ribs, inspar ribs, rudder supports, actuators and supports, and rudder assemblies. The multiple load paths provided by the skin-stringer construction attached to multiple body bulkheads and frames results in a damage tolerant structure.

6.1.1.5 Landing Gear

The model 953-815 will be capable of 400 passes on CBR = 6.0 field conditions at 150,000 pounds gross weight, with high flotation tires of a type already in service on the Boeing 737. The same size tires are used on both nose and main gear wheels. The gear is designed to turn the aircraft at 4 knots in less than 100 feet of runway width using nose wheel steering.

Main Landing Gear

Each main landing gear is supported by a stationary leg attached to the body frames. The lever-arm is pivoted at the lower end of the leg with sufficient angular excursion to provide for the total axle travel of 35 inches plus an additional travel to permit the arm to be retracted into the gear pod in flight.

The air-oil shock absorber strut reacts the moments in the lever and provides compression and recoil damping during landing, takeoff, and taxi conditions. The shock absorber strut is attached to the stationary leg by means of a linkage and lock system that locks the gear down, raises the lever, and locks the gear up in flight. Access to the lock from within the body is provided to install the ground lock-pins, and to effect emergency unlocking in-flight in the event of damage or failure of the normal control system.

Towing and jacking provisions are incorporated in all main gears.

The landing gears are housed within fairing pods attached to the body. The wheel-well cavities are covered by double-hinged full length landing gear doors. The doors are hydraulically actuated and sequenced, and can be manually released to gain increased access for tire and brake changes.

Nose Landing Gear

The nose landing gear is of the fully articulated, aft retracting design. By retracting the gear aft, the nose gear can be mounted as far forward as possible, thus reducing loads, improving steering, and providing generous access for towing and tire maintenance while retaining a simple door system.

The outer cylinder incorporates integral trunnion arms, drag brace lugs, steering collar lugs, and journal. The lever pivot tube rotates on bushings on the outside of the outer cylinder, and is steered by torque applied through a disconnect link connected to the steering collar. For towing the airplane beyond the normal steering limits, the disconnect link is disconnected from the steering collar by removing a quick release pin.

The lever arm is pivoted on the lever pivot tube and provides for a total axle stroke of 23 inches. The lever arm is connected to the shock absorber piston by means of a ball-ended link.

Primary airplane tow-bar connection is an extension of the lever pivot pin forward of the tires. Clearance is provided to rotate the nose gear $\pm$ 90° with flat shock strut.

The nose gear doors are of conventional clamshell design. The forward pair are connected to the outer cylinder by push rods, and the aft doors are hydraulically driven and sequenced to re-close after the gear is down and locked.

6.1.2 Structural Design Criteria

Requirements of specifications MIL-A-008860A (USAF) thru MIL-A-008870A (USAF) have been met except as noted here.

6.1.2.1 Design Weight Definitions

- Maximum Design Weight ($C_{Transport}$)
  Weight of the airplane with maximum internal payload (58,000 lbs) and full internal fuel.

- Basic Flight Design Weight ($C_{Transport}$)
  Maximum Design Weight less center wing tank fuel.

- Basic Flight Design Weight ($C_{Assault}$)
  Weight of the airplane with primary mission payload (28,000 lbs) and primary mission fuel.

- Alternate Flight Design Weight ($C_{Assault}$)
  Basic Flight Design Weight ($C_{Assault}$) less fuel used in arriving at the midpoint of the primary mission. Applicable to:

a) Landing and ground handling on semi-prepared fields.
b) STOL takeoff
c) Flight loads

- Landplane Landing Design Weight (CTOL)
  Maximum Design Weight ($C_{Transport}$) less half internal fuel.

- Landplane Landing Design Weight (STOL)
  Same as Alternate Flight Design Weight ($C_{Assault}$). Applicable to STOL landing.

6.1.2.2 Design Data

- Design weights and applicable load factors are presented in Table V for the 953-815

- Actual and structural center of gravity envelopes are shown in Figure 52.

- Structural design airspeeds for the clean configuration are shown in Figure 53 . Flap placard speeds are found in Figure 54.

- V-n diagrams for the basic configuration at maximum design weight, and basic flight design weight both assault and transport are presented in Figures 55 thru 57 . Landing and take-off configuration diagrams are shown in Figure 58.

- Design limit sinking speeds are:

	Landplane Landing Design Weight	Maximum Landing Design Weight
CTOL	10 FT/SEC	6.0 FT/SEC
STOL	15 FT/SEC	Not applicable

6.1.3 Stress Analyses

Stress analyses of the body, wing, and tails were performed to size the primary structural members. The structures are designed to withstand the flight and ground handling loads discussed in Section 6.1.4.

The stress analyses were performed using conventional preliminary design methods based on linear beam theory. The effects of combined shear, moment, and torsion loads and the resulting combined stresses are included.

The design criteria requirements of Section 6.1.2 are also incorporated in the analyses. The structures are designed to prevent failure at ultimate loads and pressures and to exhibit no detrimental deformations when subjected to limit loads. Material properties and

Table V: Design Weights and Load Factors

Design Condition	Weight (lb)	Maneuver Load Factor (Limit)
Maximum Design Weight	225,400	2.0, 0.0
Basic Flight Design Weight (Tranport)	204,800	2.5, -1.0
Basic Flight Design Weight (Assault)	158,000	3.0, -1.0
Alternate Flight Design Weight (Assault)	145,000	3.0, -1.0
Landplane Landing Weight (CTOL)	191,700	2.5, -1.0
Landplane Landing Weight (STOL)	145,000	3.0, -1.0
Maximum Landing Weight (CTOL)	222,350	2.0, 0.0
Minimum Flying Weight	102,760	3.0, -1.0
Zero Fuel Weight (Assault)	128,000	3.0, -1.0
Zero Fuel Weight (Transport)	158,000	2.5, -1.0

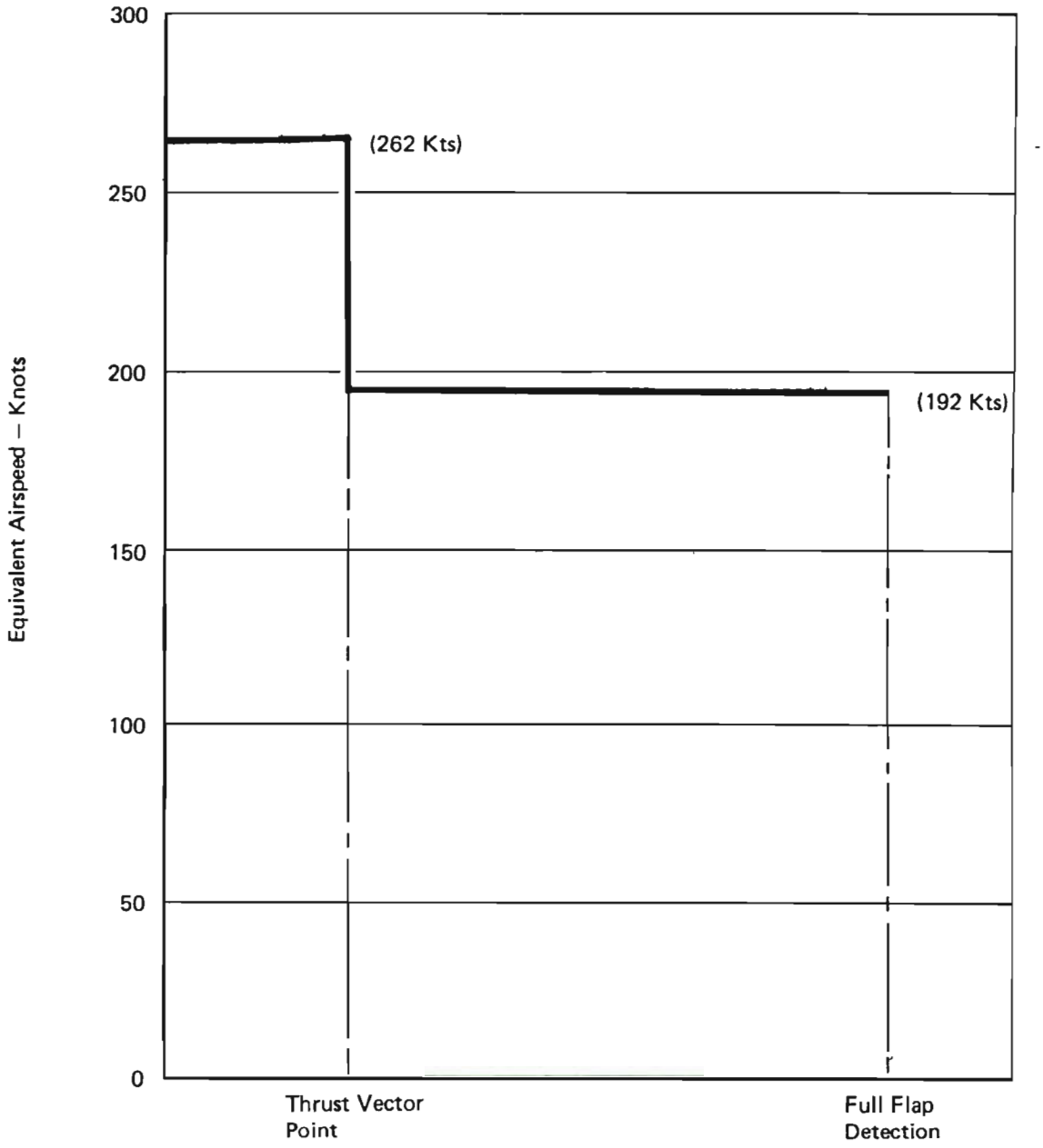

Figure 54: Variation of Flap Placard Speed (V_{LF}) With Flap Deflection

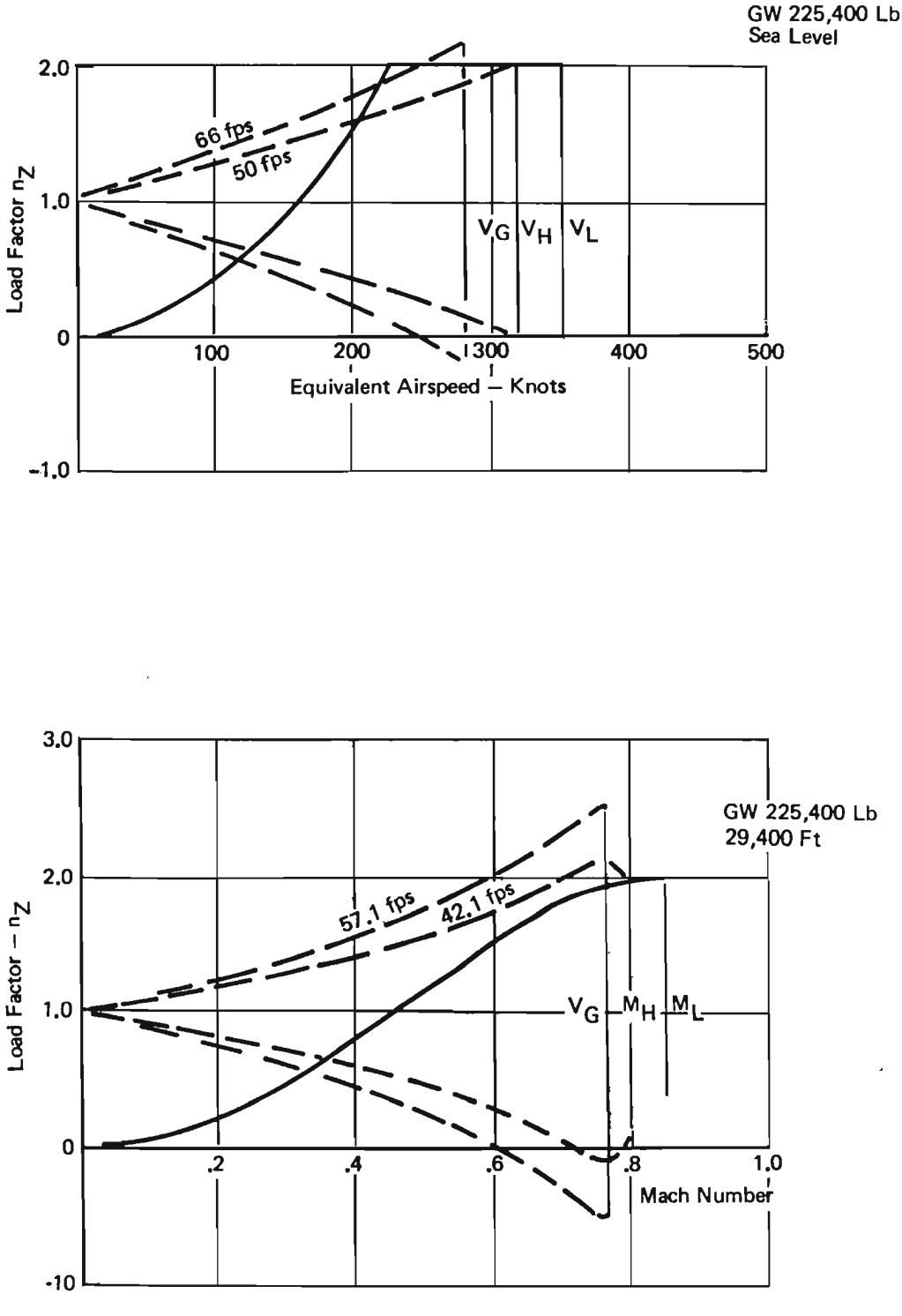

Figure 55: V-n Diagrams – Maximum Gross Weight

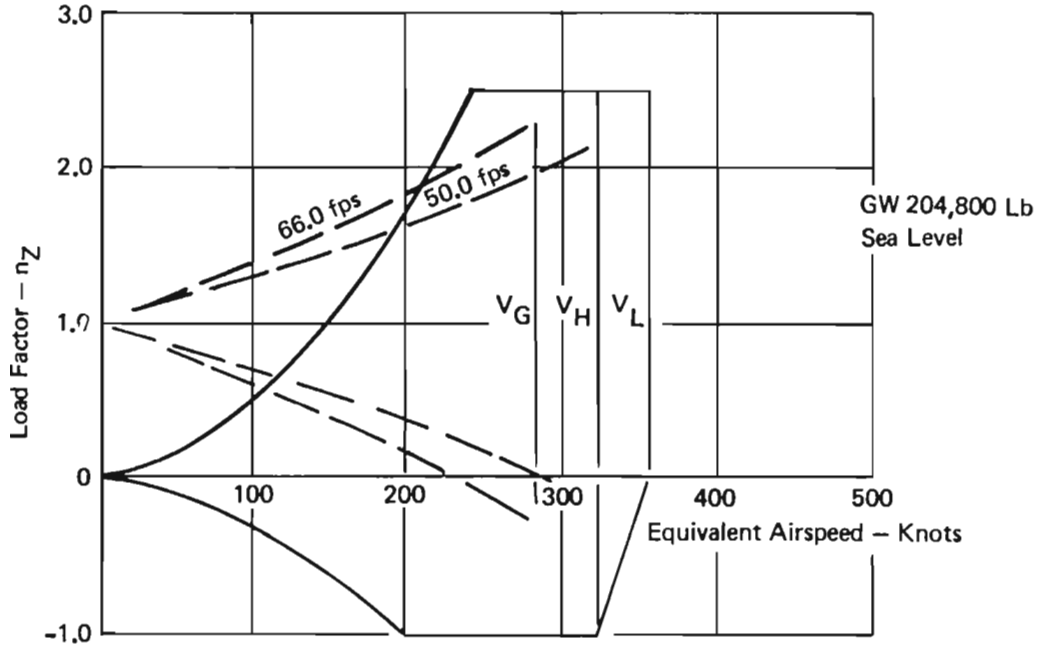

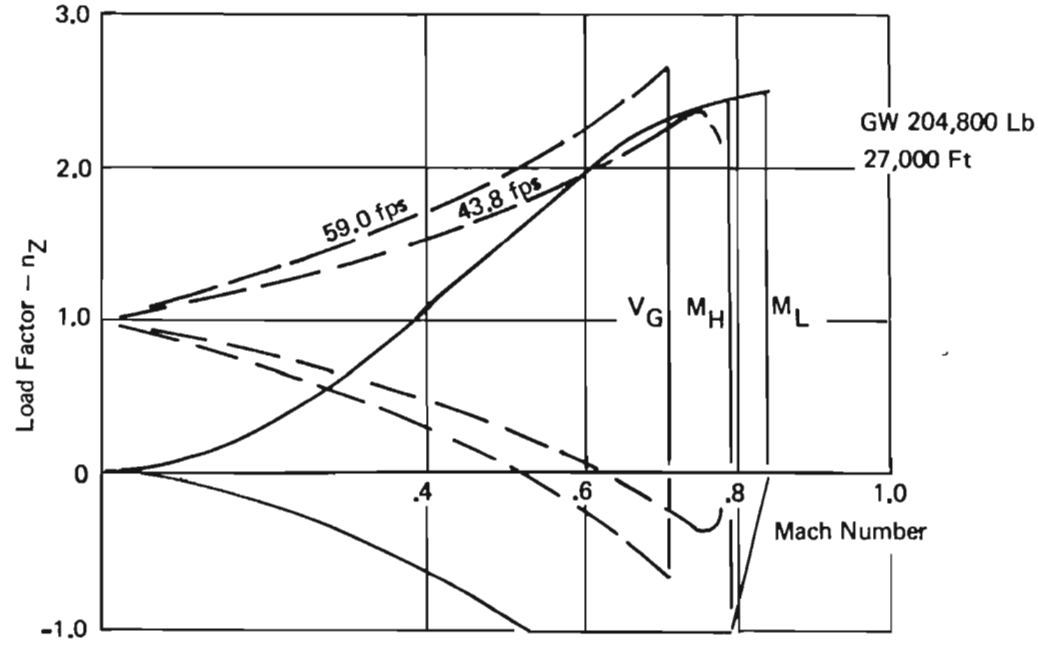

Figure 56: V-n Diagrams – Basic Flight Design Weight – $C_{Transport}$

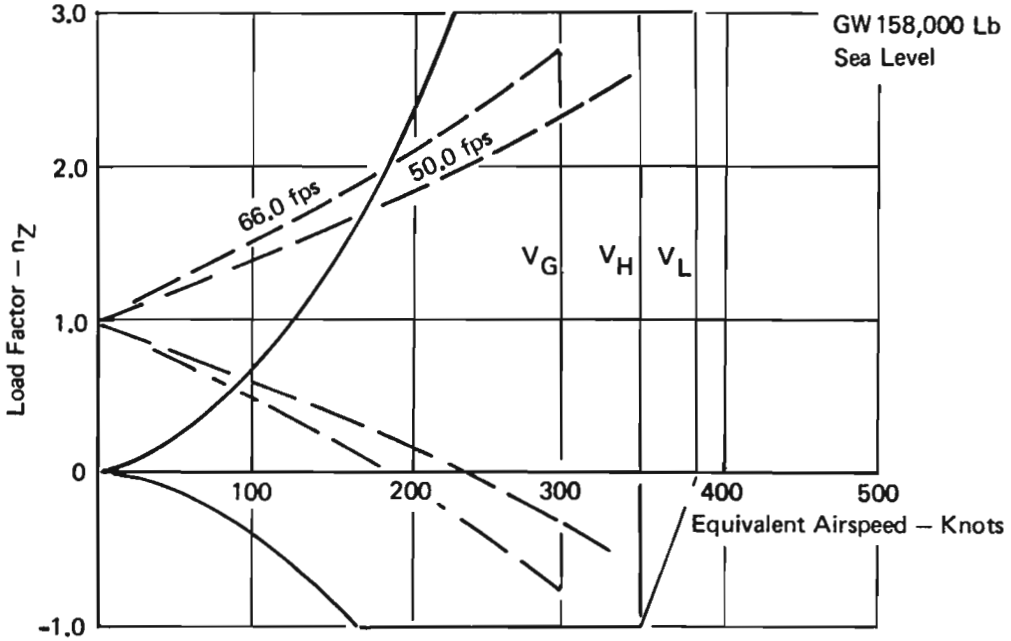

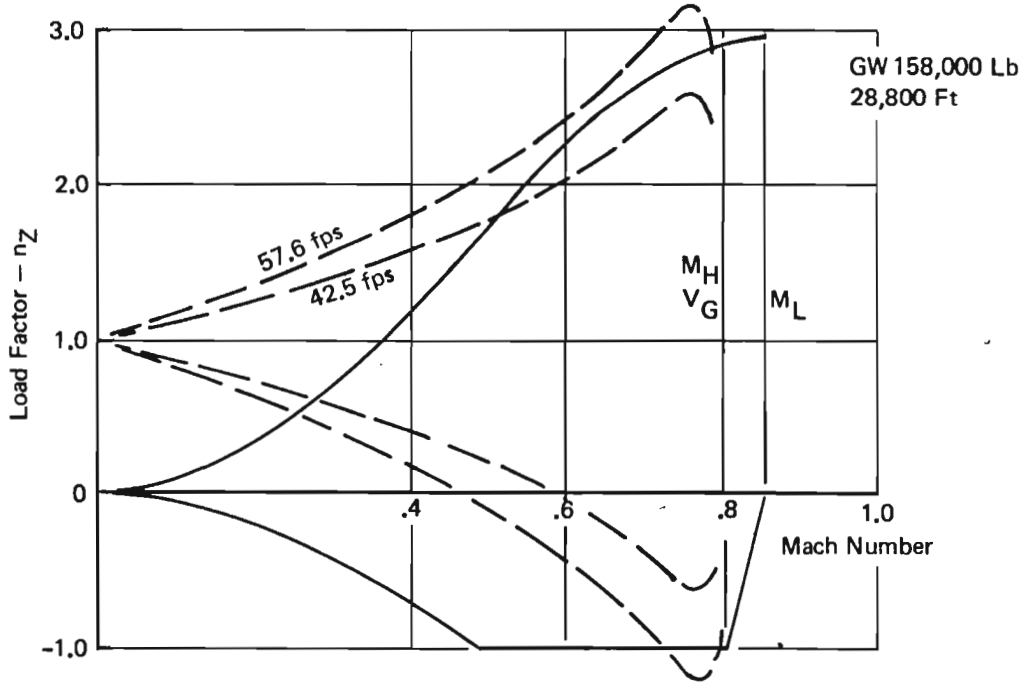

Figure 57: V-n Diagrams – Basic Flight Design Weight – $C_{Assault}$

GW 225,400 Lb
Sea Level Flaps Down

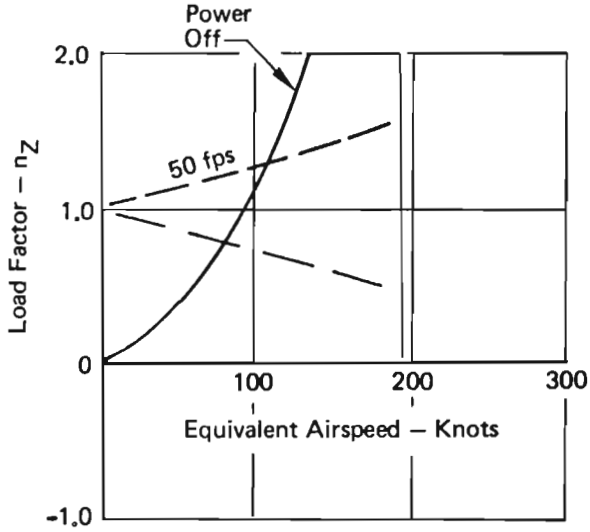

GW 191,700 Lb
Sea Level Flaps Down

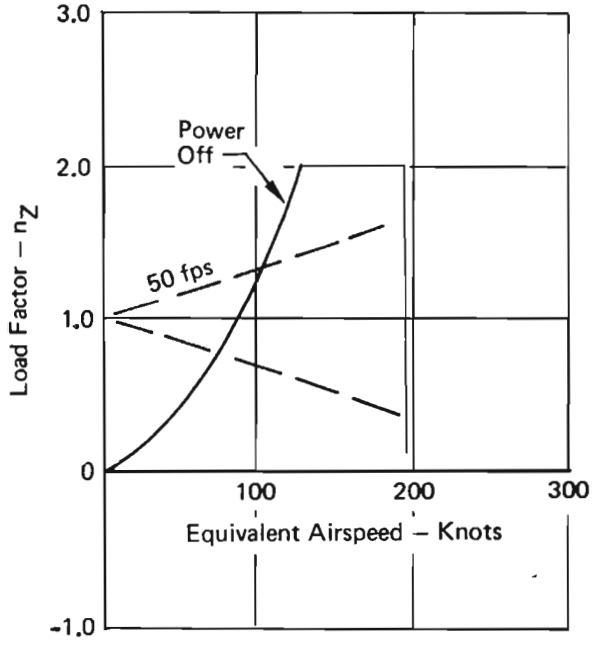

Figure 58: V-n Diagrams – Flaps Down

structural element allowables are selected in accordance with the requirements of MIL-HDBK-5A.

6.1.3.1 Wing Analysis

Analysis of the wing primary structure was done using a Boeing developed computer program "Preliminary Design Wing Structural Analysis System (ORACLE)". In this analysis the wing structure was idealized as a rectangular box consisting of the upper and lower surfaces and the front and rear spars. The upper and lower surfaces are each of uniform thickness at a cross section. Correction factors are used to improve the rectangular box structural idealization. These factors include corrections for the effects of the aerodynamic contour of the upper and lower wing skins, stringers, leading and trailing edge structure and spanwise thickness taper. This analysis is used to design both the outboard and center section wing structures.

Wing Outboard Section Design Analysis

The upper and lower wing skins were sized to the state of stress at the front spar and rear spar locations. The largest skin thickness on each wing skin was then taken as the uniform thickness for that surface. There were two material sizing calculations, one for that portion of the wing skin which is in combined compression and shear and one for the portion which is in combined tension and shear.

The compression surface failure criterion used was the interaction formula

$$R_c + R_s^2 = 1$$

where R_c is the ratio of the axial compression stress to the compression allowable stress and R_s is the ratio of the shear stress to the allowable shear stress.

On the tension surface, the more stringent of two failure criteria is used. The first is the maximum tension stress as compared with the allowable tension stress. The second is the maximum shear stress as compared with the allowable shear stress.

Spar web thicknesses are computed from the wing box depths, interspar distances and skin thicknesses to satisfy a torsional stiffness criterion based on past Boeing experience.

Wing Center Section Design Analysis

Though the aeroelastic loads on the wing are computed on an idealized beam having aerodynamic panels along its span and extending to the centerline of the airplane, the strength design analysis of the wing inside the body is to a different criterion than the rest of the wing. For the design analysis, the wing shear and torsion loads are

assumed reacted by the fuselage at the side of body. The wing center section designing loads are only wing bending moment loads and center section internal loads due to cabin pressurization and fuel contained in the wing center section. As in the outboard wing computation, the problem is separated into a compression and a tension surface problem. Upper and lower surface skin thickness requirements are established from appropriate compression and tension allowables.

Spar web thickness computations for the center section are similar to those for the outboard wing.

Analysis Results

Table VI summarizes the sizing requirements for the upper and lower surfaces and for the front and rear spars for each spanwise station investigated. The critical design condition for the wing upper and lower surfaces is the 50 fps gust occurring at M = .75 at 18,000 feet and a gross weight of 125,710 lbs. The spar webs are critical for the bending stiffness condition. Other conditions investigated included +LAA and ground taxi.

6.1.3.2 Body Analysis

The semi-monocoque body is analyzed as a curved, incomplete diagonal-tension shear web system subjected to combined loads. These combined loads included body bending, transverse shear, and torsion resulting from flight and ground handling conditions together with cabin pressure loads where critical.

Skin Analysis

The body skin is analyzed as a curved, incomplete diagonal-tension shear web taking into account the reduction in shear capability resulting from the reduced initial buckling capability of the panels due to the presence of the axial compressive stresses. In addition, the skin is analyzed to insure adequate fatigue life and fail safe capability under combined cabin pressure and flight loads by preventing the rapid uncontrolled growth of cracks. This is accomplished by the selection of proper materials and stress levels and by the use of multiple-load-path structure consisting of tear straps and frames in addition to the skin.

Stiffener Analysis

Body stringers are analyzed as beam columns subjected to axial stress resulting from flight and ground handling conditions. The effects of secondary diagonal tension loads due to skin shear stresses are included through incorporation of equivalent compression stresses in the analysis.

Table VI: Wing Structural Requirements

ETA Sta	Upper Surface		Lower Surface		Spars				
	Design Condition	Skin Thickness Inches	Stiffener Area Sq In.	Design Condition	Skin Thickness Inches	Stiffener Area Sq In.	Design Condition	Front Web Thickness Inches ▷	Rear Web Thickness Inches ▷
.95	Gust	.08000	2.392	Gust	.08000	1.288	Stiffness	.12462	.12462
.85	Gust	.08568	3.434	Gust	.08000	1.727	Stiffness	.11517	.11517
.75	Gust	.12904	6.514	Gust	.11927	3.242	Stiffness	.15924	.15924
.53	Gust	.16670	10.419	Gust	.15628	5.259	Stiffness	.19407	.19407
.53	Gust	.19311	14.003	Gust	.18777	7.332	Stiffness	.21970	.21970
.45	Gust	.18528	14.906	Gust	.18446	7.991	Stiffness	.21048	.21048
.32	Gust	.20728	19.393	Gust	.21232	10.696	Stiffness	.23721	.23721
.17	Gust	.20234	22.131	Gust	.21206	12.489	Stiffness	.24336	.24336
.05	Gust	.14747	16.316	Gust	.15839	9.436	Stiffness	.17626	.17626

▷ Includes Stiffener Area

Frame Analysis

Body frames are analyzed to insure adequate strength and stiffness to prevent general instability failure of the body shell structure and local failure of the frames due to externally applied loads. These loads include external aerodynamic pressures, local cargo loads, and secondary diagonal tension loads due to skin shear stresses.

Analysis Results

Figures 59 thru 62 summarize the sizing requirements for the body skin, stringers, and typical frames. A minimum skin gage of .063 inches with tear straps and frames at 20 inch spacing is required to insure adequate fatigue and failsafe capability under normal cabin operating pressure of 8.2 psi and a maximum relief valve setting of 9.0 psi. The skin in the vicinity of the nose wheel well is designed to carry the nose gear loads occurring during a 3 point landing. The stiffeners in the forward body are critical for vertical gust loads. The stiffeners and some skin in the aft body are critical for either vertical gust loads or lateral (fin) gust loads. The skin and stiffeners between the wing front and rear spar bulkheads are critical for the shear loads due to differential bending between the forward and aft body sections during a two point landing. The typical body frames are critical for the negative differential cabin pressure of 1.5 psi ultimate.

6.1.3.3 Horizontal Tail Analysis

Analysis Method

The primary structural components of the horizontal tail are analyzed as a box structure consisting of the front and rear spars and the upper and lower skin panels stabilized by ribs spaced at 9 inch intervals. A mid chord spar is included on the inboard sections. No spanwise stringers are used in the skin panels.

Both transverse shear loads and torsion loads are carried by the spar webs and the skin panels as intermediate diagonal-tension shear webs. Bending loads are carried by spar caps on the compression side and by the spar caps and skin panels together on the tension side. The effect of combined stresses due to tension and shear loads is included in the analysis. However, the effects of sweepback and taper are neglected.

Analysis Results

The structural sizes established by analysis are summarized in Table VII . Both unsymmetrical gust load and unsymmetrical instantaneous elevator load conditions are investigated. The spar caps are critical for gust loads. The front and mid spar webs are also critical for gust loads while the rear spar web is critical for instantaneous

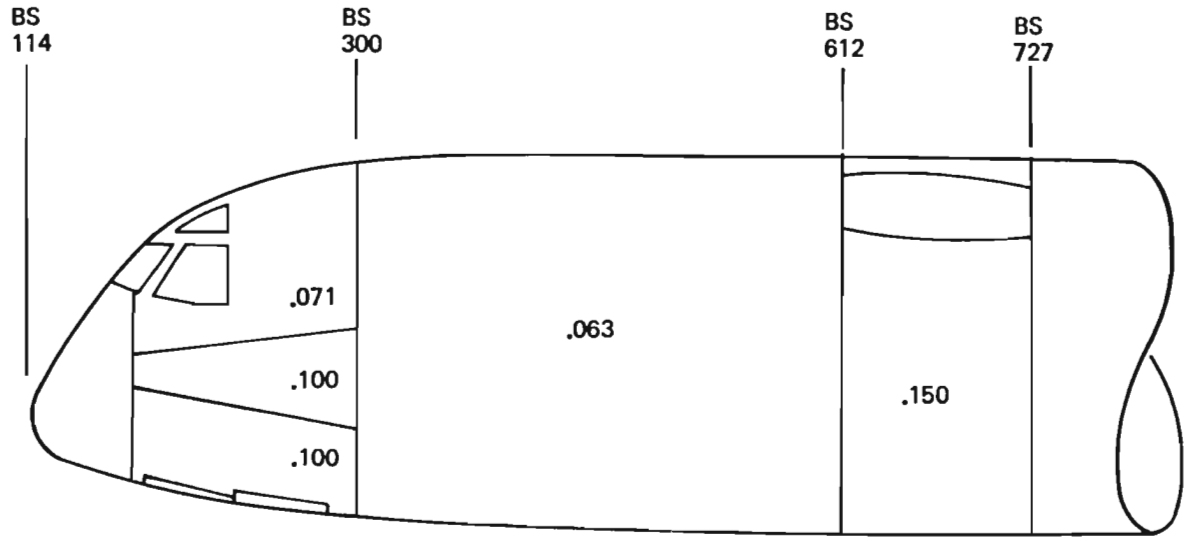

Notes: Frame Spacing 20 In. Except 10In. Forward of Sta 300.
Pressure Relief Valve Setting = 9.0 psi
Skin Material – Clad 2024-T3 or T-4
Tear Straps at Each Frame (20 In. Spacing)
Typical Frame Area = .39 $In.^2$

Figure 59 : Forward Body Skin Structural Requirements

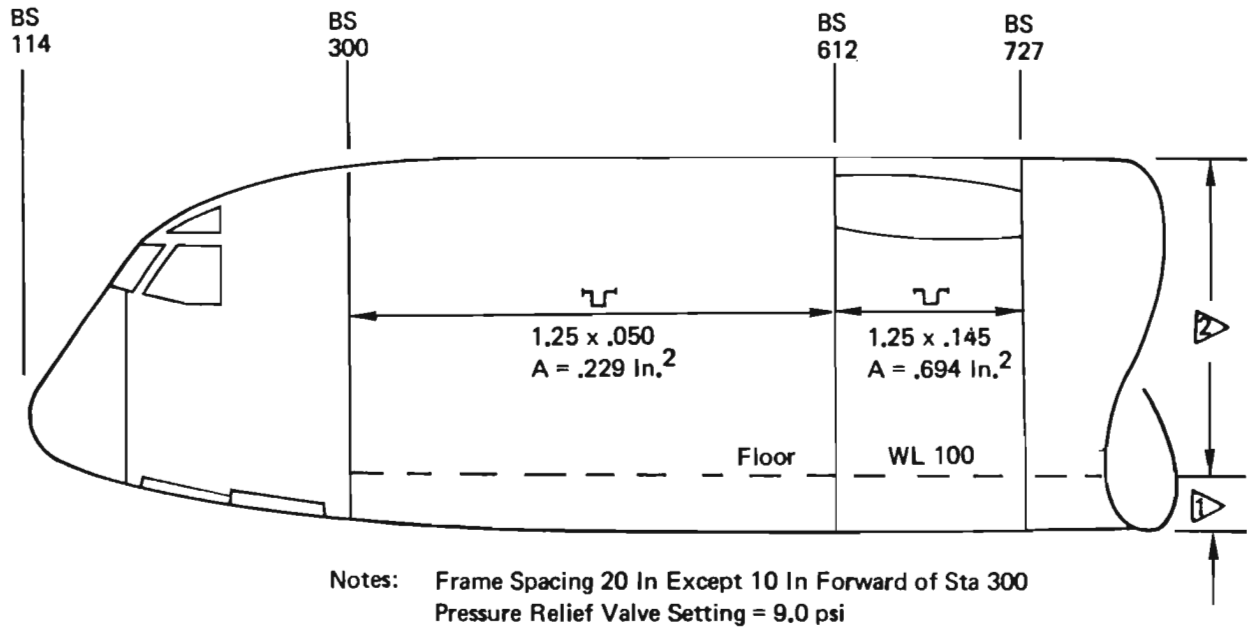

Notes: Frame Spacing 20 In Except 10 In Forward of Sta 300
Pressure Relief Valve Setting = 9.0 psi
Stringer Material Clad 7075-T6
1 Stringer Spacing = 8.25 In.
2 Stringer Spacing = 9.25 In.
Typical Frame Area = .39 $In.^2$

Figure 60 : Forward Body Stiffener Structural Requirements

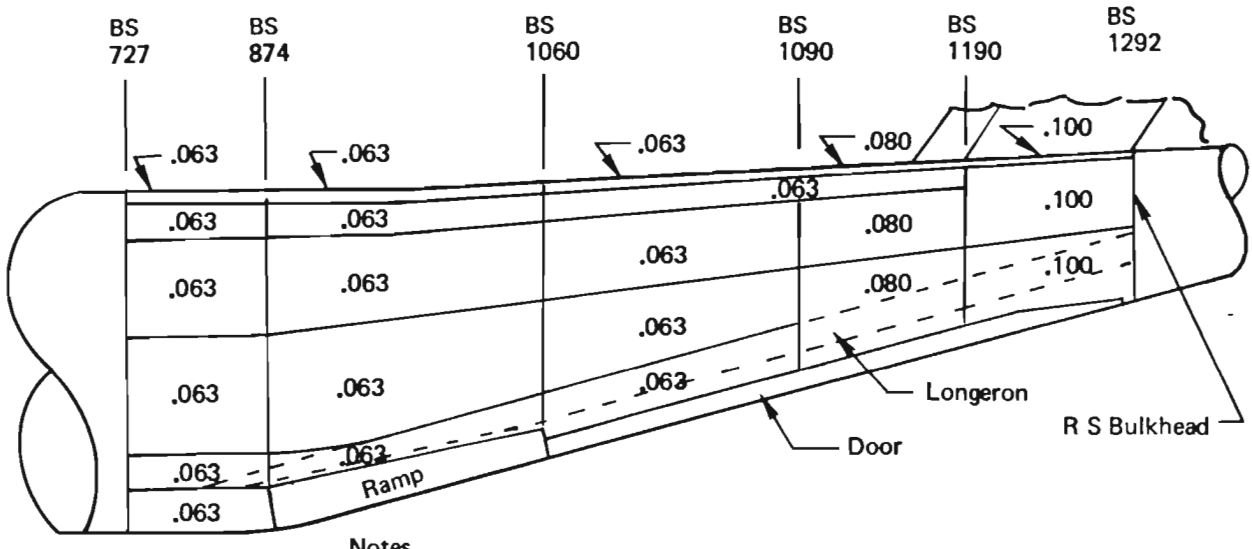

Notes
Frame Spacing = 20 In.
Pressure Relief Valve Setting = 9.0 psi
Skin Material – Clad 2024-T3 or T4
Tear Straps at Each Frame
Typical Frame Area = .39 In.^{2}

Figure 61 : Aft Body Skin Structural Requirements

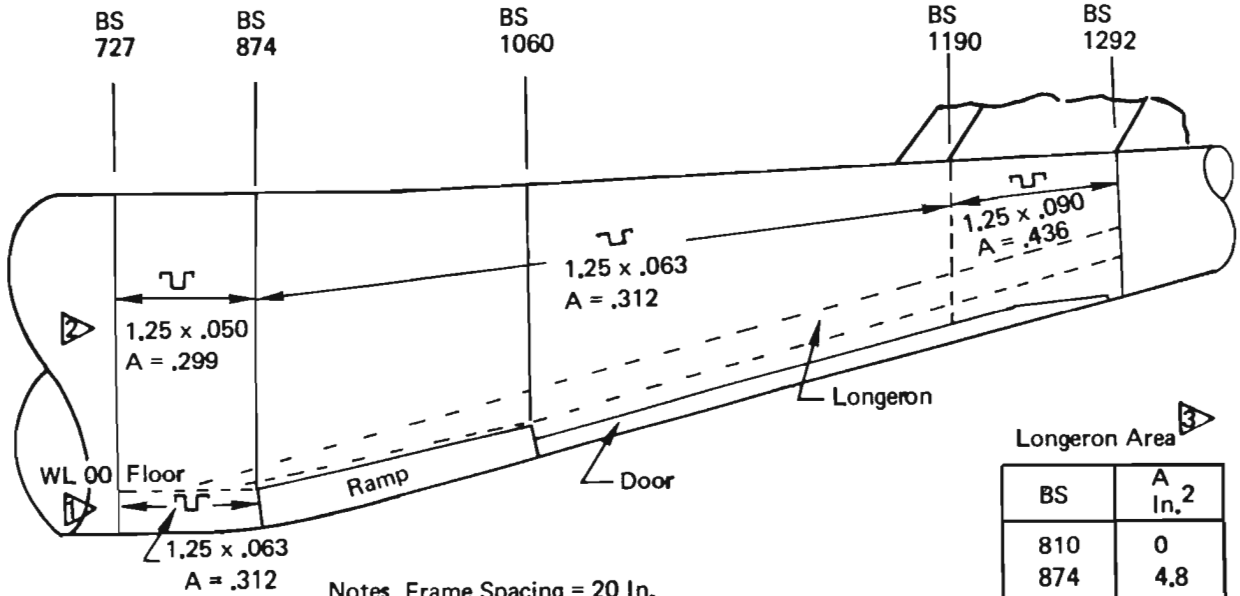

Longeron Area ③

BS	A In.^{2}
810	0
874	4.8
909	5.0
1190	3.0
1292	3.0

Notes Frame Spacing = 20 In.
Pressure Relief Valve Setting = 9.0 psi
Stringer Material @ Clad 7075-T6
① Stringer Spacing = 8.25 In.
② Stringer Spacing = 9.25 In.
③ Area Varies Linearly Between Stations. Material = 7075-T6
Typical Frame Area = .39 In.^{2}

Figure 62 : Aft Body Stiffener Structural Requirements

Table VII: Horizontal Tail Structural Requirements (1)

Sta BL	Front Spar			Mid Spar			Rear Spar			Skin Panels	
	Web Thick (2) In.	Upper Chord Area Sq In.	Lower Chord Are Sq In.	Web Thick (2) In.	Upper Chord Are Sq In.	Lower Chord Area Sq In.	Web Thick (2) In.	Upper Chord Are Sq In.	Lower Chord Area Sq In.	Upper Skin Thick In.	Lower Skin Thick In.
14	.057	1.438	1.380	.054	1.672	1.604	.072 (3)	1.672	1.604	.076 (3)	.072 (3)
100	.066	1.106	1.061	–	–	–	.060 (3)	1.114	1.069	.068	.065
200	.030	.210	.210	–	–	–	.030 (3)	.210	.210	.027 (3)	.026 (3)

(1) Critical Design Condition for All Structure is Negative Unsymmetrical Gust Load Except Where Noted

(2) Includes Stiffeners

(3) Critical Design Condition is Unsymmetrical Instantaneous Elevator Load

elevator loads. Both the upper and lower surface skin panels near the tip and near the root are critical for the instantaneous elevator condition. The skin panels at mid span however, are slightly more critical for gust loads.

6.1.3.4 Vertical Tail Analysis

Analysis Method

The primary structural components of the vertical tail are analyzed as a box structure composed of the front and rear spars and the left and right hand skin panels stiffened by spanwise stringers. Ribs at 24 inch spacing stabilize the box structure.

Both transverse shear loads and torsion loads are carried by the spar webs and the skin panels as intermediate diagonal-tension shear webs. Bending loads are carried by the stiffened skin panels. The effect of combined shear and compression stresses in the skin panels is included in the analysis by using the interaction formula $R_c + R_s^2 = 1$ as the failure criterion. R_c is the ratio of axial compression stress to the compression allowable stress and R_s is the ratio of the shear stress to the allowable shear stress. The effects of sweepback are also included.

Analysis Results

Figure 63 contains a summary of the sizes required for each primary structural component expressed as average thicknesses including stiffener material. All primary structural members are critical for the fin gust loading condition. The effects of unsymmetrical loads on the horizontal tail are included.

6.1.4 Loads

This section is divided into two parts (a) static loads where magnification of load due to structural dynamic effects is included through a simple factor and (b) dynamic loads where the structural dynamics are included as degrees of freedom. Comparative plots of the maximum loads from each approach are found in Section 4.9.3.1 and show that the factors applied to the static loads adequately cover the structural dynamic effects.

6.1.4.1 Static Loads

o Airload Distribution Methods

Conditions for loads analysis are selected using the criteria of 6.1.2. Net structural loadings on the wing, body, and empennage are calculated such that the airplane is balanced by a system of airloads and inertia loads. Aerodynamic loadings are calculated using analytical methods modified to match rigid wind

Notes:

Material = 7075-T6

Linear Taper

Thicknesses Shown Includes Stiffener Area

Rib Spacing = 24 In.

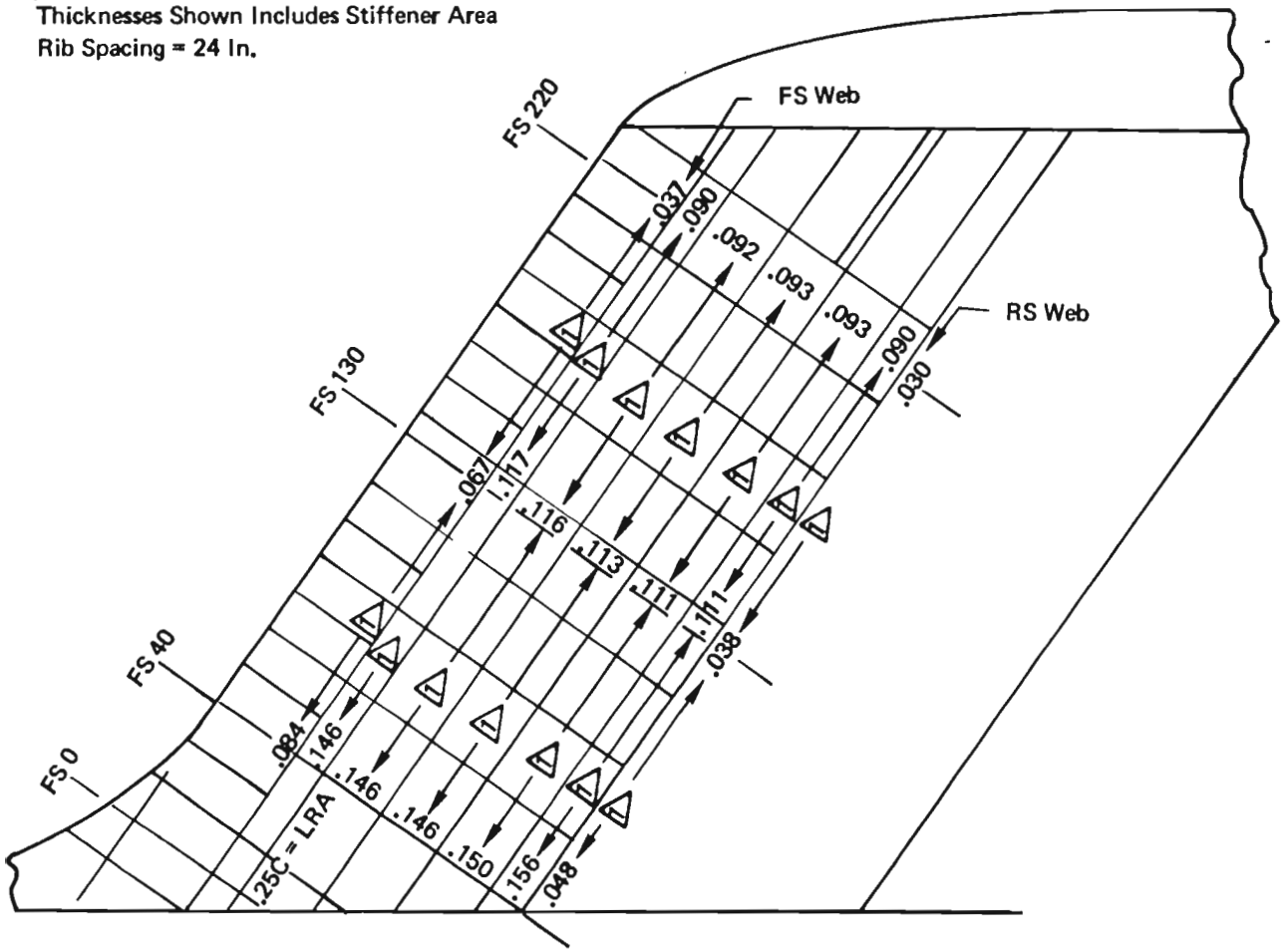

Figure 63: Vertical Tail Structural Requirements

tunnel data. Aeroelastic effects are included through the lifting line aerodynamic influence matrix of Reference 4.9-1. Since no high speed wind tunnel data has been obtained during this study, applicable data has been taken from an AMST model.

o Wing Loads

A survey of wing loads at all possible gross weights throughout the flight envelope shows that maximum wing bending moments occur during a gust at cruise altitude and Mach number with minimum wing fuel. Reduced cruise speeds with payloads heavier than that for the primary mission are selected to avoid exceeding design loads. Overall wing loads during high lift operation do not approach design values due to the reduced maneuver requirements. Conditions with flaps extended or thrust vectored design local structure. Design wing loads are presented in Figures 64 and 65 for maximum up-bending, maximum down-bending and taxiing. The highest dynamic loads due to gust and taxiing from Section 6.1.4.2 are presented for comparison.

o Empennage Loads

Critical vertical tail loads occur during a lateral gust encounter at V_H at sea level. Rudder available limits the rudder kick maneuver load to 60 percent of the gust load.

Vertical tail loads are found in Figure 66 . Maximum loads on the horizontal tail occur during up and down gusts at V_H at 18,000 ft. Nominal horizontal tail design load distributions are presented in Figure 67. These loads must be distributed on either side of the horizontal tail in a 115/85 percent ratio as required by MIL-A-008861A (USAF).

o Body Loads

Forebody design loads occur during up and down gusts at V_H at 18,000 ft. with design payload. Reducing V_H with larger payloads avoids increasing forebody loads. Loads due to landing and ground handling do not exceed the design loads shown in Figure 68 . Critical vertical bending loads on the aft body occur during a 3.0g pull-up at V_L at 13,200 ft. This gives the greatest combination of down tail load and load factor. Maximum up-bending occurs during a -1.0g push-over at negative high angle of attack. Aft body loads are found in Figure 69.

6.1.4.2 Dynamic Loads

Dynamic flight and ground loads were calculated. For reasons of economy and schedule, the dynamic analyses used equations of motion and load equations already available for the Boeing 727 airframe. The structural frequencies were corrected to match those determined in the flutter analysis of the STAI airplane, and the loads recomputed accordingly. Because of the similarity in weights and overall dimensions between the 727 and the STAI configuration, the use of those equations was considered to give sufficiently accurate results.

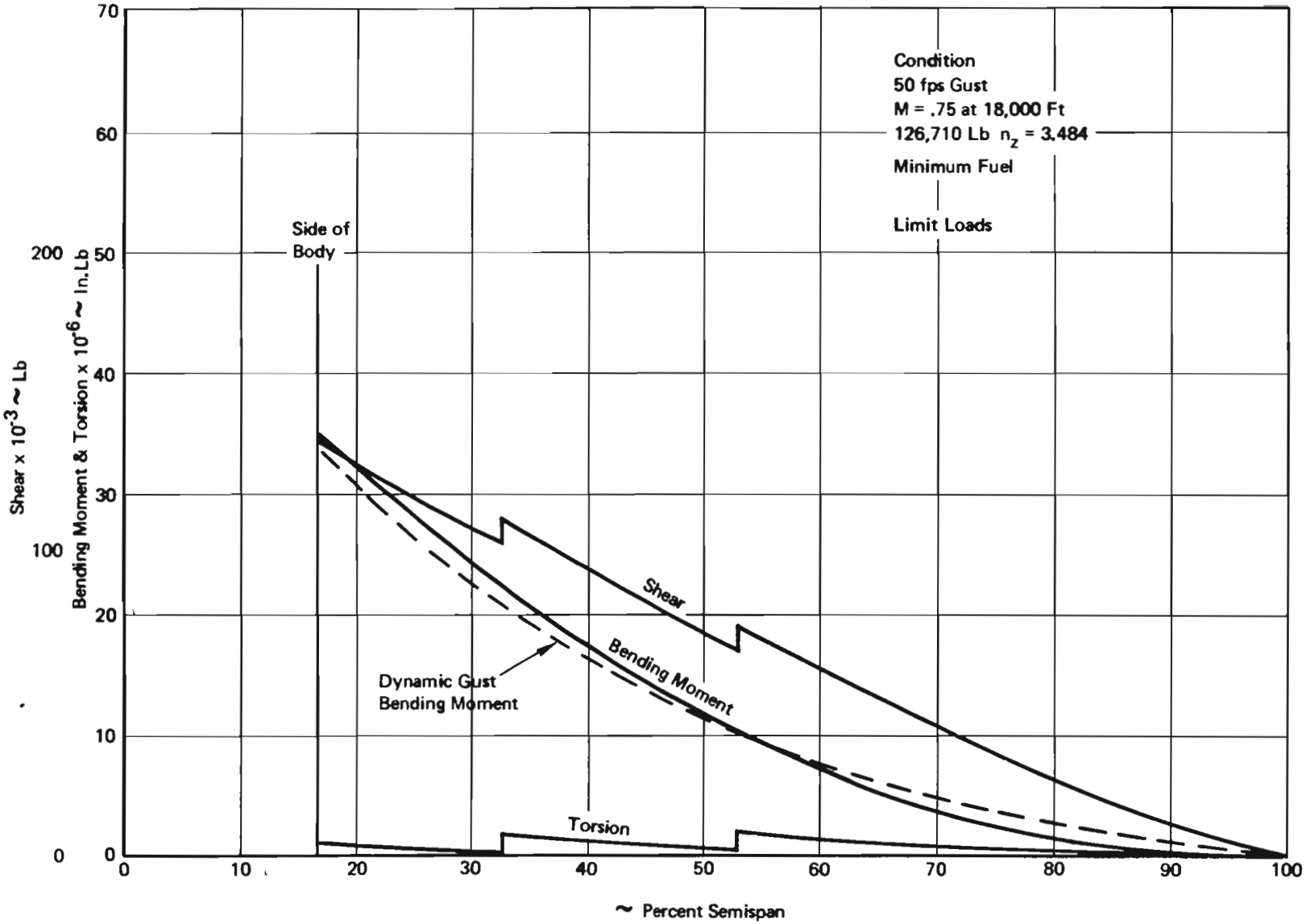

Figure 64: Wing Loads Maximum Bending

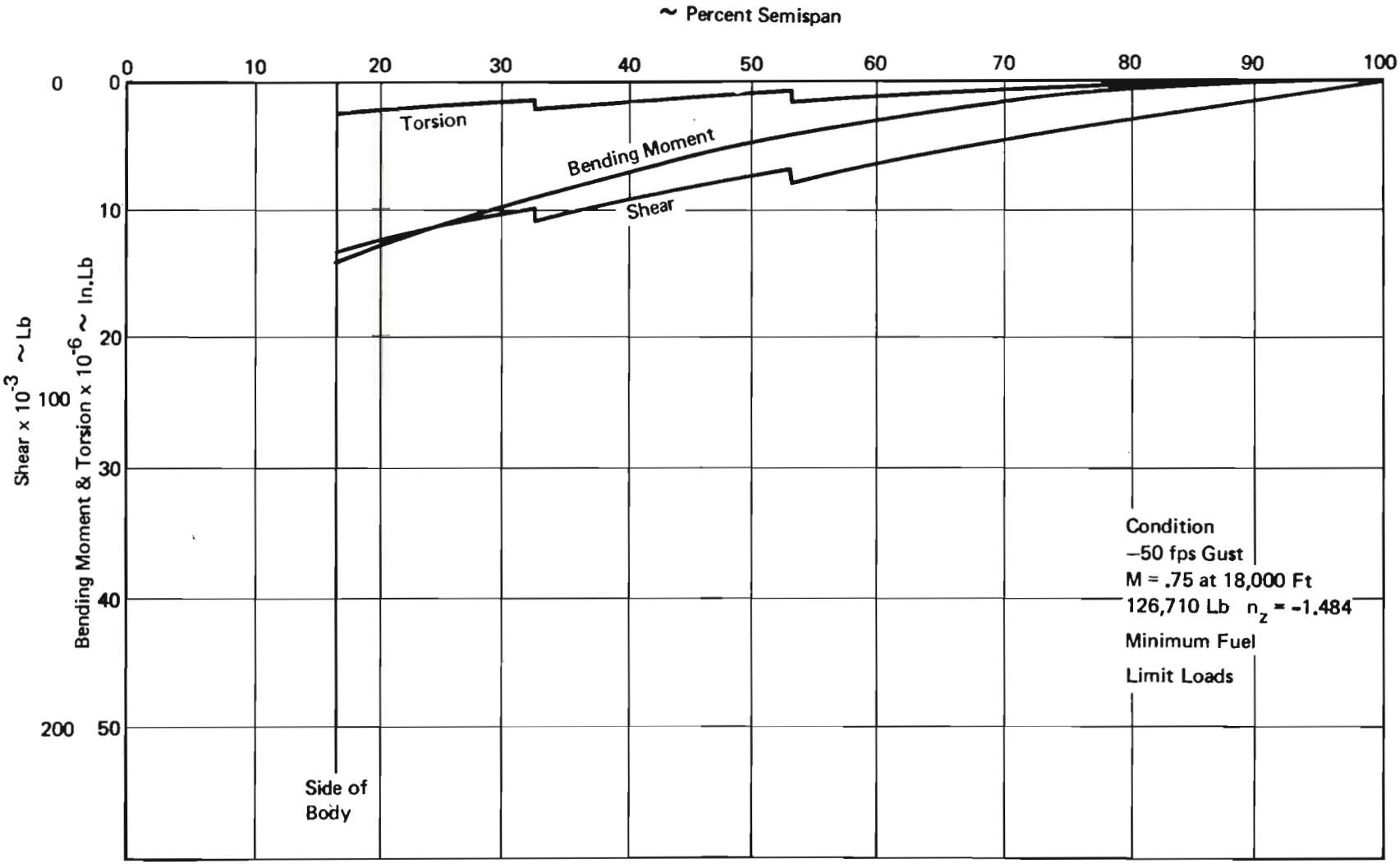

Figure 65: Negative Wing Loads

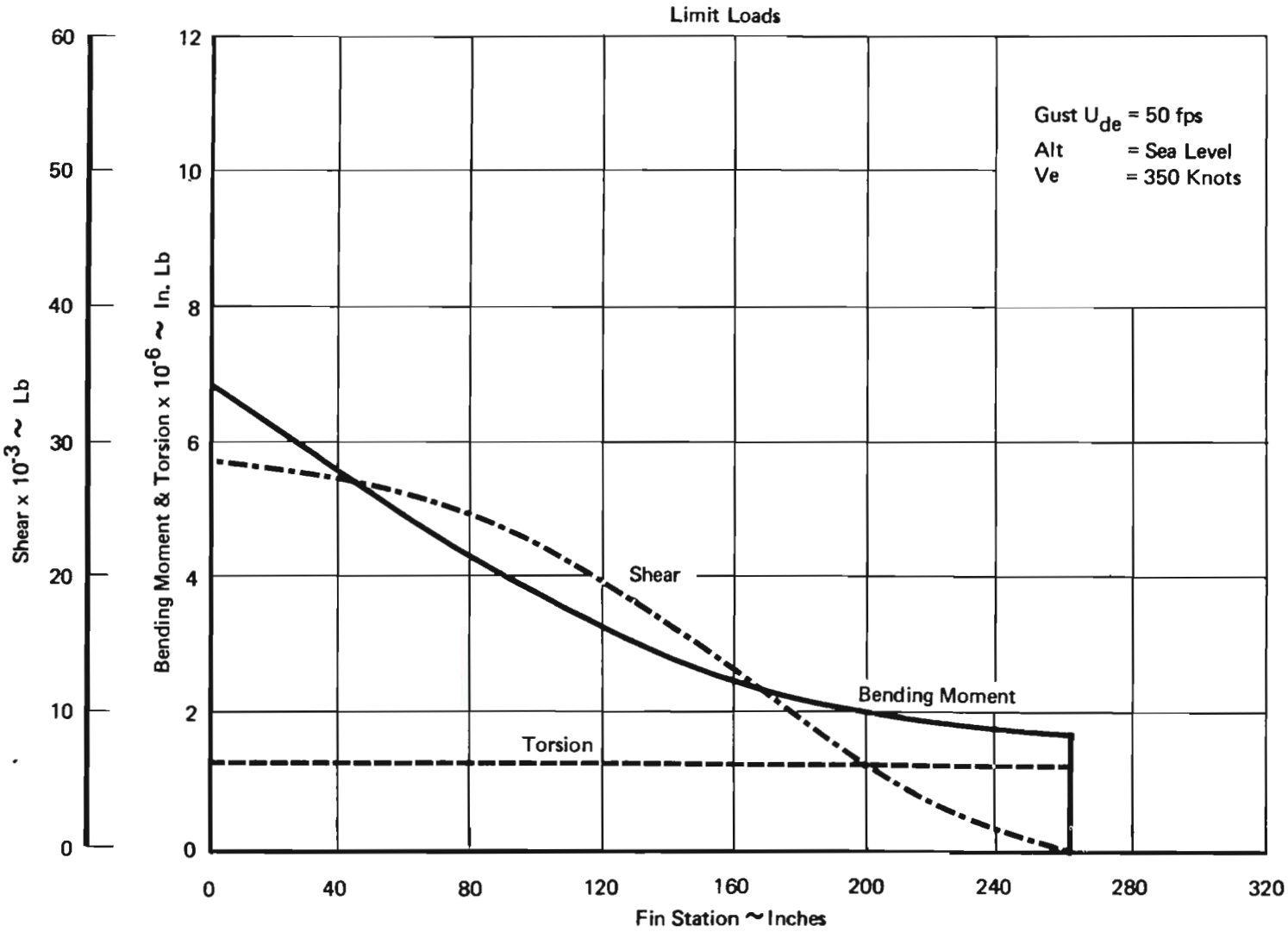

Figure 66 : Vertical Tail Loads

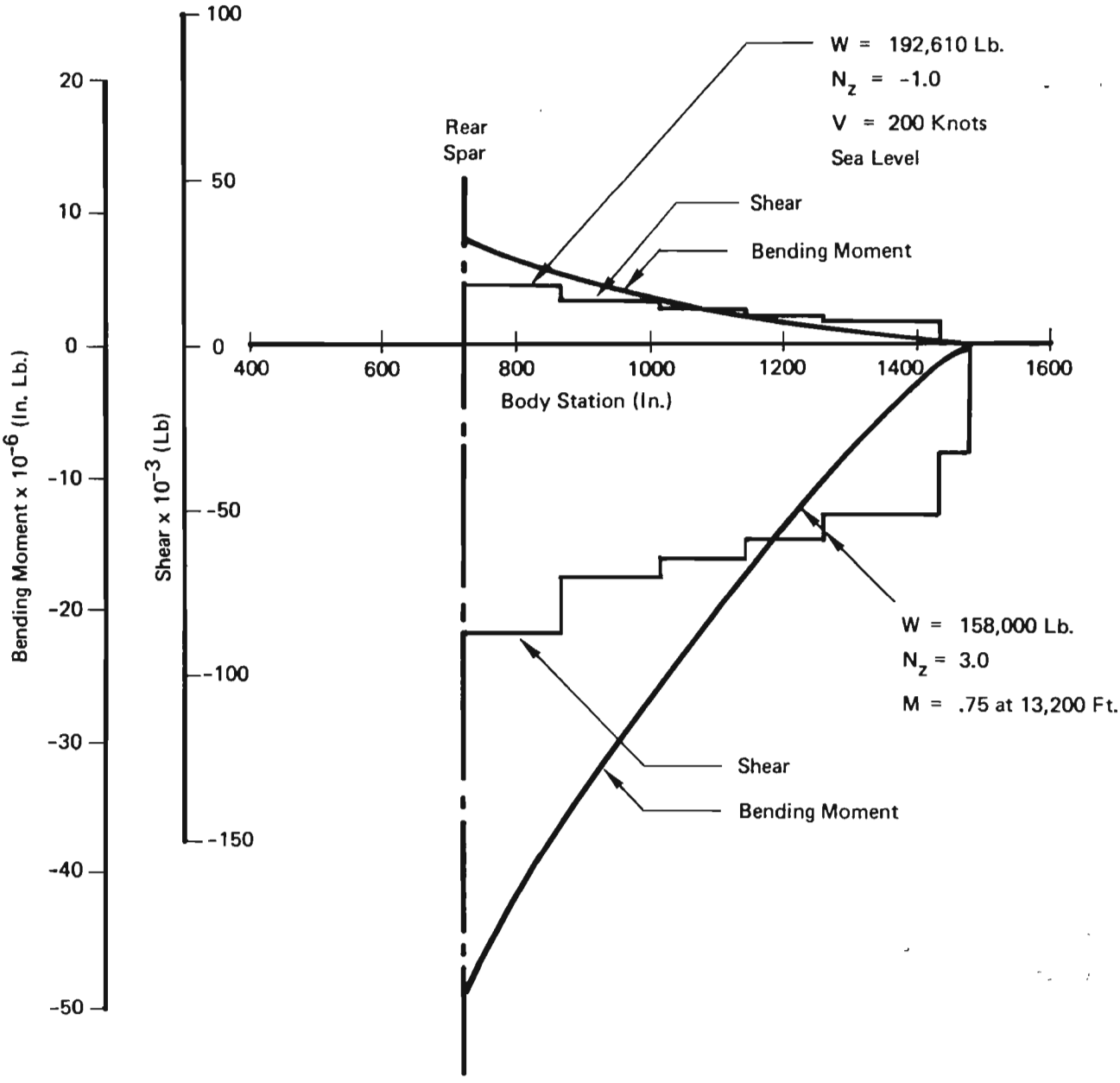

Figure 69: Aft Body Loads

Dynamic Ground Loads

The gears were sized for impact performance. The analysis conservatively assumed the gears to have fixed (unable to rotate) outer cylinders. No attempt was made to translate the analysis characteristics to their equivalent active gear counterparts.

Landing impact and taxi loads are shown in Figures 70 through 75 . The critical impact case is landplane landing at 15 fps and forward velocity of 153 fps. The critical dip has a depth of 9.47 inches and is 80 ft. long encountered at a taxi speed of 98.8 fps.

Dynamic Gust Loads

Loads due to atmospheric turbulence are shown in Figure 76 . These resulted from application of the design envelope criteria (MIL-A-008861A (USAF), 3.22.2.1.2). The critical flight condition was V_e = 390 kn at 18,900 ft.

6.1.5 Flutter

The Model 953-815 configuration was subjected to a flutter analysis using the stiffness and mass distribution for the strength-designed structure. The analysis used two-dimensional aerodynamic theory with empirical corrections for finite span and compressibility effects. Cantilevered wing structural modes were augmented with rigid airplane freedoms to obtain free-free symmetric and antisymmetric airplane modes.

The results of this analysis are shown in Figure 77 . It can be seen that the airplane with full fuel is deficient in flutter margin. Due to the antisymmetric mode of the flutter it was found that it was sensitive to both bending and torsional stiffness. The airplane was reanalyzed with bending stiffness increased by 25% and torsional stiffness by 15%. Results are given in Figure 78 . Again the full fuel antisymmetric mode is critical. While a 100 knot increment has been obtained, full flutter clearance has not been achieved.

Further trade studies on local wing stiffening show a negligible increase in flutter speed due to torsional stiffening between the nacelles. The influence of engine placement is shown in Figure 79 . Moving the engine to 58% semispan gives the required flutter clearance.

It is concluded from this work that although the STAI configuration as drawn is deficient in flutter speed, it is possible to achieve flutter clearance with a small weight penalty by configuration changes.

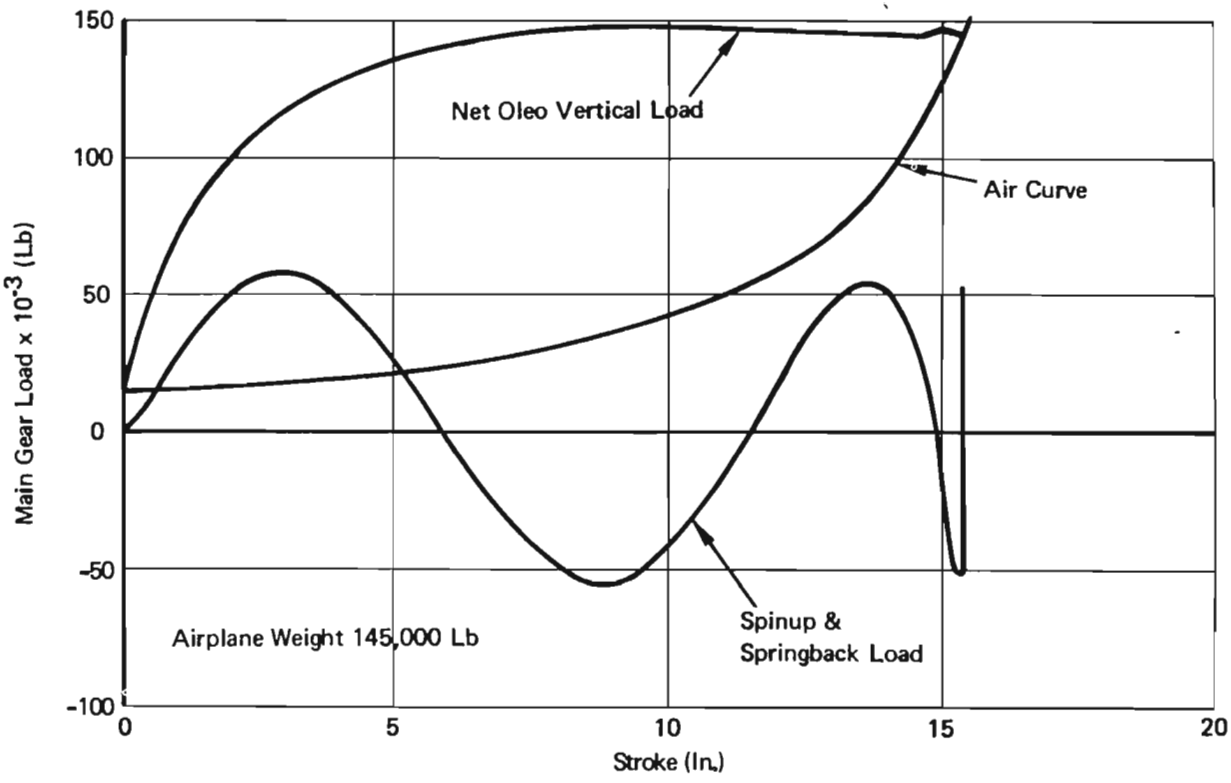

Figure 70: Main Gear Landing Impact — 15 FPS

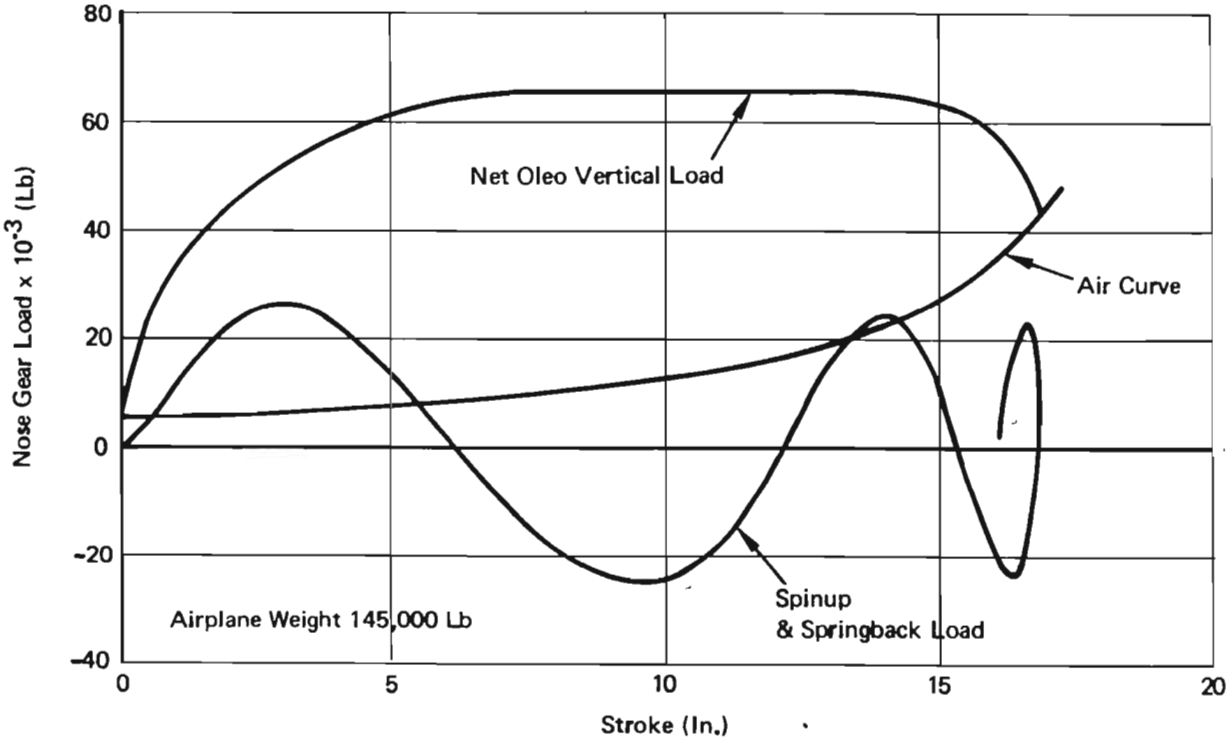

Figure 71: Nose Gear Landing Impact — 15 FPS

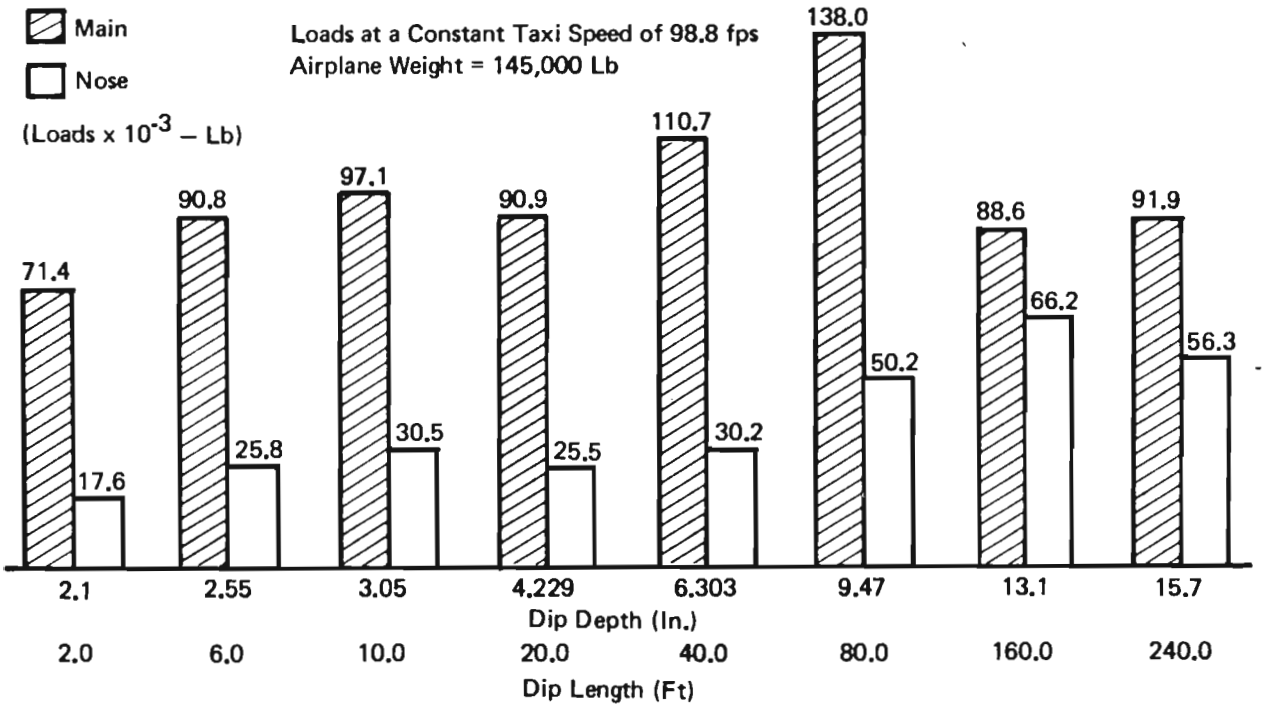

Figure 72: Taxi Loads – Varying Dip Constant Speed

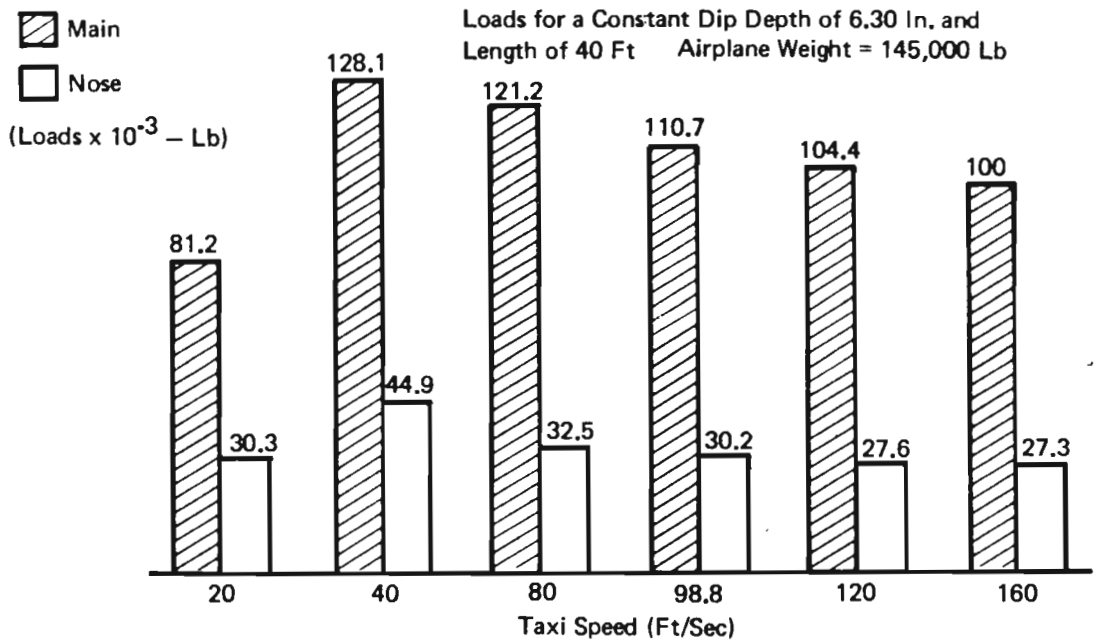

Figure 73: Taxi Loads – Speed Variation Constant Dip

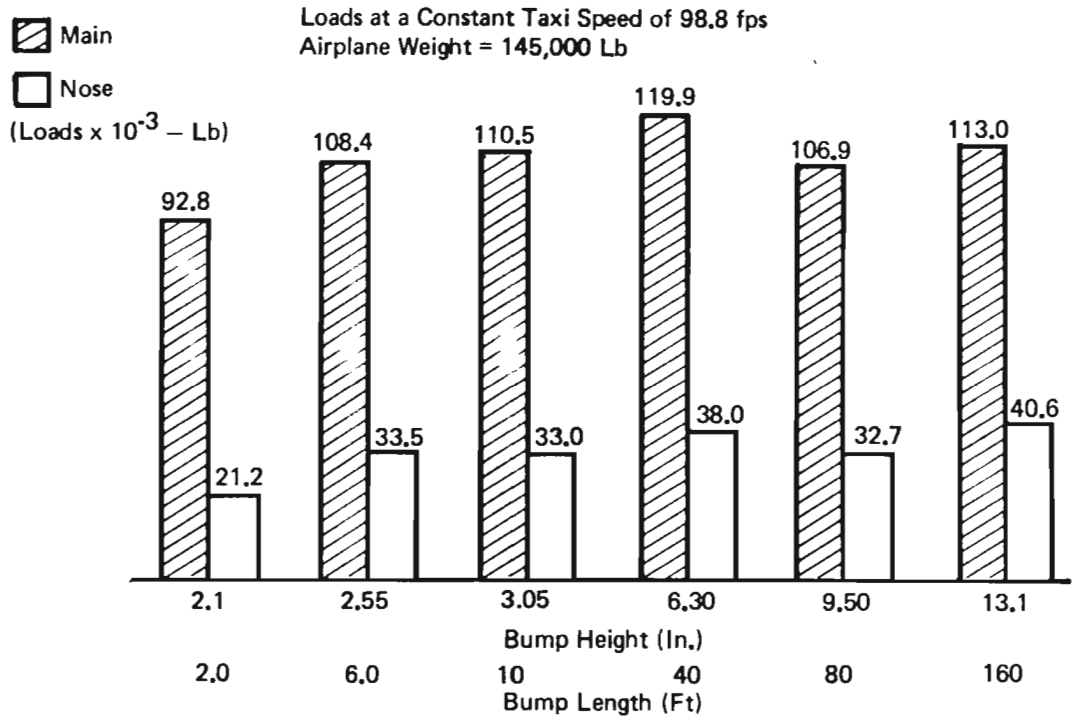

Figure 74: Taxi Loads — Varying Bump — Constant Speed

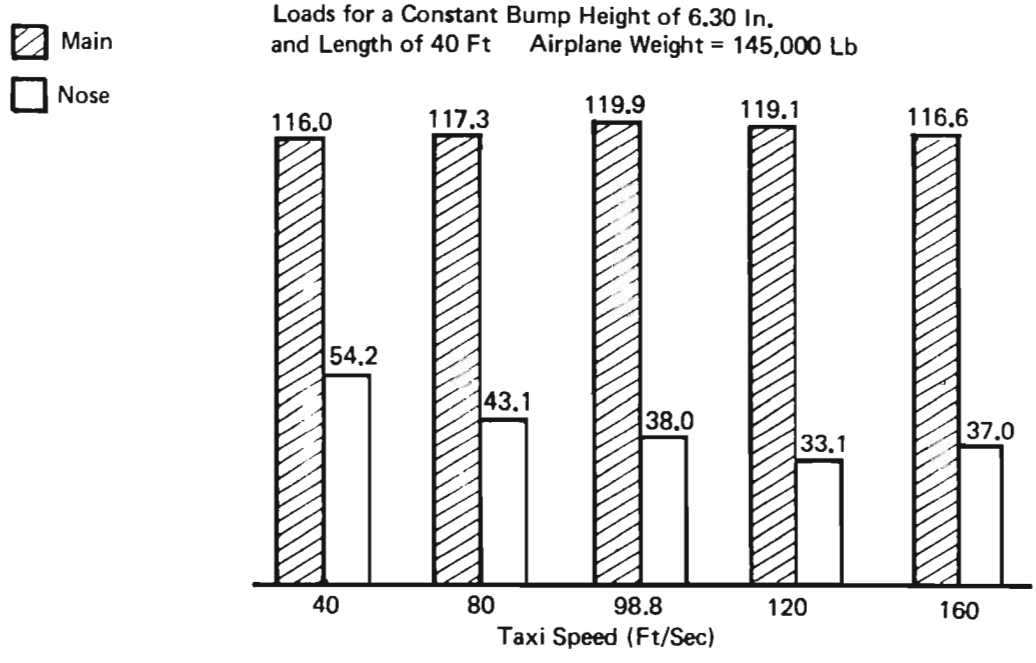

Figure 75: Taxi Loads — Speed Variation — Constant Bump

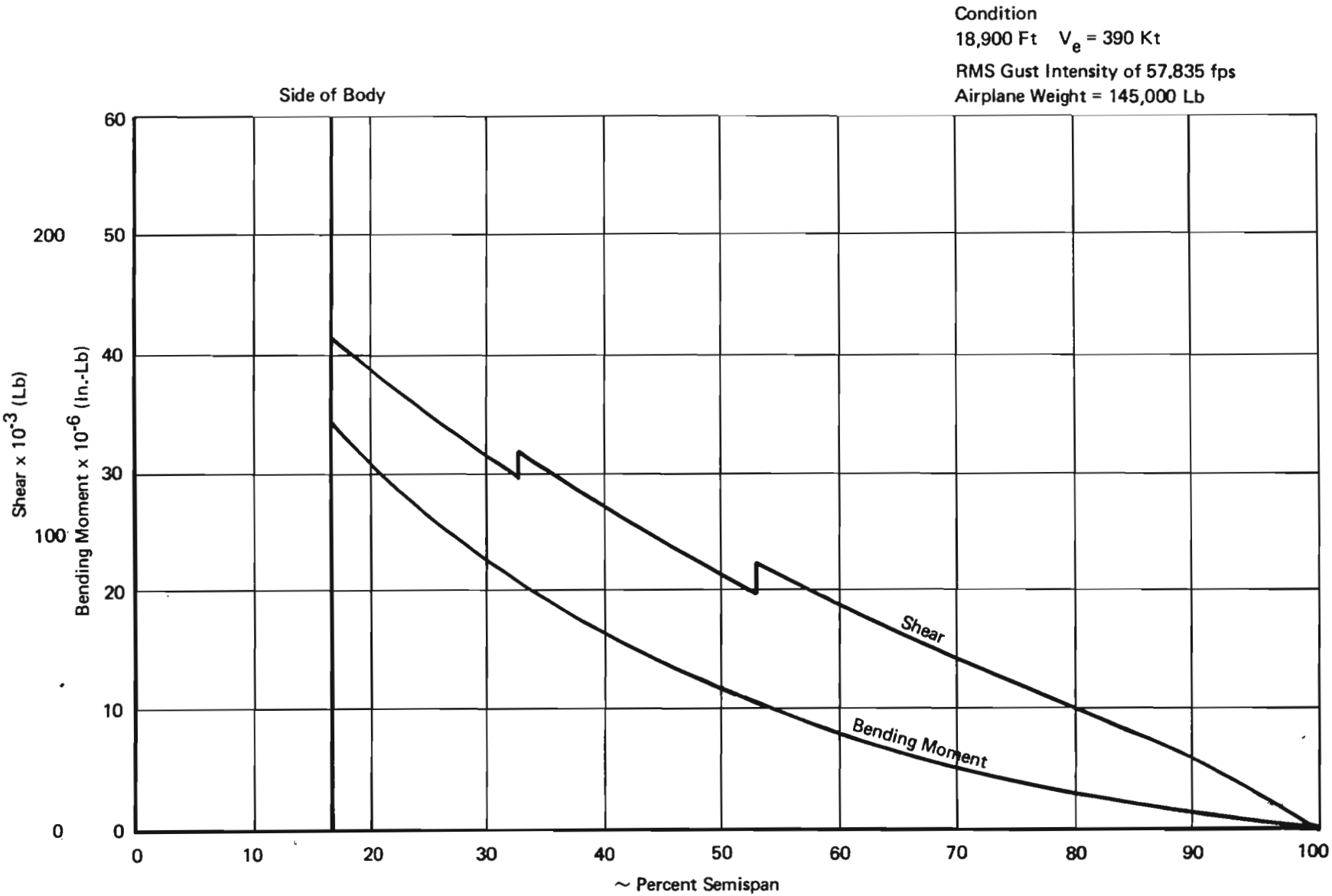

Figure 76: Wing Loads — Dynamic Gust

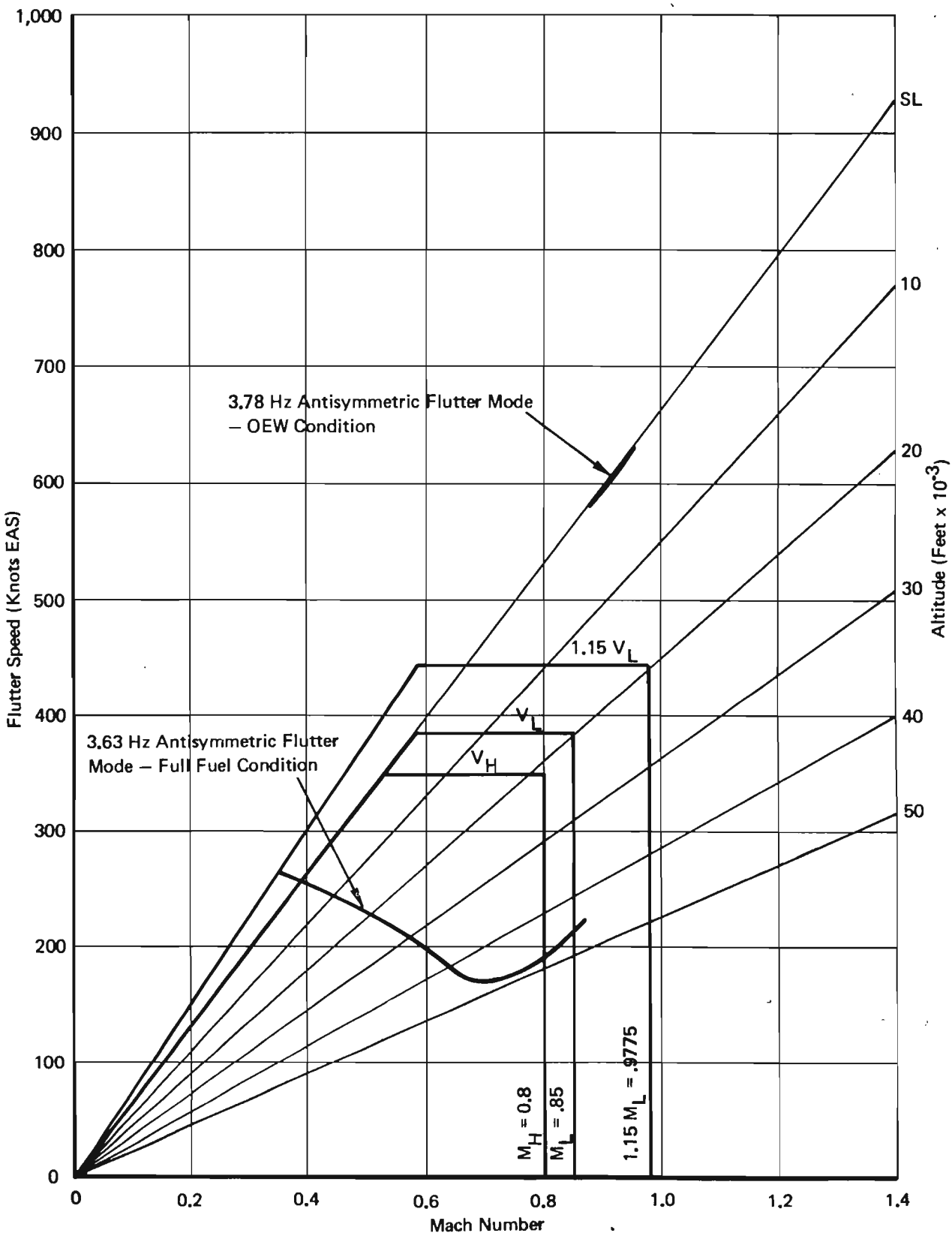

Figure 77: Comparison of Flutter Boundary to Structural Placard – Strength Design

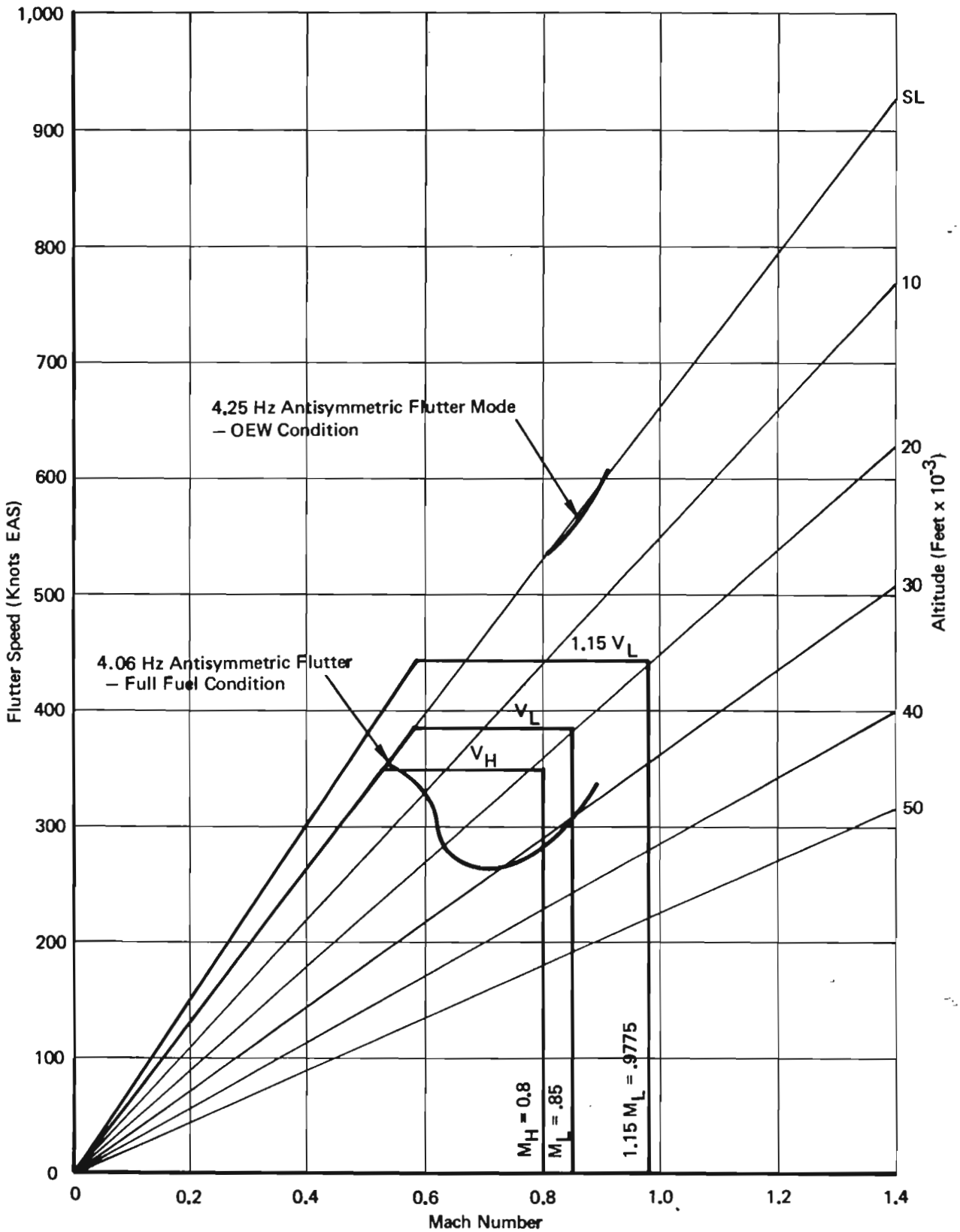

Figure 78: Comparison of Flutter Boundary to Structural Placard – Uniformly Stiffened Wing

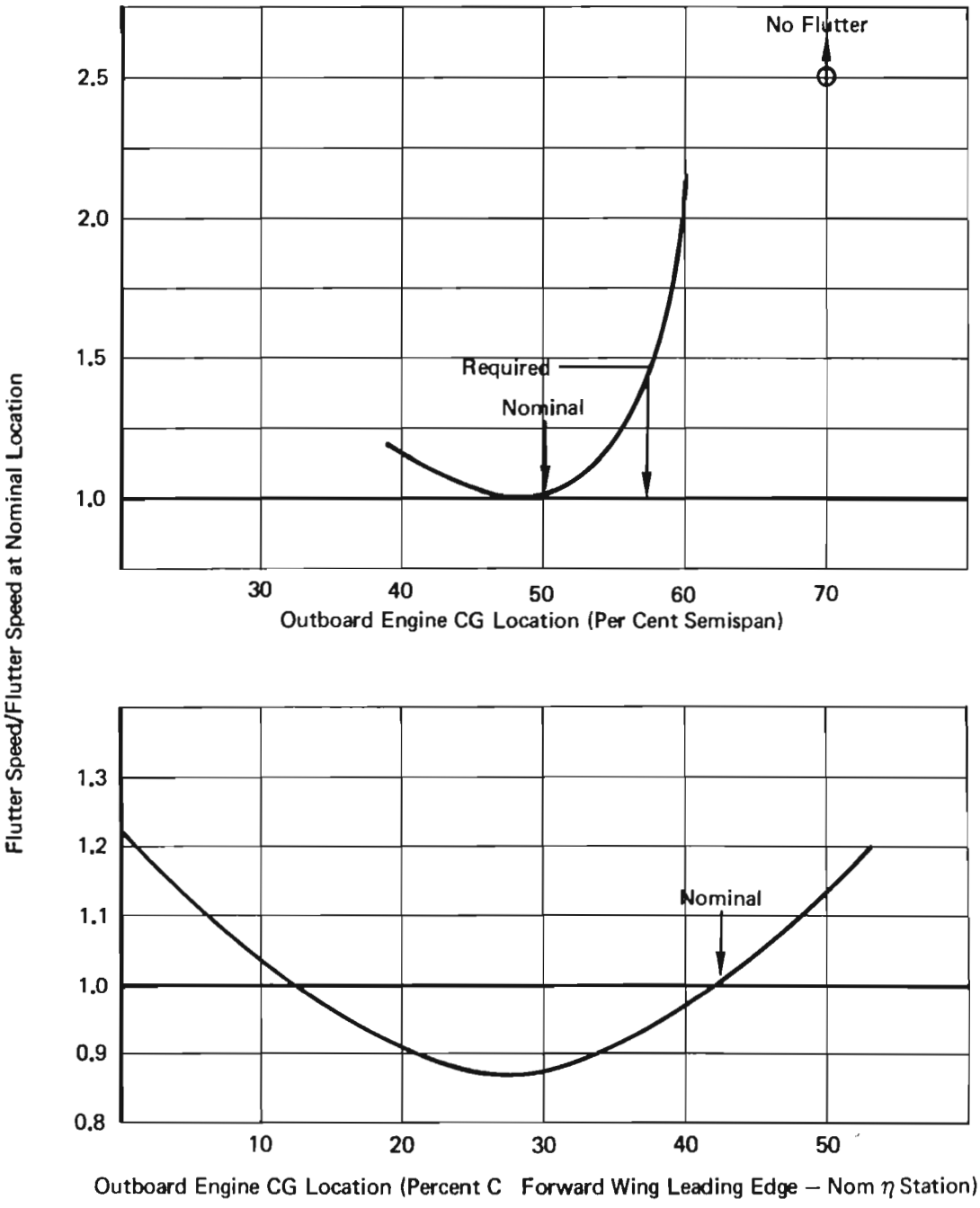

Note:
- Full Fuel
- EI Increased 25% Over Entire Wing
- GJ Increased 15% Over Entire Wing
- 19,600 Feet = Altitude

Figure 79: Engine Placement Study – Uniformly Stiffened Wing

6.2 Mass Properties

6.2.1 General

Group weight and balance statement and the "Dimensional and Structural Data" page of the AN9103D group weight statement are presented in Table VIII and IX, respectively.

Group weights were developed from the following data:

- Stress sizing of primary structure (wing, empennage and body)
- Empirical methods for secondary structure items
- Statistical methods for some propulsion and fixed equipment items
- Air Force equipment group weights, references
- Engine weights and scaling from the manufacturer
- Proposal and pre-proposal study results from Boeing AMST prototype work

The weight analyses produce weights that reflect special increments due to STOL design requirements. Weight studies accomplished by Boeing during the AMST design competition were used extensively in calculation of the Model 953-815 mass properties.

Design weights and centers of gravity used in the structural analyses are shown in Table X. Nominal values for payload and fuel c.g.'s were used to calculate the design weights center of gravities.

Effects of fuel and cargo loading on the Model 953-815 center of gravity locations are shown in Figures 80 and 81 . The limitation on placement of forward payload is determined by the forward aerodynamic c.g. limit. Aft payload placement limitation is variable, depending on the amount of fuel in the airplane. Figure 81 presents a comparison in aft payload loading capability when the airplane has full internal fuel (67,400 lbs) or basic STOL mission fuel (30,000 lbs). The curves show increased aft payload loading capability as fuel is off loaded. The fuel usage and/or loading effects (fuel vectors) on airplane center of gravity and the aerodynamic c.g. limits are shown in Figure 80 . Aerodynamic limits provide a total c.g. range of 27.7 in. for loading flexibility. Loading procedures equivalent to current military cargo transport operations can be employed. Ample flight control margin is available during air drop of cargo pallets even if the forward pallets remain in place.

Table VIII: Group Weight and Balance Statement

	Weight (Lb)	CG (In.)	
		Longitudinal	Vertical
Wing	18,470	674	260
Horizontal Tail	3,050	1,505	533
Vertical Tail	3,380	1,358	425
Body	25,720	638	164
Main Gear	6,940	724	81
Nose Gear	1,140	203	85
Nacelle or Eng Section	6,190	521	195
Structure	(64,890)	(716.9)	(215.0)
Engine	9,170	485	168
Engine Accessories	400	485	165
Fuel System	2,670	643	240
Engine Controls	320	390	240
Starting System	240	533	155
Thrust Reverse/Vector	3,940	584	172
Propulsion	(16,740)	(532.4)	(181.5)
Auxiliary Power Unit	500	620	95
Instruments & Nav Equipment	900	280	170
Surface Controls	3,010	726	305
Hydraulic/Pneumatic	900	670	250
Electrical	1,900	505	175
Avionics	2,000	250	150
Armament	700	380	190
Furnishings & Equip	4,000	423	193
Air Cond & Anti-Icing	1,600	490	114
Auxiliary Gear	100	650	100
BLC Supply System	1,300	624	248
Fixed Equipment	(16,910)	(498.4)	(200.8)
Weight Empty	98,540	648.1	206.9
Crew	860	210	210
Crew Provisions	80	210	210
Oil & Trapped Oil	200	480	168
Unavailable Fuel	320	660	250
Non-Exp Useful Load	(1,460)	(345.6)	(213.0)
Operating Weight	100,000	643.7	207.0
Payload	28,000	592	170
Fuel – Wing	30,000	665	260
STOL Gross Weight	158,000	638.5	210.5

Notes: Longitudinal CG Reference: Nose @ BS 114
Vertical CG Reference: Floor Line @ WL 100
MAC Length = 198 In.
LeMAC @ BS 597

Table IX: Group Weight Statement

AI -9103-D
NAME _____
DATE _____

GROUP WEIGHT STATEMENT
DIMENSIONAL & STRUCTURAL DATA

PAGE _____
MODEL 953-815
REPORT _____

1	LENGTH - OVERALL (FT.)	125.75		HEIGHT - OVERALL - STATIC (FT.) 44.17					
2		Main Floats	Aux. Floats	Booms	Fuse or Hull	Nacelles Inboard	Nacelles Center	Nacelles Outboard	
3	LENGTH - MAX. (FT.)				110.0	19.2		19.2	
4	DEPTH - MAX. (FT.)				17.97	6.41		6.41	
5	WIDTH - MAX. (FT.)				17.97	5.67		5.67	
6	WETTED AREA (SQ. FT.)				4,307	630.0		630.0	
*7	FLOAT OR HULL DISPL. - MAX (LBS.)								
8	FUSELAGE VOLUME (CU. FT.)		PRESSURIZED			TOTAL			
9						Wing	H. Tail	V. Tail	
10	GROSS AREA (SQ. FT.)					1700.0	533.6	385.65	
11	WEIGHT/GROSS AREA (LBS./SQ. FT.)					10.86	5.72	8.76	
12	SPAN (FT.)					113.0	45.5	22.4	
13	FOLDED SPAN (FT.)					–	–	–	
14									
15	SWEEPBACK - AT 25% CHORD LINE (DEGREES)					6.35	10.0	37.0	
16	- AT % CHORD LINE (DEGREES)								
**17	THEORETICAL ROOT CHORD - LENGTH (INCHES)					278.0	181.0	236.0	
18	- MAX. THICKNESS (INCHES)					41.7	23.5	30.7	
**19	CHORD AT PLANFORM BREAK - LENGTH (INCHES) @ .55 b/2					172.0	–	–	
20	- MAX. THICKNESS (INCHES) @ .55 b/2					22.7			
**21	THEORETICAL TIP CHORD - LENGTH (INCHES)					86.0	93.0	236.0	
22	- MAX. THICKNESS (INCHES)					11.4	12.1	30.7	
23	DORSAL AREA, INCLUDED IN (V. TAIL) AREA (SQ. FT.)							14.60	
24	TAIL LENGTH - 25% MAC WING TO 25% MAC H. TAIL (FT.)							67.33	
25	AREAS (SQ. FT.) Flaps	L.E. 170		T.E. 345					
26	Lateral Controls	Slots		Spoilers 128		Ailerons 69			
27	Speed Brakes	Wing		Fuse. or Hull					
28									
29									
30	ALIGHTING GEAR (LOCATION)						Main	Nose	
31	LENGTH - OLEO EXTENDED - ℄ AXLE TO ℄ TRUNNION (INCHES)						–	84.0	
32	OLEO TRAVEL - FULL EXTENDED TO FULL COLLAPSED (INCHES)						35.0	23.0	
33	FLOAT OR SKI STRUT LENGTH (INCHES)								
34	ARRESTING HOOK LENGTH - ℄ HOOK TRUNNION TO ℄ HOOK POINT (INCHES)								
35	HYDRAULIC SYSTEM CAPACITY (GALS.)								
36	FUEL & LUBE SYSTEMS	Location	No. Tanks	****Gals. Protected		No. Tanks	****Gals. Unprotected		
37	Fuel - Internal	Wing	7	10,370					
38		Fuse. or Hull							
39	- External								
40	- Bomb Bay								
41									
42	Oil								
43									
44									
45	STRUCTURAL DATA - CONDITION			Fuel in Wings (Lbs.)		Stress Gross Weight		Ult. L.F.	
46	FLIGHT			30,000		158,000		4.5	
47	LANDING			17,000		145,000			
48	MAX. DESIGN WEIGHT			67,400		225,400			
49	MAX. GROSS WEIGHT WITH ZERO WING FUEL					158,000			
50	CATAPULTING								
51	MIN. FLYING WEIGHT					102,760			
52	LIMIT AIRPLANE LANDING SINKING SPEED (FT./SEC.) 15					145,000			
53	WING LIFT ASSUMED FOR LANDING DESIGN CONDITION (%W)								
54	STALL SPEED - LANDING CONFIGURATION - POWER OFF (KNOTS)								
55	PRESSURIZED CABIN - ULT. DESIGN PRESSURE DIFFERENTIAL - FLIGHT (P.S.I.)							8.6	
56									
57	AIRFRAME WEIGHT (AS DEFINED IN AN-W-11) (LBS.)								

*Lbs. of sea water @ 64 lbs./cu. ft.
**Parallel to ℄ at ℄ airplane.
***Parallel to ℄ airplane.
****Total usable capacity.

GPO 807984

Table X: Design Weights

Design Condition	Weight (lb)	CG (In.)	
		Longitudinal	Vertical
Maximum Design Weight	225,400	636.7	213.3
Basic Flight Design Weight (Transport)	204,800	635.7	208.6
Basic Flight Design Weight (Assault)	158,000	638.5	210.5
Alternate Flight Design Weight (Assault)	145,000	636.2	206.1
Landplane Landing Weight (CTOL)	191,700	631.8	205.1
Landplane Landing Weight (STOL)	145,000	636.2	206.1
Maximum Landing Weight (CTOL)	222,350	636.3	212.7
Minimum Flying Weight	102,760	646.7	208.7
Zero Fuel Weight	128,000	632.4	198.9

Notes: Longitudinal CG Reference: Nose @ BS 114
Vertical CG Reference: Floor Line @ WL 100
Payload CG @ BS 592 & WL 170
MAC Length = 198 In.
LEMAC @ BS 597

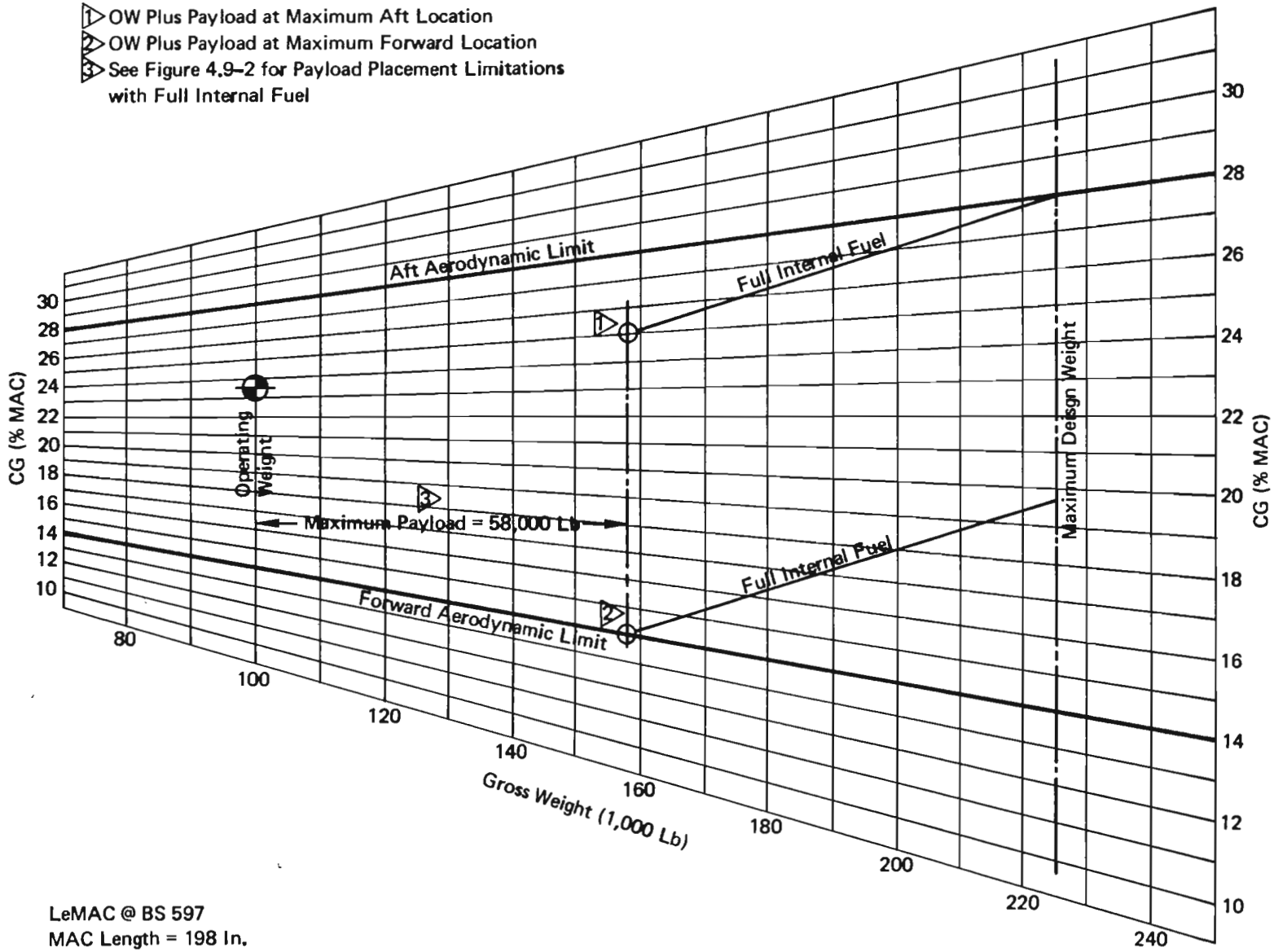

Figure 80 : Center of Gravity Envelope — Maximum Payload and Full Internal Fuel

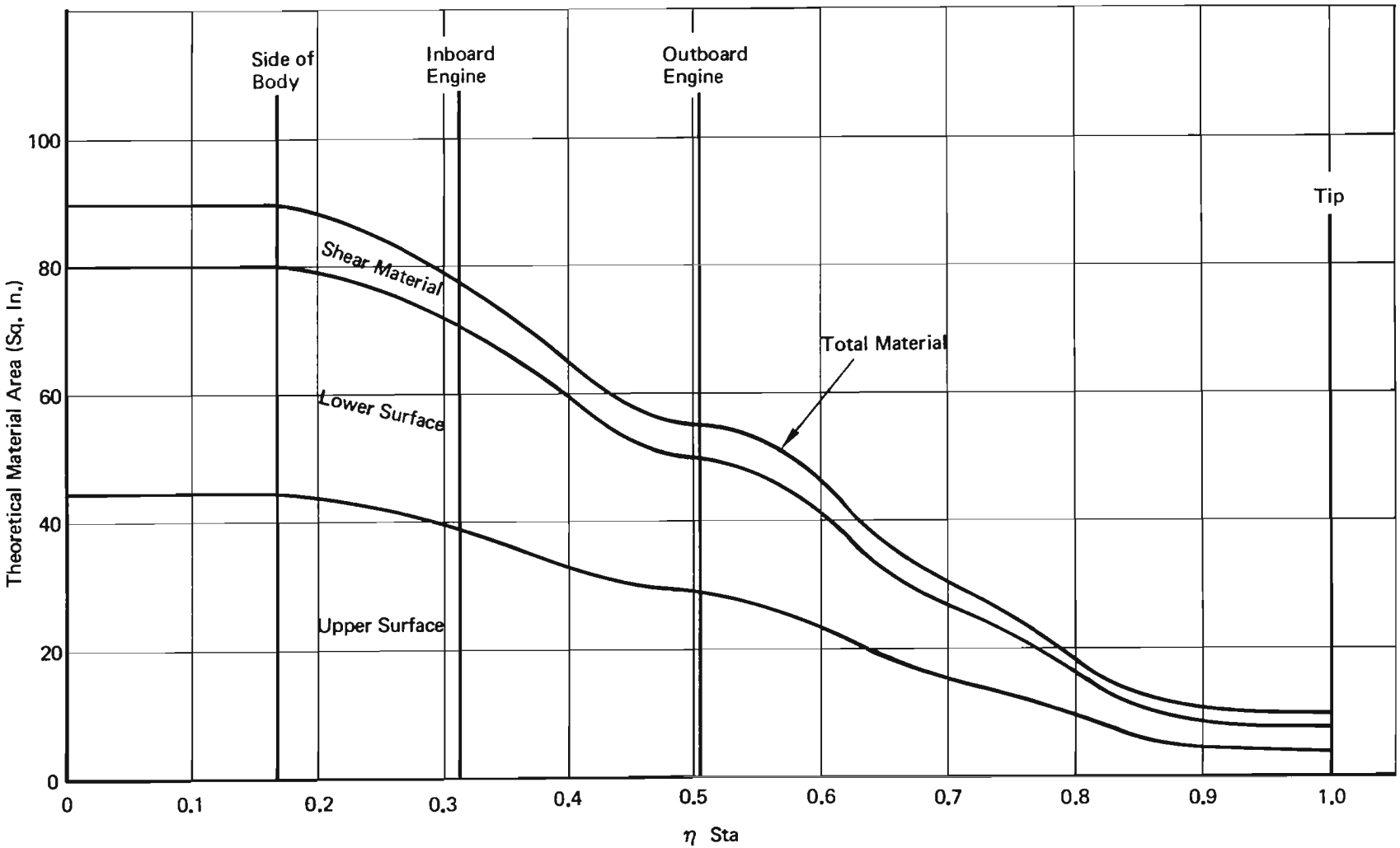

Figure 82 : Wing Box Material Requirements

Vertical Tail

Surface Material		680 lbs
Spars		490
Ribs and Joints		330
Pivot Actuator Fittings		350
Fasteners		80
Access Panels		50
Fixed Leading Edge (incl. Dorsal)		180
Fixed Trailing Edge		80
Rudders		870
Tip Fairing		210
Walkways, Steps and Grips		30
Exterior Finish		30
TOTAL VERTICAL TAIL WT.		3380 lbs

Body

Skin and Stringer		5920 lbs
Bulkheads		3830
Minor Frames		1820
Longerons		980
Flooring and Supports		5280
Cargo Floor	3060	
Cargo System	1880	
Crew Deck	340	
Windows		860
Doors		4840
Jump Door	500	
Entry	360	
Escape Hatches	130	
Aft Ramp	1960	
Aft Cargo Plug Door	1650	
Access	20	
Nose Gear Door	220	
Main Gear Fairing and Doors		1250
Stairways and Ladders		20
Walkways, Steps and Grips		150
Non-Skid Floor Protection		40
Protective Finish		180
Aerial Refueling Provision		60
Floor Protection		400
Miscellaneous		90
TOTAL BODY WT.		25720 lbs

Main Landing Gear

Running Gear	2140 lbs
Structure	2920
Controls	910
Hi-Flotation Penalty	970
TOTAL MAIN GEAR WEIGHT	6940 lbs

Nose Landing Gear

Running Gear	270 lbs
Structure	610
Controls	260
TOTAL NOSE GEAR WEIGHT	1140 lbs

Nacelle or Engine Section

Struts	3040 lbs
Inlet	1340
Fan Cowl	950
Side Cowl	595
Engine Mounts	265
TOTAL NACELLE WEIGHT	6190 lbs

6.2.3 Propulsion Group Weight

The engine description, weight and scaling curves are presented in Section 4.2. Weight breakdowns to the level of weights estimation for the propulsion groups are shown below:

Engine		9170 lbs
Engine Accessories		400
Fuel System		2670
Basic System	2060	
IFR	100	
Explosion Suppression	510	
Engine Controls		320
Throttle	120	
Start	120	
Thrust Reverse/Vector	80	
Starting System		240
Thrust Reverser/Vector		3940
External Boattail	1165	
Thrust Reverse Structure	2010	
Thrust Vector Actuation	205	
Shell Position Control	320	
Thrust Reverse Input	240	
TOTAL PROPULSION WEIGHT		16740 lbs

6.2.4 Fixed Equipment Weight

Weight breakdowns for the fixed equipment groups are shown below:

Auxiliary Power Plant		500	lbs
Instruments		900	
Surface Controls		3010	
Cockpit Controls	180		
AFCS	230		
Roll Controls	750		
Pitch Controls	550		
Yaw Controls	250		
Hi-Lift Controls	1050		
Hydraulics		900	
Electrical		1900	
Avionics		2000	
Armament		700	
Furnishings		4000	
Air-Conditioning & Anti-Icing		1600	
Auxiliary Gear		100	
BLC Supply System		1300	
Ejectors	240		
Ejector Supply Ducting	110		
Valving	90		
Supply Ducts	620		
Wire and Controls	90		
Nozzle and Ducts	150		
TOTAL FIXED EQUIPMENT WEIGHT		16910	lbs

SECTION VII

COMPARATIVE OVERVIEW OF POWERED - LIFT CONCEPTS

7.1 Candidate Powered Lift Systems

When the Tactical Airlift Technology ADP was begun, four powered lift concepts were considered candidates for the eventual AMST:

(1) Vectored thrust with mechanical flaps (VT/MF)

(2) Externally blown jet flaps (EBJF)

(3) Internally blown jet flaps (IBJF)

(4) Augmentor wing (AW)

Because the augmentor wing was already under intensive investigation by NASA, it was decided that the STAI programs should cover only the first three candidates.

After the STAI effort was well underway, the Air Force initiated the AMST Prototype program. In preparing to propose a design for the prototype, The Boeing Company re-evaluated the then available data on all the above powered lift candidates and also considered other possible approaches. That effort resulted in the selection of the Upper Surface Blown Flap (USB) as the powered lift concept for its prototype proposal.

Two contractors were eventually selected to build AMST prototype airplanes: McDonnell-Douglas with an EBJF design, and Boeing with its USB. The five concepts are diagrammed in Figure 83.

7.2 Aerodynamic Characteristics

The aerodynamic characteristics having greatest influence on the STOL transport design problem are:

(1) Usable* maximum lift coefficient. This determines minimum speed for a given wing loading.

and

(2) The range of net force along the flight path. (i.e., net drag.) This determines the maximum climb and descent angles. The capability to modulate this force for path angle control is essential.

*Trimmed in pitch, and if the design condition must consider engine failure, in roll and yaw as well.

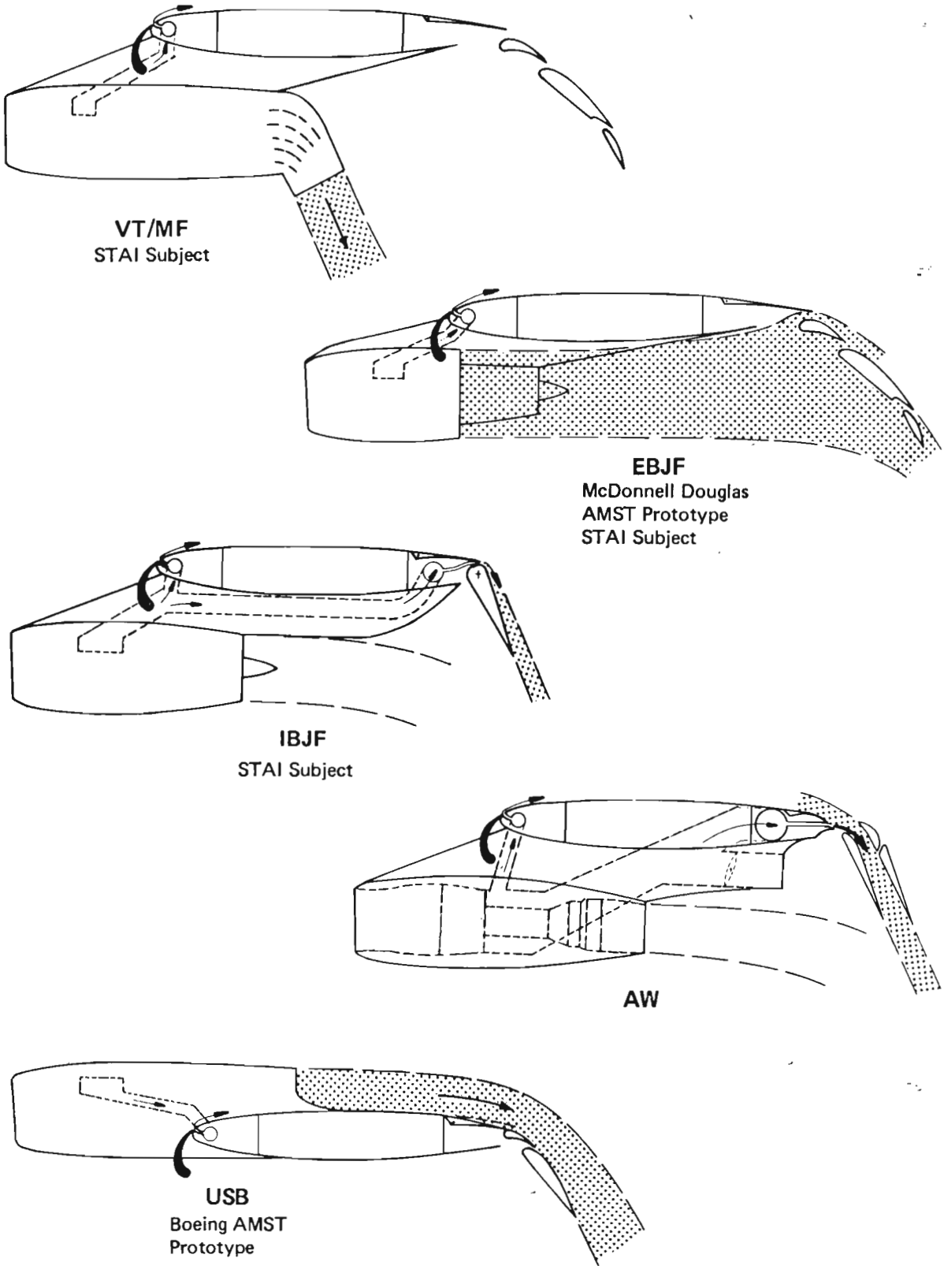

Figure 83: Powered Lift STOL Concepts

Figure 84 (from Ref. 9) shows untrimmed C_D and C_L (including propulsive forces) as measured in the Boeing V/STOL wind tunnel for all five systems. The same basic model was used for all but the IBJF case, which is STAI data adjusted for planform differences. All systems except the VT/MF show substantial lift augmentation due to "supercirculation" effects characteristic of the jet flap. The extra balancing tail load required to trim the larger negative C_m's of the four jet flap systems would reduce their C_L values by about 0.25. Their net C_L advantage remains in the range of 1.5 to 2.0.

The VT/MF system had been expected to show superior climb capability (i.e., to have a more negative C_D at a given C_L) because of the high turning efficiency of the vector nozzle. (This was determined to be better than 0.99, from static thrust measurements.) At 30° thrust vector angle, the actual effective turning efficiency (determined by the distance from the extended power-off polar to the power-on curve) is only 0.88. The difference can be explained as follows:

(1) For best effective turning efficiency, the 30° vector angle is appropriate at an overall C_L of 6.6 at $C_J = 2$. The mechanical flap system, unaided by supercirculation, never attains the required aerodynamic C_L.

(2) The jet induces adverse aerodynamic interference, as reported in Volume IV of this series. The interference decreases lift except at the highest angles of attack, and also usually increases drag.

The USB system achieves about the same turning efficiency (and thus the same climb angle capability) as the VT/MF system. The EBJF has noticeably poorer climb capability, reflecting losses due to high speed flow through the flap slots and momentum lost to spanwise flow. The AW system also shows poorer climb capability, because of the drag penalty due to separation on the upper side of the augmentor shroud.

The jet momentum coefficient (C_J) was based in each case on conditions measured at the blowing nozzle. This implies that the AW and IBJF data may be optimistic, since losses in the duct system carrying the air from the engines to the flap knee were not accounted for.

The VT/MF, EBJF, and USB systems all generate large rolling moments in case of engine failure. Because of its over-wing engine arrangement, the USB concept permits locating the engines closer to the airplane centerline on high wing configurations, and therefore has an advantage over the other two. For the IBJF and AW concepts, cross-ducting arrangements can minimize or eliminate the problem.

All five powered lift concepts provide the means to modulate net drag to control flight path angle. For VT/MF this is done by varying the thrust vector angle(σ). At the high σ required for landing approach, this results in large drag variation but very little change in total lift. The jet flap concepts can provide path angle control through variation of the trailing edge flap angle. Beyond flap

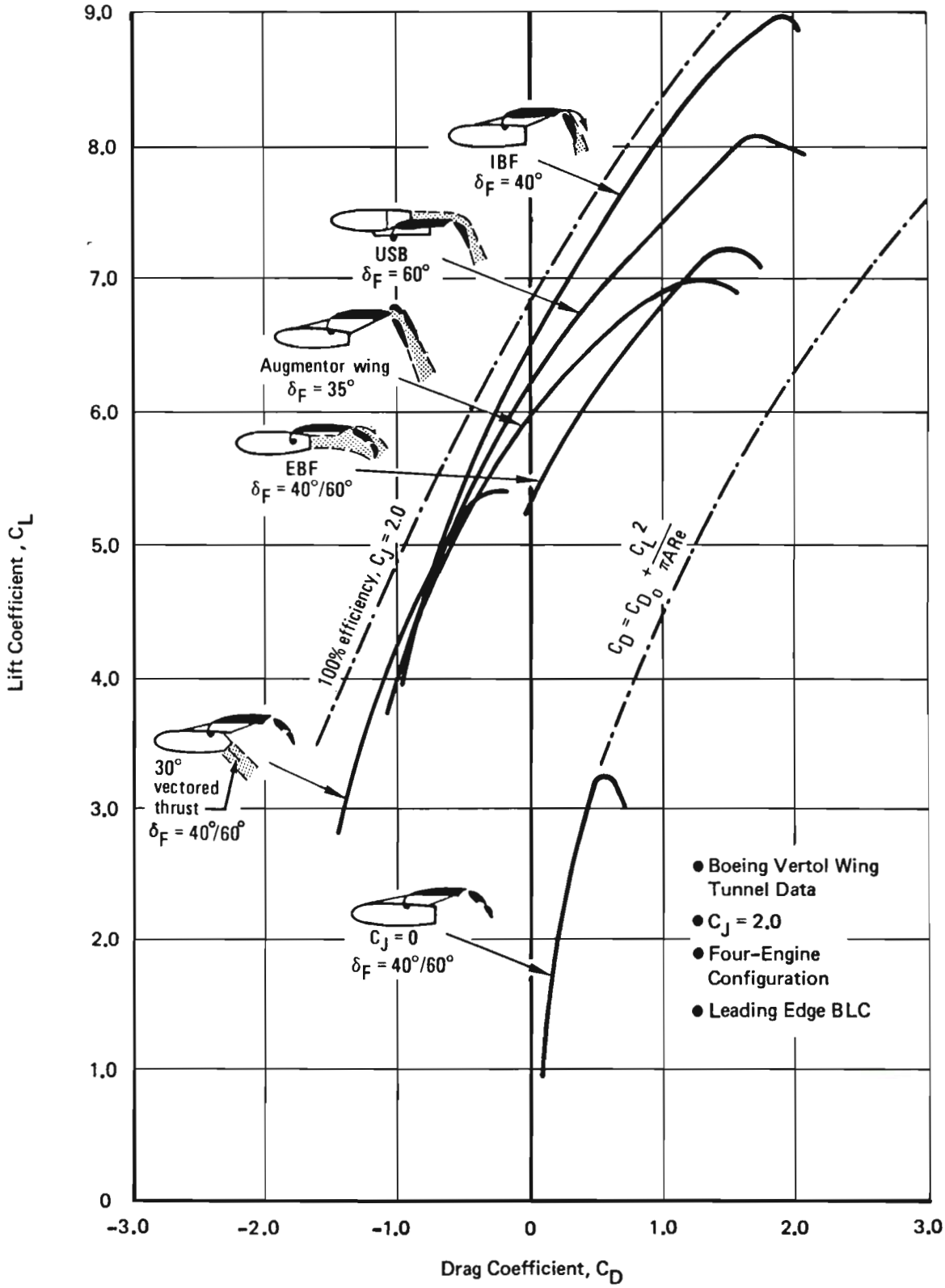

Figure 84: Drag Polars for Various Powered-Lift Concepts

deflections around 40°, this also results in drag control with little lift variation.

7.3 Design Considerations

The present study did not include a formal, detailed comparison of the refined VT/MF airplane design with configurations using the other powered lift system candidates. However, it is possible to make some observations on the basis of the results of the Baseline Configuration Study conducted early in the STAI and of an independently conducted brief study of a 4-engine AMST designed to STAI rules.

7.3.1 Vectored Thrust vs Internally Blown Jet Flap

In the Baseline Configuration Study, a VT/MF airplane and an IBJF airplane were parametrically designed to the same rules. (These baseline airplanes were described in detail in Appendix A.) The IBJF design was approximately 29,000 lbs. heavier than the Baseline VT/MF configuration. The main causes of this gross weight increase were:

(1) A reduction in wing internal fuel tank volume caused by forward relocation of the rear spar (from 65 percent to 52 percent chord) to make room for air distribution ducts. This produced an increase in wing size to maintain the required ferry range capability and a corresponding increase in horizontal tail size. Because of the resulting low wing loading, the IBJF's considerable advantage in C_L max over VT/MF was not efficiently utilized.

(2) The addition of the empty weight increment of the internally blown jet flap air distribution system.

(3) The increase in nacelle size and weight to accommodate the engine and duct system required for IBJF.

(4) The increase in propulsion system weight resulting from a lower bare-engine thrust-to-weight ratio and a larger thrust requirement.

(5) An increase in the specific fuel consumption resulting from the selection of a relatively low bypass ratio engine suited to the IBJF application.

(6) Structural weight increases in the body and landing gear to accommodate the changes listed above.

Although the refined VT/MF airplane presented in Section III was found to be somewhat heavier than the original baseline (158,000 lbs. vs 144,500 lbs. for the STOL radius mission), more than half of the original 29,000 lb. disadvantage of the original IBJF baseline remains. Furthermore, it is likely that if the IBJF design were subjected to the same refinement process, its weight would also have grown.

7.3.2 Vectored Thrust vs Upper Surface Blowing

Figure 85 shows a parametric design "thumbprint" for a four-engine USB airplane designed to STAI rules. It was obtained by adjusting the thumbprint for the VT/MF parametric design (Figure 8) for weight increments as indicated by data developed in studies for the AMST prototype program. Weight savings obtained by elimination of the thrust vectoring system and replacement of the nacelle struts by an over-wing mounting arrangement result in a gross weight reduction of 2.5% for any combination of thrust and wing loading. Superior STOL performance, due to the excellent aerodynamic characteristics of USB, and essentially unchanged ferry mission characteristics lead to a design point having a gross weight of 147,000 lbs. and a thrust to weight ratio of 0.39. This airplane is 7% lighter and requires 23% less installed engine thrust than the 953-815 VT/MF design. It is therefore reasonable to conclude that the USB powered lift concept has superior potential compared to VT/MF.

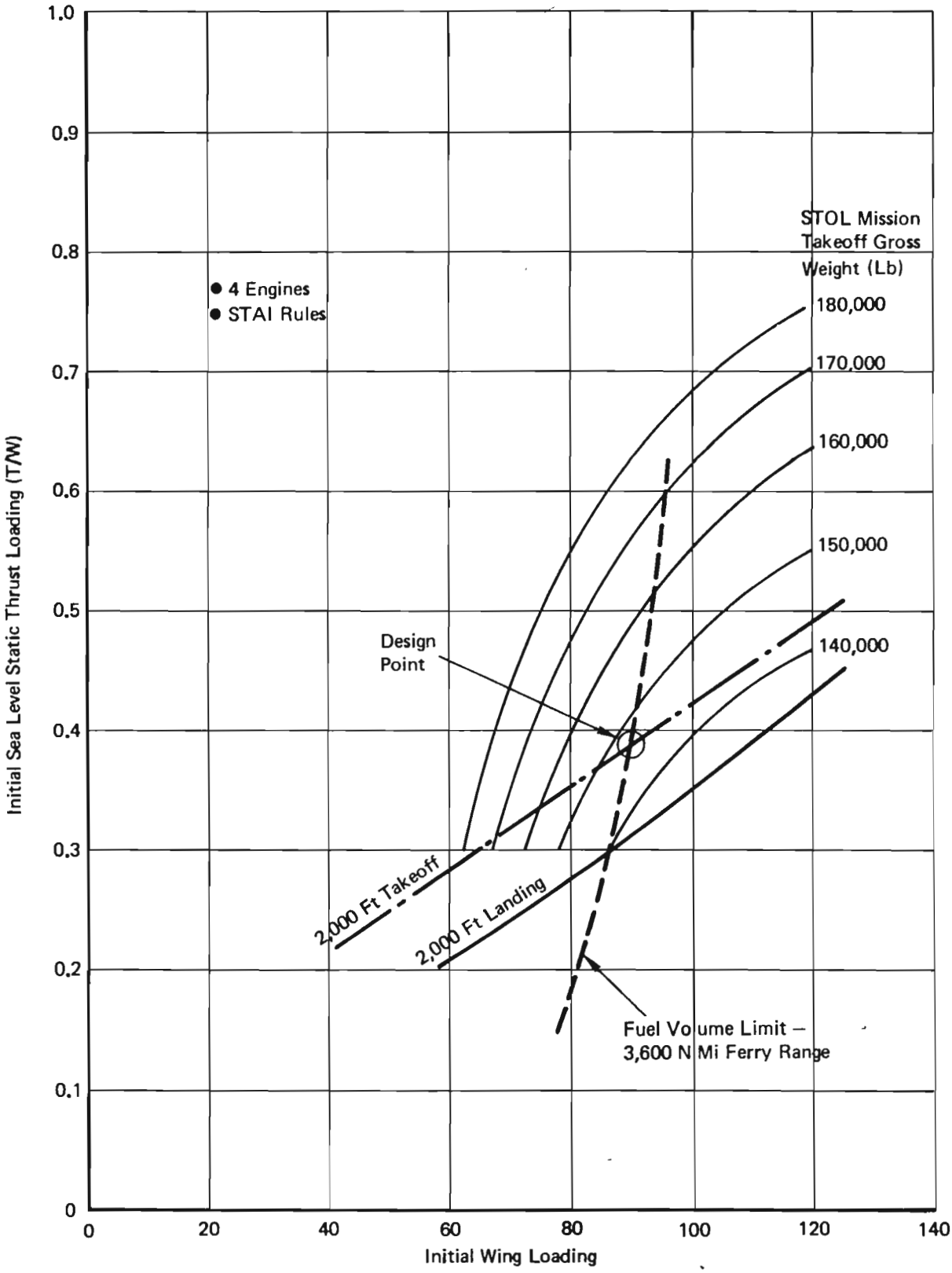

Figure 85: Parametric Design — USB Airplane

SECTION VIII

RECOMMENDED FUTURE PROGRAMS

8.1 Background

When the STAI was begun, the start of an AMST prototype program before the STAI's completion could not be foreseen. It was therefore expected that one major end product of the STAI would be a recommendation for a program of major component development, flight demonstrator aircraft construction, or the like. The AMST prototype program will accomplish the objectives of development efforts of that type, so recommendations along those lines are inappropriate.

There will nevertheless remain a number of technical areas where the AMST Prototype work, because of the austerity of that program, will not have provided all the technology base needed to exploit the full potential of a possible production AMST. Furthermore, the AMST will not be the last USAF program to benefit from advances in STOL technology. It is therefore proper that work should continue on problems relating both to tactical airlift and to STOL in general. Some recommendations for such work are presented below.

8.2 STOL Aerodynamics Technology

The upper surface blowing powered lift concept should be explored beyond the limits of what is required to make the AMST Prototype work. Specifically:

(1) The gas dynamics of turning thick jets over convex surfaces should be studied both analytically and experimentally. The objective would be to determine the limits of turning angle and turning efficiency as they are affected by viscosity and compressibility. The ultimate potential for USB in both STOL and VTOL applications would be clarified.

(2) The effects of arrangement variables, such as aspect ratio, sweepback, and engine spanwise location should be explored in a program similar to those applied to other systems in the STAI. This data would serve as a technology base for future STOL programs.

(3) The question of whether to arrange pairs of engines in Siamese pods or to spread them out along the wing should be studied. Since the Boeing AMST prototype is a twin engine design, this problem will otherwise remain unresolved. It is possible that a pair of engines in a double pod could be installed in a way which could reduce the lift and trim penalty due to engine failure by spreading the available jet thrust over the span normally occupied by both engines' exhaust. This issue could be of importance to a possible AMST production program if a new STOL engine development makes a four engine USB design appear attractive.

8.3 Flight Control Technology

While the STAI work appears to have made a substantial contribution to the development of an AMST control system which can be expected to provide excellent STOL flying qualities, pilots will still welcome any further simplification of the STOL landing task. In this area, it is recommended that a program of cockpit display development be pursued. A system is needed which will show the pilot his speed and maneuvering g margins in a format integrated with the vertical situation display.

In cruising flight, a production AMST could benefit from a flight control system using feedback techniques for gust load alleviation and suppression of undesirable structural dynamic modes. Such a system would improve ride quality, permit savings in structural weight, and extend the useful life of the aircraft.

8.4 STOL Performance Ground Rules

All the rules so far proposed for calculating takeoff and landing field lengths are based on arbitrary assumption regarding the extra runway needed to account for touch down dispersion, variations in braking technique, time to apply spoilers, etc. The ground rules suggested in Volume III of the present series (Reference 10) are, unfortunately, no exception. Analytical techniques are needed to permit estimation of the benefits which may be expected from a variety of features in both flight and ground-roll controls and decelerating devices, so their real value can be quantitatively stated. A study to develop such techniques is recommended.

8.5 Survivability/Vulnerability

The operational AMST must have some level of hardness against small-arms fire (including 7.62 mm, 14.5 mm and 23 mm HE), and laser weapons. The design hardness level for each threat should be established by evaluating the trades between reduction in attrition rate and the penalties associated with hardening.

The initial step in the S/V integration would be to establish the critical components and vulnerable areas of the configuration, including the fuel system, crew area, flight controls, propulsion system, hydraulic system and structure. Following this, a parametric trade study should be conducted to determine the penalties and benefits of hardening concepts, including gross voided foam for fuel tanks, nitrogen inerting, armor and shielding, and retrofittable passive countermeasures for protection against lasers.

The data from these studies would then be used to establish final hardness criteria for the production vehicle, and the effects on performance.

8.6 Ground Operations

8.6.1 Cargo Handling

Current Air Force cargo aircraft have experienced considerable difficulties in their cargo handling systems under the stress of actual military operations. For example, maintenance has been a problem because of excessively fragile fittings in cargo compartments. The problem of maintaining fuel supplies at forward bases for Army helicopters and ground vehicles has lead to an unforeseen heavy use of tactical transports as tankers, as well.

These problems indicate that a cargo handling system development program is needed well in advance of possible AMST production. This program would begin with a comprehensive tabulation of the items which will be carried and the frequency of their handling. The results would then determine design criteria for the cargo floor and other handling system elements. One important issue which needs resolution in this area is the question of whether or not to provide tanker capability by installation of permanent extra tank capacity and an associated fluid transfer system.

8.6.2 Ground Mobility

In the cramped environment of a short austere forward airfield, it is likely that use of engine power to taxi and reposition aircraft for loading, unloading and service would cause severe difficulties because of noise and exhaust effects.

It is therefore recommended that a ground mobility system independent of the main propulsion engines be investigated.

8.7 Advanced Structural Concepts

A potential exists for substantial savings in weight and fabrication costs through use of advanced composite structures. Advanced composites are especially beneficial where structural stiffness is required, as well as strength. Cost savings can be realized through designs having many fewer parts. A single bonding operation in an autoclave can sometimes replace an assembly of large numbers of small metal elements with many fasteners.

It is therefore recommended that presently planned conceptual studies of advanced composite structural applications for the AMST be carried through to fruitful conclusions.

APPENDIX I

SUMMARY OF PRELIMINARY BASELINE CONFIGURATION STUDY:

JANUARY 1972

1.0 Introduction

This appendix summarizes the preliminary Baseline Configuration Study portion of the STAI carried out by The Boeing Company under U.S. Air Force Flight Dynamics Laboratory Contract No. F33615-71-C-1757 through January 1972. The complete report is given in Reference 2.

The principal result of this study was a Medium STOL Transport (MST) configuration embodying the powered high-lift concept known as "Vectored Thrust Plus Mechanical Flaps" (VT + MF). Figure 86 shows the general arrangement of this airplane, Model 953-801, and lists its major characteristics. It was designed to fulfill the MST Mission Requirements and Takeoff/Landing Rules, as given in Appendix II. This configuration served as a basis for establishing wind tunnel model and test requirements and for conducting flight control system studies, and simulation, as required by Part 2 of the STAI work statement. In addition, trade data defining the impact of variations of mission requirements on aircraft weight and arrangement were developed. This data is discussed below.

2.0 Planform Parametric Study Configurations

Prior to the selection of the preliminary baseline configuration Model 953-801, parametric studies were conducted utilizing the mission requirements and preselected low speed aerodynamic characteristics (triple-slotted trailing edge flaps, aerodynamically shaped leading edge flaps, leading edge boundary layer control, blown drooped ailerons and vectored thrust). Six combinations of aspect ratios and sweepback angles were applied to these data resulting in different takeoff gross weights. These combinations are shown in Figure 87 . Figure 88 shows the gross weight comparisons of the various configurations leading to the selection of Model 953-801 based on its lower gross weight to satisfy mission requirements.

3.0 Preliminary Baseline Configuration

The selection of the preliminary baseline design, identified as the Model 953-801 (Figure 86) was made on the basis that it was the lightest of all the configurations considered in the study which met mission requirements. Its low sweepback angle also was considered advantageous because it appeared to offer more desirable stability and control characteristics in the STOL flight regime. The design selection chart for this baseline configuration is presented in Figure 89 .

4.0 Trade Studies - Mission Variations

After the selection of Model 953-801 as the baseline configuration, specific trades were made as to the sensitivity of airplane size and performance to changes in the mission requirements (Appendix II). In each case, a new airplane model was obtained by matching the airframe and engine parameters to the altered mission requirements. The STOL field length and the fuel volume required for the ferry mission generally dictated the design point selection; except in the maximum cruise Mach number trade, which was constrained by the speeds and fuel volume requirements. The bar chart of Figure 90 compares the incremental effects of the trades on the baseline airplane size and performance. A deviation from the desired maximum cruise speed of Mach .75 was made in the 2500 foot field length trade. This is explained in Section 4.3 below.

Table XI summarizes the values of the principal size and performance parameters and Table XII presents the weight statements for the airplane configurations that resulted from the trades.

4.1 750-Nautical-Mile-Mission Radius (Model 953-807)

The increase in the mission radius from 500 nautical miles to 750 nautical miles causes the airplane gross weight to increase by about 20,000 pounds, and the thrust by about 3,000 pounds. The design selection chart for the 750-nautical-mile-radius mission is presented in Figure 91 . The design point is shown there to be defined by the takeoff and fuel volume requirements. The configuration is similar to that of the baseline airplane (-801) but has increases in weight, wing area, and rated thrust as indicated in Figure 90 .

It may be noted that about 12,000 pounds of the 20,000 pounds increase from the baseline gross weight is in the fuel for the extended radius mission. The larger engines required to achieve the 2,000 foot takeoff produced additional weight but also a bonus of .02 Mach number in maximum cruise speed.

4.2 1,500 Foot Field Length (Model 953-810)

The 500 foot decrease in STOL field length from 2,000 foot to 1,500 foot produced greater increases in both wing area and rated thrust than the 750 nautical mile radius trade. Figure 92 presents the design selection chart for the 1,500 foot field length mission. In this case, the landing field length became critical and the minimum weight design was determined by the landing and takeoff field length requirements. The empty weight increase was about the same as that incurred by the 750 nautical mile trade. It is reflected in the 12,560 pound gross weight increment shown on the bar chart of Figure 90 . The thrust increase associated with the shorter field length resulted in an increase in maximum cruise Mach number of about .02.

APPENDIX I

SUMMARY OF PRELIMINARY BASELINE CONFIGURATION STUDY: JANUARY 1972

1.0 Introduction

This appendix summarizes the preliminary Baseline Configuration Study portion of the STAI carried out by The Boeing Company under U.S. Air Force Flight Dynamics Laboratory Contract No. F33615-71-C-1757 through January 1972. The complete report is given in Reference 2.

The principal result of this study was a Medium STOL Transport (MST) configuration embodying the powered high-lift concept known as "Vectored Thrust Plus Mechanical Flaps" (VT + MF). Figure 86 shows the general arrangement of this airplane, Model 953-801, and lists its major characteristics. It was designed to fulfill the MST Mission Requirements and Takeoff/Landing Rules, as given in Appendix II. This configuration served as a basis for establishing wind tunnel model and test requirements and for conducting flight control system studies, and simulation, as required by Part 2 of the STAI work statement. In addition, trade data defining the impact of variations of mission requirements on aircraft weight and arrangement were developed. This data is discussed below.

2.0 Planform Parametric Study Configurations

Prior to the selection of the preliminary baseline configuration Model 953-801, parametric studies were conducted utilizing the mission requirements and preselected low speed aerodynamic characteristics (triple-slotted trailing edge flaps, aerodynamically shaped leading edge flaps, leading edge boundary layer control, blown drooped ailerons and vectored thrust). Six combinations of aspect ratios and sweepback angles were applied to these data resulting in different takeoff gross weights. These combinations are shown in Figure 87 . Figure 88 shows the gross weight comparisons of the various configurations leading to the selection of Model 953-801 based on its lower gross weight to satisfy mission requirements.

3.0 Preliminary Baseline Configuration

The selection of the preliminary baseline design, identified as the Model 953-801 (Figure 86) was made on the basis that it was the lightest of all the configurations considered in the study which met mission requirements. Its low sweepback angle also was considered advantageous because it appeared to offer more desirable stability and control characteristics in the STOL flight regime. The design selection chart for this baseline configuration is presented in Figure 89 .

4.0 Trade Studies - Mission Variations

After the selection of Model 953-801 as the baseline configuration, specific trades were made as to the sensitivity of airplane size and performance to changes in the mission requirements (Appendix II). In each case, a new airplane model was obtained by matching the airframe and engine parameters to the altered mission requirements. The STOL field length and the fuel volume required for the ferry mission generally dictated the design point selection; except in the maximum cruise Mach number trade, which was constrained by the speeds and fuel volume requirements. The bar chart of Figure 90 compares the incremental effects of the trades on the baseline airplane size and performance. A deviation from the desired maximum cruise speed of Mach .75 was made in the 2500 foot field length trade. This is explained in Section 4.3 below.

Table XI summarizes the values of the principal size and performance parameters and Table XII presents the weight statements for the airplane configurations that resulted from the trades.

4.1 750-Nautical-Mile-Mission Radius (Model 953-807)

The increase in the mission radius from 500 nautical miles to 750 nautical miles causes the airplane gross weight to increase by about 20,000 pounds, and the thrust by about 3,000 pounds. The design selection chart for the 750-nautical-mile-radius mission is presented in Figure 91 . The design point is shown there to be defined by the takeoff and fuel volume requirements. The configuration is similar to that of the baseline airplane (-801) but has increases in weight, wing area, and rated thrust as indicated in Figure 90 .

It may be noted that about 12,000 pounds of the 20,000 pounds increase from the baseline gross weight is in the fuel for the extended radius mission. The larger engines required to achieve the 2,000 foot takeoff produced additional weight but also a bonus of .02 Mach number in maximum cruise speed.

4.2 1,500 Foot Field Length (Model 953-810)

The 500 foot decrease in STOL field length from 2,000 foot to 1,500 foot produced greater increases in both wing area and rated thrust than the 750 nautical mile radius trade. Figure 92 presents the design selection chart for the 1,500 foot field length mission. In this case, the landing field length became critical and the minimum weight design was determined by the landing and takeoff field length requirements. The empty weight increase was about the same as that incurred by the 750 nautical mile trade. It is reflected in the 12,560 pound gross weight increment shown on the bar chart of Figure 90 . The thrust increase associated with the shorter field length resulted in an increase in maximum cruise Mach number of about .02.

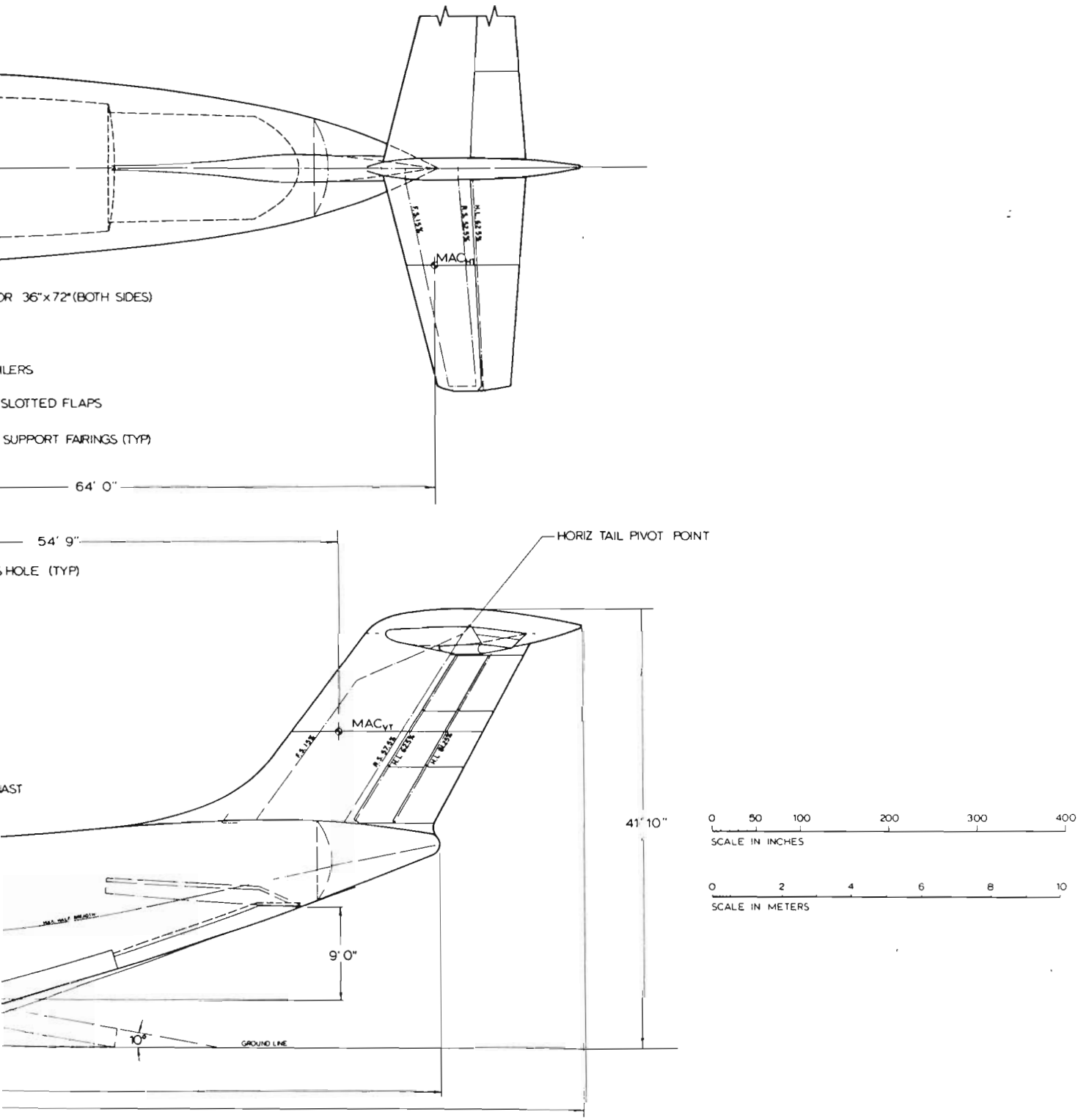

Figure 86: General Arrangement – Model 953-801

6	14,180 LB
5	13,760 LB
4	17,170 LB
	45,110 LB
NK	19,130 LB
	64,240 LB

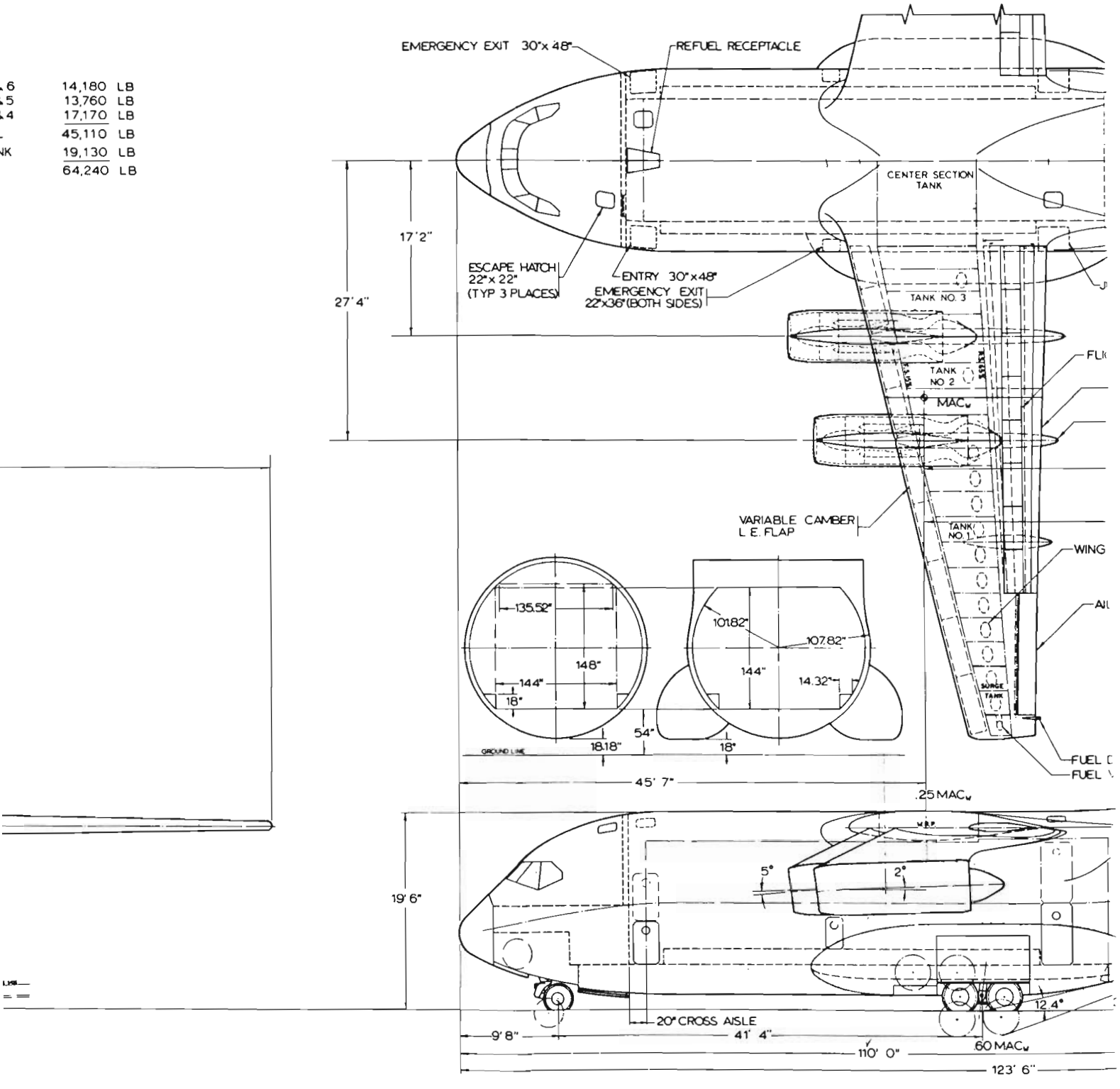

MODEL 953-801

AERODYNAMIC DATA

		WING	HORIZ. TAIL	VERT. TAIL
AREA	FT^2	1589.50	422.30	327.38
SPAN	FT	112.76	41.10	18.09
ASPECT RATIO		8.0	4.0	1.0
SWEEP, C/4		10°	10°	35°
DIHEDRAL		0°	- 4°	—
INCIDENCE		0°	+4°,-15°	—
TAPER RATIO		.3	.5	.8
THICKNESS RATIO	BODY SIDE	.150	.13	.13
	.55 b/2	.132	.13	.13
	TIP	132	.13	.13
MAC	FT	15.46	10.65	18.17
VOLUME COEFFICIENT		—	1.10	0.10

POWER PLANT

4 BY PASS 5.25 TURBOFANS WITH THRUST VECTORING 17,740 LB THRUST

LANDING GEAR

MAIN 8 42 x 15.0-16 TIRES
NOSE 2 34 x 12.0-12 TIRES

CARGO COMPARTMENT

144"w 144"/148"H 540"L

WEIGHTS

DESIGN GROSS	145,440	LB	ASSAULT MISSION
DESIGN STOL	132, 350	LB	
STOL PAYLOAD		LB	
O.E.W.	88,500	LB	
DESIGN GROSS	194,000	LB	CTOL MISSION
MAX. PAYLOAD		LB	

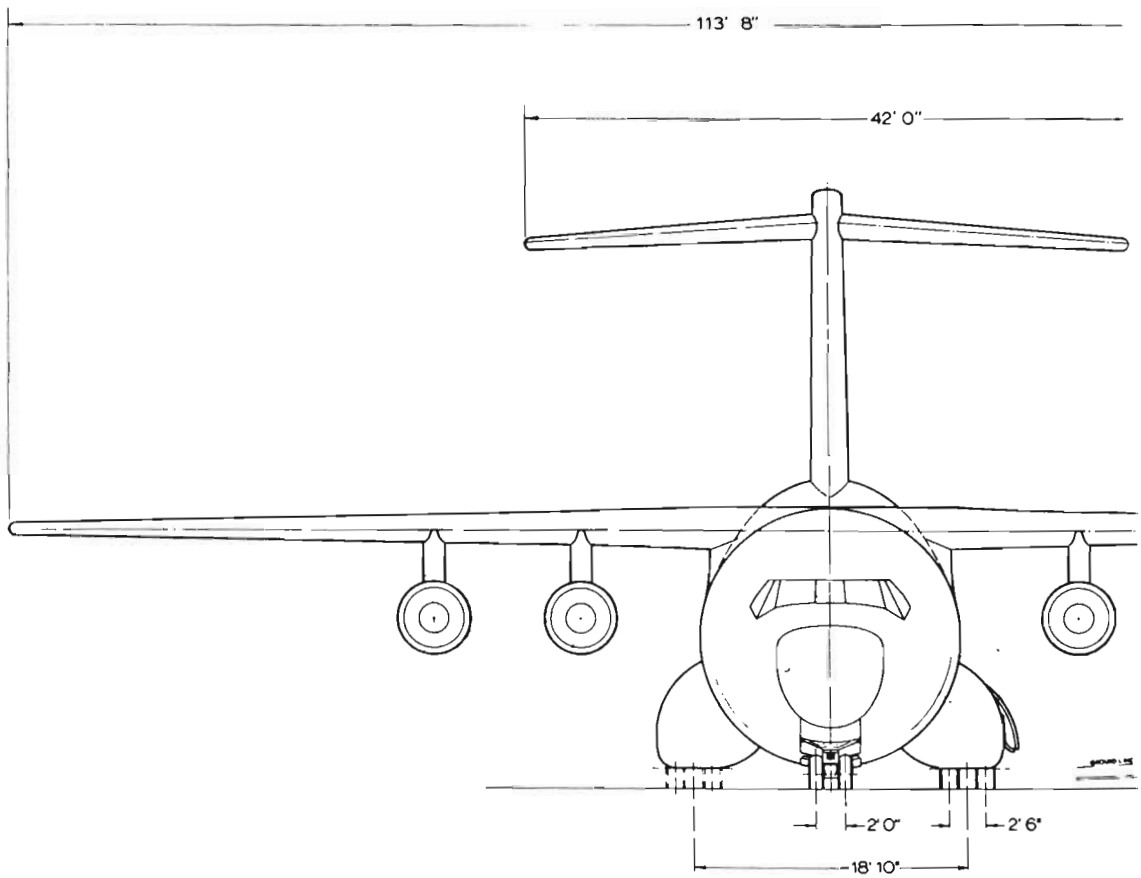

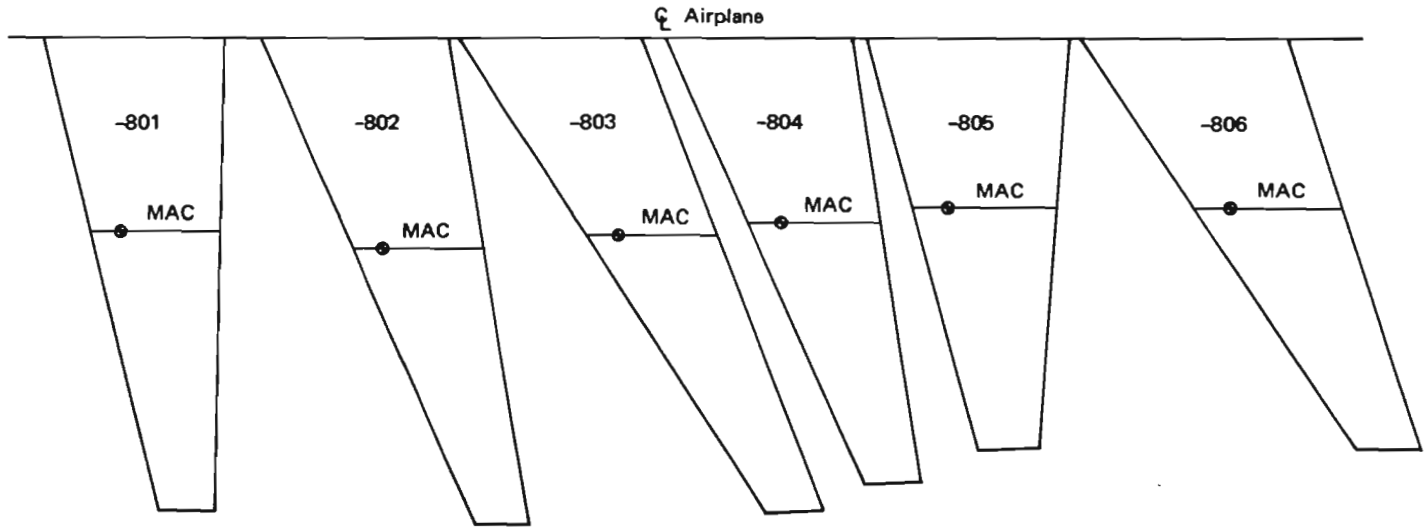

Item \ Model	-801	-802	-803	-804	-805	-806
Aspect Ratio	8.0	8.0	8.0	7.3	6.16	6.16
Area, $Ft.^2$	1590	1603	1626	1594	1567	1577
Sweep C/4	10^o	20^o	30^o	20^o	10^o	30^o
Mac, Ft.	15.46	15.52	15.63	16.20	17.49	17.55
Span, Ft.	112.76	113.24	114.05	107.87	98.25	98.56
Des. Gr. Wt.	145,440	148,300	152,000	147,460	145,900	150,780

Figure 87: WING PLANFORM PARAMETRIC STUDY CONFIGURATIONS

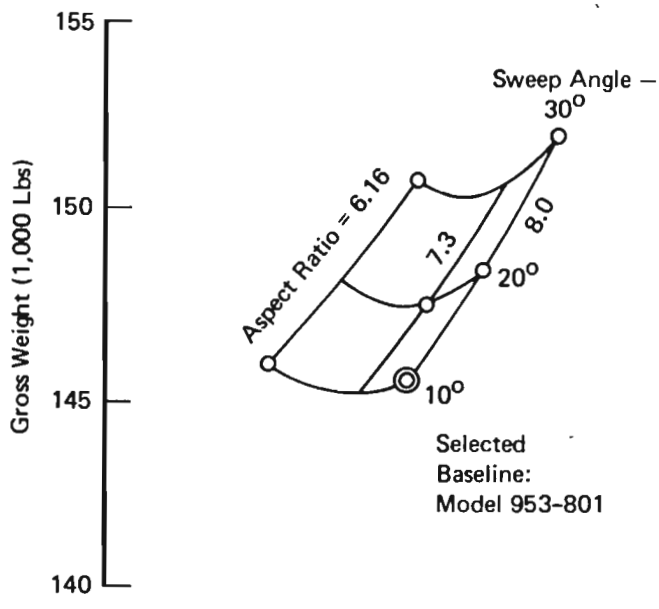

Figure 88: PLANFORM STUDY – RESULTS

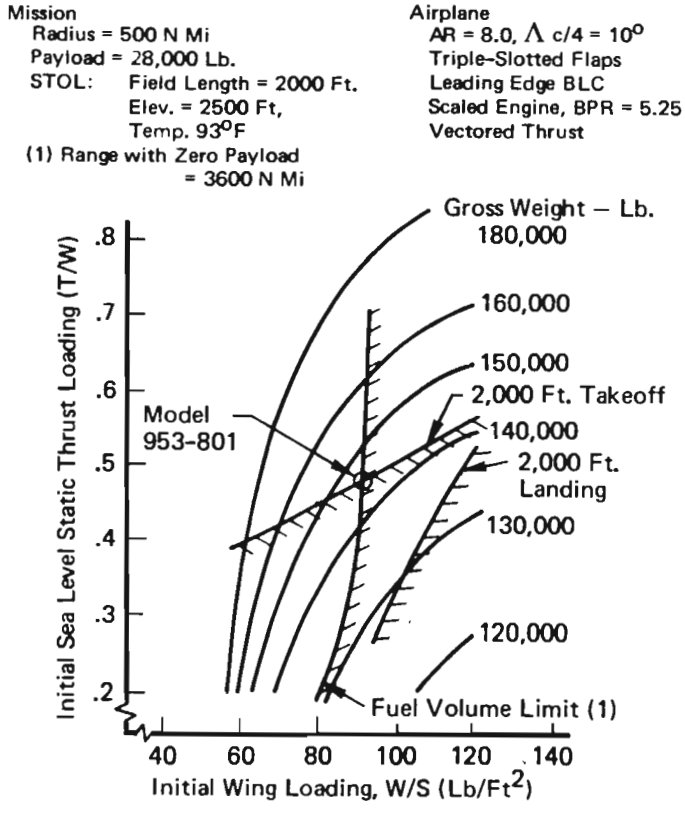

Figure 89: PARAMETRIC DESIGN CHART BASELINE AIRPLANE

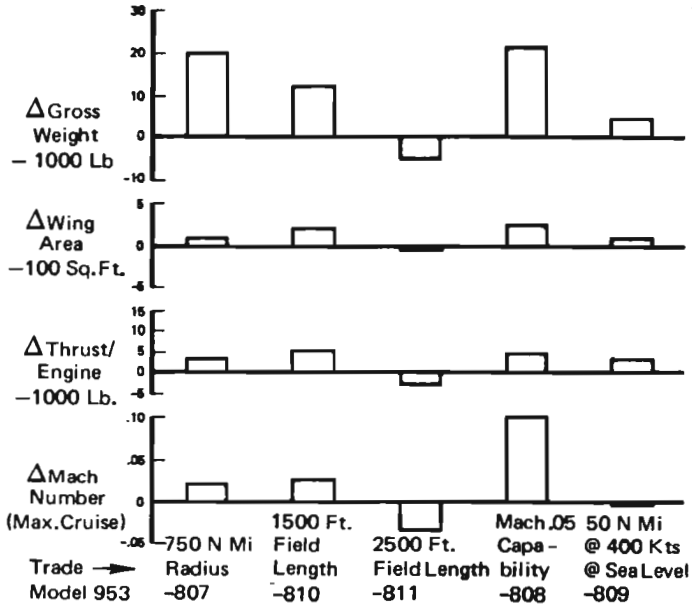

Figure 90: INCREMENTAL EFFECTS OF TRADES ON BASELINE PARAMETERS

Table XI: AIRPLANE SIZE AND PERFORMANCE FOR TRADES

Trade	Baseline	750 N MI Radius	1500 Ft. Field Length	2500 Ft. Field Length	Mach .85 Speed Capability	50 N Mi @ 400 kts @ Sea Level
Model No. 953	-.801	-807	-810	-811	-808	-809
Gross Weight (lb)	146,440	166,710	158,000	140,490	167,200	160,470
Wing Area (Sq. Ft.)	1,590	1,700	1,600	1,550	1,866	1,690
Rated Thrust (lb)	17,740	20,880	22,500	14,930	21,950	18,050
Initial Cruise Alt. (Ft)	37,900	36,400	40,600	36,700	42,300	36,900
Final Cruise Alt. (Ft)	40,900	40,700	43,800	39,500	45,500	40,600
Cruise Mach No.	0.70	0.70	0.70	0.70	0.82	0.70
Max. Level Flt. M	0.75	0.77	0.77	0.71	0.86	0.74

Table XII: TRADEOFF WEIGHT STATEMENT

Weights Group	Baseline Model 953-801	750 Mile Radius (-807)	1500 Ft. Field (-810)	2500 Ft. Field (-811)	Mach .85 Speed Capability (-808)	400K @ S.L. 50 Mi-Dash (-809)
Structure	55,550	60,290	59,400	53,430	69,940	56,950
Powerplant	15,770	18,590	19,790	13,750	19,880	15,770
Fixed Equipment	15,750	15,900	15,870	15,600	16,150	16,050
Weight Empty	87,070	94,780	95,060	82,780	105,750	88,770
Useful Load	1,430	1,950	1,880	1,750	1,950	1,430
Operating Weight	88,500	96,730	96,940	84,530	107,700	90,200
Payload	28,000	28,000	28,000	28,000	28,000	28,000
Fuel	28,940	40,980	33,060	27,960	31,500	32,270
Gross T.O. Weight	146,440	166,710	158,000	140,490	167,200	160,470

Notes: (1) The weights for the structure do not reflect a flutter analysis.

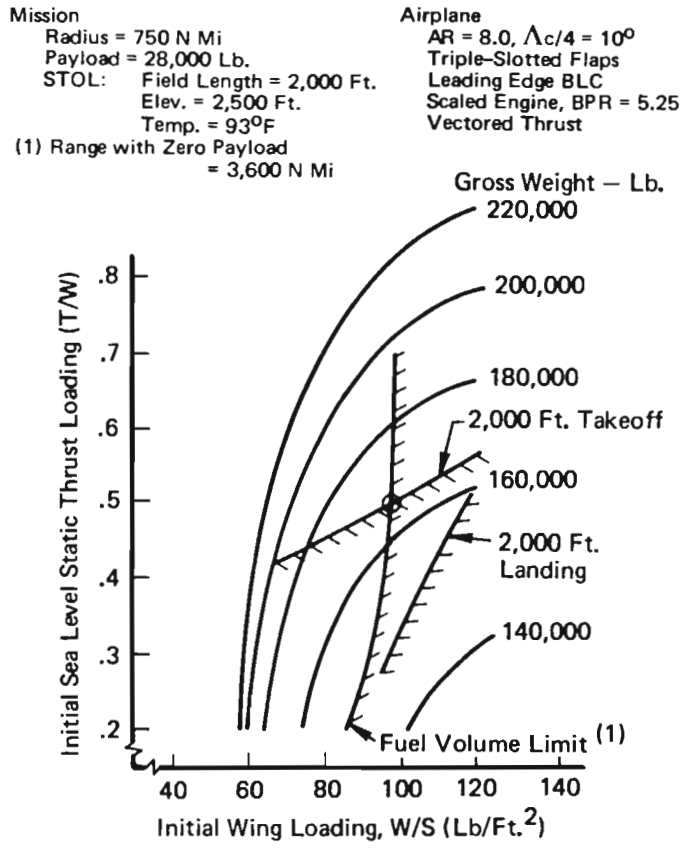

Figure 91: 750 N MI MISSION RADIUS TRADE

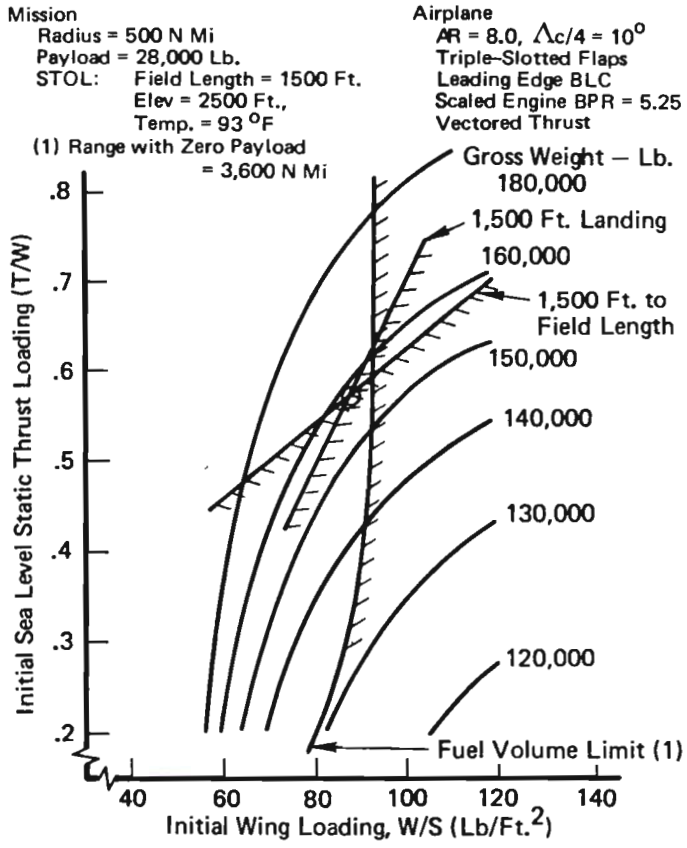

Figure 92 : 1500 FT FIELD LENGTH TRADE

4.3 2,500 Foot Field Length (Model 953-811)

The 500 foot increase in STOL field length from 2,000 feet to 2,500 feet gave reductions of about 5,000 pounds in gross weight and 2,800 pounds in rated thrust, provided a decrease of about .04 in maximum cruise Mach number is accepted. If the maximum cruise speed of Mach .75 is maintained, the advantage of the longer field length is severely limited. The 2,500 foot field length trade was takeoff-critical as shown by Figure 93 . The relaxation of the field length requirement caused decreases in wing area and thrust that saved about 4,000 pounds in empty weight. These were accompanied by a decrease in maximum cruise Mach number to 0.713. Since the long range cruise Mach number did not decrease, the lower maximum speed was retained. This let the trade variable, field length, select the design. The design selection chart indicates that the Mach .75 requirement could be reimposed for a gross weight penalty of about 3,000 pounds. The gross weight would then be within 2,000 pounds of the baseline weight, and about 60% of the effect of increasing the field length would be negated.

4.4 Mach .85 Speed Capability (Model 953-808)

The requirement for a maximum cruise speed capability of .85 Mach number caused an increase in the gross weight and thrust as expected (Figure 88). In order to attain this speed at cruise altitude, the configuration was altered considerably from that of the baseline. The quarter-chord wing sweep was changed from 10° to 35°, thickness ratio from .137 to .11, and aspect ratio from 8 to 7. An advanced technology airfoil section was used to gain an increase of 0.03 in wing critical Mach number. The empennage sweep and thickness underwent corresponding changes, and the body nose fineness ratio was increased to 2.0.

With the altered configuration, the desired maximum cruise speed was obtained at a thrust loading of .525 and a wing loading of 89.6 pounds per square foot, as indicated on the design chart of Figure 94 . With this wing, the ferry range fuel volume resulted in only slightly lower wing loading than would be dictated by the 2,000 foot takeoff. This was due, in part, to the favorable effect of the aspect ratio reduction on fuel volume. The resultant gross weight of 167,200 pounds showed an increase of 21,760 pounds over the baseline gross weight.

4.5 50 Nautical Mile Sea Level Penetration At 400 Knots (Model 953-809)

The sea level penetration trade was computed for a 50 nautical mile dash at 400 knots prior to landing at the assault airfield. This capability was achieved at the cost of about 5,000 pounds in gross weight. The trade was based on the baseline design chart of Figure 89 with appropriate adjustments for the sea level dash requirements on fuel and structural weight. These amounted to 3,230 pounds of fuel and 1,700 pounds of empty weight.

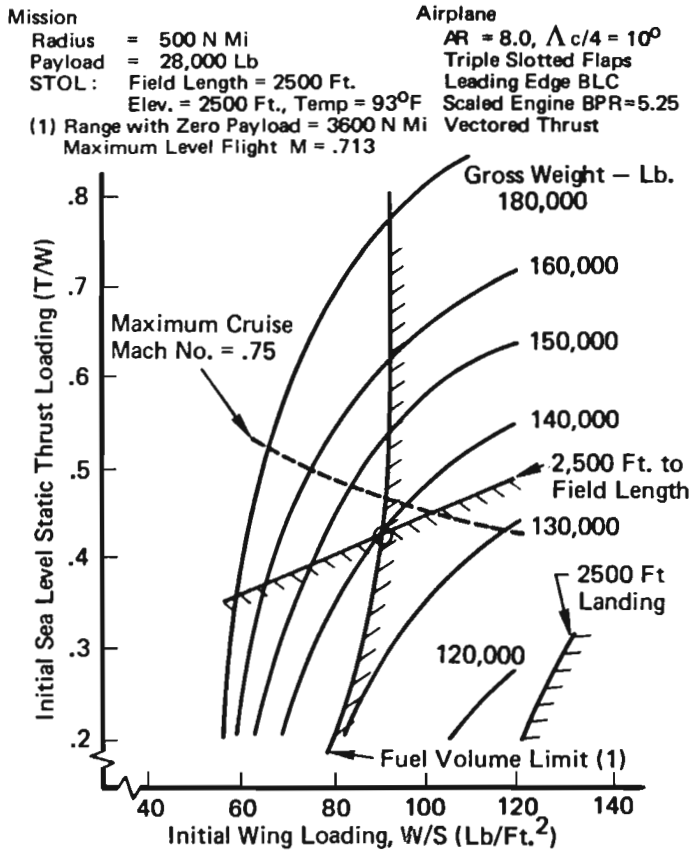

Figure 93: 2,500 FT. FIELD LENGTH TRADE

Figure 96 shows the various weight increments of the IBJF airplane relative to the Model 953-801.

The 953-812 airplane met the design requirements of the STAI except for the cruise speed requirements. The airframe-engine matching produced, at optimum altitude for initial cruise weight, a long-range cruise Mach number of 0.69 and a maximum cruise Mach number of .71.

MODEL 953-812

AERODYNAMIC DATA

		WING	HORIZ. TAIL	VERT. TAIL
AREA	FT^2	2363.00	820.40	542.31
SPAN	FT	123.93	57.29	23.29
ASPECT RATIO		6.5	4.0	1.0
SWEEP, C/4		10°	10°	35°
DIHEDRAL		0°	- 4°	—
INCIDENCE		0°	+4°,-15°	—
TAPER RATIO		.3	.5	.8
THICKNESS RATIO	BODY SIDE	.150	.13	.13
	.55 b/2	.132	.13	.13
	TIP	.132	.13	.13
MAC	FT	20.91	14.85	23.38
VOLUME COEFFICIENT		——	1.10	.10

POWER PLANT

4 P&W STF 389 TURBOFANS WITH THRUST REVERSERS

LANDING GEAR

MAIN 8 42 x 15.0 - 16 TIRES
NOSE 2 34 x 12.0 - 12 TIRES

CARGO COMPARTMENT

144"W 144"/148"H 540"L

WEIGHTS

DESIGN GROSS	174,740	LB	ASSAULT MISSION
DESIGN STOL	156,270	LB	
STOL PAYLOAD		LB	
O.E.W.	105,190	LB	
DESIGN GROSS	201,700	LB	CTOL MISSION
MAX. PAYLOAD		LB	

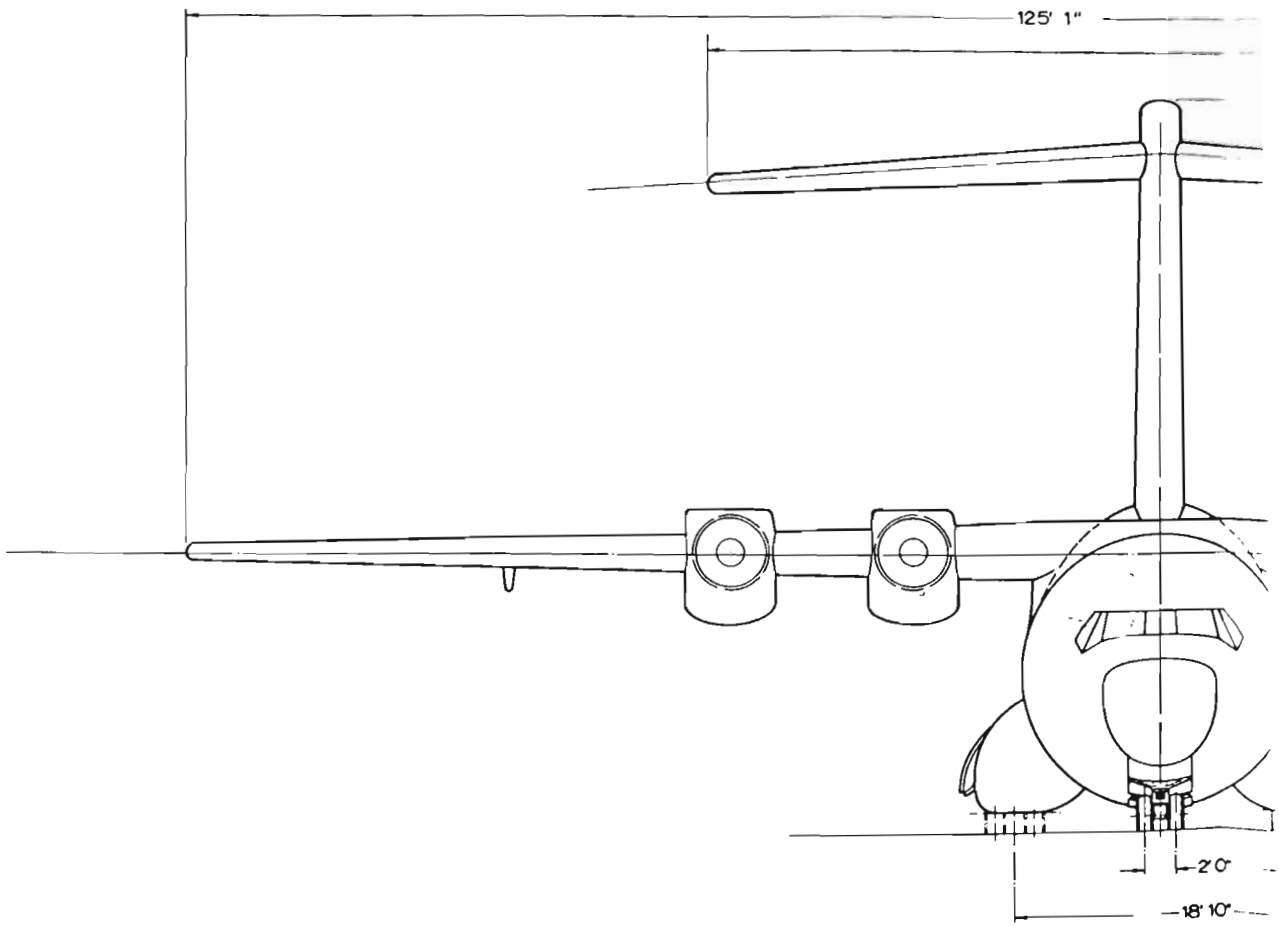

	HORIZ. TAIL	VERT. TAIL
)	820.40	542.31
3	57.29	23.29
	4.0	1.0
	10°	35°
	- 4°	—
	+4°,-15°	—
	.5	.8
0	.13	.13
2	.13	.13
2	.13	.13
	14.85	23.38
-	1.10	.10

POWER PLANT

4 P&W STF 369 TURBOFANS WITH THRUST REVERSERS 19,480 LB THRUST

LANDING GEAR

MAIN	8	42 x 15.0 - 16 TIRES
NOSE	2	34 x 12.0 - 12 TIRES

CARGO COMPARTMENT

144"W 144"/148"H 540"L

WEIGHTS

DESIGN GROSS	174,740 LB	ASSAULT MISSION
DESIGN STOL	156,270 LB	
STOL PAYLOAD	LB	
O.E.W.	105,190 LB	
DESIGN GROSS	201,700 LB	CTOL MISSION
MAX. PAYLOAD	LB	

FUEL

TANK NO. 1 & 6	16,220 LB
TANK NO. 2 & 5	21,660 LB
TANK NO. 3 & 4	28,900 LB
SUB TOTAL	66,780 LB
CENTER TANK	29,730 LB
TOTAL	96,510 LB

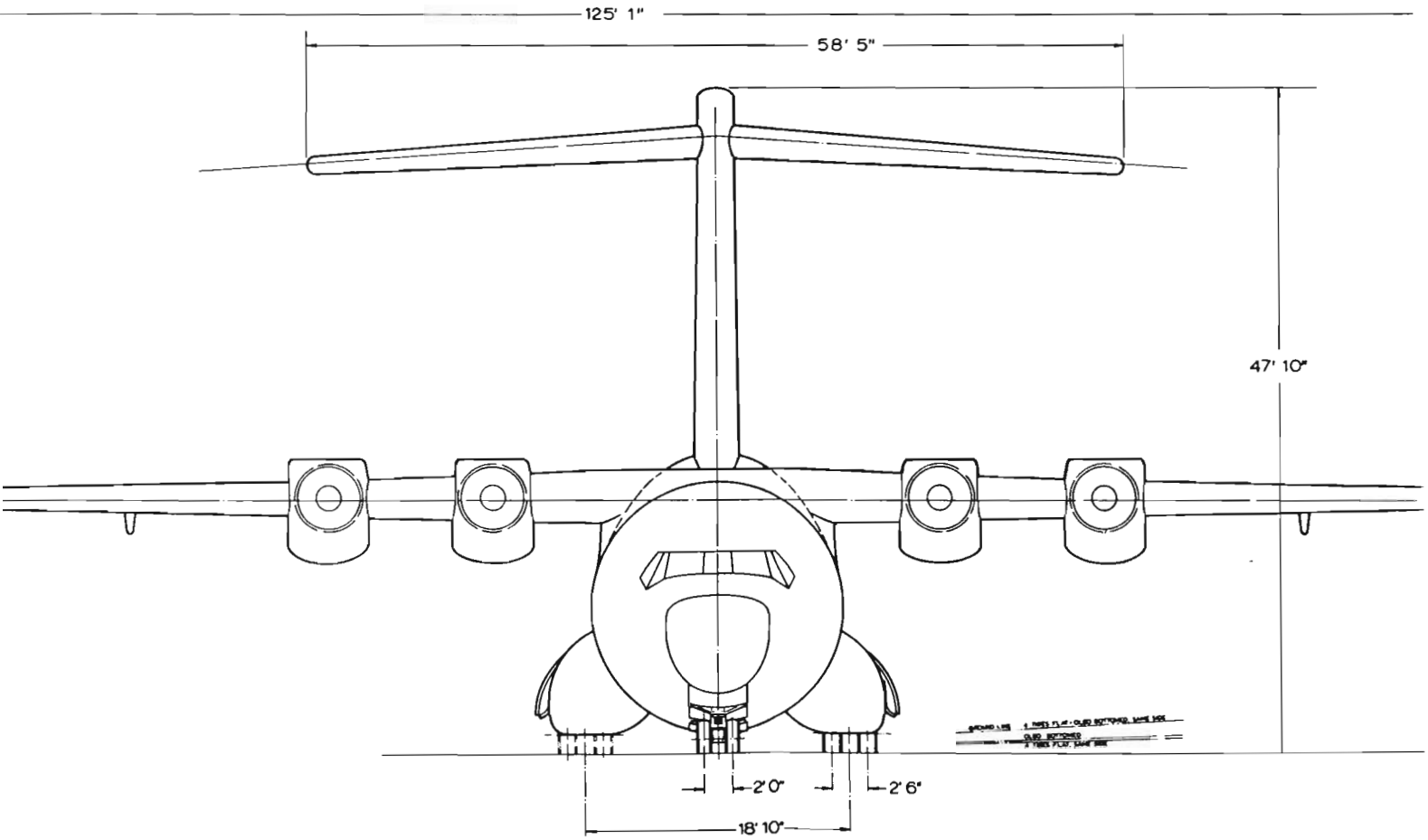

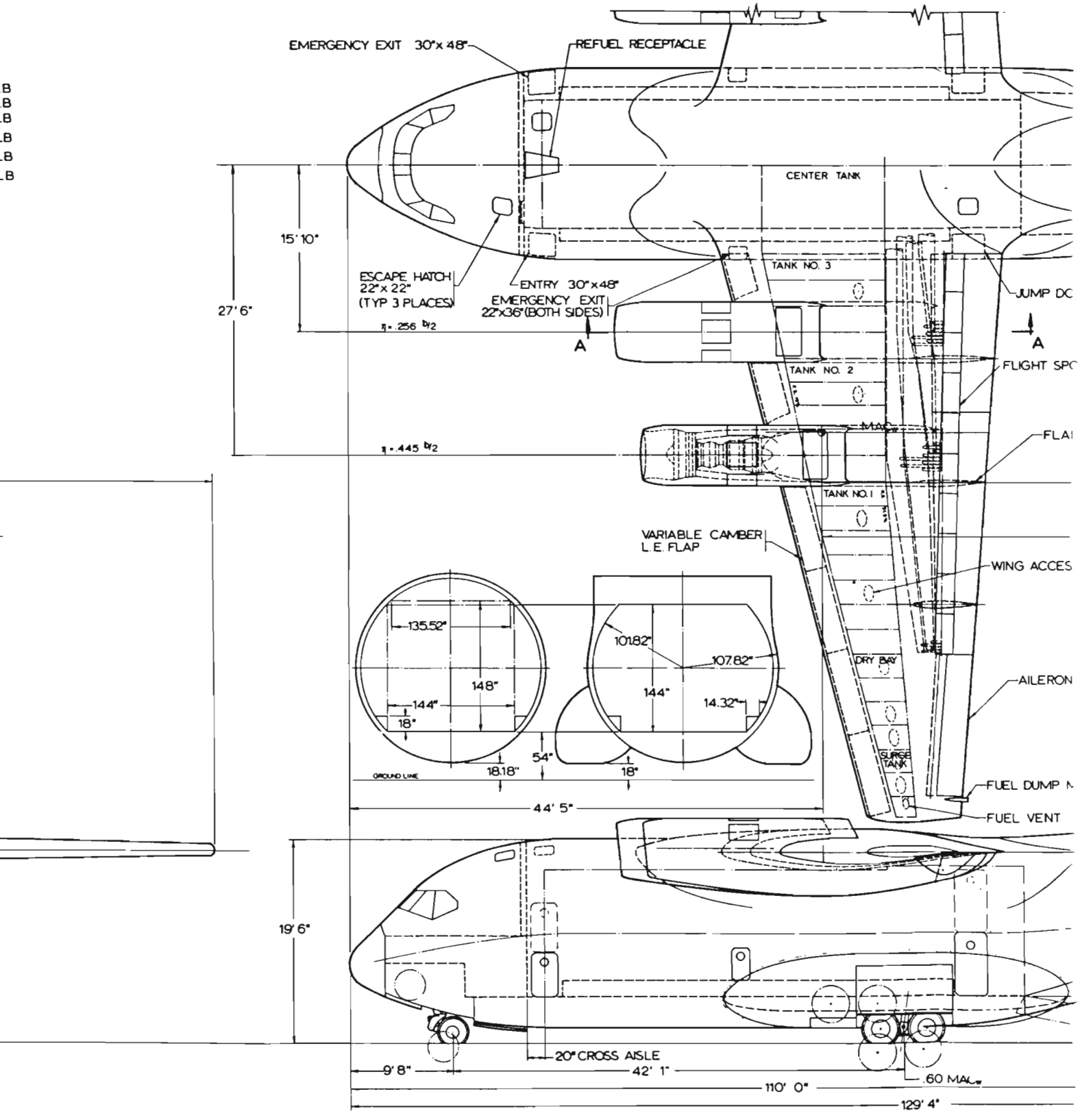
EMERGENCY EXIT 30"x 48"
REFUEL RECEPTACLE
CENTER TANK
15' 10"
27' 6"
ESCAPE HATCH
22"x 22"
(TYP 3 PLACES)
ENTRY 30"x48"
EMERGENCY EXIT
22"x36"(BOTH SIDES)
TANK NO. 3
JUMP DO
A
A
TANK NO. 2
FLIGHT SPO
MAC
FLAI
TANK NO. 1
VARIABLE CAMBER
L.E. FLAP
WING ACCES
135.52"
148"
144"
18"
101.82"
107.82"
144"
14.32"
DRY BAY
AILERON
54"
18.18"
18"
GROUND LINE
SURGE
TANK
FUEL DUMP N
FUEL VENT
44' 5"
19' 6"
20" CROSS AISLE
9' 8"
42' 1"
.60 MAC
110' 0"
129' 4"

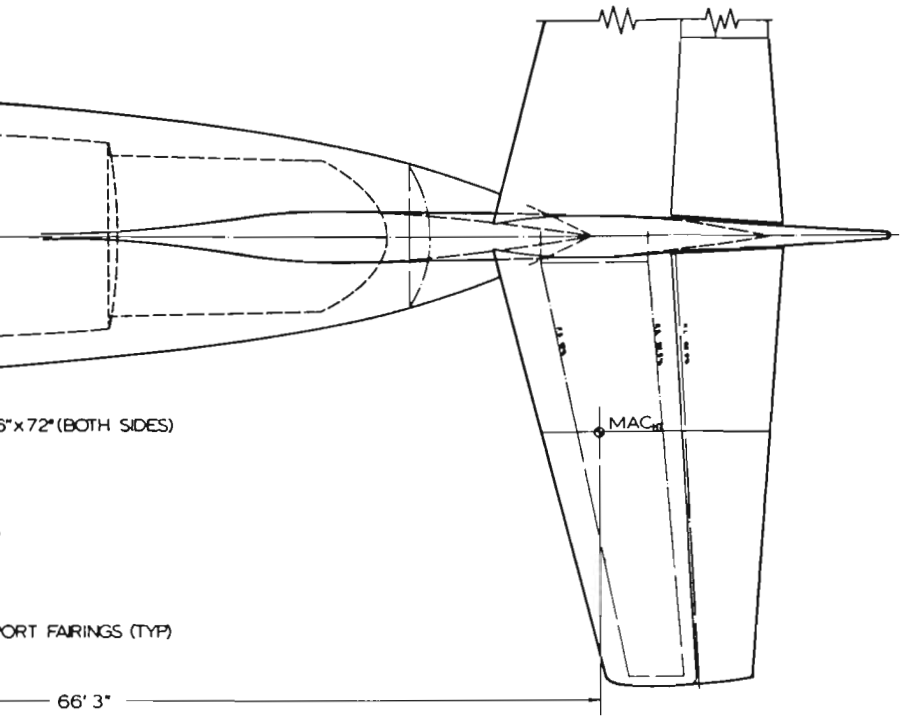

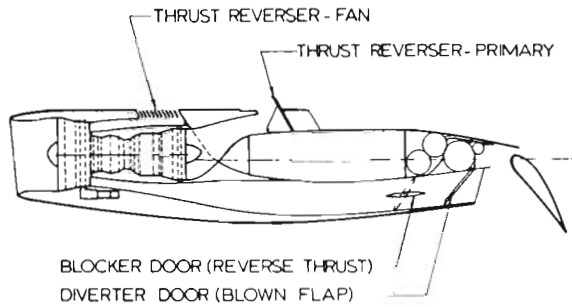

A-A

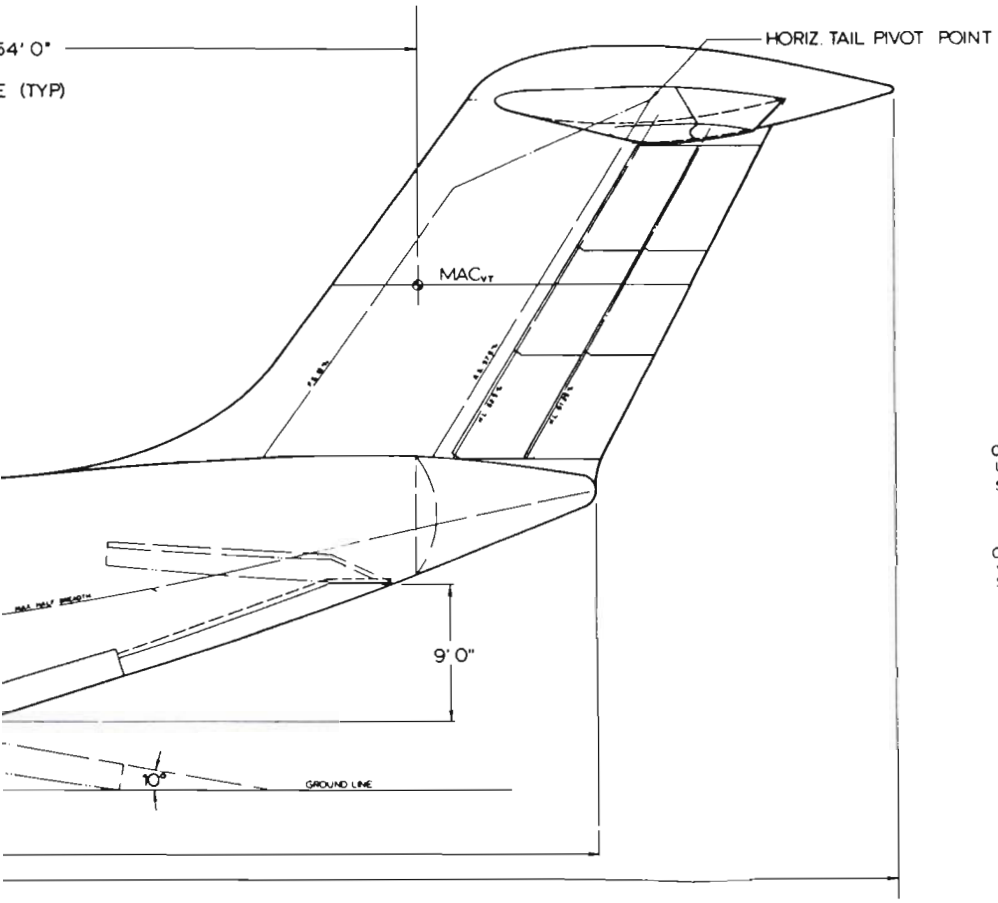

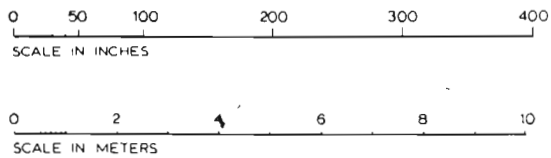

Figure 95: General Arrangement— Model 953-812

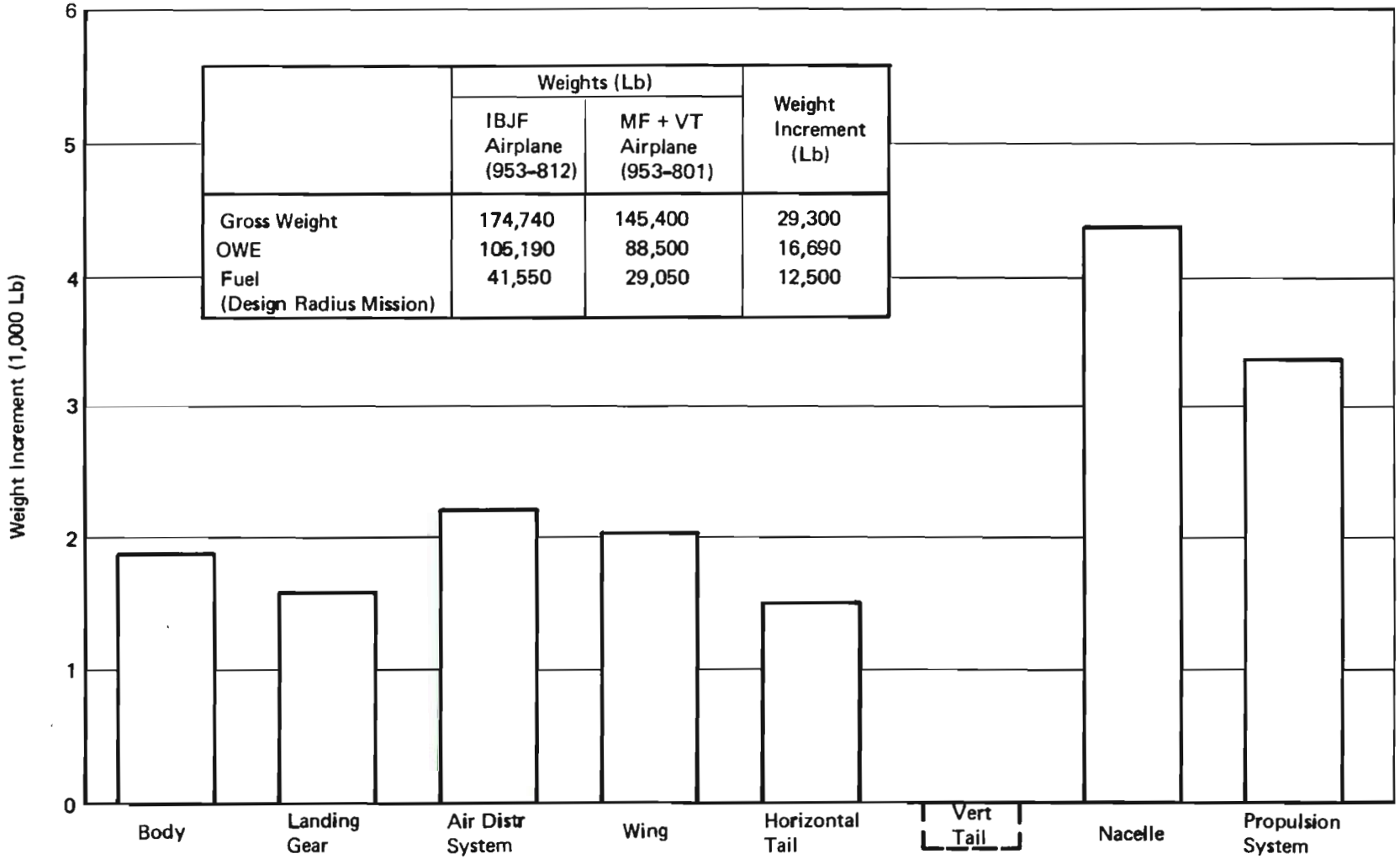

Figure 96: IBJF Airplane Weights Relative to VT + MF Airplane Weights

APPENDIX II

MISSION, AND TAKEOFF AND LANDING RULES

1.0 Mission Rules

1.1 Missions shall be computed according to the rules of Military Specification MIL-C-5011A, 5 November 1951, except as provided in the following rules.

1.2 The radius mission shall depart from and return to an airfield at sea level, standard atmospheric conditions (U.S. Standard Atmosphere, 1962) and arrive and depart from a midpoint assault strip at 2,500 feet elevation with hot day conditions per MIL-STD-210A, 30 November 1958.

1.3 The baseline radius shall be 500 nautical miles.

1.4 A payload of 28,000 pounds shall be carried both ways on the radius mission.

1.5 A ferry mission of 3,600 nautical miles without cargo shall be performed from the sea level base.

1.6 The airplane shall be capable of carrying a payload of 58,000 pounds in an overloaded condition.

1.7 The maximum cruise Mach number shall be at least 0.75.

2.0 Takeoff and Landing Rules

2.1 Takeoff

2.1.1 The ground run friction coefficient shall be 0.1.

2.1.2 Liftoff speed shall be determined by:

2.1.2.1 Load factor equal to or greater than 1.1 g with one engine inoperative.

2.1.2.2 105 percent or greater air minimum control speed, one engine inoperative in ground effect.

2.1.3 The pitch rotation rate shall not exceed 8 degrees per second.

2.1.4 The takeoff climbout speed shall be equal to or greater than 110 percent air minimum control speed with one engine out and out of ground effect.

2.1.5 Climbout speed load factor shall be equal to or greater than 1.3 g with all engines operating and out of ground effect.

2.1.6 The engine failure speed shall be equal to or greater than ground minimum control speed.

2.1.7 Engine failure recognition time shall be one second.

2.1.8 The climb angle in the takeoff climb shall be at least 3 degrees with an engine inoperative.

2.2 Landing

2.2.1 Approach speed shall be determined by:

2.2.1.1 Load factor equal to or greater than 1.3 g with one engine inoperative.

2.2.1.2 Go-around capability from 50 feet altitude with all engines operating or from 100 feet with one engine inoperative.

2.2.1.3 Equal to or greater than 110 percent air minimum control speed, one engine inoperative.

2.2.2 Touchdown speed shall be giverned by:

2.2.2.1 No flare.

2.2.2.2 Touchdown rate of sink shall be equal to or less than 2/3 of the landing gear design rate of sink, and aircraft design R/S must be equal to or less than 1000 fpm.

2.2.2.3 The touchdown pitch attitude shall be such that main gear touch before the nose gear touches.

2.2.2.4 Load factor equal to or greater than 1.15 g, one engine inoperative and in ground effect.

2.2.2.5 Equal to or greater than 110 percent minimum touchdown speed, one engine inoperative and in ground effect.

2.2.3 The pitch rotation rate shall not exceed 8 degrees per second.

2.2.4 Deceleration on the ground shall be giverned by:

2.2.4.1 Two-second delay in actuating and deploying deceleration devices.

2.2.4.2 Braking friction coefficient of 0.30.

2.2.4.3 Symmetrical reverse thrust equal to or less than 50 percent of two-engine thrust for four-engine designs.

2.3 General

2.3.1 The "obstacle height," or threshold height requirement, shall be 50 feet.

2.3.2 The field length for STOL operation shall be 2,000 feet.

2.3.3 The airplane shall be capable of performing the 2,000-foot takeoff from the midpoint assault strip with one engine inoperative, no cargo and sufficient fuel to return 500 nautical miles to its sea level base.

Table XIII: Streamwise Airfoils — Wing

X/C	η = 0		η = 0.1		η = 0.2		η = 0.3		η = 0.4		η = 0.55 → Tip	
	Z/C_u	Z/C_ℓ	Z/C_u	Z/C_ℓ	Z/C_u	Z/C_ℓ	Z/C_u	Z/C_ℓ	Z/C_u	Z/C_ℓ	Z/C_u	Z/C_ℓ
0.0	0.0	0.0	0.0	0.0	0.0	0.0	0.0	0.0	0.0	0.0	0.0	0.0
.0025	.012362	-.009428	.011460	-.008526	.010847	-.007913	.010428	-.007494	.010170	-.007235	.009977	-.007043
.0050	.017879	-.012771	.016609	-.011501	.015748	-.010640	.015158	-.010050	.014795	-.009687	.014523	-.009415
.0075	.022271	-.014933	.020430	-.013692	.019384	-.012646	.018668	-.011930	.018228	-.011490	.0178979	-.011160
.0125	.028058	-.018712	.026120	-.016774	.024806	-.015460	.023906	-.014560	.023353	-.014007	.022938	-.013592
.025	.038527	-.024183	.035929	-.021585	.034167	-.019823	.032961	-.018617	.032219	-.017875	.031662	-.017318
.050	.052123	-.032021	.048638	-.028536	.046273	-.026171	.044655	-.024553	.043659	-.023551	.042912	-.022810
.075	.060690	-.037980	.056603	-.033893	.053830	-.031120	.051932	-.029222	.050765	-.028055	.049889	-.027179
.100	.067188	-.043174	.062617	-.038603	.059515	-.035501	.057373	-.033359	.056087	-.032073	.055107	-.031093
.125	.072258	-.048026	.067276	-.043044	.063895	-.039663	.061582	-.037350	.060159	-.035927	.059091	-.034859
.15	.076510	-.052278	.071176	-.046944	.067556	-.043324	.065079	-.040847	.063555	-.039323	.062412	-.038180
.20	.083155	-.060335	.077211	-.054391	.073178	-.050358	.070419	-.047599	.068721	-.045901	.067447	-.044627
.25	.087491	-.066627	.081108	-.060244	.076776	-.055912	.073812	-.052948	.071988	-.051124	.070620	-.049756
.30	.090949	-.071497	.084221	-.064769	.079655	-.060203	.076531	-.057079	.074609	-.055157	.073167	-.053715
.35	.093061	-.074697	.086112	-.067748	.081397	-.063033	.078171	-.059807	.076186	-.057822	.074697	-.056333
.40	.093628	-.075372	.086628	-.068372	.081878	-.063622	.078628	-.060372	.076623	-.058372	.075128	-.056872
.45	.093462	-.074120	.086521	-.067179	.081810	-.062468	.078588	-.059246	.076604	-.057262	.075117	-.055775
.50	.092423	-.070907	.085658	-.064142	.081067	-.059551	.077926	-.056410	.075994	-.054473	.074544	-.053028
.55	.090040	-.066026	.083575	-.059561	.079189	-.055175	.076188	-.052174	.074341	-.050327	.072956	-.048942
.60	.085739	-.059877	.079707	-.053845	.075615	-.049753	.072814	-.046952	.071091	-.045229	.069799	-.043937
.65	.078938	-.052860	.073479	-.047401	.069774	-.043696	.067240	-.041162	.065680	-.039602	.064510	-.038432
.70	.070281	-.045397	.065489	-.040605	.062238	-.037354	.060013	-.035129	.058645	-.033761	.057618	-.032734
.75	.059984	-.037272	.055955	-.033243	.053222	-.030510	.051351	-.028639	.050200	-.027488	.049337	-.026625
.80	.048608	-.029158	.045387	-.025937	.043202	-.023752	.041706	-.022256	.040786	-.021336	.040036	-.020646
.85	.036523	-.020875	.034146	-.018498	.032533	-.016885	.031429	-.015781	.030749	-.015101	.030240	-.014592
.90	.024394	-.012984	.022842	-.011432	.021796	-.010386	.021077	-.009667	.020635	-.009225	.020303	-.008853
.95	.012078	-.005992	.011329	-.005243	.010822	-.004736	.010474	-.004388	.010460	-.004174	.010100	-.004014
1.00	0.0	0.0	0.0	0.0	0.0	0.0	0.0	0.0	0.0	0.0	0.0	0.0

Note: Streamwise Airfoil Untwisted—Twist Given Separately

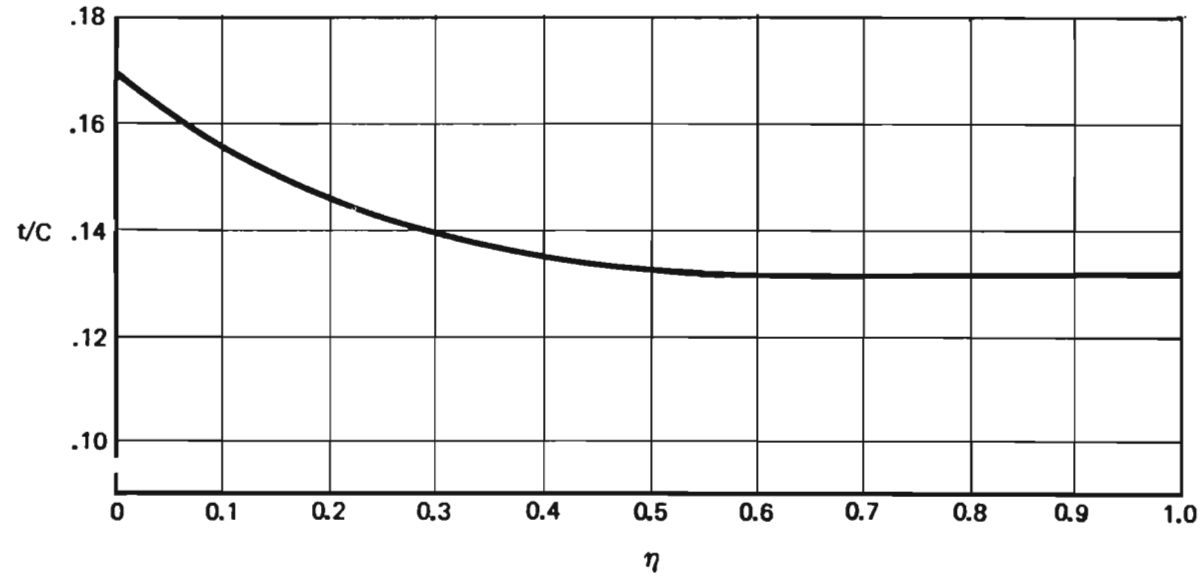

Figure 97: Wing Thickness Distribution

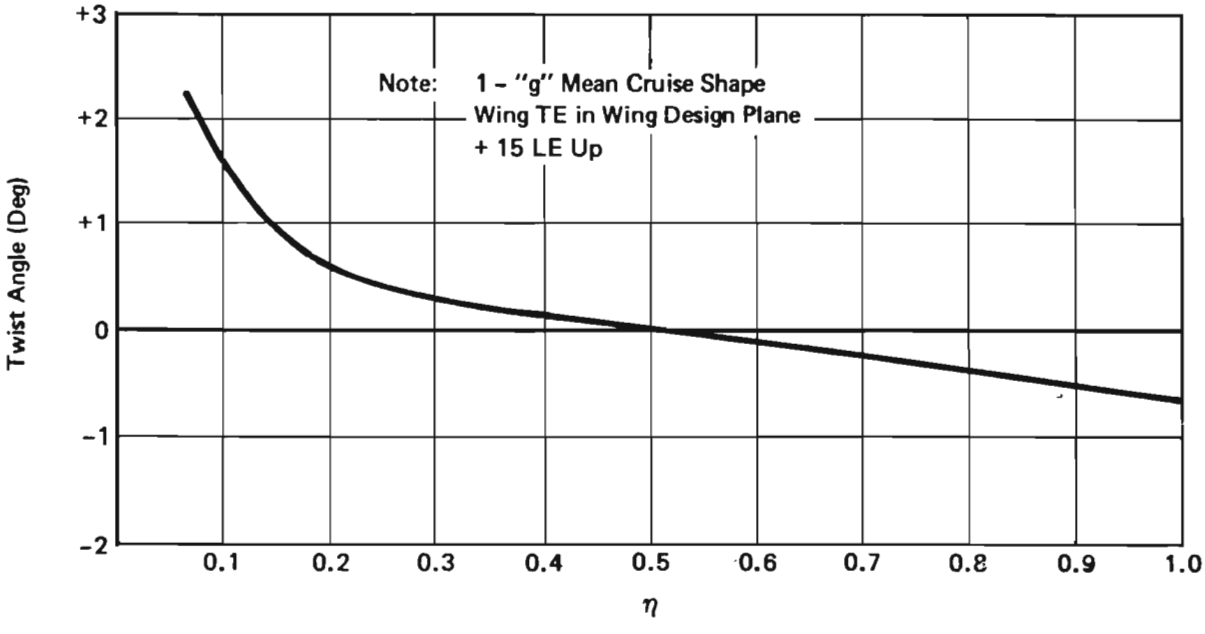

Figure 98: Wing Twist

X/C	Z/C_u	Z/C_l
0.0	0.0	0.0
.005	.01445	-.01666
.0075	.01637	-.01963
.0125	.01960	-.02473
.025	.02391	-.03602
.05	.02809	-.04582
.075	.02847	-.05387
.10	.02988	-.05990
.15	.03281	-.06847
.20	.03585	-.07418
.25	.03894	-.07831
.30	.04207	-.08126
.305	.04246	-.08132
.35	.04483	-.08294
.40	.04603	-.08226
.45	.04734	-.08266
.50	.04732	-.08086
.55	.04669	-.07774
.60	.04481	-.07313
.65	.04200	-.06671
.70	.03695	-.05819
.75	.03098	-.04848
1.00	0.0	0.0

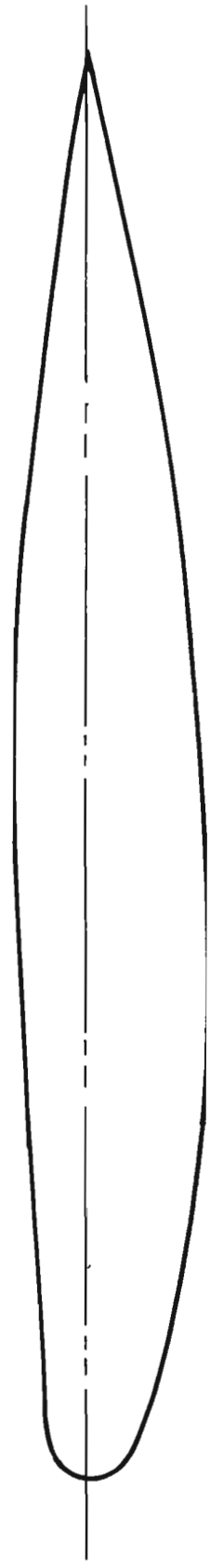

Figure 99: Horizontal Tail Airfoil

BAC 448

X/C	Z/C
0.0	0.0
.0025	±.00723
.0050	±.01002
.0075	±.01207
.0100	±.01377
.0125	±.01524
.025	±.02082
.050	±.02849
.075	±.03444
.10	±.03951
.15	±.04770
.20	±.05389
.25	±.05850
.30	±.06176
.35	±.06386
.40	±.06488
.425	±.06500
.45	±.06489
.50	±.06401
.55	±.06209
.60	±.05891
.65	±.05418
.70	±.04745
.75	±.03955
1.00	0.0

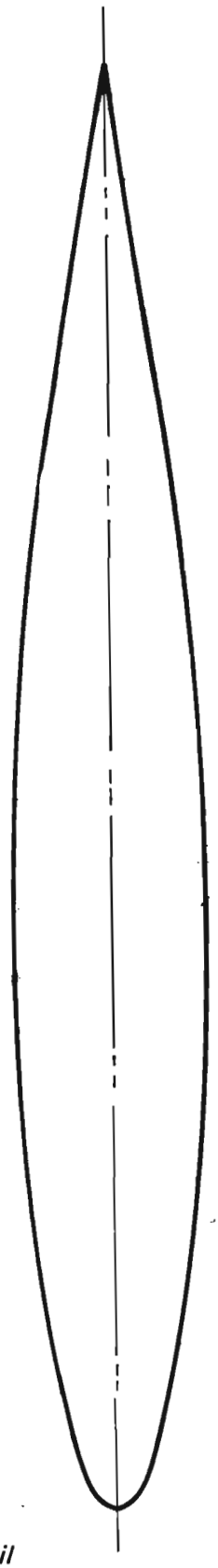

Figure 100: Vertical Tail Airfoil

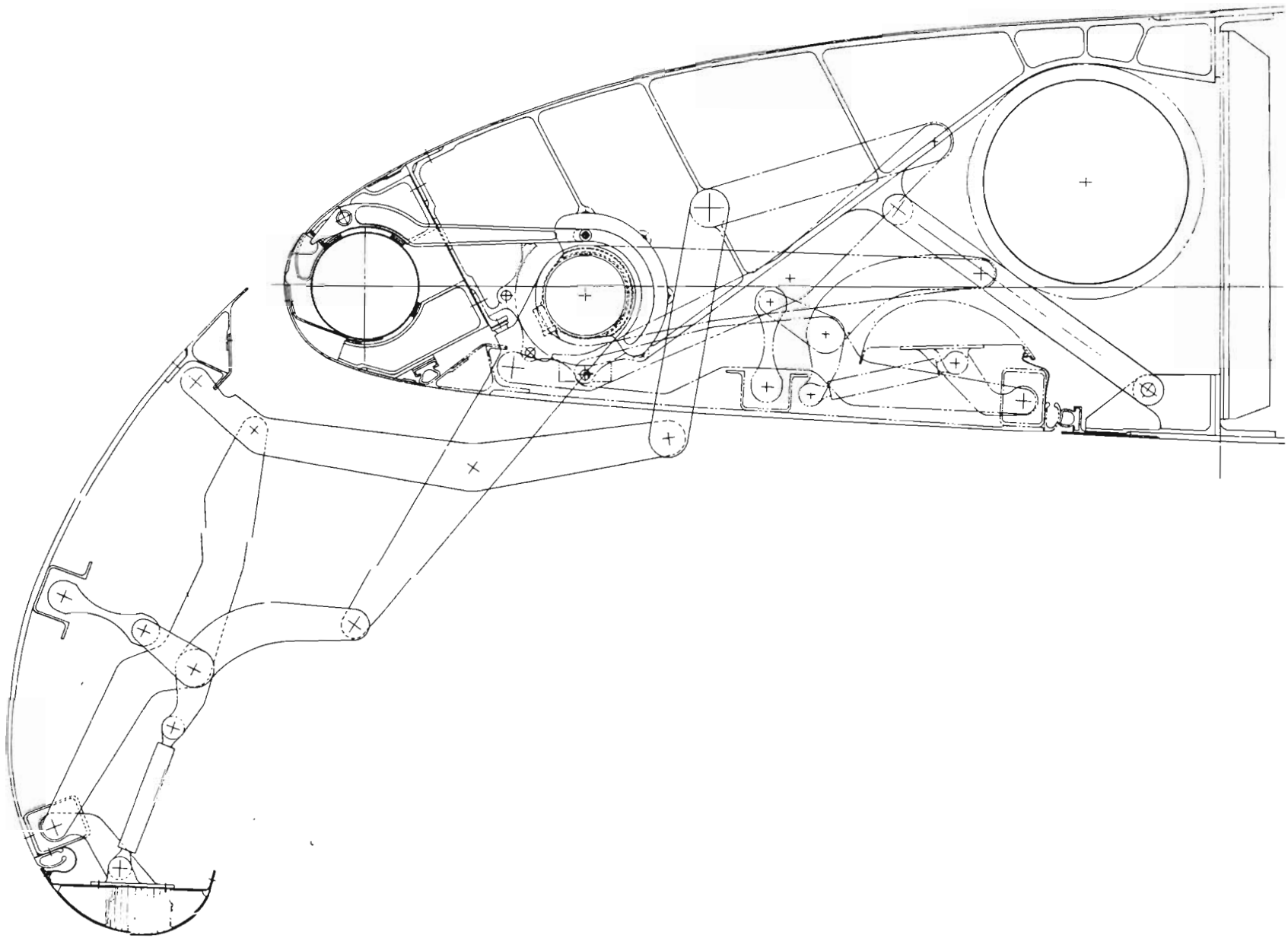

Figure 103: Leading Edge Flap Mechanization

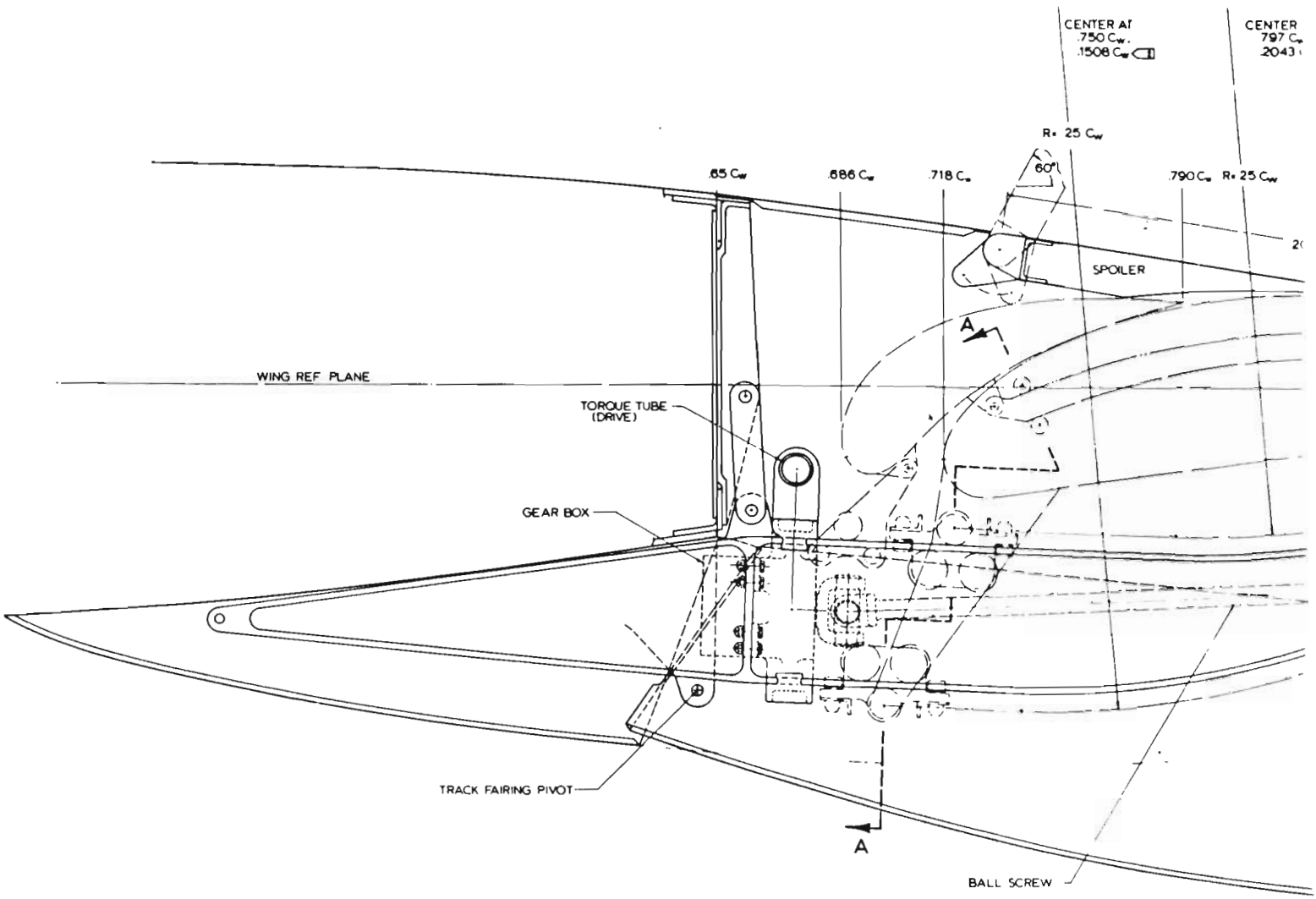

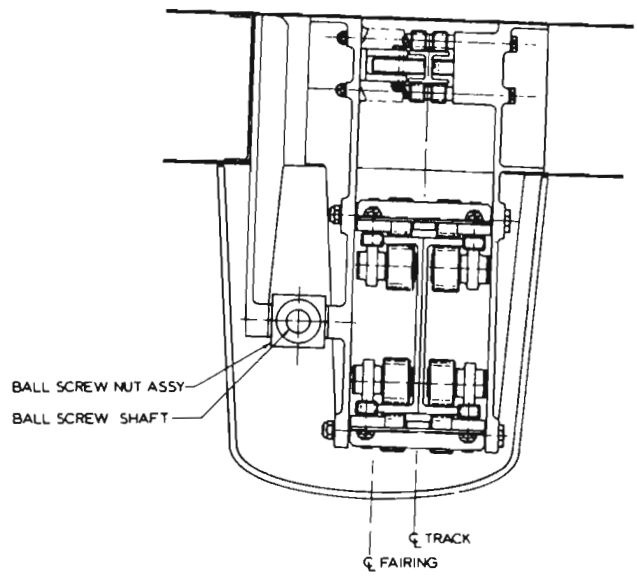

SECTION A-A (FLAP UP)

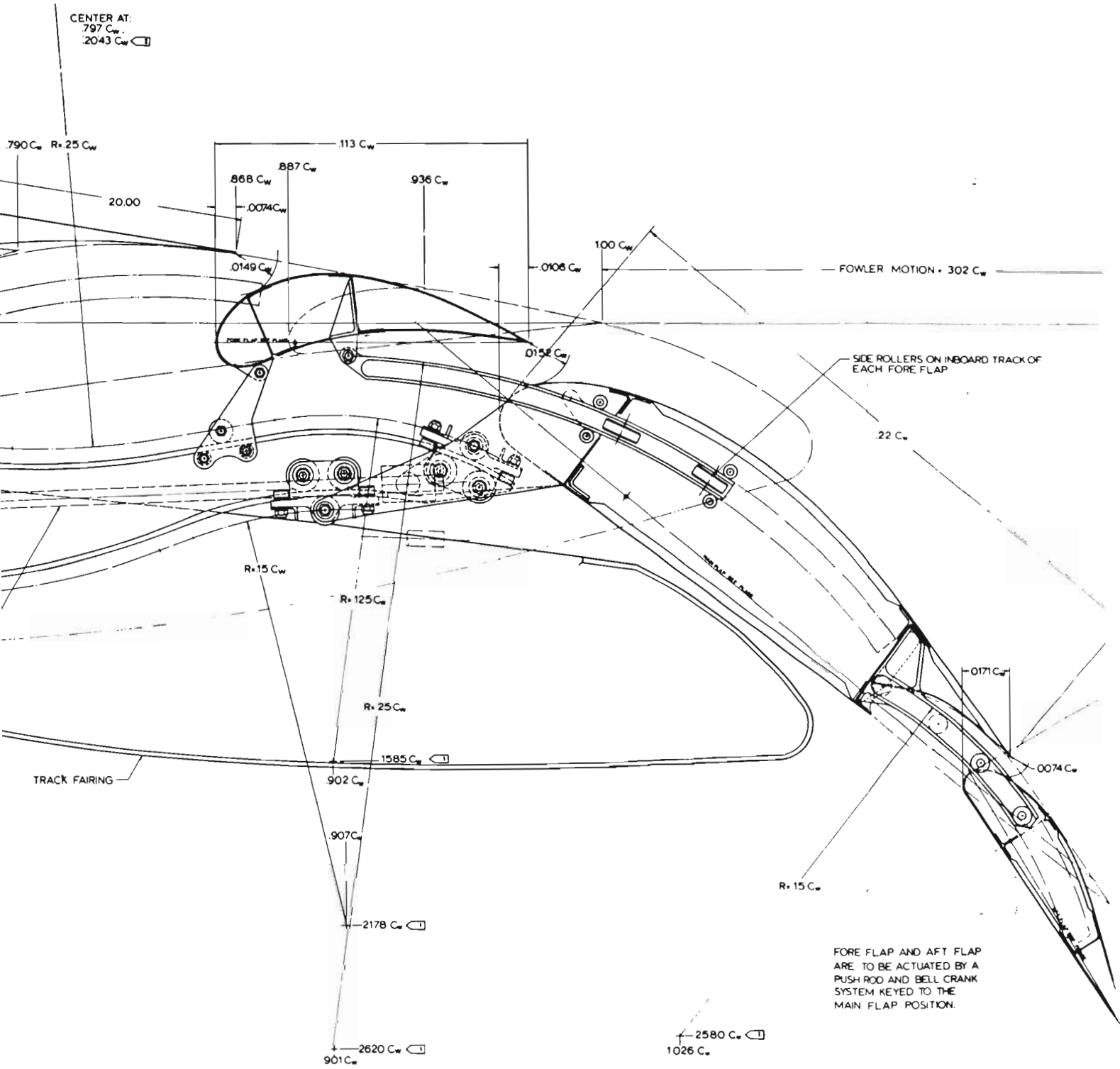
CENTER AT:
.797 Cw ,
.2043 Cw
.790 Cw R= 25 Cw
20.00
.868 Cw
.887 Cw
.936 Cw
.113 Cw
.0074 Cw
.0149 Cw
.0108 Cw
1.00 Cw
FOWLER MOTION = 302 Cw
.0152 Cw
SIDE ROLLERS ON INBOARD TRACK OF EACH FORE FLAP
.22 Cw
R= 15 Cw
R= 125 Cw
R= 25 Cw
.0171 Cw
.0074 Cw
1585 Cw
.902 Cw
TRACK FAIRING
.907 Cw
2178 Cw
R= 15 Cw
FORE FLAP AND AFT FLAP ARE TO BE ACTUATED BY A PUSH ROD AND BELL CRANK SYSTEM KEYED TO THE MAIN FLAP POSITION.
2580 Cw
1026 Cw
2620 Cw
901 Cw

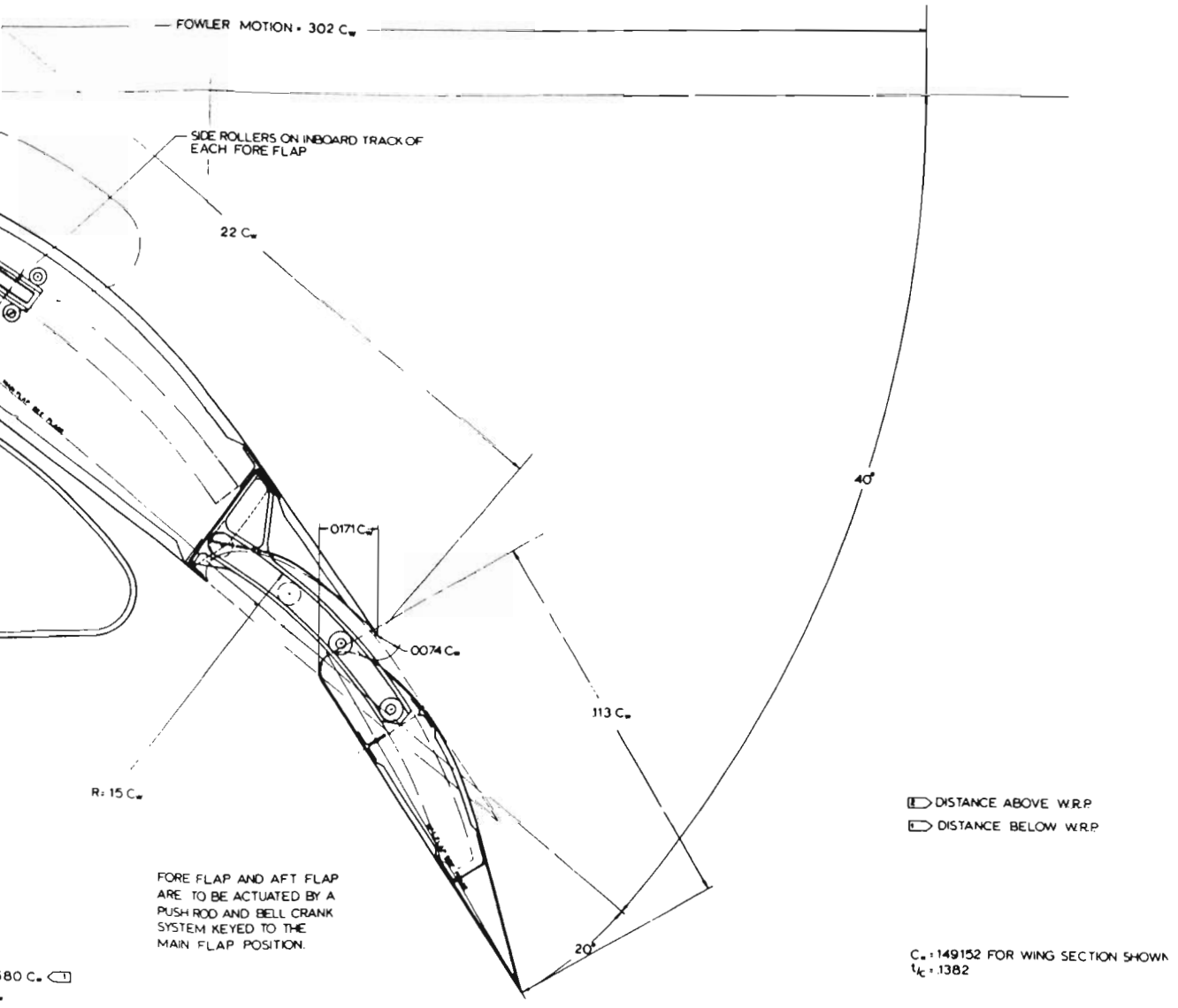

Figure 104: Trailing Edge Flap Mechanization

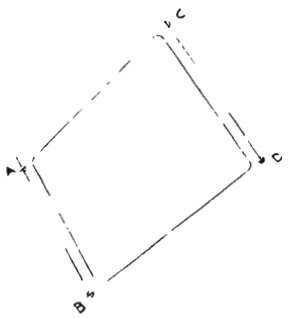

TRUE VIEW
FRONT WINDSHIELD

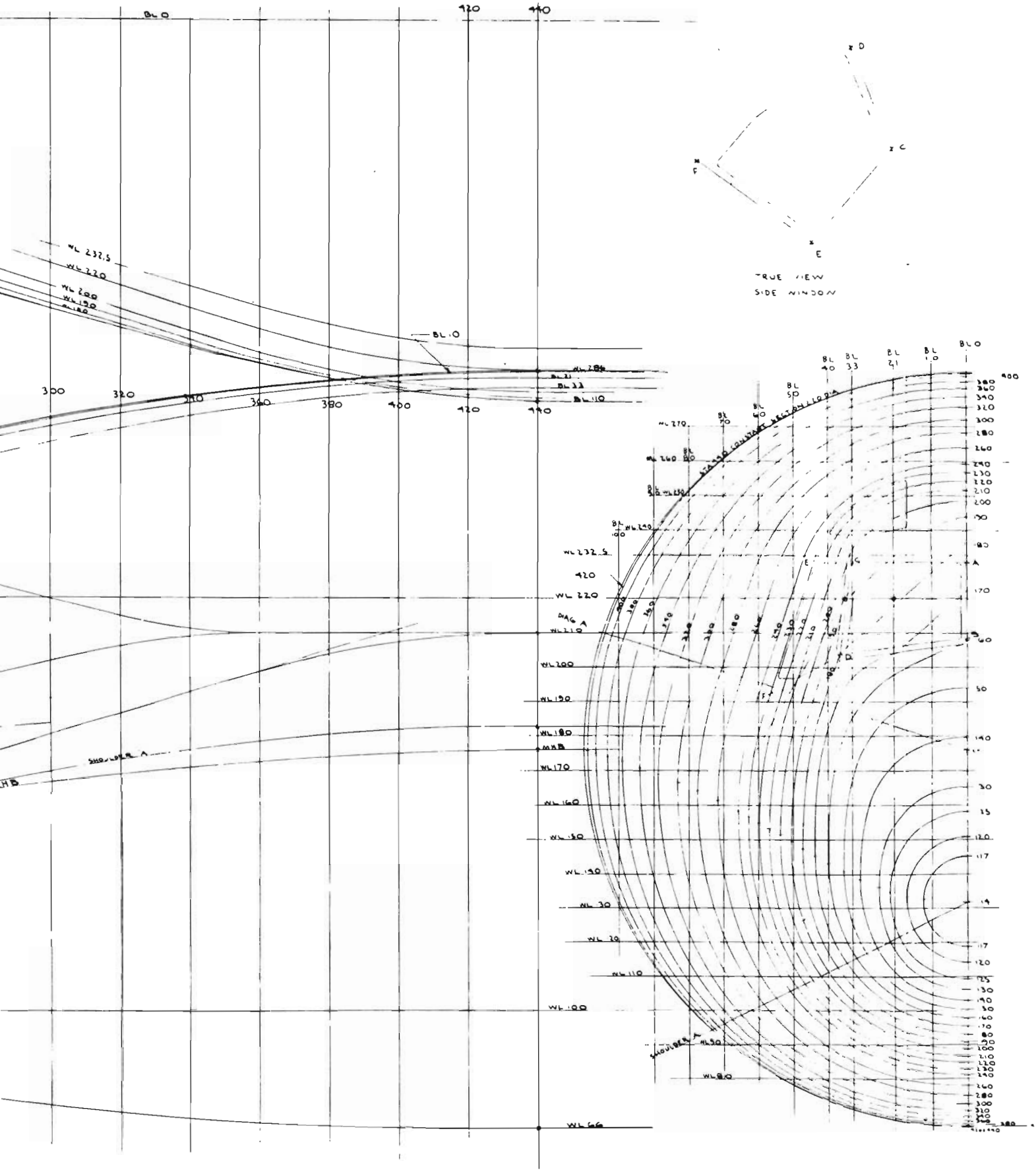
BL 0
420
440
WL 232.5
WL 220
WL 200
WL 190
WL 180
BL 0
BL 21
BL 33
BL 110
300
320
340
360
380
400
420
440
WL 270
WL 260
WL 250
WL 240
WL 232.5
420
WL 220
WL 210
WL 200
WL 190
WL 180
WL 170
WL 160
WL 150
WL 140
WL 130
WL 120
WL 110
WL 100
WL 90
WL 80
WL 66
BL 40
BL 33
BL 21
BL 10
BL 0
BL 50
BL 40
BL 30
BL 20
BL 10
BL 0
SHOULDER A
SHOULDER A
D
E
F
TRUE VIEW
SIDE WINDOW

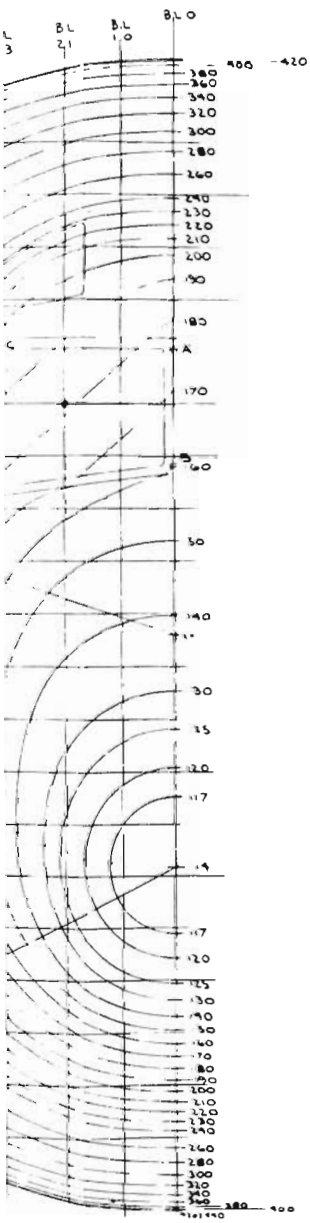

SCALE

FBL-1

Figure 105: Fore Body Loft

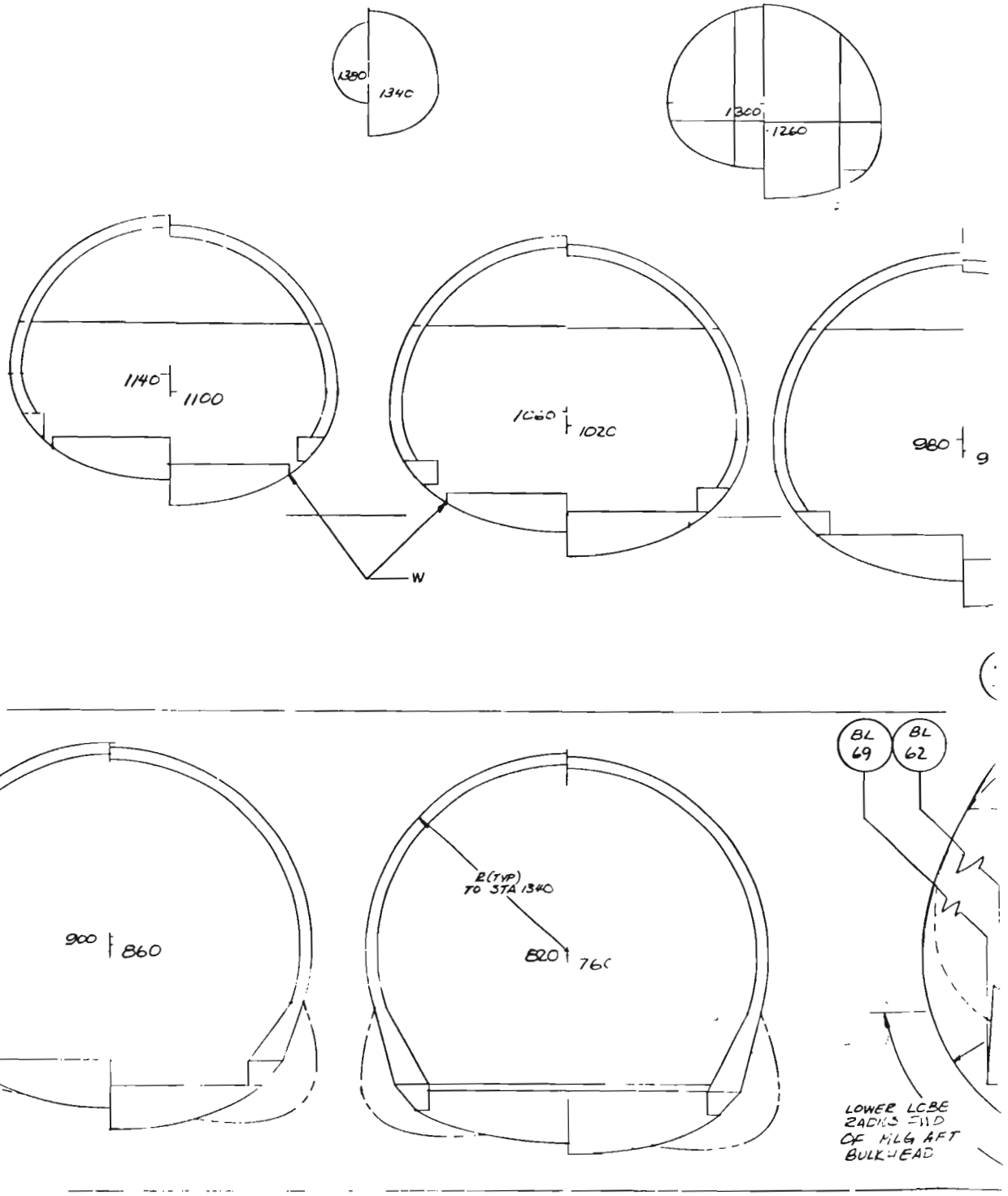
1380
1340
1300
1260
1140
1100
1060
1020
980
W
900
860
R(TYP)
TO STA 1340
820
760
BL
69
BL
62
LOWER LOBE
RADIUS END
OF MLG AFT
BULKHEAD

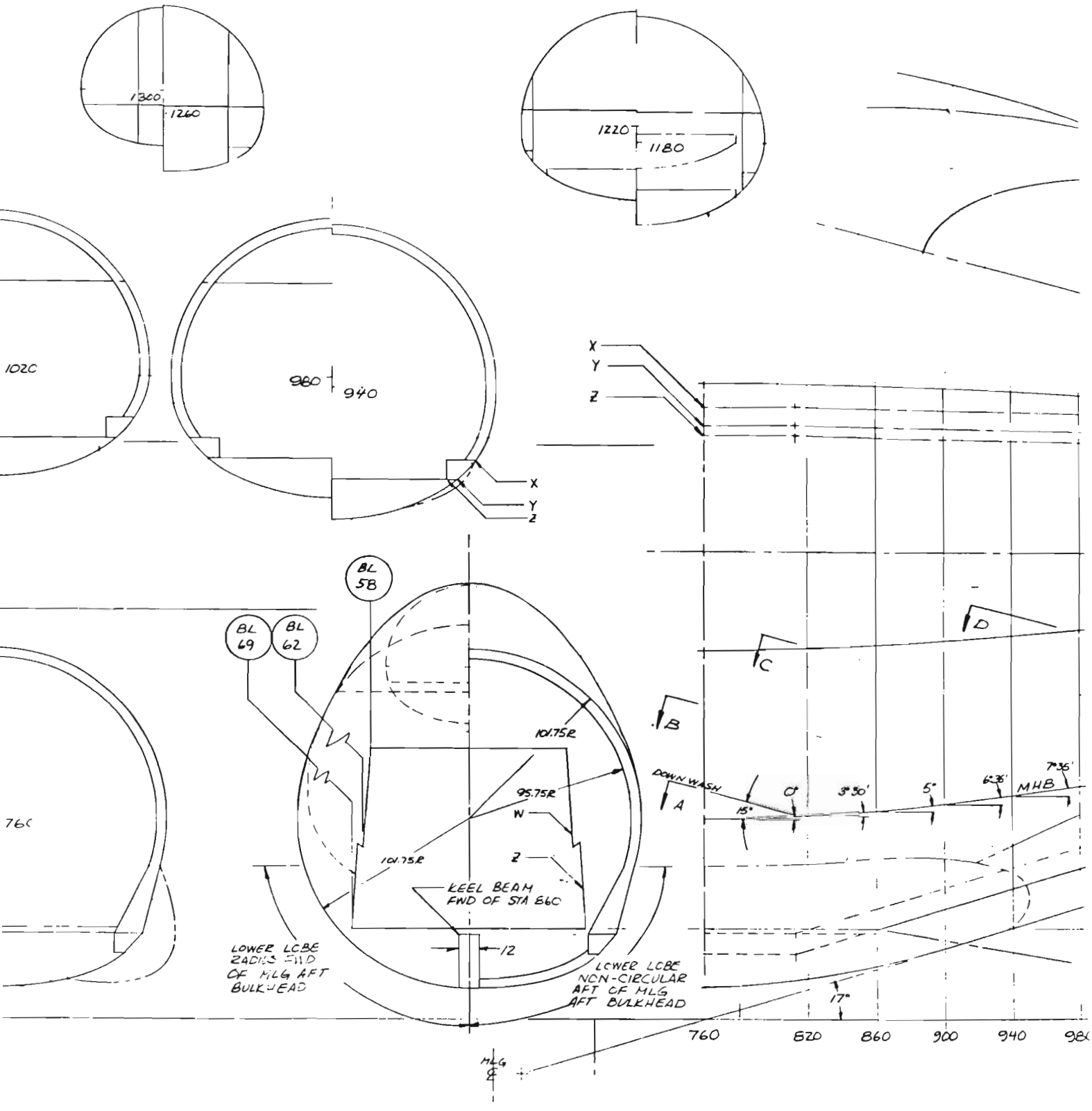
1300
1260
1220
1180
1020
980
940
X
Y
Z
BL 58
BL 69
BL 62
101.75R
95.75R
W
Z
KEEL BEAM FWD OF STA 860
12
LOWER LOBE RADIUS FWD OF MLG AFT BULKHEAD
LOWER LOBE NON-CIRCULAR AFT OF MLG AFT BULKHEAD
DOWNWASH
A
B
C
D
15°
0°
3°30'
5°
6°38'
7°36'
MHB
17°
760
820
860
900
940
MLG

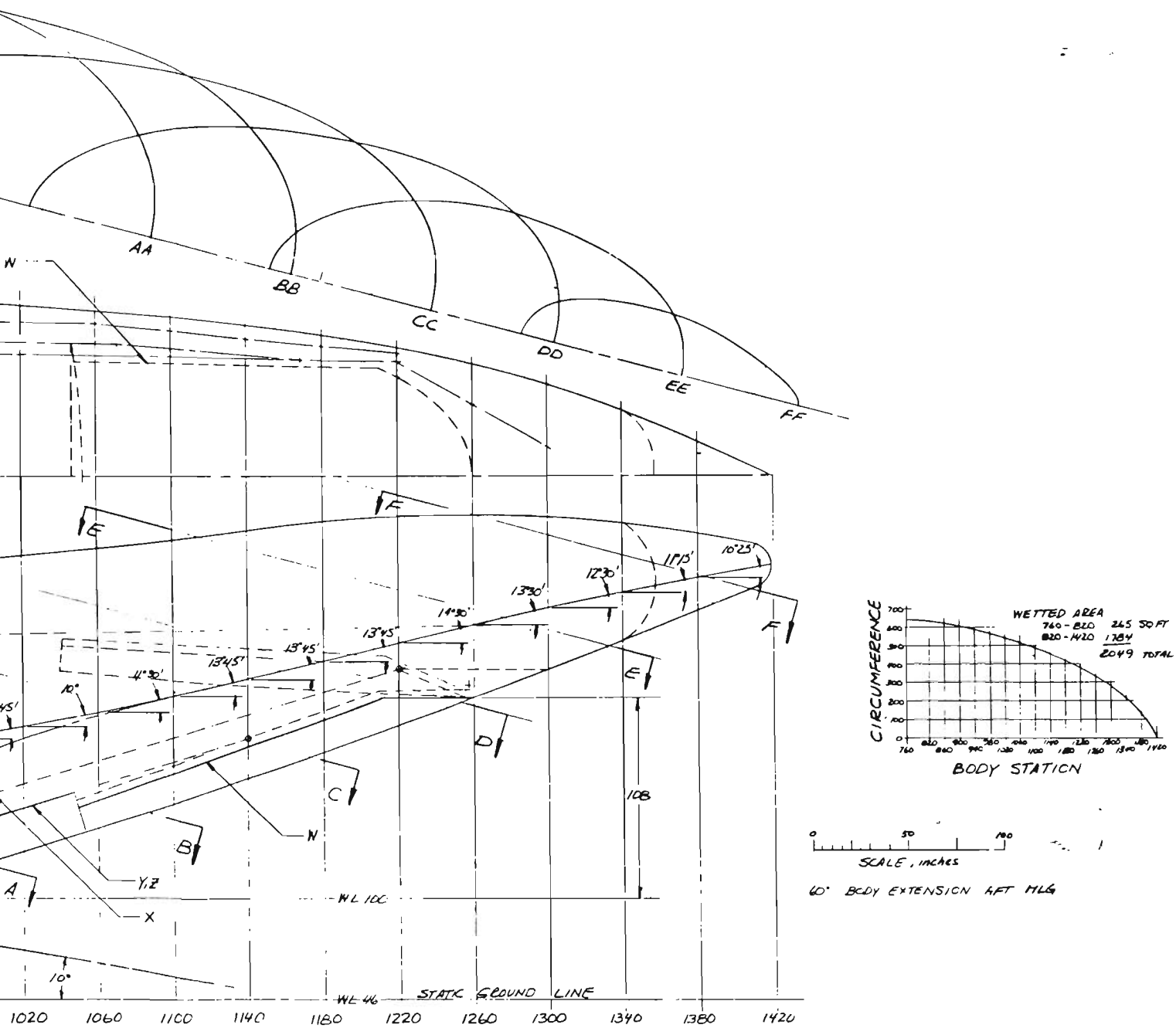

Figure 106: Aft Body Loft

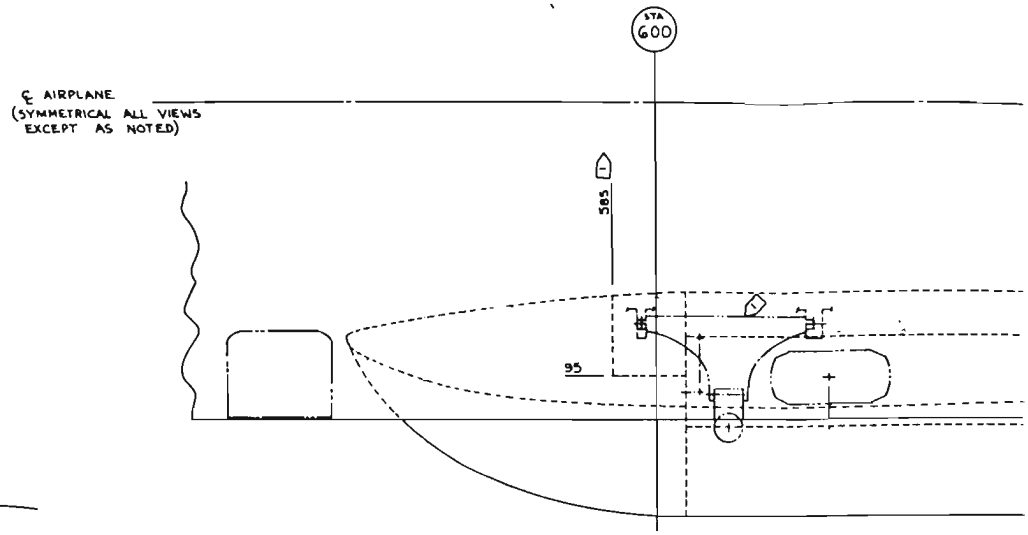

PLAN VIEW

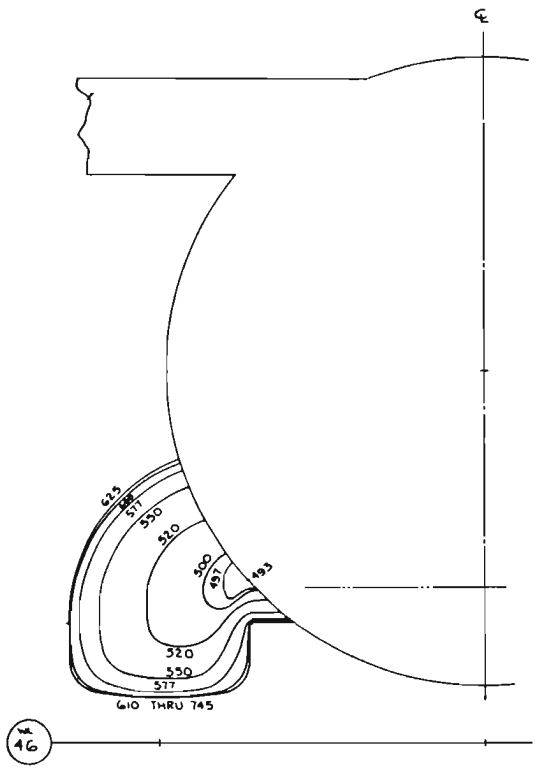

A-A

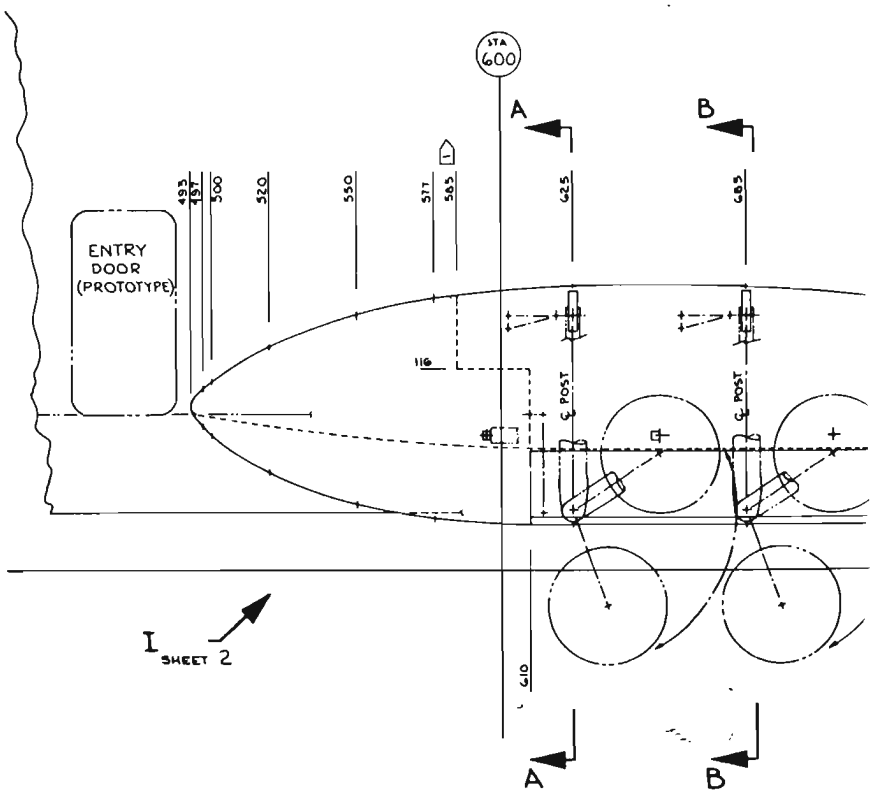

L SIDE VIEW

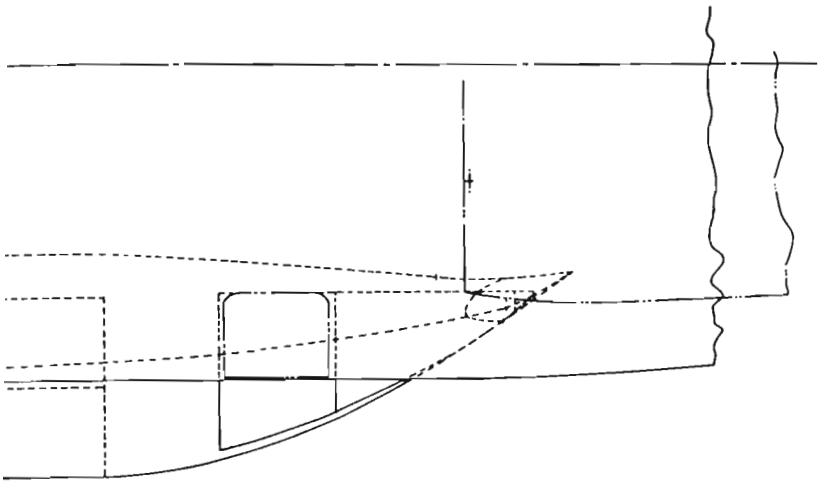

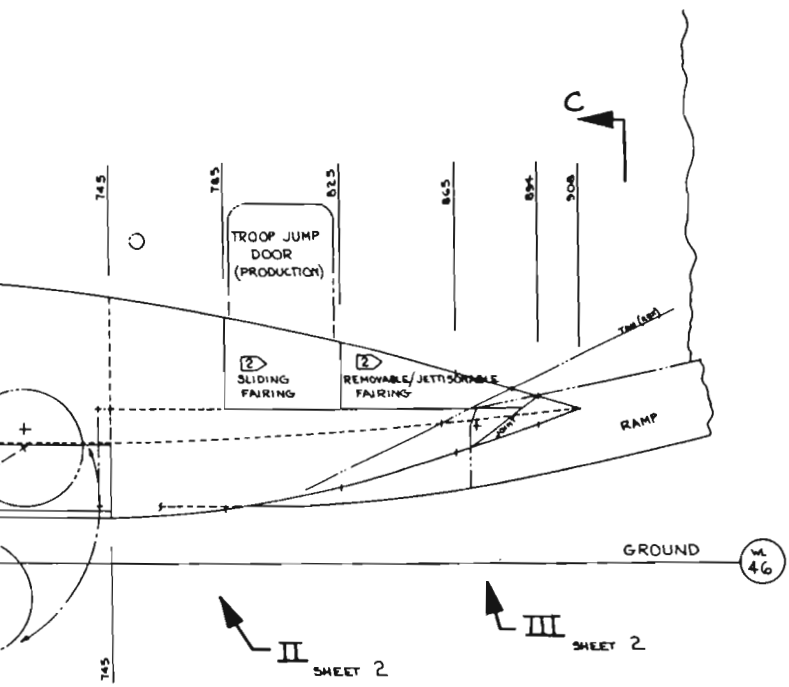

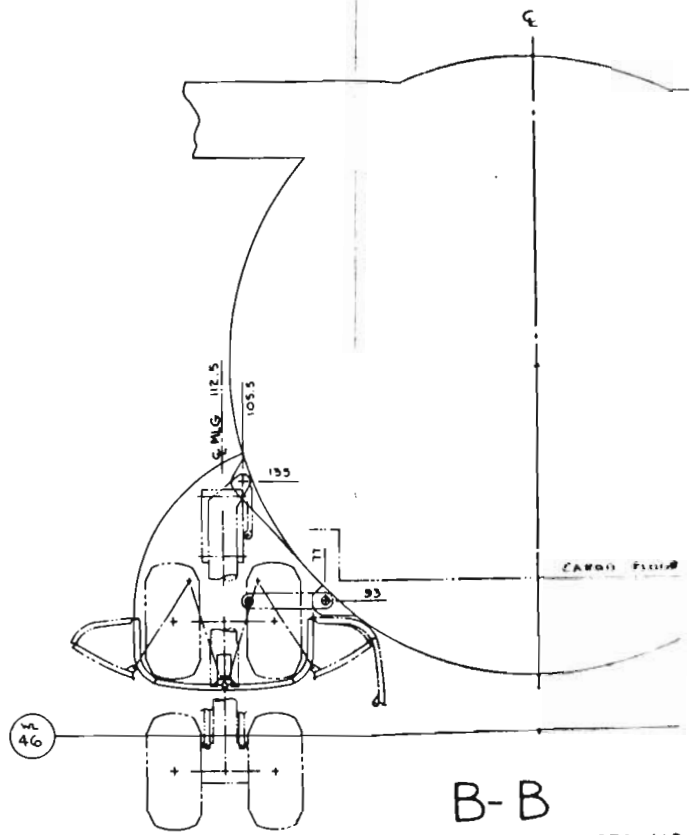

B-B

MLG WHEEL WELL STA 61C
(CONSTANT-SECTION MLG D
ABOUT ℄ MLG)

— MLG FAIRING STRUCTURE & ACC
1 PROTOTYPE AIRPLANE ONLY
2 PRODUCTION AIRPLANE ONLY
3 SPACE SHOWN MUST ALSO AC
4 APU ATTACH - L SIDE, PRODUC

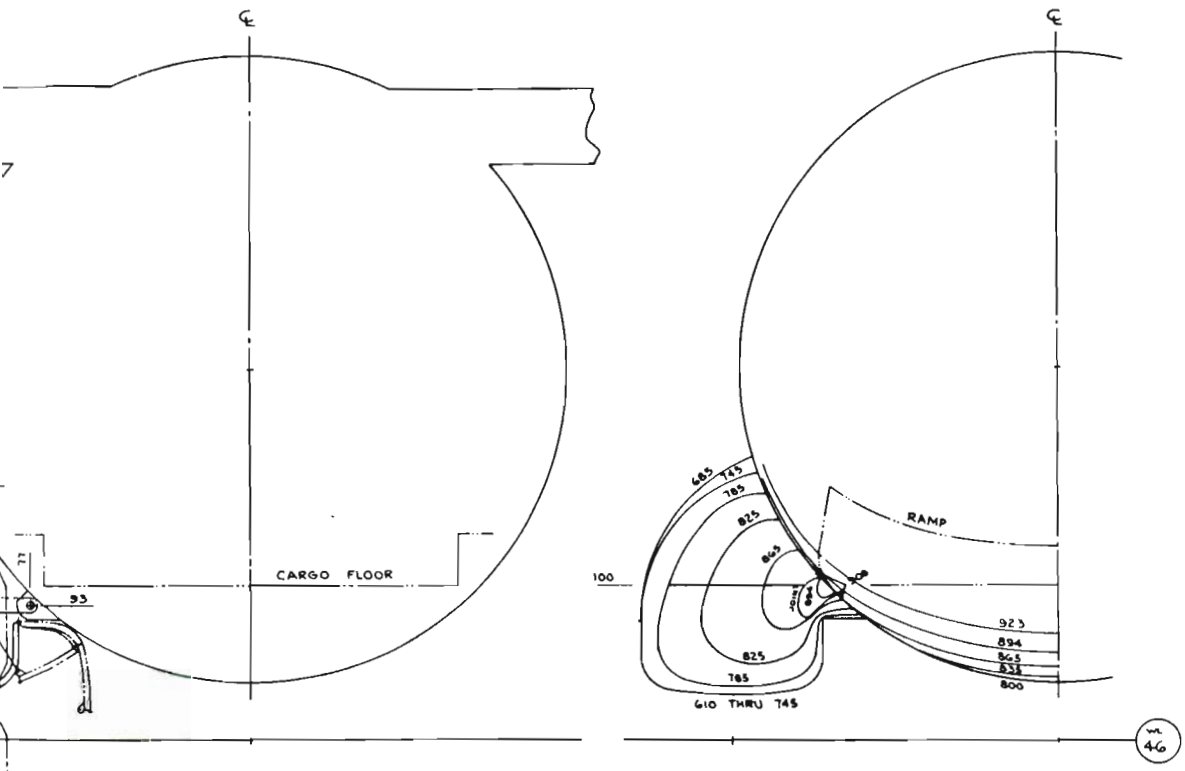

B-B

C-C

MLG WHEEL WELL STA 610-745
(CONSTANT-SECTION MLG DOORS, SYMMETRICAL ABOUT ℄ MLG)

LGFL-3

— MLG FAIRING STRUCTURE & ACCESS DOORS NOT SHOWN

(1) PROTOTYPE AIRPLANE ONLY

(2) PRODUCTION AIRPLANE ONLY

(3) SPACE SHOWN MUST ALSO ACCOMMODATE FAIRING STRUCT.

(4) APU ATTACH - L SIDE, PRODUCTION AIRPLANE ONLY

Figure 107: MLG Fairing Loft

REFERENCES

1. Petit, J. E., and Scholey, M. B., STOL Transport Thrust Reverser/ Vectoring Program, AFAPL-TR-72-109, December 1972.

2. daCosta, A. L., et al, STOL Tactical Aircraft Investigation - Baseline Configuration Study - Mechanical Flaps with Vectored Thrust, Boeing Company Document D180-14406-1, January 1972.

3. Hopkins, G. L., et al, STOL Tactical Aircraft Investigation - Baseline Configuration Study - Internally Blown Jet Flap Study, Boeing Company Document D180-14406-2, January 1972.

4. Vincent, J. H., STOL Tactical Aircraft Investigation - Flight Control Technology: Piloted Simulation of a Medium STOL Transport with Vectored Thrust/Mechanical Flaps, AFFDL-TR-73-19, Vol. V, Part II, May 1973.

5. Crandall, K. J., et al, STOL Tactical Aircraft Investigation - Flight Control Technology: System Analysis and Trade Studies for a Medium STOL Transport with Vectored Thrust/Mechanical Flaps, AFFDL-TR-73-19, Vol. V, Part I, May 1973.

6. Monk, J. R., et al, STOL Tactical Aircraft Investigation - Analysis of Wind Tunnel Data, Vectored Thrust/Mechanical Flaps and Internally Blown Jet Flaps, AFFDL-TR-73-19, Vol. IV, May 1973.

7. Runciman, W. J., STOL Tactical Aircraft Investigation - Aerodynamic Technology: Design Compendium, Vectored Thrust/Mechanical Flaps, AFFDL-TR-73-19, Vol. II, Part I, May 1973.

8. Goodmanson, L. T., and Gratzer, L. B., Recent Advanced in Aerodynamics for Transport Aircraft, AIAA Paper No. 73-9, January 1973.

9. Davenport, F. J., et al, STOL Tactical Aircraft Investigation - Takeoff and Landing Performance Ground Rules for Powered Lift STOL Transport Aircraft, AFFDL-TR-73-19, Vol. III, May 1973.

Unclassified

Security Classification

DOCUMENT CONTROL DATA - R & D

(Security classification of title, body of abstract and indexing annotation must be entered when the overall report is classified)

1. ORIGINATING ACTIVITY *(Corporate author)* Boeing Aerospace Company (A Division of The Boeing Co.) P.O. Box 3999 Seattle, Washington 98124	2a. REPORT SECURITY CLASSIFICATION UNCLASSIFIED 2b. GROUP — — —

3. REPORT TITLE

STOL Tactical Aircraft Investigation - Configuration Definition: Medium STOL Transport with Vectored Thrust/Mechanical Flaps.

4. DESCRIPTIVE NOTES *(Type of report and inclusive dates)*

Final Technical Report - 8 June 1971 through 12 January 1973

5. AUTHOR(S) *(First name, middle initial, last name)*

Richard H. Carroll
John W. Jants
Peter Milns

6. REPORT DATE	7a. TOTAL NO. OF PAGES	7b. NO. OF REFS
May 1973	179	10

8a. CONTRACT OR GRANT NO.	9a. ORIGINATOR'S REPORT NUMBER(S)
F33615-71-C-1757 b. PROJECT NO. 643A c. d.	D180-14408-1 9b. OTHER REPORT NO(S) *(Any other numbers that may be assigned this report)* AFFDL-TR-73-19, Volume I

10. DISTRIBUTION STATEMENT

Approved for public release; distribution unlimited.

11. SUPPLEMENTARY NOTES	12. SPONSORING MILITARY ACTIVITY
	Air Force Flight Dynamics Laboratory Wright-Patterson Air Force Base Ohio 45433

13. ABSTRACT

A configuration for an Advanced Medium STOL Transport (AMST) using vectored thrust for powered lift is defined in detail. Capability to operate from an austere forward airfield of 2000 feet length at the midpoint of 500 nm radius mission with 28,000 lbs. of payload is substantiated by aerodynamic, propulsion, structural, and weights data. The vectored thrust powered lift concept is compared with other powered lift schemes considered for the AMST. A program of continuing research and development in tactical airlift and STOL technology is recommended.

DD FORM 1 NOV 65 1473

Security Classification

14. KEY WORDS	LINK A		LINK B		LINK C	
	ROLE	WT	ROLE	WT	ROLE	WT
Short Takeoff and Landing (STOL)						
Medium STOL Transport						
Performance						
Parametric Design						
Aerodynamic Characteristics						
Flight Control						
Propulsion						
Thrust Reversing/Vectoring						
Boundary Layer Control (BLC)						
Structural Analysis						
Mass Properties						
Mission Rules						
Takeoff and Landing Rules						
Vectored Thrust/Mechanical Flap						

☆U.S. Government Printing Office: 1973 — 758-425/06